

***Organocatalyzed Regio-regular Polymerization of α -Aryl
Trimethylene Carbonates and Synthesis of Diblock
Copolymers Containing Donor and Acceptor Blocks***

A Thesis Submitted for the Degree of

Doctor of Philosophy

by

M. S. Ramesh



New Chemistry Unit

Jawaharlal Nehru Centre for Advanced Scientific Research

Jakkur, Bangalore-560064

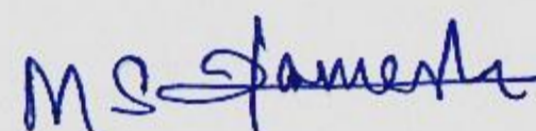
India

July-2022

Declaration

I hereby declare that the matter embodied in this thesis entitled “*Organocatalyzed Regio-regular Polymerization of α -Aryl Trimethylene Carbonates and Synthesis of Diblock Copolymers Containing Donor and Acceptor Blocks*” is the result of investigations carried out by me at the New Chemistry Unit, Jawaharlal Nehru Centre for Advanced Scientific Research, Bangalore India under the supervision of **Prof. Sridhar Rajaram** and that it has not been submitted elsewhere for the award of any degree or diploma.


In keeping with the general practice in reporting the scientific observations, due acknowledgement has been made whenever the work described is based on the findings of other investigators. Any omission that might have occurred due to oversight or error in judgement is regretted.



M. S. Ramesh
(Ph.D.student)

Certificate

I hereby certify that the matter embodied in this thesis entitled "*Organocatalyzed Regio-regular Polymerization of α -Aryl Trimethylene Carbonates and Synthesis of Diblock Copolymers Containing Donor and Acceptor Blocks*" has been carried out by **Mr. M. S. Ramesh** at the New Chemistry Unit, Jawaharlal Nehru Centre for Advanced Scientific Research, Bangalore, India under my supervision and that it has not been submitted elsewhere for the award of any degree or diploma



Prof. Sridhar Rajaram
(Research Supervisor)

Acknowledgement

I thank my parents, grandparents, brother, and sister. I would like to thank research supervisor, Prof. Sridhar Rajaram for his guidance and support. I would like to thank my course instructors: Prof. Subi. J. George, Prof. T. Govindaraju, and Prof. Jayanta Haldar. I thank Prof. K. S. Narayan for allowing me to use their glove box and I thank his students for being co-operative. I thank Prof. Satish Patil (IISc-SSCU) and his student Dr. Nilabja Maity for helping me in recording AFM images in SSCU and CeNSE. I thank Prof Subi. J. George and his student Dr. Raju Laishram for helping me in recording AFM images at their lab during optimization studies. I thank my labmates: Dr. Kavita Sharma, Dr. G. Ramana Reddy, Dr. Arjun Kumar Chittoory, Mr. Robi Sankar Patra, and Mr. Ankur Bishnoi. I thank Mr. Deepak, Mr. Mahesh, Mr. Shiva, and Mr. Vasu for their help in characterization of various compounds. I thank my friends A. P. Shikas, J. Nagaraju, T. M. Subrahmanya, K. Raja, and P. Sathish Kumar.

Thesis Synopsis

Organocatalyzed Regio-regular Polymerization of α -Aryl Trimethylene Carbonates and Synthesis of Diblock Copolymers Containing Donor and Acceptor Blocks

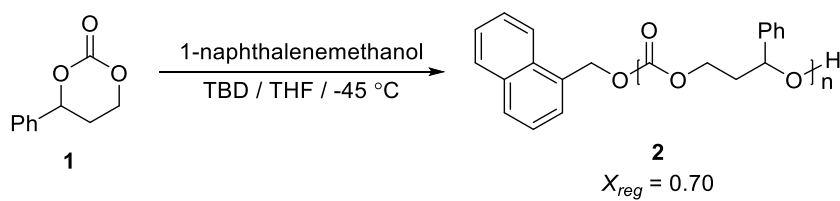
Aliphatic polycarbonates are one of the potential alternatives to the commercially available aromatic polycarbonates. The most commonly used aromatic polycarbonates upon degradation releases Bisphenol-A which has been identified as an endocrine disruptor. Aliphatic polycarbonates can be made either by copolymerization of epoxides and CO₂ or by ring opening polymerization of cyclic carbonates. These polymerization processes proceed *via* a controlled chain growth polymerization and as a result precise control of molar mass and dispersity can be achieved. As cyclic carbonates are made up of diols, a wide variety of functionalized diols can be synthesized and therefore various kinds of functionalized aliphatic polycarbonates can be obtained *via* ROP. A variety of metal-based and organocatalysts are available to carry out the ROP of cyclic monomers. Although various kinds of aliphatic polycarbonates were synthesized using available catalytic systems, their physical properties were yet to match the favorable properties of aromatic polycarbonates.

In this thesis, we were interested in introducing the favorable properties of aromatic polycarbonates into aliphatic polycarbonates under living polymerization conditions. For this purpose, we had developed regio-regular ring opening polymerization of racemic α -Aryl-trimethylene carbonate (α -ArTMC) using organocatalysts. Subsequently diblock copolymers with electron-rich and electron-deficient blocks were made in an attempt to further enhance the physical properties of aliphatic polycarbonates.

We began our optimization of ROP using commercially available phosphazene base as it has been already shown to polymerize α -MeTMC in a highly regio-regular manner. In the case of our monomer, this catalyst yielded a regio-random poly(α -PhTMC). The regio-regularity of polymer was calculated using a formula expressed as $X_{reg} = [1 - (\text{relative intensity of H-H linkages} + \text{relative intensity of T-T linkages})]$ after normalizing the H-T linkages to one. Similarly, the well-known catalytic system consisting of thiourea and DBU also yielded a regio-random polycarbonate. The commercially available strong base TBD turned out to be a useful catalyst for this class of monomers. The reaction in THF at room temperature resulted in a promising regio-regularity with $X_{reg} = 0.40$. We were able to achieve a maximum regio-regularity of $X_{reg} = 0.70$ by lowering the temperature to $-45\text{ }^\circ\text{C}$ (Figure 1). Under this optimized condition we synthesized poly(α -PhTMC)s of various DPs by varying monomer to initiator ratios and also shown that the ROP of α -PhTMC exhibits living polymerization behavior.

In order to study the effect of substituents on regio-regularity we carried out ROP of other monomers *viz* α -4-Me-PhTMC, α -4-Br-PhTMC, and α -4-CF₃-PhTMC under the optimized condition. The ROP of α -4-Me-PhTMC was observed to be slower than that of α -PhTMC and also yielded polycarbonate with lower regio-regularity ($X_{reg} = 0.60$). On the other hand, the ROP of α -4-Br-PhTMC and α -4-CF₃-PhTMC were found to be faster than

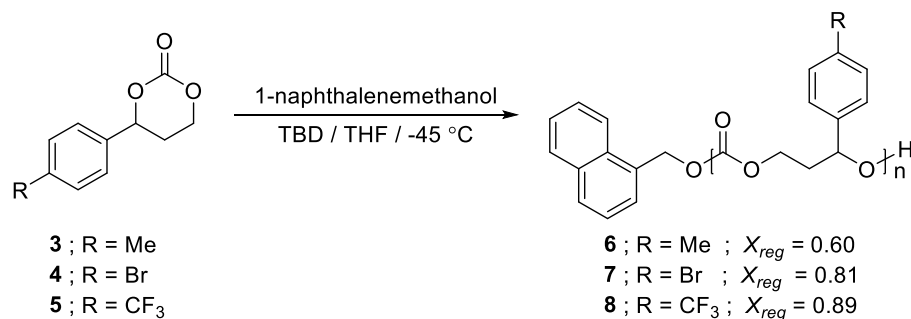
Figure 1. ROP of α -PhTMC Using TBD as Catalyst



that of α -PhTMC. The polymerization of α -4-Br-PhTMC exhibited greater regio-regularity with $X_{reg} = 0.81$ while the polymerization of α -4-CF₃-PhTMC was highly regio-regular with an $X_{reg} = 0.89$ (Figure 2). The increase in regio-regularity with electron withdrawing substituents in the aromatic ring suggests that the ROP of monomer results in a secondary alcohol as the active chain-end.

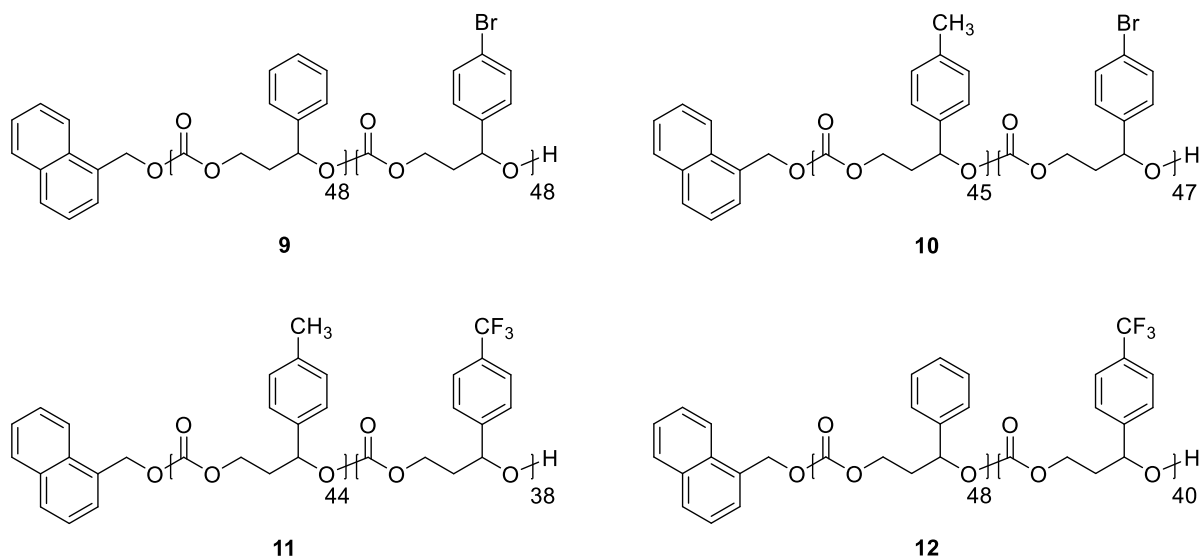
We carried out DSC studies on poly(α -ArTMC)s to determine their glass transition temperatures (T_g s) and also analyzed the effect of regio-regularity on T_g . The poly(α -PhTMC) with $X_{reg} = 0.01$ exhibits T_g of 39 °C which is greater than stereo and regio-regular poly(α -MeTMC) ($T_g = -2$ °C). For a polymer with a higher regio-regularity ($X_{reg} = 0.40$), the T_g was found to be 50 °C. Further increase in regio-regularity did not result in an increase in T_g . This trend clearly indicates that T_g increases with X_{reg} to a certain extent and beyond that it remains unchanged for the poly(α -PhTMC). This effect was not significant in the case of substituted poly(α -PhTMC)s, but their T_g s were found to be better than poly(α -PhTMC). The T_g of poly(α -4-Me-PhTMC), poly(α -4-Br-PhTMC), and poly(α -4-CF₃-PhTMC) were found to be 52 °C, 65 °C, and 63 °C, respectively.

Figure 2. ROP of α -ArTMC Using TBD as Catalyst



We believed that the physical properties of aliphatic polycarbonates can be further enhanced *via* intermolecular π - π interactions between electron-rich and electron-deficient blocks of diblock copolymers. To achieve our goal, we need to overcome the micro-phase separation of diblock copolymers which arise due to incompatibility of two blocks. In order to prevent micro-phase separation, we had decided to synthesize diblock copolymers having almost identical backbone and side-chains. With this in mind we synthesized diblock copolymers having electron-rich and electron-deficient blocks from α -ArTMCs that we previously made (Figure 3). These diblock copolymers have a common backbone and almost similar side-chains. To minimize the effect of transesterification, we polymerized electron-rich monomer first followed by electron-deficient monomer. We carried out these polymerization reactions using TBD as catalyst in THF at -45 °C to obtain maximum regio-regularity. The block lengths of diblock copolymers were successfully determined using ^1H NMR. Low dispersity and a unimodal SEC traces of synthesized diblock copolymers indicated good block purity.

Figure 3. Structures of Diblock Copolymers Containing Donor and Acceptor Blocks



All the diblock copolymers were found to form smooth phase mixed thin films with RMS roughness less than 0.5 nm. Thermal annealing of these thin films at 55 °C for 30 mins resulted in dewetting. The RMS roughness of pin hole free areas in all films were still less than 0.5 nm, which suggests that the diblock copolymers were phase mixed at least up to their T_g (Figure 4).

Figure 4. AFM images of a Diblock Copolymer (10): (A) As spun-cast; (B) Thermally annealed at 55 °C for 30 mins

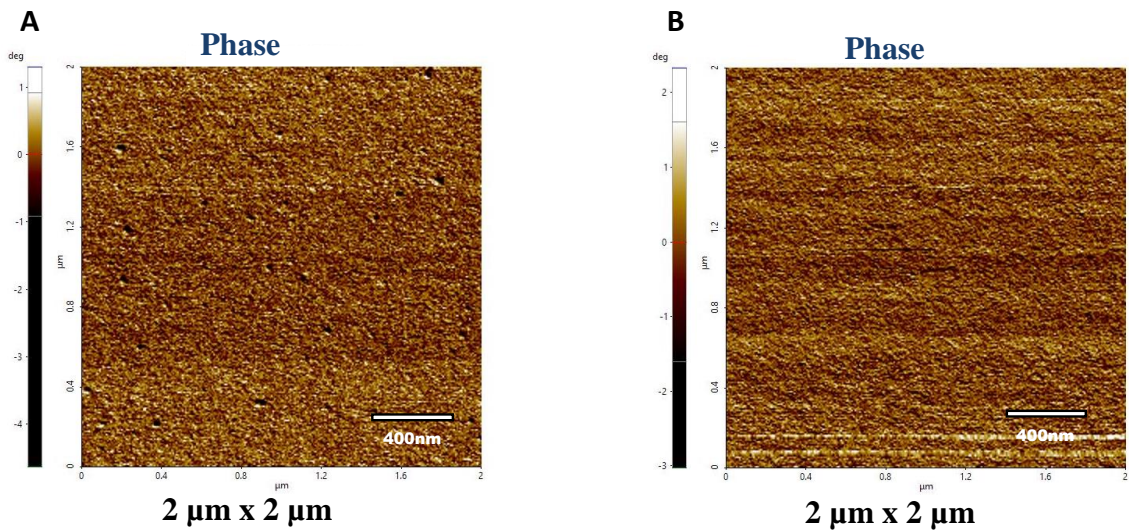


TABLE OF CONTENTS

Acknowledgement		vii
Synopsis		ix
List of Abbreviations		xvii
List of Figures		xix
List of Tables		xxiii
Chapter 1	Polycarbonates and Ring Opening Polymerization	
1.1	Introduction	1
1.2	Polycarbonates	2
<i>1.2.1</i>	Properties of Polycarbonates	3
<i>1.2.2</i>	Synthesis of Aromatic Polycarbonates	3
<i>1.2.3</i>	Synthesis of Aliphatic Polycarbonates	5
1.3	Ring Opening Polymerization (ROP)	10
<i>1.3.1</i>	Thermodynamics and Kinetics of ROP	10
<i>1.3.2</i>	ROP of Five-Membered Cyclic Carbonates	13
<i>1.3.3</i>	ROP of Six-Membered Cyclic Carbonates	17
<i>1.3.4</i>	Metal Catalyzed ROP	18
<i>1.3.5</i>	Organocatalyzed ROP	21
1.4	Conclusions	43
1.5	References	44
Chapter 2	Organocatalyzed Regio-regular Polymerization of α-Aryl Trimethylene Carbonates	
2.1	Introduction	53
2.2	Background	53
<i>2.2.1</i>	Sugar Based Cyclic Carbonates	54
<i>2.2.2</i>	β -Substituted Trimethylene Carbonates	55
<i>2.2.3</i>	α -Substituted Cyclic Carbonates	56

2.3	Initial Hypothesis	60
2.4	Results and Discussion	60
2.5	Conclusions	75
2.6	Experimental Section	76
2.7	References	92
Chapter 3	Synthesis of Diblock Copolymers Containing Donor and Acceptor Blocks and Its AFM Studies	
3.1	Introduction	97
3.2	Background	99
3.3	Our Approach	103
3.4	Results and Discussion	106
3.5	Conclusions	121
3.6	Experimental Section	122
3.7	References	131
Appendix 1	NMRs	135
Appendix 2	SEC Traces	179
Appendix 3	DSC Traces	189

List of Abbreviations

AFM	:	Atomic force microscopy
ATRP	:	Atom transfer radical polymerization
BEMP	:	2-tert-Butylimino-2-diethylamino-1,3-dimethyl-perhydro-1,3,2-diazaphosphorine
Bis-MPA	:	2,2-bishydroxy(methyl)propionic acid
BPA	:	Bisphenol-A
CDI	:	1,1'-Carbonyldiimidazole
DBU	:	1,8-Diazabicyclo[5.4.0]undec-7-ene
DCM	:	Dichloromethane
DMAP	:	4-Dimethylaminopyridine
DMSO	:	Dimethyl sulfoxide
DP	:	Degree of polymerization
DSC	:	Differential scanning calorimetry
EC	:	Ethylene carbonate
EO	:	Ethylene oxide
EtOAc	:	Ethyl acetate
IR	:	Infrared spectroscopy
M.P.	:	Melting point
MTBD	:	7-Methyl-1,5,7-triazabicyclo[4.4.0]dec-5-ene
NMR	:	Nuclear magnetic resonance
NHC	:	N-Heterocyclic carbene
PET	:	Poly(ethylene terephthalate)
PPY	:	4-pyrrolidinopyridine
RAFT	:	Reversible addition-fragmentation chain-transfer
ROP	:	Ring opening polymerization
SEC	:	Size exclusion chromatography

TBD : 1,5,7-triazabicyclo[4.4.0]dec-5-ene
THF : Tetrahydrofuran
TMC : Trimethylene carbonate

List of Figures

Figure 1.1.	3
Structures of Various Aromatic Polycarbonates	
Figure 1.2.	8
Different Kinds of Carbonate Linkages and Stereo-regularities of H-T Linkage	
Figure 1.3.	13
(a) Plots of $\ln[M]_0/[M]$ versus time with various k_i/k_p ratios ($[M]_0/[I]_0 = 100$); (b) Plots of degree of polymerization and molar mass distribution versus time with various k_i/k_p ratios ($[M]_0/[I]_0 = 100$)	
Figure 1.4.	21
Structures of Al and Zn Based Single-Site Catalysts Used for Stereo-regular ROP of Lactides	
Figure 1.5.	24
Structures of Different Lactones and Cyclic Carbonates	
Figure 1.6.	26
Structure of DMAP and PPY	
Figure 1.7.	30
Structure of Various <i>N</i> -Heterocyclic Carbenes Used for ROP	
Figure 1.8.	33
Structure of Guanidines and Amidine	
Figure 1.9.	35
Structure of Phosphazene Bases	
Figure 1.10.	37
Structure of Some of Bifunctional Hydrogen-Bonding Organocatalysts Used for ROP of Cyclic Monomers	
Figure 1.11.	39
Mode of Activation of Monomer and Initiator Using Bifunctional Organocatalysts	
Figure 1.12.	40
Structure of (Thio)Ureas and Amines	

Figure 1.13.	41
Cooperative and Anion Hydrogen-Bonding Mechanisms	
Figure 1.14.	42
Structures of (Thio)Urea Anions Used for the ROP of Cyclic Monomers	
Figure 2.1.	55
Structures of Sugar Based Cyclic Carbonates	
Figure 2.2.	56
Structures of β -Substituted Trimethylene Carbonates	
Figure 2.3.	57
Structures of α -Substituted Cyclic Carbonates	
Figure 2.4.	61
$^{13}\text{C}\{^1\text{H}\}$ NMR Spectrum of Non-Regioselective ROP of α -PhTMC	
Figure 2.5.	63
Structure of catalysts used in the regio-regular polymerization of α -PhTMC 2.18	
Figure 2.6.	66
Identification of End-Group Using ^1H NMR: (a) Expansion of Aromatic Region of ^1H NMR (CDCl_3) of Synthesized Carbonate 2.21 ; (b) Expansion of Aromatic Region of ^1H NMR (CDCl_3) of poly(α -PhTMC) 2.20	
Figure 2.7.	68
Kinetic plot of $\ln([M]/[M]_0)$ versus time for ROP of 2.18	
Figure 2.8.	69
Plots of M_n and M_w/M_n versus monomer conversion for ROP of 2.18	
Figure 2.9.	72
Ring opening pathway for the formation of primary and secondary alcohol end groups	
Figure 3.1.	97
Representation of Three kinds of Block Copolymers	
Figure 3.2.	100
Folding of a Single Block Copolymer Chain via Intramolecular Hydrogen Bonding Interactions: (a) Barner-Kowollik and coworkers report; (b) Meijer and coworkers report	

Figure 3.3.	101
(a) Chemical Structure and Representation of Secondary Structure of Foldamer Based on Donor and Acceptor Interactions; (b) Chemical and Crystal Structure of β -Sheet Foldamer Based on face-to-face π - π interactions.	
Figure 3.4.	102
Schematic Representation of the Single-chain Folding of PS ₃₀ -PDMAA ₂₀ -PPFS ₃₀ Block Copolymer in Solution	
Figure 3.5.	102
Chemical Structure of Coil-Helix Diblock Copolymer Comprised of Poly(styrene) and Poly(pentafluorophenyl isocyanide) Blocks and Representation of π - π Stacking Interactions Between Phenyl and Pentafluorophenyl Rings in Coil-Helix Diblock Copolymer	
Figure 3.6.	103
Chemical Structure of ABCA Tetrablock Copolymer Comprised of Poly(<i>p</i> -phenylene vinylene) (PPV) and Poly(norbornene) (PNB) Blocks and Schematic Representation of Synthetic β -Sheet Formation of PPV-(PNB-PNB-PPV) ₅	
Figure 3.7.	105
Structure of Poly(3-hexylthiophene- <i>b</i> -perylene bisimide acrylate) and SFM Phase Image of the Diblock Copolymer (a) As spun cast; (b) After thermal annealing at 150 °C for 20 min; (c) After annealing for 2h in toluene/chloroform vapor	
Figure 3.8.	112
An Example to Show the Block Lengths of a Diblock Copolymer Using ¹ H NMR	
Figure 3.9.	118
AFM Images of As Spun-Cast Thin Films of Diblock Copolymers: (A) 3.5 ; (B) 3.6	
Figure 3.10.	118
Curve Fitting of Histogram of Diblock Copolymers: (A) 3.5 ; (B) 3.6	
Figure 3.11.	119
AFM Images of As Spun-Cast Thin Films of Diblock Copolymers: (A) 3.7 ; (B) 3.8	
Figure 3.12.	120
AFM Images of Thermally Annealed Thin Films of Diblock Copolymers: (A) 3.5 ; (B) 3.6 ; (C) 3.7 ; (D) 3.8	

List of Tables

Table 1.1.	9
Copolymerization of <i>rac</i> -Propylene Oxide and CO ₂ <i>via</i> Kinetic Resolution	
Table 1.2.	27
ROP of Lactide Using DMAP and PPY as Catalysts	
Table 1.3.	30
ROP of Cyclic Monomers Using Various NHCs	
Table 1.4.	33
Details of Guanidines and Amidine Catalyzed ROP of Cyclic Monomers	
Table 1.5.	35
Details of Phosphazenes Catalyzed ROP of Cyclic Monomers	
Table 1.6.	37
Details of ROP of Cyclic Monomers Using Bifunctional Hydrogen-Bonding Organocatalysts	
Table 1.7.	40
Details of ROP of Cyclic Monomers Catalyzed by the Combinations of (Thio)Ureas and Bases	
Table 1.8.	42
Details of (Thio)Urea Anions Catalyzed ROP of Cyclic Monomers	
Table 2.1.	59
Regio-Regular ROP of <i>R</i> - α -MeTMC	
Table 2.2.	63
Optimization of Ring opening polymerization of α -PhTMC 2.18	
Table 2.3.	67
ROP of α -PhTMC 2.18 using TBD by varying monomer to initiator ratios.	
Table 2.4.	70
ROP of α -ArTMC 2.22-2.24 using TBD as catalyst	
Table 2.5.	73
Comparison of Polycarbonate 2.20 of Varying X_{reg} with T _g	

Table 2.6.	74
Comparison of Polycarbonate 2.25 of Varying X_{reg} with T_g	
Table 2.7.	74
Comparison of Polycarbonate 2.26 of Varying X_{reg} with T_g	
Table 2.8.	75
Comparison of Polycarbonate 2.27 of Varying X_{reg} with T_g	
Table 3.1.	109
Synthesis of Different kinds of Diblock Copolymers Containing Electron-Rich and Electron-Deficient Blocks	
Table 3.2.	115
TBD Catalyzed Ring Opening Polymerization of α -PhTMC (3.1)	
Table 3.3.	116
DSC Studies of Diblock Copolymers	

Chapter 1

Polycarbonates and Ring Opening Polymerization

1.1 Introduction

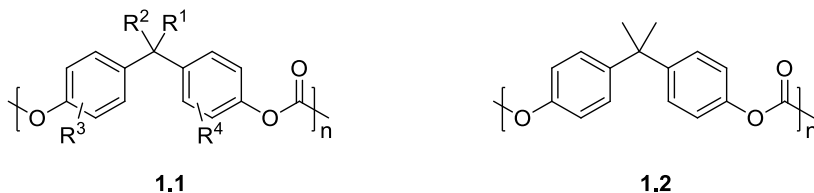
Nature has synthesized a variety of polymers like carbohydrates, proteins, DNAs, RNAs and many others. Each polymer plays its own significant role in daily life. Human society has played its part in synthesizing a variety of polymers over past 100 years. The synthetic polymers made by mankind has not yet matched the complexity and the precision of nature's work. However, in terms of practical applications synthetic polymers have gained a lot of interest and recognition worldwide. In fact, the current world cannot carry out its day-to-day life without using synthetic polymers. Among synthetic polymers, polycarbonate is one of the most widely used polymers in the world. Polycarbonates, especially aromatic polycarbonates are produced in industrial scale every year worldwide and used in various fields. Aromatic polycarbonates derived from BisPhenol-A (BPA) have found application in a wide range of fields such as optics (as CDs/DVDs), electronics (as computer covers, cell phone case), household items (as food carrier, water bottles), construction (as transparent multiwall sheets, windows), medical (as blood filters, dialyzers), and automobile (as headlamp diffuser lenses). Since aromatic polycarbonates possess some adverse effect on the environment (*vide infra*), aliphatic polycarbonates have started to gain academic and industrial interest. Among the available methods for the synthesis of aliphatic

polycarbonates, ring opening polymerization (ROP) appears to be an efficient route. The ROP proceeds by chain growth mechanism and unlike step-growth polymerization, it is possible to synthesize polymers of desired molar mass with narrow dispersity. There are a number of organometallic catalysts and organocatalysts that carry out ROP. In this chapter, we will discuss about the synthesis of polycarbonates and its important properties. Also, we will discuss the thermodynamic, and kinetic parameters that dictate the outcome of ROP, and the role played by catalysts in ensuring an efficient ROP.

1.2 Polycarbonates

Polycarbonates belong to a broad class of synthetic polymers, where the repeating units are linked by carbonate moieties [-O-C(O)-O-]. Polycarbonates can be divided into aromatic or aliphatic based on the nature of carbon atom bound to the carbonate linkage. If the carbon atom bound to the carbonate moiety is part of an aromatic system, then it is termed as aromatic polycarbonate. Polycarbonates with a non-aromatic carbon atom bound to the carbonate linkage are termed as aliphatic polycarbonates. The first report on the synthesis of polycarbonate was in the 19th century by the polycondensation of resorcinol and phosgene.¹ This was followed by various reports on using other dihydroxy phenols and phosgene or diphenyl carbonate to prepare polycarbonates.^{2, 3} H. Schnell from Bayer AG in Germany reported the synthesis of various types of aromatic polycarbonates (**1.1**, Figure 1.1) derived from 4,4'-dihydroxydiarylalkanes, which showed interesting structural properties.⁴⁻⁶ Among the various types of polycarbonates, the polycarbonate (**1.2**, Figure 1.1) derived from 2,2-bis(4-hydroxy-phenyl) propane (BPA or BisPhenol-A) possessed remarkable structural properties. This led Bayer to commercialize the production of BPA-based polycarbonate under the trade name Makrolon in 1959. In 1960, D. W. Fox from General Electric in USA

Figure 1.1. Structures of Various Aromatic Polycarbonates



also produced BPA-based polycarbonate in industrial scales and commercialized the product under the trade name Lexan.⁷ Today, there are companies all over the world that manufacture BPA-based polycarbonates in ton scales. Examples include, Mitsubishi Chemical Group (Japan, China), Teijin Group (Japan, Singapore), Sabic Group (Japan, USA, Spain), Bayer Group (Germany, Belgium, USA, China), and Dow Chemical Group (USA, Germany).⁸

1.2.1 Properties of Polycarbonates

Among the aromatic polycarbonates, BPA-based polycarbonate exhibits a range of useful properties. Some of the important properties include high thermal stability ($T_g = 145-155$ °C and melting point in the range 220-230 °C), resistance to low temperatures (upto -100 °C), high flame retardancy, electrical insulation, impact resistance, dimensional stability, moldability and greater transparency.⁸⁻¹⁰ Aliphatic polycarbonates on the other hand, have an elastic backbone and generally exists as oily polymers. Many researchers are currently interested in improving the mechanical properties of aliphatic polycarbonates.

1.2.2 Synthesis of Aromatic Polycarbonates

There are two important methods available for the synthesis of aromatic polycarbonates namely, (i) Interfacial Polycondensation and (ii) Melt Polycondensation. Both processes follow step-growth polymerization mechanism.

1.2.2.1 Interfacial Polycondensation

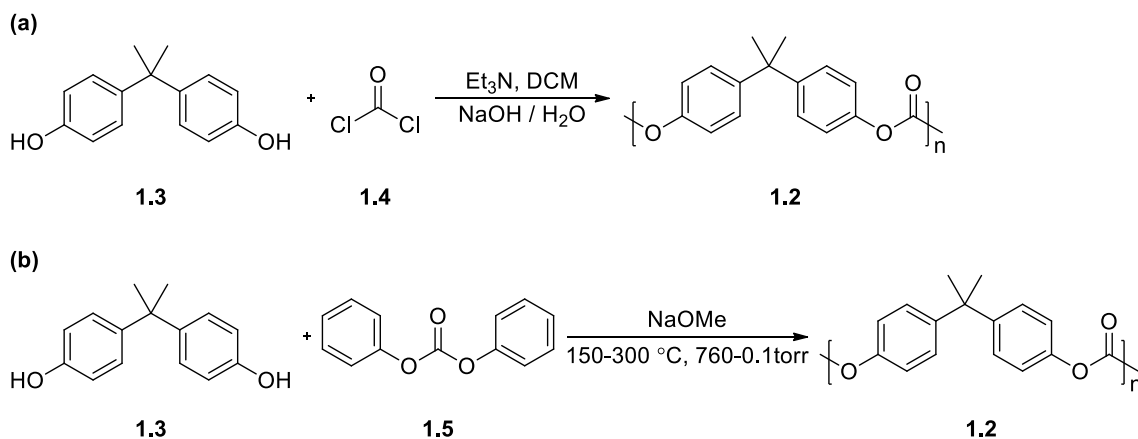
Interfacial polycondensation is the most commonly used industrial method for the production of BPA-based polycarbonates.^{4-6, 11} In this process, phosgene is purged into a biphasic suspension containing bisphenol-A under rigorous stirring (Scheme 1.1a). The sodium salt of bisphenol-A reacts with phosgene at the interface and forms oligomers with chloro formate ester end group. These oligomers enter the organic phase and the tertiary amine (catalyst) accelerates the polycondensation of oligomers. The polymerization can be terminated by the addition of phenol or substituted phenol. Therefore, the amount of addition of chain terminator determines the molecular mass of the polycarbonate. In this method, polycarbonate with the molecular mass in the range of 50,000-200,000 Da can be prepared.

1.2.2.2 Melt Polycondensation

Melt polycondensation or transesterification process avoids the usage of harmful phosgene and chlorinated solvents. In this method bisphenol-A and diphenyl carbonate are subjected to melt polycondensation with the elimination of phenol (Scheme 1.1b).^{5, 7, 10} The raw materials along with catalytic amount of sodium methoxide are initially heated to 150 °C under moderate vacuum with rigorous stirring. During the course of polycondensation, the byproduct phenol is removed. The reaction temperature is gradually increased up to 300 °C along with increase in vacuum to obtain high molecular mass polycarbonates.

Although, aromatic polycarbonates are produced in ton scales worldwide and used in various applications, it possesses some major drawbacks. Bisphenol-A, the main raw material for the industrial production of polycarbonates has been identified as an endocrine disruptor.^{12, 13} Current studies indicate bisphenol-A has been detected in urine, breast milk,

Scheme 1.1. Synthesis of BPA-based Polycarbonates by Interfacial and Melt Polycondensation



placental tissue and in fetal liver due to its environmental persistence.¹⁴ Prolonged exposure to bisphenol-A might have adverse effects on human health. Another drawback in the synthesis of aromatic polycarbonate is the difficulty in precisely controlling the molar mass. Also, aromatic polycarbonates display broad dispersity mainly because of step-growth polymerization. On the other hand, aliphatic polycarbonates have gained attention, as they biodegrade into non-hazardous compounds. There are many ongoing efforts on improving the mechanical properties of aliphatic polycarbonates for a better alternative to aromatic polycarbonates.

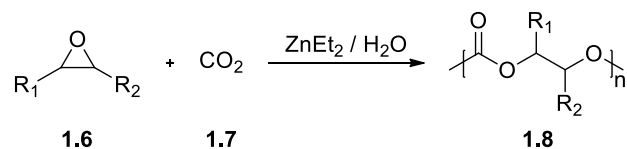
1.2.3 Synthesis of Aliphatic Polycarbonates

The polycondensation methods available for the synthesis of aromatic polycarbonates can be used for the synthesis of aliphatic polycarbonates. Apart from this, other specialized polymerization methods are available for the synthesis of aliphatic polycarbonates namely (i) Copolymerization of CO₂ and cyclic ethers (epoxides), (ii) Ring opening polymerization of cyclic carbonates. These polymerization processes proceed *via* a controlled chain growth polymerization and as a result precise control of molar mass and dispersity can be achieved.

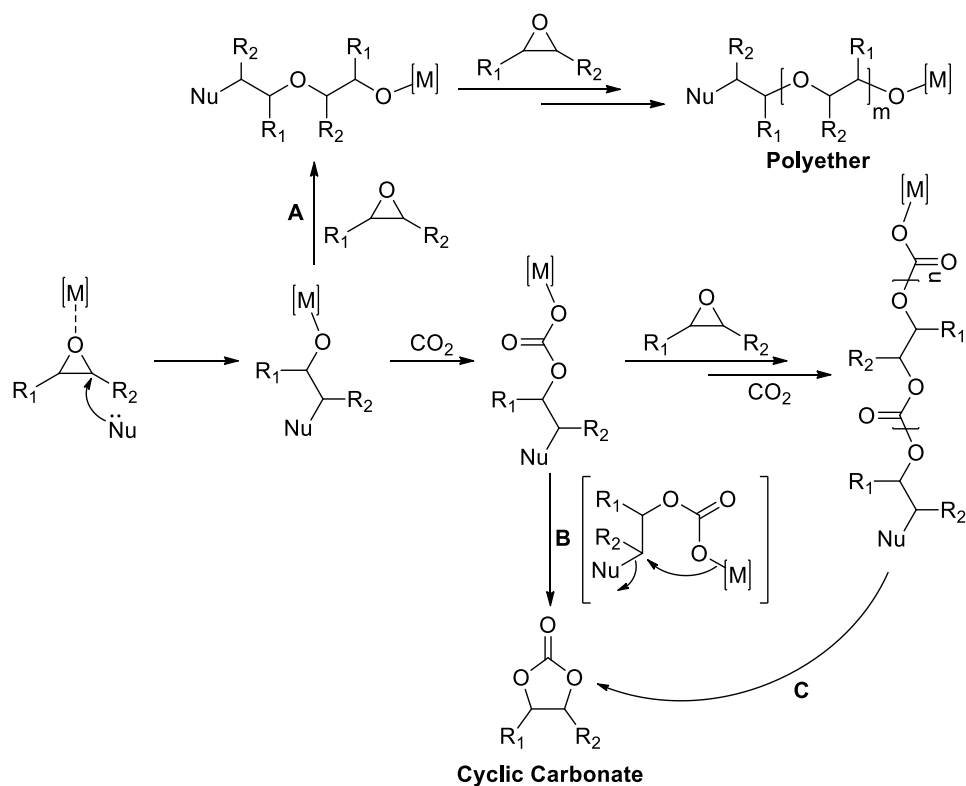
Carbon dioxide, an inexpensive, inert, and abundant material has been used as monomer for the synthesis of aliphatic polycarbonates. Initially, the copolymerization of CO₂ and epoxide was carried out using diethylzinc-water system as catalyst to obtain polycarbonate (Scheme 1.2).^{15, 16} Subsequently, several heterogeneous metal based catalysts have been reported for the copolymerization of CO₂ and epoxides.¹⁷⁻²⁰ Under these conditions, along with the formation of polycarbonates, some undesired side products are generated. Mechanistically, the reaction proceeds by alternate enchainment of an epoxide and carbon dioxide. Sequence errors can occur when two epoxides are enchainned successively, resulting in ether linkages (Scheme 1.3, path A). This is one of two unwanted side reactions. The other is the formation of thermodynamically stable five membered cyclic carbonate by intramolecular back-biting mechanism (Scheme 1.3, path B & C).²¹

In the copolymerization of CO₂ and unsymmetrical epoxides, regioselectivity plays a significant role in determining the uniformity of carbonate linkages in the polycarbonate. The epoxide ring can open either by the cleavage of methylene C-O bond or by the cleavage of methine C-O bond (Scheme 1.4). Based on the nature of ring opening of unsymmetrical epoxides, the carbonate linkages in the polymer can be classified into three types (Figure 1.2a). Head-to-tail linkages can be obtained either by the successive ring opening of epoxides at methylene C-O bond or methine C-O bond. On the other hand, head-to-head and tail-to-tail linkages are obtained by alternative cleavage of epoxides at methylene C-O bond and methine C-O bond. Polymers with greater content of head-to-tail linkages are termed as regio-regular polymers. Highly regio-regular polymer chains can potentially pack in an ordered manner and increase the degree of crystallinity of the polymer.²²⁻²⁴ Both regio-regular and irregular polycarbonates can possess another important structural property called

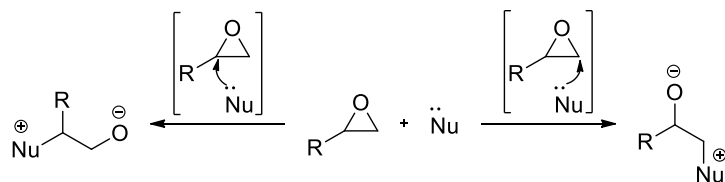
Scheme 1.2. Copolymerization of CO₂ and Epoxide



Scheme 1.3. Side Reactions Involved in the Copolymerization of CO₂ and Epoxides



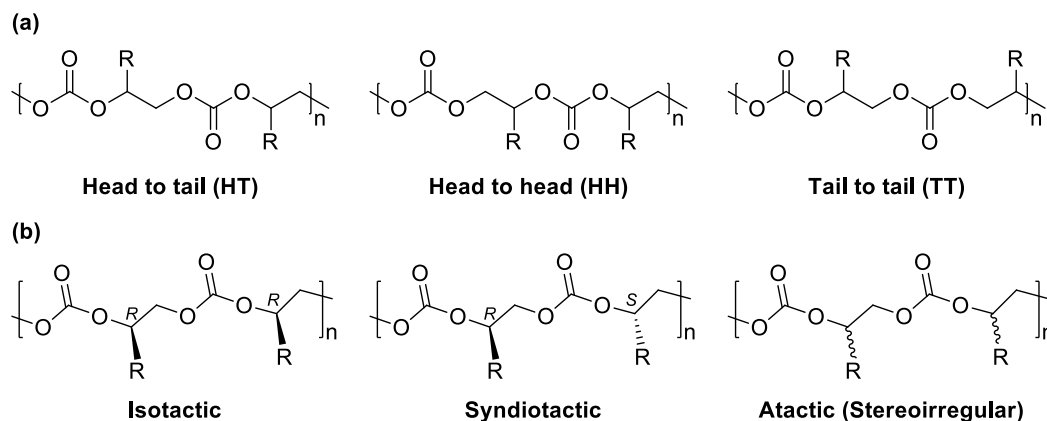
Scheme 1.4. Pathways of Ring Opening of Unsymmetrical Epoxide



stereo-regularity. Polycarbonates can exhibit two kinds of stereo-regularity namely, isotactic and syndiotactic (Figure 1.2b). In isotactic polymers each repeating unit has the same stereo configuration (either *R* or *S*), while, in syndiotactic polymers the repeating units will have alternating configurations. Like regio-regularity, stereo-regularity also plays a significant role in enhancing the degree of crystallinity of the polymer.²²⁻²⁴ Therefore, both regio and stereo-regularity influence physical properties such as glass transition temperature (T_g) and melting temperature (T_m).

Extensive research carried out in this field led to the development of several organometallic homogenous catalysts to obtain polycarbonates without the formation of ether linkages or cyclic carbonate.²⁵ Also, many organometallic catalysts were developed to induce regio and stereoselectivity in the polycarbonates.^{21, 23, 25-29} Racemic epoxides with various substituents are more readily accessible than the enantiopure epoxides. Also, racemic epoxides provide the scope for the synthesis of isotactic polycarbonate *via* kinetic resolution avoiding the use of enantiopure epoxide. Several cobalt-based complexes have been reported to yield high regio and stereoselective copolymerization of CO₂ and racemic

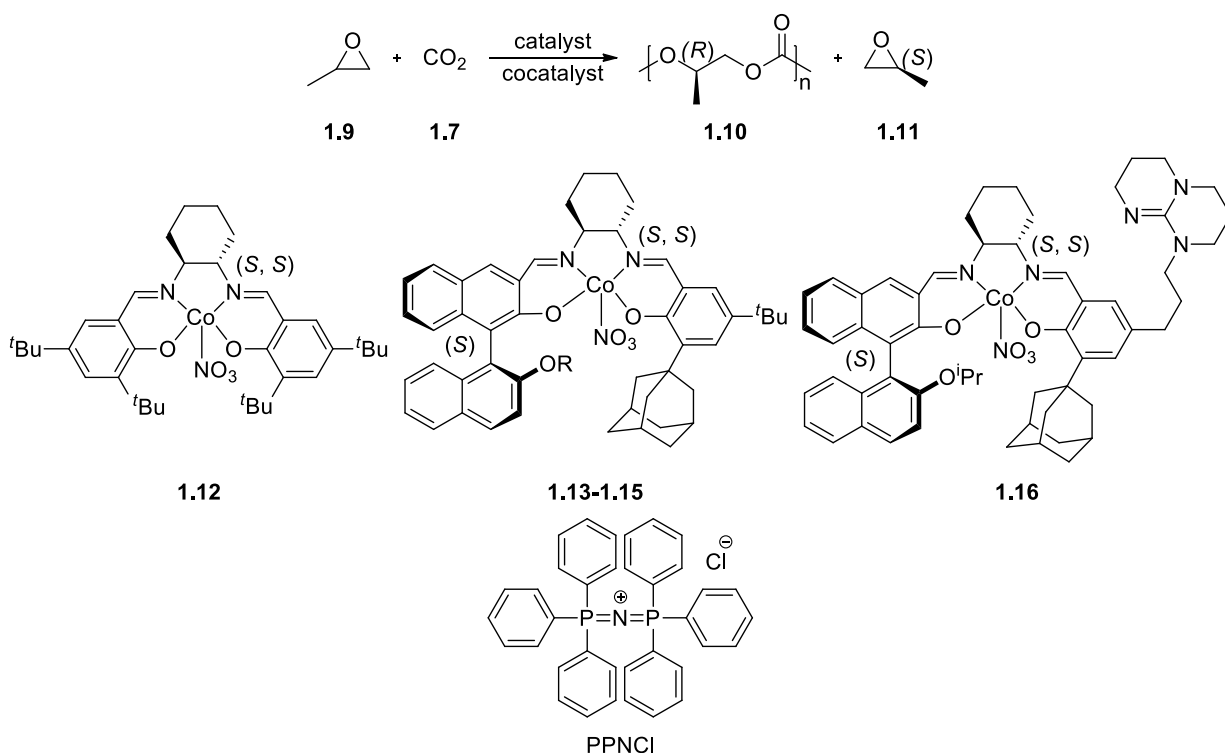
Figure 1.2. Different Kinds of Carbonate Linkages and Stereo-regularities of H-T Linkage



propylene oxide.²⁶⁻²⁹ Amongst them, the complexes mentioned in the Table 1.1 shows better results in obtaining higher regio and stereoselective polycarbonates by kinetic resolution of racemic propylene oxide. Other epoxides, such as cyclohexene oxide have been copolymerized with CO₂ stereoselectively using zinc-based³⁰⁻³² and cobalt-based complexes.³³⁻³⁵

Copolymerization of other cyclic ethers with CO₂ have been less explored. The current method of polymerization is not possible beyond five membered cyclic ethers.^{8, 36, 37}

Table 1.1. Copolymerization of *rac*-Propylene Oxide and CO₂ via Kinetic Resolution



entry	catalyst	R	cocatalyst	T (°C)	M _n (kDa)	Đ	k _{rel}	ref
1	1.12	-	PPNCI	25	28.0	1.16	4.6	28
2	1.13	Me	PPNCI	25	29.9	1.13	9.8	28
3	1.14	ⁿ Bu	PPNCI	25	29.0	1.12	10.6	28
4	1.15	ⁱ Pr	PPNCI	25	28.7	1.13	12.4	28
5	1.15	ⁱ Pr	PPNCI	-25	6.5	1.18	23.7	28
6	1.16	-	-	-20	20.4	1.15	24.3	29

This becomes a major drawback of the method and thus there is need for new methods having broader scope. One such method is the ring opening polymerization of cyclic carbonates and it is discussed in the next section.

1.3 Ring Opening Polymerization

Ring opening polymerization of cyclic carbonates is an efficient method of synthesizing aliphatic polycarbonates. A wide range of catalyst system have been developed for the ring opening polymerization of a variety of monomers. For the synthesis of cyclic carbonates, diols are the most commonly used precursor. Some of the diols can be extracted easily from the natural resources in racemic or in enantiopure form. A variety of functionalized diols can be synthesized in few steps using well known reactions such as aldol, Claisen and hydroxylation reactions. Therefore, ring opening polymerization of cyclic carbonates provides wide scope for the functionalization of aliphatic polycarbonates. To obtain polycarbonates *via* ROP of cyclic carbonates, the ring opening reaction must be thermodynamically and kinetically favored. Among the different ring sizes, five, six and seven membered cyclic carbonates are the most commonly used monomers.

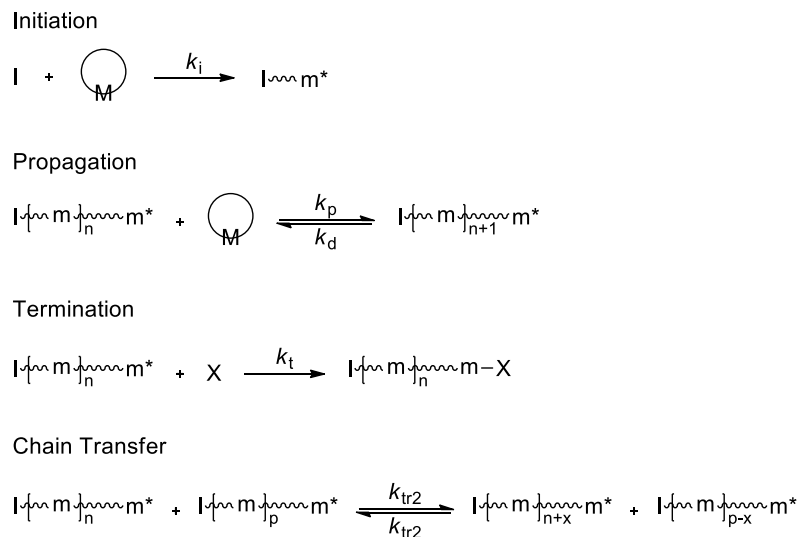
1.3.1 Thermodynamics and Kinetics of Ring Opening Polymerization

The Gibbs free energy of polymerization (represented as $\Delta G_p = \Delta H_p - T\Delta S_p$) determines whether the ROP is thermodynamically favored or not. Similar to all chemical reactions, the ROP will be thermodynamically favored only when the $\Delta G_p < 0$. The ΔG_p in turn depends on the ΔH_p (enthalpy of polymerization), ΔS_p (entropy of polymerization) and T (absolute temperature). Considering the Gibbs free energy equation, monomers having $\Delta H_p < 0$ and $\Delta S_p > 0$ can be polymerized at any given temperature, provided the kinetics are

favorable. In the case of monomers having $\Delta H_p > 0$ and $\Delta S_p < 0$, the polymerization is thermodynamically forbidden at any given temperature. For the case where $\Delta H_p < 0$ and $\Delta S_p < 0$, the polymerization is thermodynamically favored only when ΔH_p is greater in magnitude than $T\Delta S_p$ (which will result in $\Delta G_p < 0$). In such cases, as the temperature increases the concentration of monomer at equilibrium ($[M]_{eq}$) increases.³⁸ At certain temperature called ceiling temperature (T_c), $[M]_{eq}$ and $[M]_o$ (initial concentration of monomer) becomes equal and as a result formation of polymer does not take place at or above T_c . For example, ROP of THF fails above its ceiling temperature ($T_c = 84\text{ }^\circ\text{C}$).^{38, 39} On the other hand, for monomers possessing $\Delta H_p > 0$ and $\Delta S_p > 0$, the polymerization is thermodynamically favored only when $T\Delta S_p$ is greater in magnitude than ΔH_p (which will result in $\Delta G_p < 0$). In this case as the temperature increases, $[M]_{eq}$ decreases. Therefore, the temperature at which $[M]_{eq} = [M]_o$ is termed as floor temperature (T_f) and the polymerization is thermodynamically disfavored at or below the floor temperature. For example, ROP of cyclo-octasulfur cannot be carried out below its floor temperature ($T_f = 159\text{ }^\circ\text{C}$).^{40, 41} Most of the cyclic monomers studied in the ROP possess ring strain and the release of ring strain drives the ROP, as it leads to $\Delta H_p < 0$ which prevails over $T\Delta S_p$ contribution to ΔG_p .

Living polymerization is one of the special features of ROP and it is determined by the kinetics of reactions involved in the ROP (Scheme 1.5).³⁸ Firstly, in the initiation step the initiator (I) opens up the cyclic monomer to generate linear active propagating species (k_i is the rate constant of initiation). The propagating species reacts repeatedly with the monomer molecules to form linear polymer in the propagation step (k_p is the rate constant of propagation and k_d is the rate constant of depropagation). The linear polymer can undergo termination by intramolecular cyclization or by reacting with terminating agent to give a

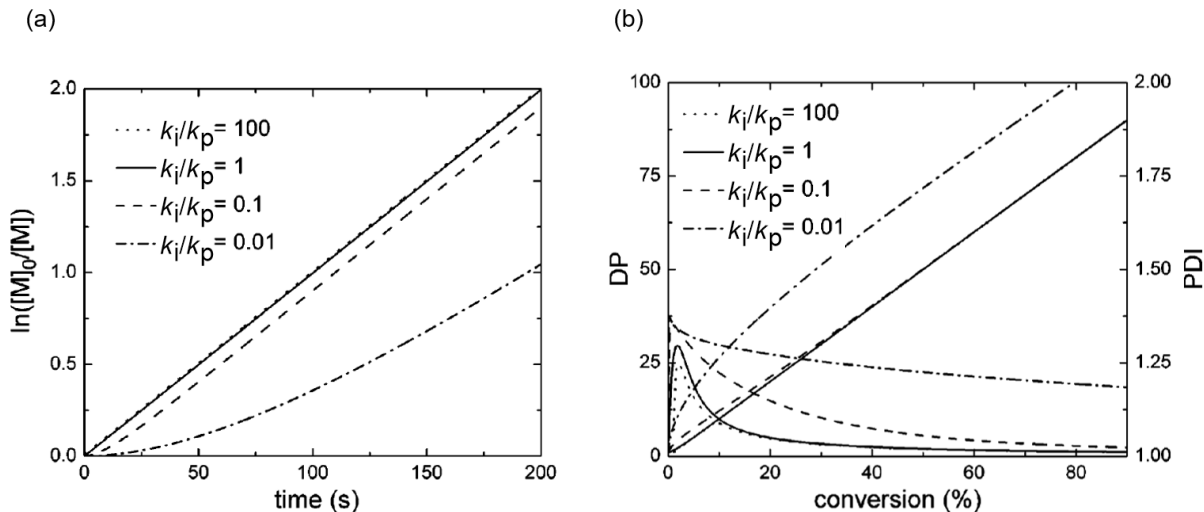
Scheme 1.5. Kinetics of Reactions Involved in the Ring Opening Polymerization



dead polymer (k_t is the rate constant of termination). Another possible side reaction is chain transfer, wherein polymer molecules react with each other and can lead to rupturing of polymer chains (k_{tr2} is the rate constant of bimolecular chain transfer).

The conditions for the ROP to become living polymerization are as follows (i) the rate of initiation should be greater than or equal to the rate of propagation ($k_i \geq k_p$); (ii) the ROP should be devoid of chain termination ($k_t = 0$); (iii) the rate of chain transfer reaction leading to chain scission (observed commonly in ROP) should be negligible ($k_{tr2} \geq 0$). The above mentioned conditions to exhibit living polymerization behavior, lead to two important experimental outcomes. The plots of $\ln[M]_0/[M]$ versus time (Figure 1.3a) and degree of polymerization (M_n) versus conversion of monomer (Figure 1.3b) should be linear with the intercept at the origin.^{40, 42} Deviations from the linearity of the plots observed in Figure 1.3a and 1.3b can be either due to the slower initiation or existence of side reactions such as chain transfer and chain termination reactions. These side reactions in the ROP also lead to higher dispersity.

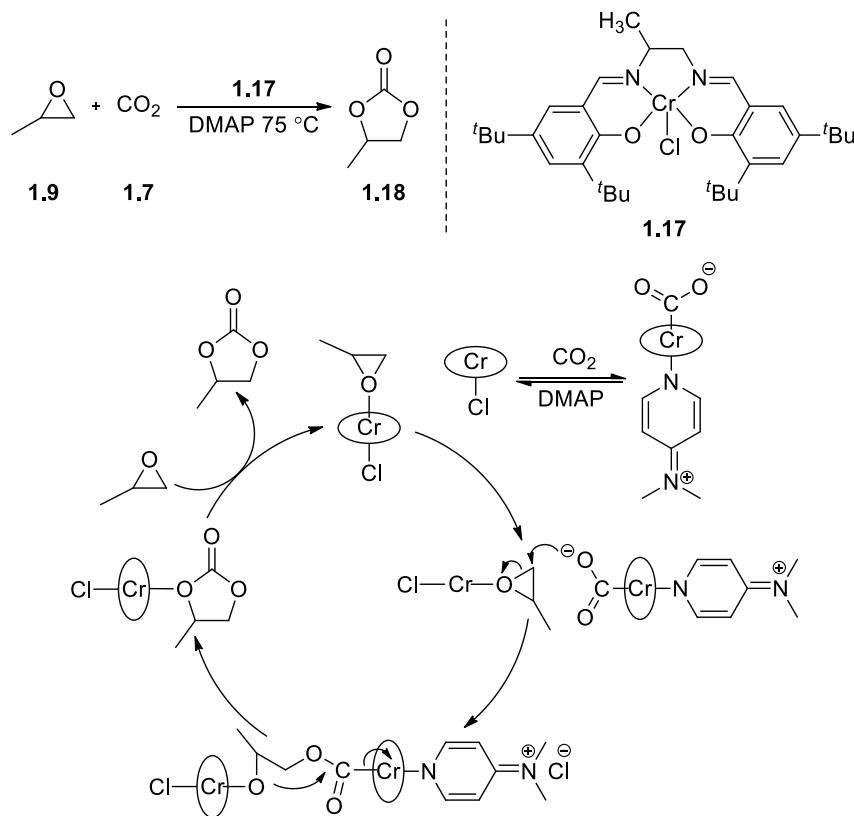
Figure 1.3. (a) Plots of $\ln([M]_0/[M])$ versus time with various k_i/k_p ratios ($[M]_0/[I]_0 = 100$); (b) Plots of degree of polymerization and molar mass distribution versus time with various k_i/k_p ratios ($[M]_0/[I]_0 = 100$). Reprinted (adapted) with permission from Kamber, N. E.; Jeong, W.; Waymouth, R. M. *Chem. Rev.* **2007**, *107*, 5813-5840. Copyright 2007 American Chemical Society.



1.3.2 Ring Opening Polymerization of Five-Membered Cyclic Carbonates

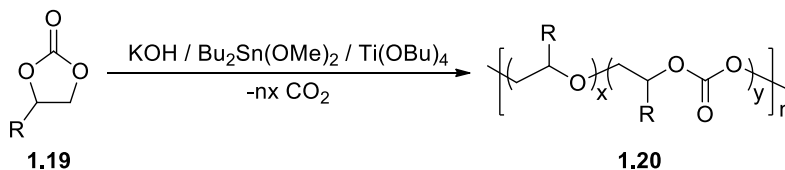
Five-membered cyclic carbonates can be synthesized either by treating 1,2-diol with dialkyl carbonate (phosgene equivalent)^{43, 44} or by the reaction between CO₂ and epoxide.⁴⁵⁻⁴⁹ As the coupling of CO₂ and epoxide to produce five-membered cyclic carbonate is completely atom economical (no byproducts formed) and avoids the usage of hazardous materials it is a more efficient synthetic route than the condensation reaction. A wide range of organometallic⁵⁰⁻⁵⁷ and organocatalysts⁵⁸⁻⁶¹ have been developed for the coupling of CO₂ and epoxides. Transition metal complexes have been found to be efficient at catalyzing this reaction with low catalyst loadings.⁵³⁻⁵⁷ Amongst organocatalysts, DBU and imidazole based salts were efficient at catalyzing this reaction at ambient temperature and pressure.^{60, 61} A chromium-salen complex catalyzed reaction of CO₂ and propylene oxide is represented as an example in Scheme 1.6.

Scheme 1.6. Coupling of CO₂ and Propylene Oxide by Chromium Complex and its Proposed Mechanism



Ring opening polymerization of five-membered cyclic carbonates is thermodynamically disfavored, as the standard enthalpy of polymerization ΔH_p^0 is positive and standard entropy of polymerization ΔS_p^0 is negative. At high temperatures (>150 °C) five-membered cyclic carbonates undergoes polymerization to give poly(alkylene ether-carbonates) with a mixture of ether and carbonate repeating units (Scheme 1.7).^{9, 62-68} This is possible with the decarboxylation during the course of polymerization. For ethylene carbonate, at 170 °C the standard enthalpy of polymerization with decarboxylation ΔH_{pd}^0 becomes negative and also the decarboxylation leads to positive ΔS_p^0 value.

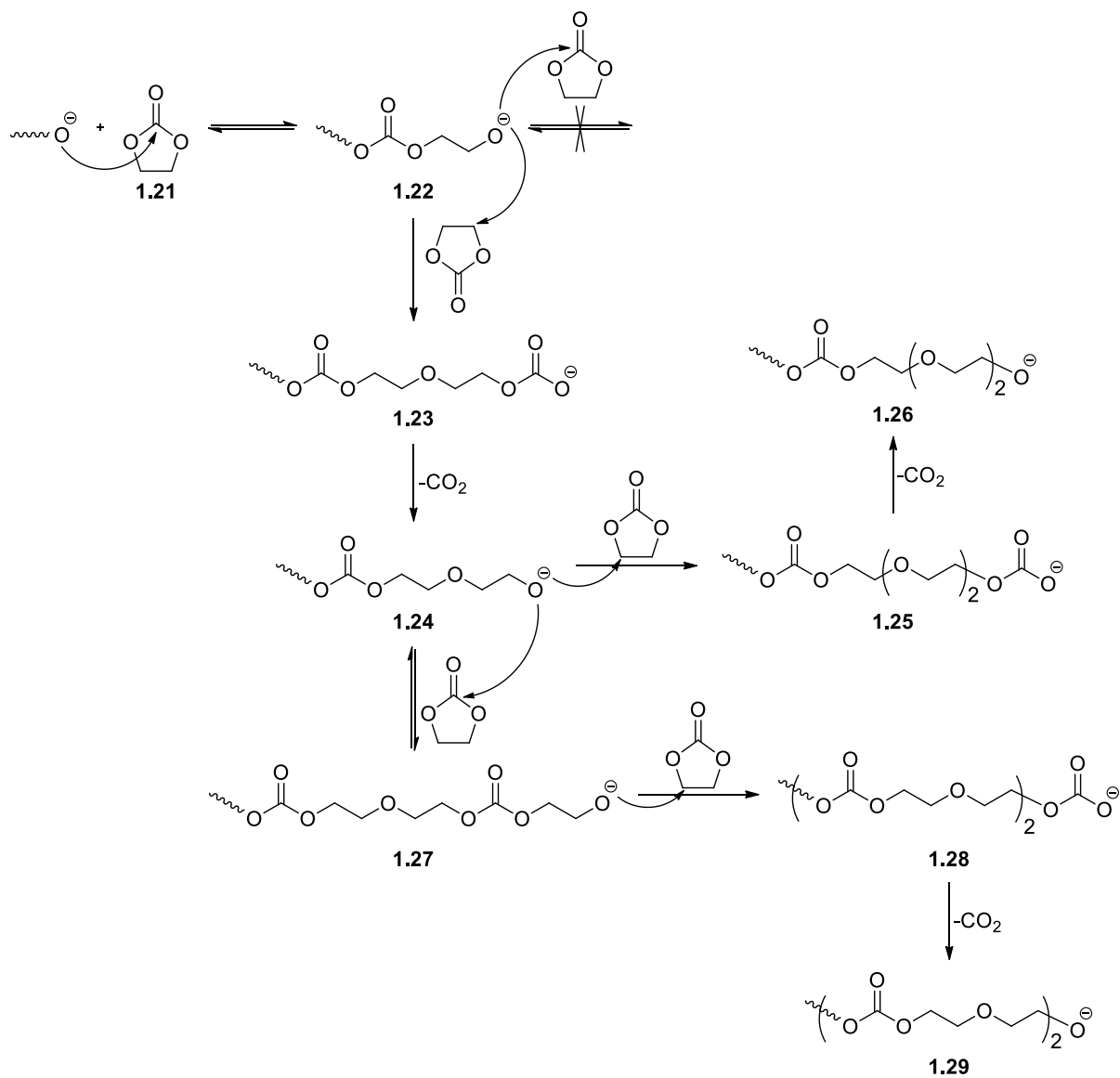
Scheme 1.7. Ring Opening Polymerization of Five-Membered Cyclic Carbonates



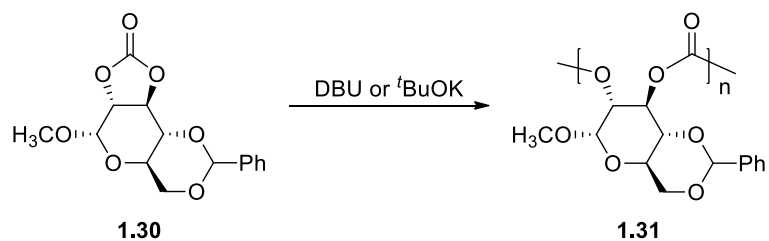
Let us consider ethylene carbonate (EC) as the monomer to explain the probable mechanism for the formation of poly(alkylene ether-carbonates) (Scheme 1.8).⁶⁹ The polymer possesses mainly two kinds of repeating unit sequences namely ethylene carbonate-ethylene oxide (EC-EO) and ethylene carbonate-(ethylene oxide)₂ (EC-EO-EO). Initially, the alkoxide (part of the initiator or catalyst) attacks the carbonyl carbon of the EC (**1.21**) to form an alkoxide and a carbonate linkage (**1.22**). This reaction is reversible and thermodynamically forbidden. A fraction of **1.22** irreversibly attacks the alkylene carbon of EC to form **1.23** which upon decarboxylation releases CO₂ and forms alkoxide **1.24** having both carbonate and ether linkage. The alkoxide **1.24** can again attack the alkylene carbon of EC to form **1.25** which upon decarboxylation generates **1.26** which is an EC-EO-EO repeating unit sequence. On the other hand, if the alkoxide **1.24** attacks the carbonyl carbon of EC it forms alkoxide **1.27** (reversible reaction) which subsequently attacks alkylene carbon of EC to generate **1.28**. Decarboxylation of **1.28** leads to the formation of **1.29** which is an EC-EO repeating unit sequence. In this manner two kinds of repeating unit sequences becomes part of poly(alkylene ether-carbonates).

The ring opening polymerization of five-membered cyclic carbonate without the elimination of CO₂ can be achieved by employing a strained monomer (Scheme 1.9).⁷⁰ The five-membered cyclic carbonate **1.32** derived from methyl 4,6-*O*-benzylidene-glucopyranoside undergoes ring opening polymerization without the elimination of CO₂ to

Scheme 1.8. Probable Mechanism of Ring Opening Polymerization of Ethylene Carbonate



Scheme 1.9. Ring Opening Polymerization of Strained Five-Membered Cyclic Carbonate

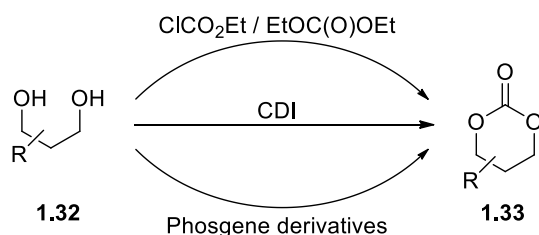


obtain pure polycarbonate.⁷¹ The monomer exhibits ring strain due to the trans-configuration at the five-six ring junction. The release of ring strain upon ring opening drives the polymerization in the forward direction.

1.3.3 Ring Opening Polymerization of Six-Membered Cyclic Carbonates

Six-membered cyclic carbonates are of prime interest for the preparation of aliphatic polycarbonates. Unlike five-membered cyclic carbonate, the presence of carbonyl group induces ring strain in the six-membered cyclic carbonate.^{9, 38} Therefore, six-membered cyclic carbonates undergo ring opening polymerization to yield polycarbonates without the elimination of CO₂. An efficient method of synthesizing six-membered cyclic carbonates is the transesterification between 1,3-diols and phosgene equivalents such as ethyl chloroformate,^{72, 73} diethyl carbonate,^{43, 44, 74} 1,1'-carbonyldiimidazole (CDI),^{75, 76} and other phosgene derivatives⁷⁷ (Scheme 1.10). A wide range of six-membered cyclic carbonates can be found in the literature which are mainly derived from substituted or functionalized 1,3-diols,⁷⁸⁻⁸² sugars,⁸³⁻⁸⁵ and 2,2-bishydroxy(methyl)propionic acid (bis-MPA).⁸⁶⁻⁸⁸ The ROP of six-membered cyclic carbonates will be explained in sections 1.3.4 and 1.3.5.

Scheme 1.10. Synthesis of Six-Membered Cyclic Carbonates Using Various Methods



There are four different classes of ROPs: (i) cationic, (ii) anionic, (iii) radical and (iv) ring opening metathesis. As the thesis is about the ROP of cyclic carbonates, only cationic and anionic ROP of selected cyclic monomers (lactides, lactones and cyclic carbonates) will be explained in this chapter. The success of ROP of these cyclic monomers is mainly attributed to the availability of wide range of catalysts. The requirements for a good catalyst are (i) it needs to be very selective in catalyzing the polymerization of monomer rather than catalyzing unwanted reactions such as chain rupturing of polymer chains, (ii) it should have ability to induce chemoselectivity, regioselectivity, and stereoselectivity in the ROP. Based on the nature of catalyst used in the polymerization, ROP can be broadly classified into (i) metal catalyzed ROP and (ii) organocatalyzed ROP.

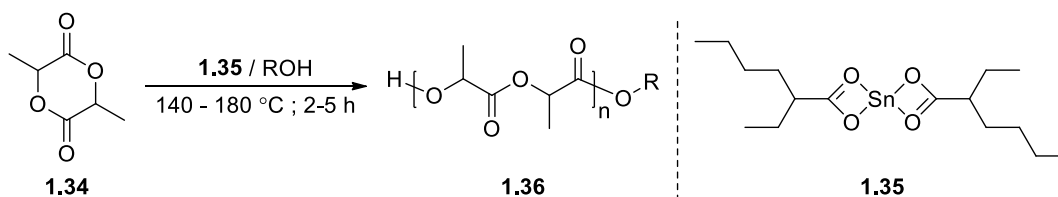
1.3.4 Metal Catalyzed Ring Opening Polymerization

Most of the early work in this area focused on developing catalysts for the ROP of lactide (cyclic diester of lactic acid), as polylactide has well developed applications. Although there were reports on the ROP of cyclic carbonates and other cyclic monomers, most of the reports employed the catalysts that were used for the ROP of lactide.^{9, 89, 90} Hence, to understand the design and development of catalysts used for ROP, it is useful to study the catalysts used for the ROP of lactide. One of the well-known and widely used metal-based catalyst for the ROP of lactide and other cyclic monomers is tin(II)bis(2-ethylhexanoate), also termed as tin(II)octanoate ($\text{Sn}(\text{Oct})_2$).⁹¹⁻⁹³ $\text{Sn}(\text{Oct})_2$ is a commercially available catalyst, carries out ROP of lactide (Scheme 1.11) under bulk condition around 140-180 °C to yield high molar mass polylactide (ranging from 10^5 - 10^6 g mol⁻¹).⁹³

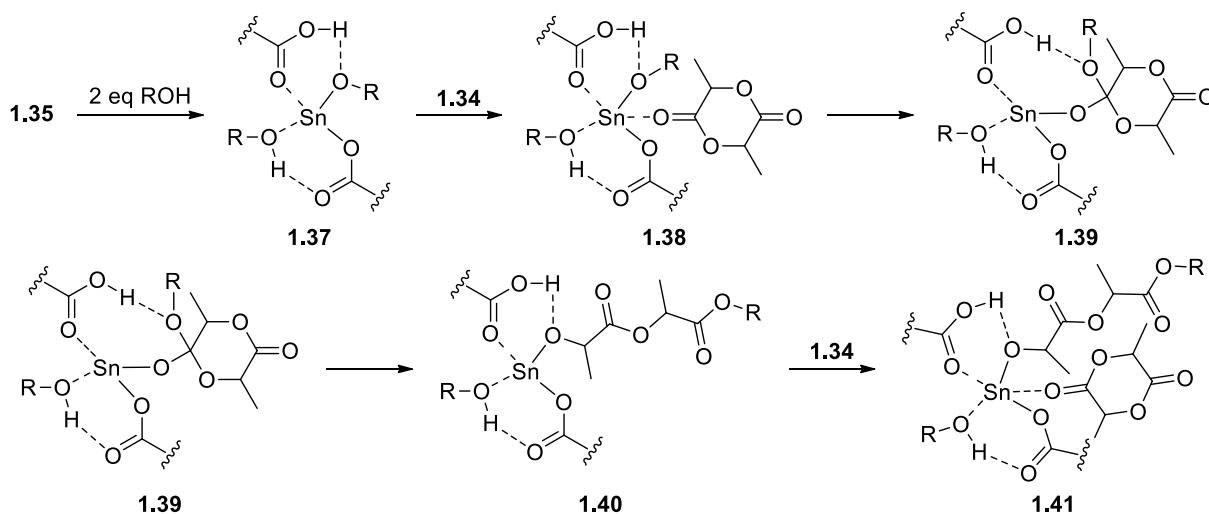
Mechanistic studies on the $\text{Sn}(\text{Oct})_2$ catalyzed ROP showed that the reaction follows coordination-insertion mechanism.⁹³⁻⁹⁵ In this mechanism (Scheme 1.12), two equivalents of

alcohol (initiator) react with $\text{Sn}(\text{Oct})_2$ to generate tin (II) alkoxide (**1.37**). The attack of alcohol can lead to either retention of octanoate or release of octanoic acid.⁹⁶ The monomer coordinates with the metal center of **1.37** to form **1.38**. The alkoxide part of **1.38** inserts into the monomer to generate tetrahedral intermediate **1.39**. The intermediate **1.39** upon ring opening, generates a linear molecule **1.40**. The linear molecule is capped with ester group at one end of the chain, while the other end is bound to the metal center and becomes the active chain end. This chain end attacks the newly bound monomer in **1.41** to carry forward the propagation process.

Scheme 1.11. ROP of Lactide Using Tin(II)Octanoate



Scheme 1.12. Coordination-Insertion Mechanism of ROP of Lactide Catalyzed by $\text{Sn}(\text{Oct})_2$

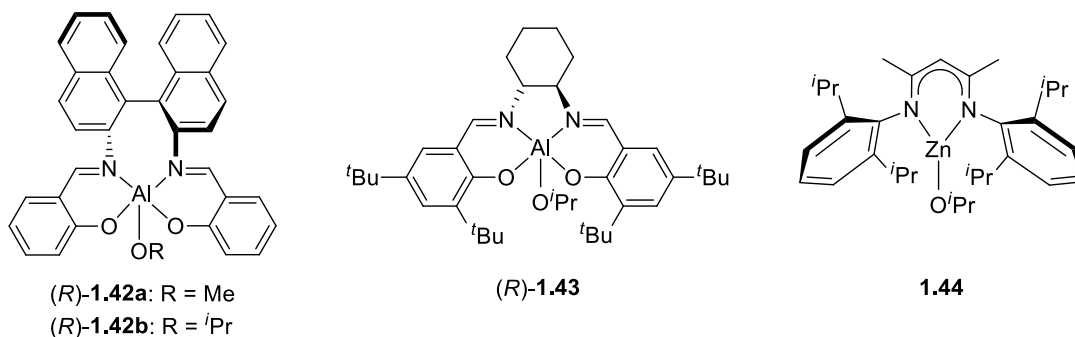


$\text{Sn}(\text{Oct})_2$, in spite of being a highly active catalyst for the ROP poses some major drawbacks. Polymers with remnant tin impurities cannot be used in biomedical fields. Chain transfer reactions lead to high dispersity in the resulting in polylactide.^{91, 92} Also, the impurities in the monomer react with the catalyst and retard the initiation process. As a result, other metal-based catalysts started to gain more importance for achieving efficient ROP. Since the tin alkoxide was identified as the catalytic species in the above mechanism, various metal based alkoxides were synthesized and employed in the ROP.^{91, 97-105}

Like $\text{Sn}(\text{Oct})_2$, the ROP catalyzed by metal alkoxides follow coordination-insertion mechanism. Although some of the metal alkoxides show good efficiency, the major disadvantages of metal alkoxides includes its aggregation behavior and the presence of multiple alkoxide groups. Aggregation of catalyst leads to slowing down of the reaction and formation of an indeterminate number of bridging alkoxide that cannot initiate ROP. The presence of multiple alkoxide initiators on the same metal leads to growth of multiple polymer chains attached to the same metal center. All of this put together results in poorly controlled polymerizations. Therefore, polymer chemists have pursued single-site catalysts to minimize the disadvantages.

Extensive research had been carried out for the design and synthesis of single-site metal catalysts. The general structural formula of single-site metal catalyst is L_nMR . The design of single-site metal catalysts is mainly aimed at minimizing the aggregation of catalyst and side reactions. Using various combination of ligands and metals, an array of single-site metal catalysts were synthesized and used for the ROP (Figure 1.4).^{9, 89, 90, 106-108}

Figure 1.4. Structures of Al and Zn Based Single-Site Catalysts Used for Stereo-regular ROP of Lactides



1.3.5 Organocatalyzed Ring Opening Polymerization

Small organic molecules without metals have proved to be versatile catalyst for conventional and asymmetric organic synthesis. A wide range of organocatalysts with different functionalities and catalytic activities have been reported in the literature and have proved to be highly efficient for ROP of cyclic monomers.^{42, 89, 114, 115} Based on the mechanism, organocatalyzed ROP of cyclic monomers can be broadly classified into (i) cationic ROP and (ii) anionic ROP.

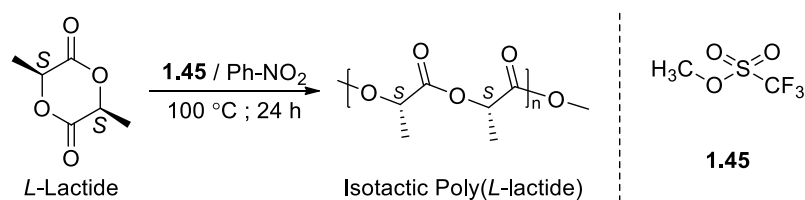
1.3.5.1 Cationic Ring Opening Polymerization

Cationic ROP can be accomplished either by the activation of monomer or by the activation of chain-end. The most common mode of activation for the cationic ROP of lactides, lactones and cyclic carbonates is the activation of monomer. The catalysts that were commonly used for the activation of cyclic monomers includes, alkylating agents, protic acids, and Lewis acids.^{9, 42, 89} Although the mode of activation of monomers remains common for these catalysts, the way in which the ring opens or cleaves is the differing aspect between alkylating agents and rest of the catalysts.

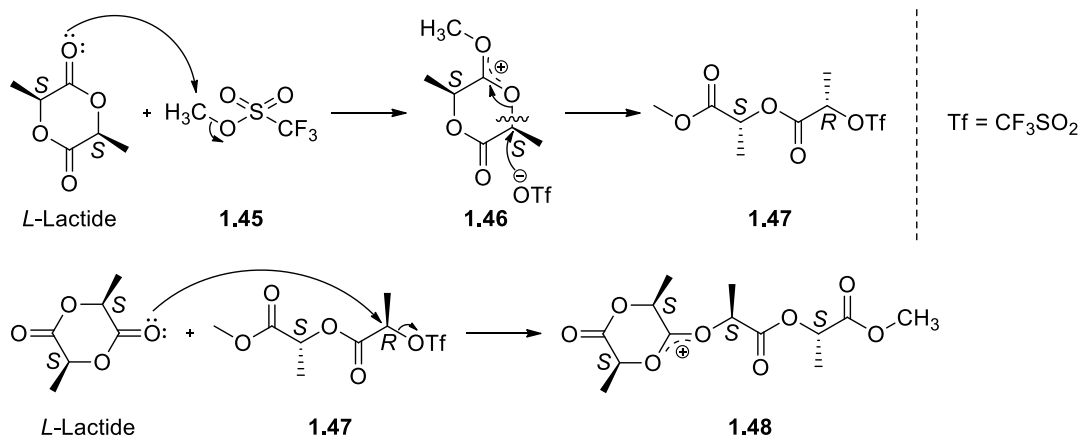
Methyl triflate is one of the most commonly used alkylating agent for the ROP of lactides, lactones and cyclic carbonates (ROP of *L*-lactide is depicted in Scheme 1.13).^{42, 116-120} The polymers obtained from the ROP of cyclic monomers using methyl triflate as an initiator contains methyl ester as one of the end-groups (by ¹H NMR). This suggests that the methyl group from methyl triflate has been incorporated into the polymer chain. It also suggests that the monomer should have ring opened by the cleavage of alkyl-oxygen bond rather than the usual acyl-oxygen bond. The proposed mechanism for the ROP of *L*-lactide is shown in Scheme 1.14.¹¹⁷ Here, the initiator methyl triflate activates the monomer by methylating the carbonyl oxygen atom to generate **1.46** (Scheme 1.14). The triflate anion carries out an S_N2 attack on the carbon attached to the alkyl-oxygen leading to the formation of **1.47** with an inversion of stereochemistry. This is followed by an attack of the carbonyl oxygen of another monomer on the carbon attached to the triflate in **1.47** to generate **1.48**. Inversion of stereochemistry in this step results in net retention.¹¹⁷

The cationic ROP of cyclic monomers using methyl triflate fails to exhibit living polymerization behavior and the molar mass of the synthesized polymer did not change with the variation of monomer to initiator ratios. Hence, to achieve the controlled cationic ROP of cyclic monomers other catalyst systems such as protic acids and Lewis acids have been used.

Scheme 1.13. ROP of *L*-Lactide Using Methyl Triflate as an Initiator



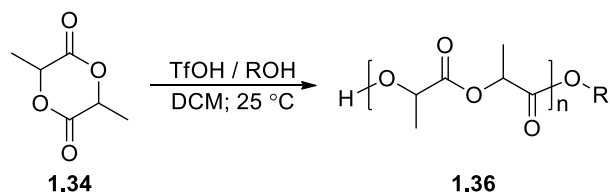
Scheme 1.14. Proposed Mechanism of ROP of *L*-Lactide Using Methyl Triflate



Among the available protic acids, triflic acid (TfOH) along with an initiator (alcohol) carries out the ROP of lactides, lactones and cyclic carbonates in a controlled manner (ROP of lactide is represented in Scheme 1.15).^{118, 120-122} TfOH/alcohol catalyzes the ROP of lactide in 3 to 28 h depending on the monomer to initiator ratios. This polymerization yields polylactide with M_n up to 18000 g/mol with narrow dispersity in the range of 1.1-1.4 and exhibits living polymerization behavior.¹²¹ Analysis by ^1H NMR shows the presence of an alkyl ester end-group formed from the initiating alcohol. Based on this observation, a mechanism for this cationic ROP was postulated as shown in Scheme 1.16.¹²¹ First, the triflic acid activates the monomer **1.34** by protonating the carbonyl oxygen and then the initiator (alcohol) attacks the electrophilic carbonyl carbon of **1.49**. The monomer ring opens by the cleavage of acyl-oxygen bond (path A) rather than alkyl-oxygen bond (path B) to produce **1.50** with alkyl ester group as one of the chain-end.

Other protic acids such as trifluoroacetic acid and $\text{HCl}\cdot\text{Et}_2\text{O}$ were used for the controlled cationic ROP of lactones (**1.52-1.54**) and cyclic carbonates (**1.55, 1.56**)¹²³⁻¹²⁷ as shown in Figure 1.5. Lewis acids ($\text{BF}_3\cdot\text{Et}_2\text{O}$, BBr_3 and BCl_3) have also been shown to carry

Scheme 1.15. ROP of Lactide Using Triflic Acid/Alcohol



Scheme 1.16. Proposed Mechanism for ROP of Lactide Using Triflic Acid/Alcohol

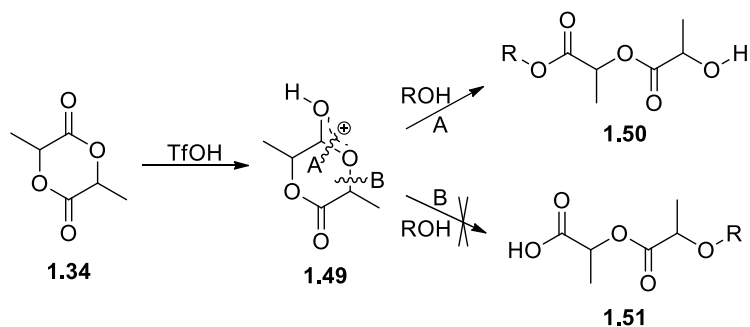
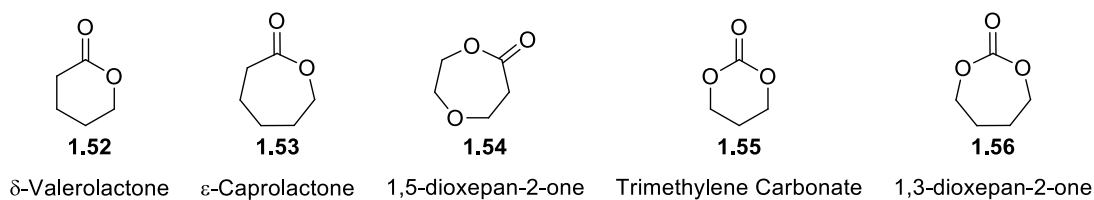


Figure 1.5. Structures of Different Lactones and Cyclic Carbonates



out controlled cationic ROP of above mentioned lactones and cyclic carbonates.^{9, 128, 129} The cationic ROP using these catalysts exhibit living polymerization behavior and also yields polymers with narrow dispersity ($\mathcal{D} = 1.1-1.3$).¹²³⁻¹²⁵ The mechanism of cationic ROP using the above mentioned catalysts is similar to that of ROP using TfOH/alcohol.

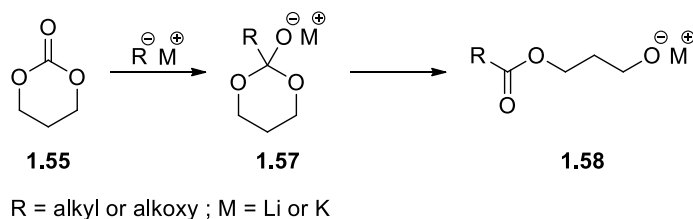
1.3.5.2 Anionic Ring Opening Polymerization

In the anionic ROP, the initiator should be negatively charged or at least it should be nucleophilic enough to attack the monomer to produce active propagating species. Initially,

organolithiums such as *n*-BuLi or *sec*-BuLi and potassium or lithium alkoxides were used as initiators for the anionic ROP of cyclic monomers¹³⁰⁻¹³⁴ These anionic initiators attack the carbonyl carbon of lactides, lactones, and cyclic carbonates and generate anionic propagating species (**1.58**, Scheme 1.17). The major disadvantages of using anionic initiators for ROP includes racemization, back-biting, and chain transfer reactions, which eventually lead to an uncontrolled ROP and broader dispersity.

Other than anionic initiators, there are a number of neutral organic compounds that can be used as catalysts for anionic ROP of lactides, lactones, and cyclic carbonates. Based on the mechanism of ROP, neutral organocatalysts can be broadly classified into two types; (i) Nucleophilic organocatalysts: here, the catalyst acts as a nucleophile and attacks the monomer to produce a reactive electrophilic species, which upon reacting with initiator generates pseudo anionic propagating species; (ii) Hydrogen-bonding organocatalysts: here, the ROP is effected either by increasing the nucleophilicity of initiator or by simultaneously increasing the nucleophilicity of initiator and also the electrophilicity of monomer. This facilitates the attack of initiator on the monomer to generate a pseudo anionic propagating species. In both of these catalyst systems, side reactions like transesterification and back-biting are suppressed (*vide infra*).

Scheme 1.17. Anionic ROP of Trimethylene Carbonate Using Anionic Initiators



1.3.5.2.1 Nucleophilic Organocatalysts for Anionic ROP

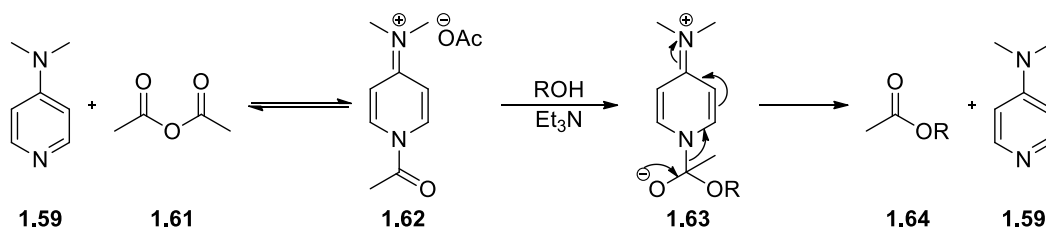
In organic synthesis, pyridine-based compounds have been recognized as efficient nucleophilic catalysts for acylation, condensation, and transesterification reactions. Among them, 4-(dimethylamino)pyridine (DMAP) and 4-pyrrolidinopyridine (PPY) (Figure 1.6) have been shown to accelerate the rate of acylation of alcohols and amines and are the most commonly used catalysts.¹³⁵⁻¹³⁷

Mechanistic studies revealed that the DMAP or PPY catalyzed acylation of alcohols proceed by the nucleophilic attack of DMAP (**1.59**) or PPY (**1.60**) on the carbonyl carbon of an electrophile to generate an acyl pyridinium intermediate **1.62** (Scheme 1.18).¹³⁶ The alcohol attacks the carbonyl carbon of **1.62** to form tetrahedral intermediate **1.63** and then it leads to the formation of ester **1.64** along with the release of catalyst.

Figure 1.6. Structure of DMAP and PPY



Scheme 1.18. Proposed Mechanism of DMAP Catalyzed Acylation of Alcohol



As the above mechanism fulfills the criteria for an anionic ROP, DMAP and PPY were used for the ROP of lactide and trimethylene carbonate. DMAP and PPY catalyzes the ROP of lactide (**1.34**) and yields polylactide with narrow dispersity (Table 1.2, entries 1-4).¹³⁸ The ROP of lactide carried out at 35 °C in solution (Table 1.2, entries 1 & 2) was found to be slower than the ROP carried out under bulk condition (Table 1.2, entries 3 & 4). The observed narrow dispersity indicates negligible transesterification of polylactide. Also, DMAP catalyzes the ROP of trimethylene carbonate (**1.55**) under bulk conditions to produce polycarbonate with slightly higher dispersity (Table 1.2, entry 5).¹³⁹ The ROP catalyzed by DMAP and PPY exhibits living polymerization behavior.

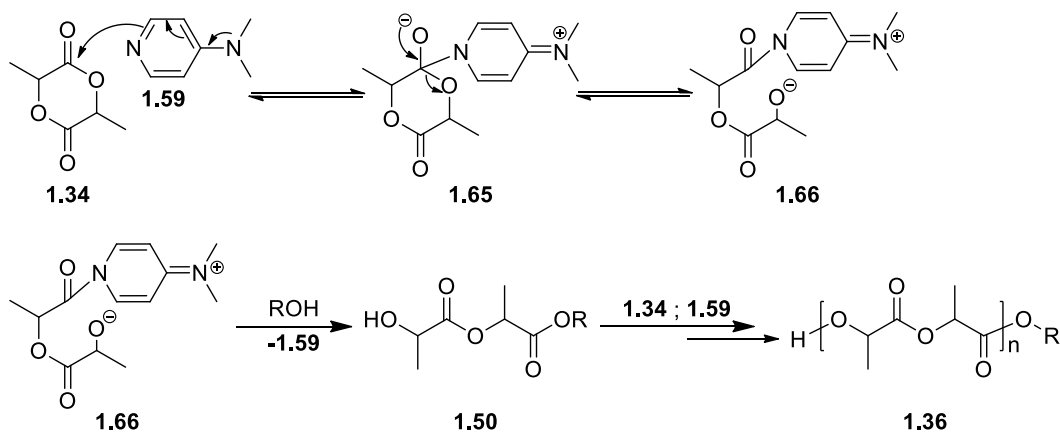
In the above ROP, initial attack of DMAP on the carbonyl carbon produces a zwitterion **1.66** (Scheme 1.19).¹³⁸ The alkoxide part of zwitterion **1.66** abstracts a proton from the initiator (alcohol) to form an alkoxide. Attack of the alkoxide on the activated acyl pyridinium center of **1.66** leads to formation of propagating species **1.50** with secondary alcohol as the end group (identified by ¹H NMR). The propagating species **1.50** transforms into polymer **1.36** by repeated attacks on the acyl pyridinium center of **1.66**.

Table 1.2. ROP of Lactide Using DMAP and PPY as Catalysts

entry ^{a,b}	catalyst	initiator	temp (°C)	time	[M] ₀ /[I] ₀	DP ^{c,d}	Đ ^e
1 ^a	1.59	EtOH	35	36 h	30	29	1.13
2 ^a	1.60	EtOH	35	20 h	30	31	1.08
3 ^b	1.59	BnOH	135	20 min	100	77	1.19
4 ^b	1.60	BnOH	135	10 min	30	32	1.16
5 ^b	1.59	BnOH	110	5 min	100	110 ^d	1.43

Entries 1-4 correspond to ROP of lactide (**1.34**) and entry 5 corresponds to ROP of trimethylene carbonate **1.55**; ^aDCM was used as solvent; ^bbulk polymerization; ^cDegree of polymerization by ¹H-NMR; ^dDegree of polymerization by SEC; ^eM_w/M_n

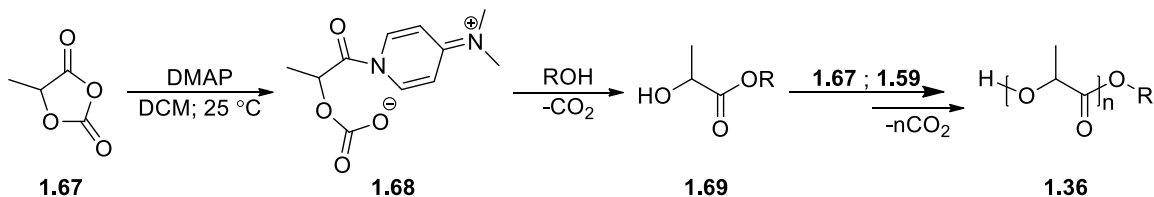
Scheme 1.19. Mechanism of ROP of Lactide Using DMAP as Catalyst



Preparation of polylactide or polylactic acid using DMAP can be accomplished in a very mild and faster rate by employing lactide equivalent, namely lactide-*O*-carboxyanhydride (lac-OCA).¹⁴⁰ *O*-carboxyanhydrides, which are similar to *N*-carboxyanhydrides of α -amino acids^{141, 142} were found to be more reactive than the cyclic diesters of α -hydroxy acids and have been used in polymerization. ROP of lac-OCA carried out using DMAP yielded polylactic acid (Scheme 1.20) at room temperature in 5-90 mins with varying of $[M]_0/[I]_0$ (10 to 100).¹⁴⁰ The nucleophilic catalyst DMAP attacks the carbonyl carbon of lac-OCA **1.67** and generates zwitterion **1.68**. The initiator (alcohol) attacks the activated carbonyl carbon of **1.68** and with simultaneous decarboxylation, it leads to the formation of propagating species **1.69**. The propagating species **1.69** later transforms into polylactic acid **1.36**. Release of CO₂ is the driving force for lac-OCA's faster reaction rate.¹⁴⁰ The ROP of lac-OCA proceeds under living condition with narrow dispersity and also racemization was not observed for enantiopure monomer.

Other than lactide, lac-OCA, and trimethylene carbonate, DMAP was also used as nucleophilic catalysts for the ROP of alkyl substituted lactides and ϵ -caprolactone.¹⁴³⁻¹⁴⁵ At

Scheme 1.20. ROP of lac-OCA Using DMAP as Catalyst



the same time, DMAP was found to be inactive for the ROP of β -butyrolactone (yielding oligomers with degree of polymerization <8).¹⁴⁶

Apart from DMAP, phosphines were also used as nucleophilic catalyst for the ROP of lactide. Phosphines catalyze the ROP of lactide under bulk conditions at high temperatures (135-180 °C) to yield polylactide with narrow dispersity ($\mathcal{D} = 1.1-1.4$) and also exhibits living polymerization behavior.^{147, 148} Among the different kinds of phosphines used, $P^n(\text{Bu})_3$ and $P^t(\text{Bu})_3$ were found to be most active catalyst and the activity decreases with the introduction of aryl substituents on the phosphorus. The ROP of lactide using phosphines proceeds through the nucleophilic attack mechanism similar to that of DMAP catalyzed ROP. Phosphines catalyzed ROP of lactide were found to be slower than DMAP catalyzed ROP. To enhance the rate of ROP stronger nucleophiles like *N*-heterocyclic carbenes (NHCs) can be employed.

N-heterocyclic carbenes (NHCs) are one of the strongest nucleophilic catalysts used in organic synthesis.¹⁴⁹⁻¹⁵¹ NHCs are also recognized as an efficient transesterification catalyst and have been used successfully in step-growth polymerization to obtain poly(ethylene terephthalate) (PET).¹⁴⁹ Due to their high nucleophilicity, NHCs have been extensively used in the ROP of cyclic monomers.^{115, 152-156} Some of the different kinds of NHCs employed for the ROP are shown in the Figure 1.7.

Among the different kinds of NHCs used for the ROP, imidazolium based NHCs were found to be more active than the thiazolium based NHCs (Table 1.3, entries 1-5). While considering the ROP of lactone (ϵ -caprolactone **1.53**) and trimethylene carbonate **1.55**, it was evident that the NHCs with less bulky substituents were found to be more active than the sterically crowded carbenes (Table 1.3, entries 7-11). NHC catalyzed ROPs have shown high end-group fidelity and exhibit living polymerization behavior.¹⁵²⁻¹⁵⁶

Figure 1.7. Structure of Various *N*-Heterocyclic Carbenes Used for ROP

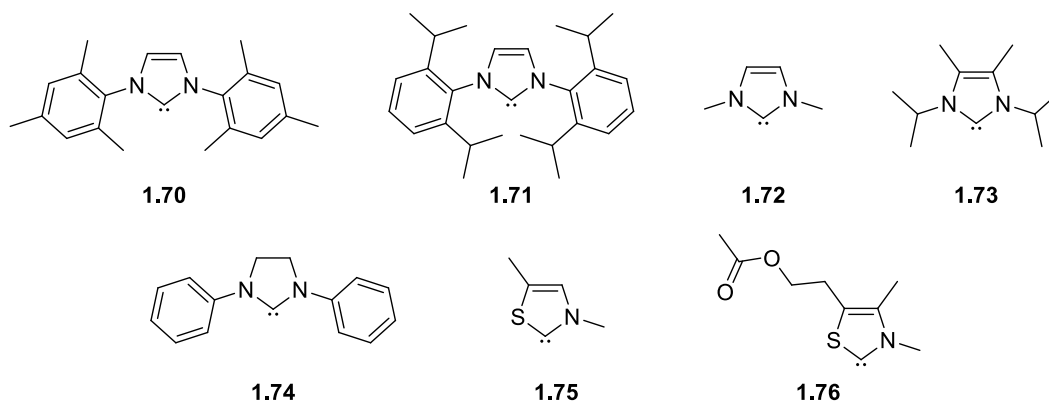


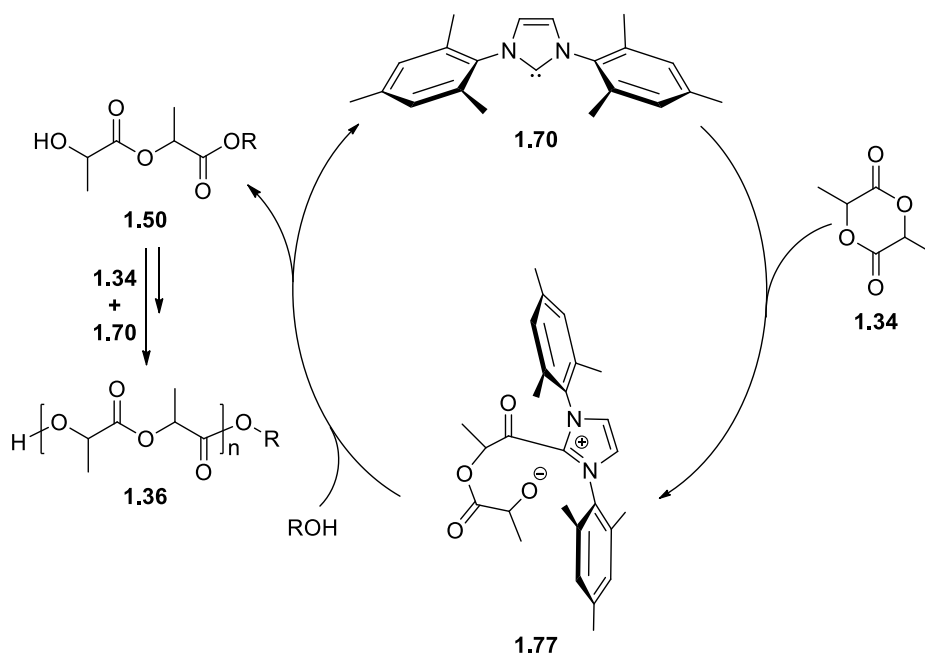
Table 1.3. ROP of Cyclic Monomers Using Various NHCs

entry ^a	monomer	catalyst ^b	[M] ₀ /[I] ₀	time	DP	\bar{D}
1	1.34	1.70	200	15 min	173	1.18
2	1.34	1.71	200	15 min	185	1.18
3	1.34	1.74	200	15 min	197	1.46
4	1.34	1.75	120	72 h	100	1.08
5	1.34	1.76	60	48 h	52	1.10
6	1.52	1.72	200	3 h	185	1.32
7	1.53	1.70	60	20 h	56	1.30
8	1.53	1.72	200	6 h	188	1.16
9	1.53	1.74	100	0.5 h	98	1.55
10	1.55	1.71	50	0.5 h	49	1.06
11	1.55	1.73	50	0.1 min	50	>2

^aTHF used as solvent for monomer **1.34** and THF or toluene used as solvent for other monomers; ^b0.5-0.75 mol% with respect to monomer

Regarding the mechanism of NHC catalyzed ROP, two pathways were proposed. The first one involves nucleophilic activation of the monomer similar to that of DMAP catalyzed ROP and the second one is the activation of the initiator by NHC to facilitate the attack on the monomer. The formation of zwitterionic species by trapping of NHC with carbon disulfide¹⁵⁴ and the formation of cyclic poly lactides in the absence of initiator¹⁵⁷ support the nucleophilic activation mechanism.¹⁵²⁻¹⁵⁶ Also, the faster rate observed for the ROP catalyzed by less bulky NHCs supports the nucleophilic activation mechanism (Scheme 1.21). Mechanistically, the reaction is initiated by the attack of NHC on the carbonyl carbon of monomer to generate zwitterion **1.77**. The initiator (alcohol) transfers the proton to the alkoxide part of zwitterion **1.77**. Then the generated alkoxide of initiator attacks the activated carbonyl carbon of **1.77** to form the propagating species **1.50**. The propagating species then transforms into polymer after repeated enchainment of monomer in this manner.

Scheme 1.21. Mechanism of ROP of Lactide Using NHC



1.3.5.2.2 Hydrogen-Bonding Organocatalysts for Anionic ROP

Hydrogen-bonding organocatalysts, catalyze the ROP of lactides, lactones and cyclic carbonates either by the activation of initiator (nucleophile) or by the simultaneous activation of monomer (electrophile) and initiator (nucleophile). Based on the nature of hydrogen bonding moiety and the mode of activation, most of them can be classified into following types: (i) guanidines and amidines; (ii) phosphazene bases, (iii) bifunctional catalysts and (iv) combination of (thio)ureas and amines.

The commercially available TBD, MTBD (guanidines) and DBU (amidine) are some of the most commonly used hydrogen-bonding catalysts for the ROP of cyclic monomers (Figure 1.8).^{42, 114, 158-162} These nitrogen bases are regarded as strong bases, with the corresponding $^{\text{MeCN}}\text{p}K_{\text{a}}$ s of 26.0; 25.5, 24.3, respectively. The high basicity of these catalysts can potentially increase the nucleophilicity of initiator (alcohol) by hydrogen-bonding to facilitate the attack on the monomer.

The more basic TBD (**1.78**) catalyzes ROP of lactide (**1.34**), δ -valerolactone (**1.52**), ϵ -caprolactone (**1.53**), and trimethylene carbonate (**1.55**) with lower catalyst loading to afford polymer with narrow dispersity and exhibits living polymerization behavior (Table 1.4, entries 1-5).^{139, 156, 159, 160} If the polymerization reaction is left unquenched after high monomer conversions, it can lead to broadening of the dispersity due to transesterification. Similarly, MTBD (**1.79**) and DBU (**1.80**) catalyze the ROP of lactide (**1.34**) and trimethylene carbonate (**1.55**) to produce polymers with narrow dispersity (Table 1.4, entries 6-9). MTBD and DBU were found to be inactive for the ROP of δ -valerolactone (**1.52**) and ϵ -caprolactone (**1.53**) (Table 1.4, entries 10-13) even under high catalyst loadings.^{156, 160} In the case of ROP of β -butyrolactone, both guanidines and amidine were found to be inactive.¹⁶⁰

Figure 1.8. Structure of Guanidines and Amidine

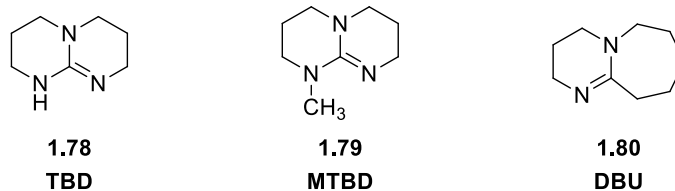


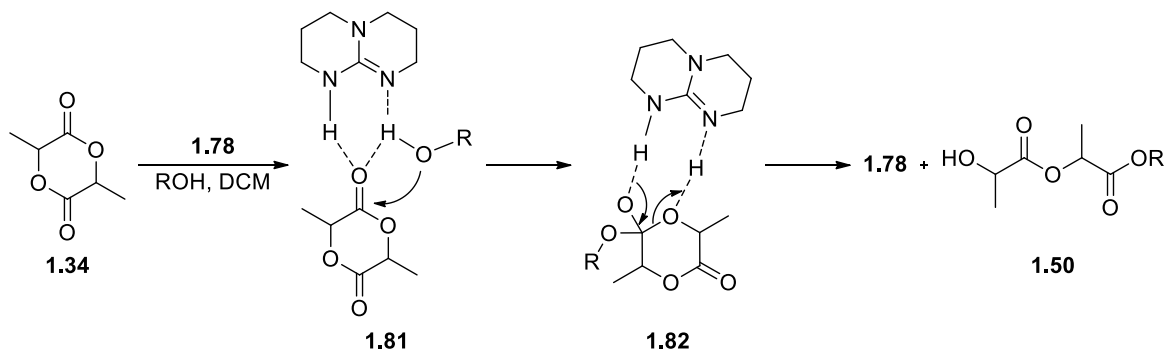
Table 1.4. Details of Guanidines and Amidine Catalyzed ROP of Cyclic Monomers

entry ^a	monomer	catalyst	mol % ^b	solvent	time	[M] ₀ /[I] ₀	DP	Đ
1	1.34	1.78	0.1	DCM	20 s	100	120	1.19
2	1.34	1.78	0.1	DCM	1 min	500	435	1.11
3	1.52	1.78	0.5	C ₆ D ₆	0.5 h	100	125	1.09
4	1.53	1.78	0.5	C ₆ D ₆	8 h	100	140	1.16
5	1.55	1.78	0.02	DCM	15 min	50	50	1.31
6	1.34	1.79	1.0	CDCl ₃	0.5 h	100	120	1.05
7	1.55	1.79	0.02	DCM	3 h	50	48	1.28
8	1.34	1.80	1.0	CDCl ₃	1 h	100	130	1.05
9	1.55	1.80	0.02	DCM	8 h	50	51	1.04
10	1.52	1.79	5.0	C ₆ D ₆	72 h	100	-	-
11	1.53	1.79	5.0	C ₆ D ₆	72 h	100	-	-
12	1.52	1.80	5.0	C ₆ D ₆	72 h	100	-	-
13	1.53	1.80	5.0	C ₆ D ₆	72 h	100	-	-

^aReactions were run at 25 °C; ^bRelative to monomer

A detailed investigation on the mechanism of TBD catalyzed ROP of lactide reveals that the TBD activates both initiator and monomer through hydrogen-bonding (bifunctional). TBD with its hydrogen-bond acceptor center increases the nucleophilicity of initiator (alcohol) while the hydrogen-bond donor center increases the electrophilicity of monomer (Scheme 1.22; **1.81**).¹⁶³ The pseudo alkoxide of initiator (part of **1.81**) attacks the carbonyl carbon of monomer to form the tetrahedral intermediate **1.82**. TBD stabilizes the **1.50** intermediate and assists the ring opening of monomer to produce propagating species through hydrogen-bonding.

Scheme 1.22. TBD Catalyzed Ring Opening of Lactide



On the other hand, MTBD and DBU, have only a hydrogen-bond acceptor center, and therefore activate the initiator, but not the monomer (Scheme 1.23).¹⁶⁰ The activation of initiator by MTBD or DBU is good enough for the ROP of lactide and trimethylene carbonate, but for the ROP of δ -valerolactone and ϵ -caprolactone the activation of monomer is also necessary. Therefore, TBD catalyzes ROP of cyclic monomers more effectively than MTBD and DBU.

Phosphazene bases are the another set of super bases used as hydrogen-bonding organocatalysts for the ROP of cyclic monomers (Figure 1.9).¹⁶⁴⁻¹⁶⁶ Phosphazenes are stronger bases than guanidines and amidines, with $^{\text{MeCN}}\text{p}K_{\text{a}} \text{P}_1\text{-}t\text{-BuH}^+ = 26.9$; $^{\text{MeCN}}\text{p}K_{\text{a}} \text{BEMPH}^+ = 27.6$; and $\text{P}_2\text{-}t\text{-BuH}^+ = 33.5$. These phosphazene bases possess only the hydrogen-bond acceptor center similar to MTBD and DBU.

The phosphazene base $\text{P}_1\text{-}t\text{-Bu}$ (**1.83**) catalyzes the ROP of lactide (**1.34**) and δ -valerolactone (**1.52**) to yield polymers with narrow dispersity (Table 1.5, entries 1 & 2).¹⁶⁵ BEMP (**1.84**), a slightly stronger base catalyzes the ROP of lactide significantly faster than $\text{P}_1\text{-}t\text{-Bu}$ (**1.83**) (Table 1.5, entry 3). Also, BEMP catalyzes the ROP of δ -valerolactone and

Scheme 1.23. Mode of Activation of Initiator by MTBD and DBU for ROP of Lactide

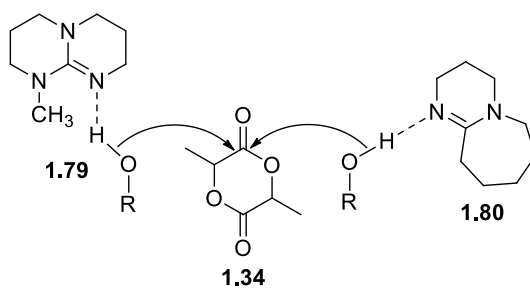


Figure 1.9. Structure of Phosphazene Bases

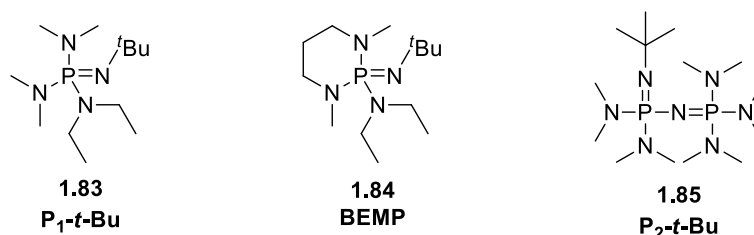


Table 1.5. Details of Phosphazenes Catalyzed ROP of Cyclic Monomers

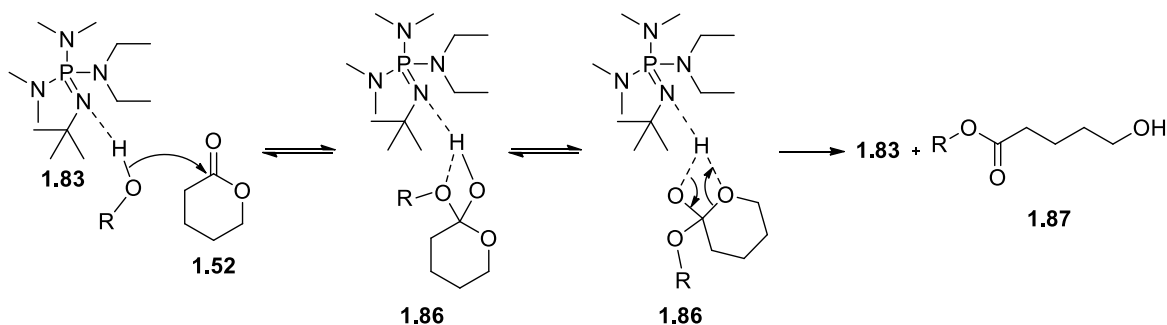
entry ^a	monomer	catalyst	time	conv ^b (%)	DP	Đ
1 ^c	1.34	1.83	70 h	82	71	1.06
2 ^d	1.52	1.83	70 h	56	68	1.11
3 ^c	1.34	1.84	23 h	76	68	1.08
4 ^d	1.52	1.84	73 h	69	68	1.12
5 ^e	1.55	1.84	30 min	80	70	1.27
6 ^f	1.53	1.84	240 h	14	15	1.08
7 ^c	1.34	1.85	25 min	84	76	1.08

^aReactions were run at 25 °C with $[M]_0/[I]_0/[C]_0 = 100/1/1$; ^bConversion of monomer was measured using ¹H NMR; ^cToluene was used as solvent; ^dbulk polymerization; ^ebulk polymerization at 60 °C with $[M]_0/[I]_0/[C]_0 = 100/1/0.2$; ^fbulk polymerization at 80 °C;

trimethylene carbonate (**1.55**) (Table 1.5, entries 4 & 5). However, BEMP was found to be inactive for the ROP of ϵ -caprolactone (**1.53**) with only 14% conversion in 10 days at 80 °C (Table 1.5, entry 6).¹⁶⁵ The highly basic P_2 -*t*-Bu (**1.85**) catalyzes the ROP of lactide (Table 1.5, entry 7) at a much faster rate compared to P_1 -*t*-Bu and BEMP.¹⁶⁶ The phosphazene catalyzed ROPs exhibit living polymerization behavior. However, higher conversions of monomers lead to broadening of molar mass distribution due to transesterification. The above ROPs proceed through a hydrogen-bonding mechanism similar to that of MTBD and DBU (Scheme 1.24).¹⁶⁵

Bifunctional hydrogen-bonding organocatalysts being the next kind of catalysts possess both a hydrogen-bond donor and a hydrogen-bond acceptor. As mentioned earlier, the hydrogen-bond donor center is responsible for activating the monomer and the hydrogen-bond acceptor center is responsible for activating the initiator. Therefore, both the reacting species can be activated using these organocatalysts. Some of the bifunctional organocatalysts (other than TBD) used for the ROP of cyclic monomers are shown in Figure 1.10.

Scheme 1.24. Mechanism of Ring Opening of δ -valerolactone Using P_1 -*t*-Bu



Takemoto's catalyst **1.88** was the first thiourea based organocatalyst used for the ROP of lactide (**1.34**) and yielded polylactide with narrow dispersity (Table 1.6, entry 1). Minimal transesterification of polylactide was observed even after extended reaction times (upto 4 days).¹⁶⁷⁻¹⁶⁹ In the case ROP of trimethylene carbonate (**1.55**) of $[M]_0/[I]_0 = 50$, the catalyst **1.88** took 6 days for the complete conversion of monomer (Table 1.6, entry 2).¹⁵⁶ Catalysts **1.89** and **1.90** were also used for the ROP of lactide (**1.34**), δ -valerolactone, (**1.52**)

Figure 1.10. Structure of Some of Bifunctional Hydrogen-Bonding Organocatalysts Used for ROP of Cyclic Monomers

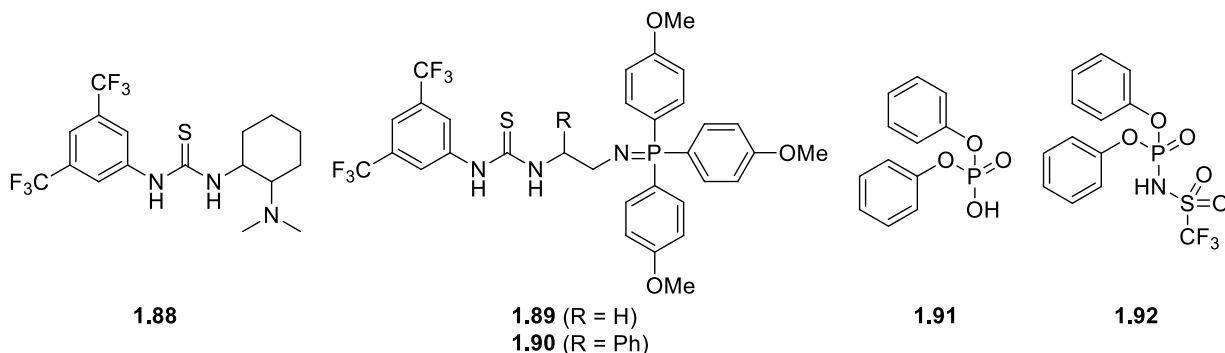


Table 1.6. Details of ROP of Cyclic Monomers Using Bifunctional Hydrogen-Bonding Organocatalysts

entry ^a	monomer	catalyst	cat ^b mol %	$[M]_0/[I]_0$	solvent	time ^c	DP	\bar{M}_w/\bar{M}_n
1	1.34	1.88	5	100	DCM	48 h	103	1.05
2	1.55	1.88	10	50	DCM	6 d	45	1.09
3	1.34	1.89	1	100	DCM	10 min	98	1.04
4	1.52	1.90	5	100	PhCl	9 h	100	1.13
5	1.53	1.90	5	100	PhMe	100 h	45 ^d	1.23
6 ^e	1.34	1.91	1	50	-	22 h	47 ^d	1.23
7	1.52	1.91	2	100	PhMe	2.5 h	100	1.07
8 ^f	1.53	1.91	2	80	PhMe	9 h	60 ^d	1.07
9	1.55	1.91	2	50	PhMe	36 h	51	1.09
10 ^f	1.53	1.92	2	80	PhMe	5.5 h	70 ^d	1.07
11	1.55	1.92	1	100	PhMe	30 h	97	1.13

^aReactions were run at 25 °C; ^bRelative to monomer; ^cHigher conversion time points

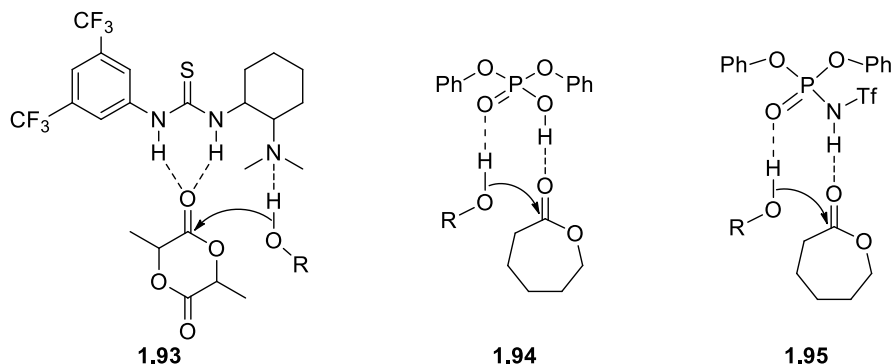
^dDegree of polymerization determined from GPC; ^eBulk polymerization at 130 °C;

^fReaction temperature = 30 °C

and ϵ -caprolactone (**1.53**) (Table 1.6, entries 3-5) and the polymerization proceeded at a faster rate compared to **1.88**.¹⁷⁰ Other than thiourea based catalysts, organic acids such as phosphoric acid **1.91** and phosphoramidic acid **1.92** were also used as bifunctional hydrogen-bonding organocatalysts for the ROP of cyclic monomers. Phosphoric acid **1.91** catalyzes the ROP of lactide, δ -valerolactone, ϵ -caprolactone and trimethylene carbonate (Table 1.6, entries 6-9) to yield polymers with narrow dispersity.¹⁷¹⁻¹⁷⁴ The more acidic catalyst **1.92** catalyzes the ROP of ϵ -caprolactone and trimethylene carbonate (Table 1.6, entries 10 & 11) at faster rate than **1.91**.^{173, 175} Overall the ROP of cyclic monomers catalyzed by the bifunctional catalysts exhibits living polymerization behavior with good end-group fidelity.

Binding studies of bifunctional organocatalysts (**1.88-1.92**) with the monomer and initiator revealed that the thiourea moiety of **1.88-1.90** activates the monomer by hydrogen-bonding to the carbonyl oxygen atom (**1.93**, Figure 1.11). The basic nitrogen was responsible for the activation of initiator (alcohol) by hydrogen-bonding.¹⁶⁷⁻¹⁷⁰ In the case of acidic catalysts **1.91** and **1.92**, the acidic proton (O-H in the case of **1.91**; N-H in the case of **1.92**) activates the monomer by hydrogen-bonding to the carbonyl oxygen atom (**1.94** and **1.95**, Figure 1.11). The initiator was activated by the oxygen atom of P(O) through hydrogen-bonding.^{173, 175} Also, the binding ability of these bifunctional organocatalysts with the linear ester molecule was found to be very weak. Coupled with the lower electrophilicity of the polymer, this slows down the transesterification of obtained polymers ensuring narrow dispersity.

Figure 1.11. Mode of Activation of Monomer and Initiator Using Bifunctional Organocatalysts



The hydrogen-bond donor and acceptor centers need not be present within the same molecular entity. Combinations of (thio)ureas (hydrogen-bond donors) and amines (hydrogen-bond acceptors) can make up the required catalytic system for the simultaneous activation of monomer and initiator for an effective ROP of cyclic monomers. Some of the (thio)ureas and amines used for making combined hydrogen-bonding catalytic systems are shown in Figure 1.12.^{42, 114, 163, 168, 176-178}

Combination of thiourea **1.96** and tertiary amine **1.99** (NCyMe₂) catalyzes the ROP of lactide (**1.34**) in 72 h to yield polylactide (Table 1.7, entry 1).¹⁶⁸ When the thiourea is replaced with urea **1.98** and NCyMe₂ with DBU, the reaction is completed within 20 seconds (Table 1.7, entry 2).¹⁷⁶ MTBD and DBU which are known to be inactive for the ROP of δ -valerolactone (**1.52**), become active in catalyzing the ROP of δ -valerolactone when combined with (thio)ureas (Table 1.7, entries 3-6). Combination of DBU and urea **1.98** shows faster reaction rate for the ROP of δ -valerolactone (within 600 seconds) compared to the mixture of DBU and other (thio)ureas (Table 1.7, entry 6).^{160, 176} The rate of ROP of δ -valerolactone can be further increased by replacing DBU with BEMP in the presence of **1.98** (within 45 seconds) (Table 1.7, entry 7). MTBD and DBU also catalyzes the ROP of ϵ -caprolactone

(**1.53**) only in combination with (thio)urea (Table 1.7, entries 8 & 9).¹⁶⁰ ROP catalyzed by combination of (thio)ureas and amines exhibits living polymerization behavior and also yields polymers with narrow dispersity. These reactions follow either cooperative hydrogen-bonding or anion hydrogen-bonding mechanism. If the pK_a of (thio)urea is greater than or equal to the pK_a of BH^+ (for examples Table 1.7, entries 1-5) the ROP of cyclic monomers follows a cooperative hydrogen-bonding mechanism, where the (thio)urea (hydrogen-bond

Figure 1.12. Structure of (Thio)Ureas and Amines

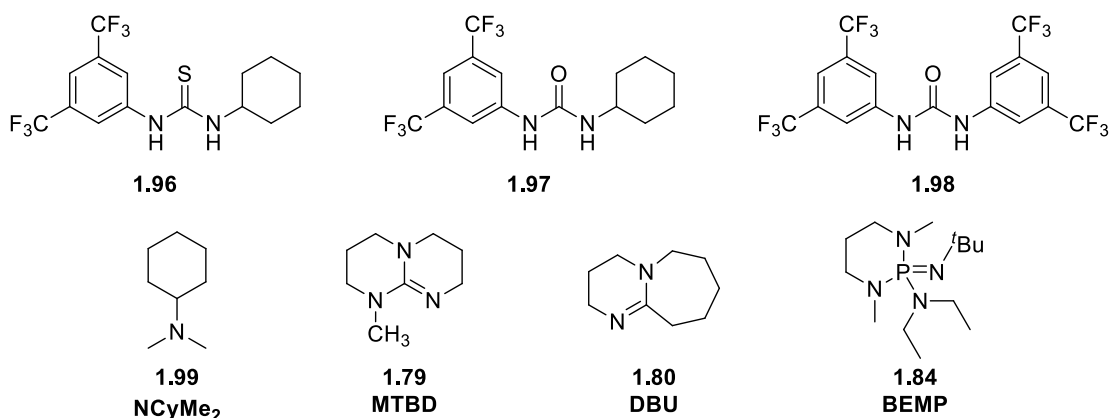


Table 1.7. Details of ROP of Cyclic Monomers Catalyzed by the Combinations of (Thio)Ureas and Bases

entry ^a	monomer	(thio)urea	base	solvent	time	conv (%)	DP ^b	Đ
1 ^c	1.34	1.96	NCyMe ₂	CDCl ₃	72 h	97	126	1.08
2	1.34	1.98	DBU	THF	20 s	89	130	1.02
3 ^d	1.52	1.96	MTBD	C ₆ D ₆	4 h	92	120	1.06
4	1.52	1.96	DBU	THF	7 h	93	102	1.03
5	1.52	1.97	DBU	THF	7 h	94	115	1.02
6	1.52	1.98	DBU	THF	600 s	91	110	1.02
7	1.52	1.98	BEMP	PhMe	45 s	93	105	1.02
8 ^d	1.53	1.96	MTBD	C ₆ D ₆	120 h	78	66	1.05
9 ^d	1.53	1.96	DBU	C ₆ D ₆	120 h	78	71	1.04

^aReactions were run at 25 °C with $[M]_0/[I]_0/[(\text{thio})\text{urea}]_0/[\text{base}]_0 = 100/1/2.5/2.5$;

^bDegree of polymerization determined from SEC; ^c10 mol% of thiourea and base used with respect to monomer; ^d5 mol% of thiourea and base used with respect to monomer.

donor center) activates the monomer and the amine (hydrogen-bond acceptor center) activates the initiator (**1.100**, Figure 1.13).¹⁷⁶ If the pK_a of (thio)urea is far less than the pK_a of BH^+ (for example Table 1.7, entry 7), the amine deprotonates the acidic proton of (thio)urea resulting in the formation of a (thio)urea anion. The (thio)urea anion activates the monomer and initiator simultaneously with its hydrogen-bond donor and acceptor centers (**1.101**, Figure 1.13).¹⁷⁶

Based on this idea, many (thio)urea anions were made and employed for the ROP of cyclic monomers to simultaneously activate monomer and initiator. Anions of (thio)urea can be readily generated in-situ by treating the (thio)urea with bases such as KOMe and KH. Some of the (thio)urea anions used for the ROP of cyclic monomers are represented in the Figure 1.14.

(Thio)urea anions catalyze the ROP of cyclic monomers at a faster rate than the previously mentioned bifunctional organocatalysts.^{179, 180} The ROP catalyzed by (thio)urea anions yields polymers with narrow dispersity and also exhibits living polymerization behavior. Urea anion (**1.103**) catalyzes the ROP of lactide (**1.34**) faster than the thiourea anion (**1.102**) (Table 1.8, entries 1 & 2). There is no clear trend observed for the activity

Figure 1.13. Cooperative and Anion Hydrogen-Bonding Mechanisms

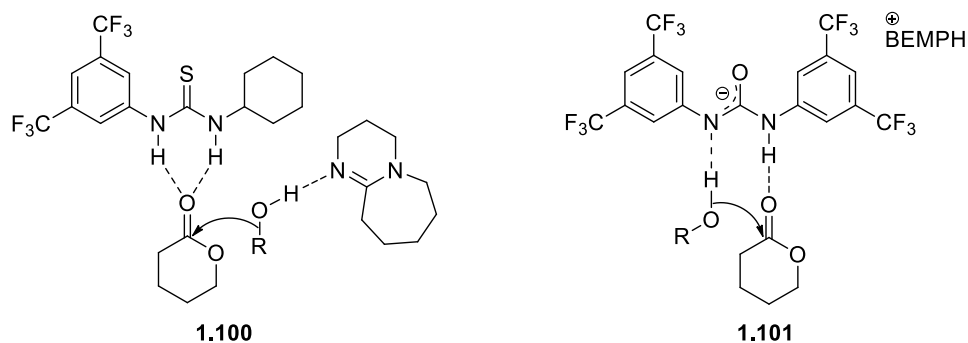
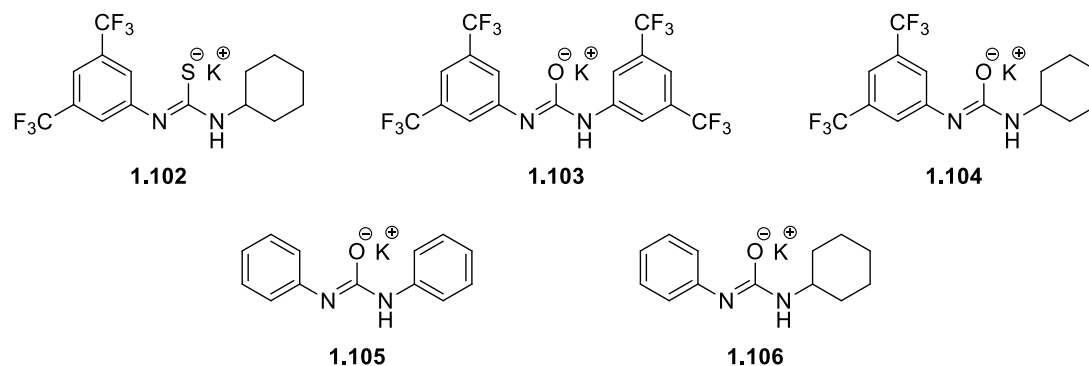


Figure 1.14. Structures of (Thio)Urea Anions Used for the ROP of Cyclic Monomers**Table 1.8.** Details of (Thio)Urea Anions Catalyzed ROP of Cyclic Monomers

entry ^a	monomer	catalyst	time	conv ^b (%)	k_{obs} (min ⁻¹)	DP ^c	\bar{D}
1	1.34	1.102	90 s	89	1.05±0.05	170	1.07
2	1.34	1.103	6 s	94	26.8±1.5	140	1.07
3	1.52	1.103	630 s	58	0.082±1×10 ⁻⁴	-	-
4	1.52	1.105	9 s	90	23.7±0.1	150	1.06
5	1.52	1.106	1 s	85	>110	150	1.09
6	1.53	1.103	720 s	5	0.00385±7×10 ⁻⁵	-	-
7	1.53	1.104	1840 s	90	0.0.74	160	1.09
8	1.53	1.106	12 s	89	1.08±0.1	150	1.14

^aReactions were run at 25 °C in THF with $[M]_0/[I]_0/[C]_0 = 100$; ^bConversion of monomer measured using ¹H NMR; ^cDegree of polymerization determined from GPC

between thiourea and urea anions of similar structures. If the pK_a s of thiourea and urea matches, then the urea anion exhibits better activity due to stronger binding with the carbonyl group of the monomer. Among the urea anions, **1.106** was observed to be the most active catalyst for the ROP of δ -valerolactone (**1.52**) and ϵ -caprolactone (**1.53**) (Table 1.8, entries 3-8).¹⁸⁰ From the Table 1.8, it can be concluded that the activity of urea anion increases with its basicity (basicity of the urea anion increases with the decrease in the number of CF₃ substituents) (Table 1.8, entries 3 & 4 and entries 7 & 8).¹⁸⁰

Apart from the above mentioned bifunctional catalysts, there were many other varieties of neutral bifunctional catalysts used for the ROP of cyclic monomers. Some of them include combinations of either hexafluoro alcohols or phenols or sulfonamide with tertiary amines.¹⁸¹⁻¹⁸³ Also, various kinds of ionic bifunctional catalysts such as mixture of DMAP and its conjugate acid (protonated DMAP), combination of DBU and benzoic acid, protonated TBD with varying anions and imidazolium trifluoroacetate were used for the ROP.¹⁸⁴⁻¹⁸⁸

1.4 Conclusions

Aromatic polycarbonates, mainly BisPhenol-A based polycarbonate are synthesized in industrial scale worldwide for number of applications. The health hazards involved in the usage of BisPhenol-A based polycarbonates has made the scientific community to seriously think of non-hazardous alternatives. Aliphatic polycarbonates are gaining attention as alternatives for aromatic polycarbonates. They can be effectively synthesized either by the copolymerization of CO₂ and epoxides or by the ring opening polymerization of cyclic carbonates. Ring opening polymerization is considered to be the better method to access polycarbonates in a simple way. Also this method has an advantage of functionalizing polycarbonates by using functionalized diols obtained from well-established synthetic approaches. A variety of metal based catalysts and organocatalysts are available for the ROP of cyclic carbonates. The synthesized aliphatic polycarbonates are yet to meet the physical properties required to replace aromatic polycarbonates from the market. In chapter two we will discuss the role of substituents and the need of regio-regularity in affecting the physical property of aliphatic polycarbonates. In chapter three, we will discuss the morphological studies of di-block aliphatic polycarbonates with different regio-regularities.

1.5 References

- 1 Birnbaum, K.; Lurie, G. *Ber. Dtsch. Chem. Ges.* **1881**, *14*, 1753-1755.
- 2 Einhorn, A. *Liebigs Ann. Chem.* **1898**, *300*, 135-155.
- 3 Bischoff, C. A.; von Hendenström, A. *Chem. Ber.* **1902**, *35*, 3431-3437.
- 4 Schnell, H. *Angew. Chem.* **1956**, *68*, 633-640.
- 5 Schnell, H. *Ind. Eng. Chem.* **1959**, *51*, 157-160.
- 6 Schnell, H. U.S. Patent 3,294,741, **1966**.
- 7 Fox, D. W. U.S. Patent 3,153,008, **1964**.
- 8 Takeuchi, K. *Chemistry and Technology of Polycondensates / Polycarbonates*; Polymer Reference: A Comprehensive Reference, Volume 5, 2012.
- 9 Rokicki, G.; Parzuchowski, P. G. *Chemistry and Technology of Polycondensates / ROP of Cyclic Carbonates and ROP of Macrocycles*; Polymer Reference: A Comprehensive Reference, Volume 4, 2012.
- 10 Wehrmann, R. *Encyclopedia of Materials: Science and Technology / Polycarbonate*, 2001.
- 11 Fry, J. S. U.S. Patent 3,035,020, **1962**.
- 12 Khan, D.; Ahmed, S. A. *Front. Endocrinol.* **2015**, *6*, 1-7.
- 13 Bahelka, I.; Stupka, R.; Citek, J.; Sprysl, M. *Chemosphere*, **2021**, *263*, 128203-128211.
- 14 Rochester, J. R. *Reprod. Toxicol.* **2013**, *42*, 132-155.
- 15 Inoue, S.; Koinuma, H.; Tsuruta, T. *Polym. Lett.* **1969**, *7*, 287-292.
- 16 Inoue, S.; Koinuma, H.; Tsuruta, T. *Makromol. Chem.* **1969**, *130*, 210-220.
- 17 Kobayashi, M.; Inoue, S.; Tsuruta, T. *Macromolecules* **1971**, *4*, 658-659.
- 18 Kuran, W.; Pasynekiewicz, S.; Skupinska, J.; Rokicki, A. *Makromol. Chem.* **1976**, *177*, 11-20.
- 19 Soga, K.; Imai, E.; Hattori, I. *Polym. J.* **1981**, *13*, 407-410.
- 20 Ree, M.; Bae, J. Y.; Jung, J. H.; Shin, T. J. *J. Polym. Sci. Part A* **1999**, *37*, 1863-1876.
- 21 Lu, X. B.; Ren, W. M.; Wu, G. P. *Acc. Chem. Res.* **2012**, *45*, 1721-1735.
- 22 Schilling, F. C.; Tonelli, A. E. *Macromolecules* **1986**, *19*, 1337-1343.
- 23 Childers, M. I.; Longo, J. M.; Van Zee, N. J.; LaPointe, A. M.; Coates, G. M. *Chem. Rev.* **2014**, *114*, 8129-8152.

- 24 DeRosa, C. A.; Luke, A. M.; Anderson, K.; Reineke, T. M.; Tolman, W. B.; Bates, F. S.; Hillmyer, M. A. *Macromolecules* **2021**, *54*, 5974-5984.
- 25 Coates, G. W.; Moore, D. R. *Angew. Chem. Int. Ed.* **2004**, *43*, 6618-6639.
- 26 Qin, Z.; Thomas, C. M.; Lee, S.; Coates, G. W. *Angew. Chem.* **2003**, *115*, 5642-5645.
- 27 Lu, X. B.; Wang, Y. *Angew. Chem. Int. Ed.* **2004**, *43*, 3574-3577.
- 28 WeiMin, R.; WenZhen, Z.; XiaoBing, L. *Sci. China: Chem.* **2010**, *53*, 1646-1652.
- 29 Ren, W.-M.; Liu, Y.; Wu, G.-P.; Liu, J.; Lu, X.-B. *J. Polym. Sci., Part A: Polym. Chem.* **2011**, *49*, 4894-4901.
- 30 Nozaki, K.; Nakano, K.; Hiyama, T. *J. Am. Chem. Soc.* **1999**, *121*, 11008-11009.
- 31 Cheng, M.; Darling, N. A.; Lobkovsky, E. B.; Coates, G. W. *Chem. Commun.* **2000**, 2007-2008.
- 32 Nakano, K.; Nozaki, K.; Hiyama, T. *J. Am. Chem. Soc.* **2003**, *125*, 5501-5510.
- 33 Cohen, C. T.; Thomas, C. M.; Peretti, K. L.; Lobkovsky, E. B.; Coates, G. W. *Dalton Trans.* **2006**, 237-249.
- 34 Shi, L.; Lu, X.-B.; Zhang, R.; Peng, X.-J.; Zhang, C.-Q.; Li, J.-F.; Peng, X.-M. *Macromolecules* **2006**, *39*, 5679-5685.
- 35 Wu, G. P.; Ren, W. M.; Luo, Y.; Li, B.; Zhang, W. Z.; Lu, X. B. *J. Am. Chem. Soc.* **2012**, *134*, 5682-5688.
- 36 Baba, A.; Kashiwagi, H.; Matsuda, H. *Tetrahedron Lett.* **1985**, 1323-1324.
- 37 Sugimoto, H.; Inoue, S. *Pure Appl. Chem.* **2006**, *78*, 1823-1834.
- 38 Duda, A.; Kowalski, A. In *Handbook of Ring-Opening Polymerization*; Dubois, P., Coulembier, O., Raquez, J. M., Eds.; (Wiley-VCH Verlag: Weinheim, Germany, 2009; p 1).
- 39 Vofsi, D.; Tobolsky, A. V. *J. Polym. Sci. Part A* **1965**, *3*, 3261-3273.
- 40 Tobolsky, A. V.; Eisenberg, A. *J. Am. Chem. Soc.* **1959**, *81*, 780-782.
- 41 Tobolsky, A. V.; Eisenberg, A. *J. Am. Chem. Soc.* **1960**, *82*, 289-293.
- 42 Kamber, N. E.; Jeong, W.; Waymouth, R. M. *Chem. Rev.* **2007**, *107*, 5813-5840.
- 43 Sarel, S.; Pohoryles, L. A.; Ben-Shoshan, R. *J. Org. Chem.* **1959**, *24*, 1873-1878.
- 44 Carothers, W. H.; Van Natta, F. J. *J. Am. Chem. Soc.* **1930**, *52*, 314-326.
- 45 Nomura, R.; Ninagawa, A.; Matsuda, H. *J. Org. Chem.* **1980**, *45*, 3735-3738.
- 46 Yano, T.; Matsui, H.; Koike, T.; Ishiguro, H.; Fujihara, H.; Yoshihara, M.; Maeshima, T. *Chem. Commun.* **1997**, *12*, 1129-1130.

- 47 Yamaguchi, K.; Ebitani, K.; Yoshida, T.; Yoshida, H.; Kaneda, K. *J. Am. Chem. Soc.* **1999**, *121*, 4526-4527.
- 48 Zhao, T.; Han, Y.; Sun, Y. *Phys. Chem. Chem. Phys.* **1999**, *1*, 3047-3051.
- 49 Iwasaki, T.; Kihara, N.; Endo, T. *Bull. Chem. Soc. Jpn.* **2000**, *73*, 713-719.
- 50 De Pasquale, R. J. *J. Chem. Soc. Chem. Commun.* **1973**, 157-158.
- 51 Darensbourg, D. J.; Holtcamp, M. W. *Coord. Chem. Rev.* **1996**, *153*, 155-174.
- 52 Kim, H. S.; Kim, J. J.; Lee, B. G.; Jung, O. S.; Jang, H. G.; Kang, S. O. *Angew. Chem. Int. Ed.* **2000**, *39*, 4096-4098.
- 53 Li, F.; Xia, C.; Xu, L.; Sun, W.; Chen, G. *Chem. Commun.* **2003**, *16*, 2042-2043.
- 54 Paddock, R. L.; Hiyama, Y.; McKay, J. M.; Nguyen, S. T. *Tetrahedron Lett.* **2004**, *45*, 2023-2026.
- 55 Paddock, R. L.; Nguyen, S. T. *J. Am. Chem. Soc.* **2001**, *123*, 11498-11499.
- 56 Jutz, F.; Grunwaldt, J. D.; Baiker, A. *J. Mol. Catal. A: Chem.* **2008**, *279*, 94-103.
- 57 Chen, S. W.; Kawthekar, R. B.; Kim, G. J. *Tetrahedron Lett.* **2007**, *48*, 297-300.
- 58 Barbarini, A.; Maggi, R.; Mazzacani, A.; Mori, G.; Sartori, G.; Sartorio, R. *Tetrahedron Lett.* **2003**, *44*, 2931-2934.
- 59 Shen, Y. M.; Duan, W. L.; Shi, M. *Adv. Synth. Catal.* **2003**, *345*, 337-340.
- 60 Mosteirín, F. N.; Jehanno, C.; Ruipérez, F.; Sardon, H.; Dove, A. P. *ACS Sustainable Chem. Eng.* **2019**, *7*, 10633-10640.
- 61 Guo, L.; Lamb, K. J.; North, M. *Green Chem.* **2021**, *23*, 77-118.
- 62 Soga, K.; Hosoda, S.; Tazuke, Y.; Ikeda, S. *J. Polym. Sci., Polym. Lett. Ed.* **1976**, *14*, 161-165.
- 63 Vogdanis, L.; Martens, B.; Uchtmann, H.; Hensel, F.; Heitz, W. *Makromol. Chem.* **1990**, *191*, 465-472.
- 64 Soga, K.; Tazuke, Y.; Hosoda, S.; Ikeda, S. *J. Polym. Sci., Part A: Polym. Chem.* **1977**, *15*, 219-229.
- 65 Harris, R. F. *J. Appl. Polym. Sci.* **1989**, *37*, 183-200.
- 66 Storey, R. F.; Hoffman, D. C. *Macromolecules* **1992**, *25*, 5369-5382.
- 67 Kuran, W.; Listos, T. *Makromol. Chem.* **1992**, *193*, 945-956.
- 68 Storey, R. F.; Hoffman, D. C. *Polymer* **1992**, *33*, 2807-2816.
- 69 Lee, J. C.; Litt, M. H. *Macromolecules* **2000**, *33*, 1618-1627.

- 70 Doane, W. M.; Shasha, B. S.; Stout, E. I.; Russell, C. R.; Rist, C. E. *Carbohydr. Res.* **1967**, *4*, 445-451.
- 71 Haba, O.; Tomizuka, H.; Endo, T. *Macromolecules* **2005**, *38*, 3562-3563.
- 72 Matsuo, J.; Aoki, K.; Sanda, F.; Endo, T. *Macromolecules* **1998**, *31*, 4432-4438.
- 73 Ariga, T.; Takata, T.; Endo, T. *Macromolecules* **1997**, *30*, 737-744.
- 74 Sarel, S.; Pohoryles, L. A. *J. Am. Chem. Soc.* **1958**, *80*, 4596-4599.
- 75 Merkley, N.; Warkentin, J. *Can. J. Chem.* **2002**, *80*, 1187-1195.
- 76 Mindemark, J.; Bowden, T. *Polymer* **2011**, *52*, 5716-5722.
- 77 Ludwig, B. J.; Piech, E. C. *J. Am. Chem. Soc.* **1951**, *73*, 5779-5781.
- 78 Keul, H.; Höcker, H. *Makromol. Chem.* **1988**, *189*, 2303-2321.
- 79 Matsuo, J.; Sanda, F.; Endo, T. *Macromol. Chem. Phys.* **1998**, *199*, 2489-2494.
- 80 Cai, J.; Zhu, K. J.; Yang, S. L. *Polymer* **1998**, *39*, 4409-4415.
- 81 Yu, C.; Zhang, L.; Shen, Z. *Polym. Int.* **2004**, *53*, 1485-1490.
- 82 Chen, X.; McCarthy, S. P.; Gross, R. A. *Macromolecules* **1998**, *31*, 662-668.
- 83 Mikami, K.; Lonnecker, A. T.; Gustafson, T. P.; Zinnel, N. F.; Pai, P. J.; Russell, D. H.; Wooley, K. L. *J. Am. Chem. Soc.* **2013**, *168*, 6826-6829.
- 84 Song, Y.; Ji, X.; Dong, M.; Li, R.; Lin, Y. N.; Wang, H.; Wooley, K. L. *J. Am. Chem. Soc.* **2018**, *140*, 16053-16057.
- 85 Gregory, G. L.; Jenisch, L. M.; Charles, B.; Kociok-Kohn, G.; Buchard, A. *Macromolecules* **2016**, *49*, 7165-7169.
- 86 Weilandt, K. D.; Keul, H.; Höcker, H. *Macromol. Chem. Phys.* **1996**, *197*, 3851-3868
- 87 Al-Azemi, T. F.; Bisht, K. S. *Macromolecules* **1999**, *32*, 6536-6540.
- 88 Sanders, D. P.; Fukushima, K.; Coady, D. J.; Nelson, A.; Fujiwara, M.; Yasumoto, M.; Hedrick, J. L. *J. Am. Chem. Soc.* **2010**, *132*, 14724-14726.
- 89 Dechy-Cabaret, O.; Martin-Vaca, B.; Bourissou, D. *Chem. Rev.* **2004**, *104*, 6147-6176.
- 90 Ajellal, N.; Carpentier, J. F.; Guillaume, C.; Guillaume, S. M.; Helou, M.; Poirier, V.; Sarazin, Y.; Trifonov, A. *Dalton Trans.* **2010**, *39*, 8363-8376.
- 91 Degee, P.; Dubois, P.; Jerome, R.; Jacobsen, S.; Fritz, H.-G. *Macromol. Symp.* **1999**, *144*, 289-302.
- 92 Kricheldorf, H. R.; Stricker, A. *Macromol. Chem. Phys.* **2000**, *201*, 2557-2565.

- 93 Ryner, M.; Stridsberg, K.; Albertsson, A.-C.; von Schenck, H.; Svensson, M. *Macromolecules* **2001**, *34*, 3877-3881.
- 94 Kricheldorf, H. R.; Kreiser-Saunders, I.; Boettcher, C. *Polymer* **1995**, *36*, 1253-1259.
- 95 Kricheldorf, H. R.; Kreiser-Saunders, I.; Stricker, A. *Macromolecules* **2000**, *33*, 702-709.
- 96 Kricheldorf, H. R. *Macromol. Symp.* **2000**, *153*, 55-65.
- 97 Kowalski, A.; Duda, A.; Penczek, S. *Macromolecules* **1998**, *31*, 2114-2122.
- 98 Wurm, B.; Keul, H.; Hocker, H. *Macromol. Chem. Phys.* **1994**, *195*, 3489-3498.
- 99 Carter, K. R.; Richter, R.; Kricheldorf, H. R.; Hedrick, J. L. *Macromolecules* **1997**, *30*, 6074-6076.
- 100 Stevels, W. M.; Ankone, M. J. K.; Dijkstra, P. J.; Feijen, J. *Macromolecules* **1996**, *29*, 3332-3333.
- 101 Ling, J.; Shen, Z.; Huang, Q. *Macromolecules* **2001**, *34*, 7613-7616.
- 102 Zhong, Z.; Dijkstra, P. J.; Birg, C.; Westerhausen, M.; Feijen, J. *Macromolecules* **2001**, *34*, 3863-3868.
- 103 Westerhausen, M.; Schneiderbauer, S.; Kneifel, A. N.; Sotl, Y.; Mayer, P.; Noth, H.; Zhong, Z.; Dijkstra, P. J.; Feijen, J. *Eur. J. Inorg. Chem.* **2003**, 3432-3439.
- 104 Stevels, W. M.; Ankone, M. J. K.; Dijkstra, P. J.; Feijen, J. *Macromol. Chem. Phys.* **1995**, *196*, 1153-1161.
- 105 O'Keefe, B. J.; Monnier, S. M.; Hillmyer, M. A.; Tolman, W. B. *J. Am. Chem. Soc.* **2001**, *123*, 339-340.
- 106 Bourget-Merle, L.; Lappert, M. F.; Severn, J. R. *Chem. Rev.* **2002**, *102*, 3031-3065.
- 107 Wu, J.; Yu, T.-L.; Chen, C.-T.; Lin, C.-C. *Coord. Chem. Rev.* **2006**, *250*, 602-626.
- 108 Wheaton, C. A.; Hayes, P. G.; Ireland, B. J. *Dalton Trans.* **2009**, 4832-4846.
- 109 Spassky, N.; Wisniewski, M.; Pluta, C.; Le Borgne, A. *Macromol. Chem. Phys.* **1996**, *197*, 2627-2637.
- 110 Zhong, Z.; Dijkstra, P. J.; Feijen, J. *Angew. Chem., Int. Ed.* **2002**, *41*, 4510-4513.
- 111 Ovitt, T. M.; Coates, G. W. *J. Am. Chem. Soc.* **1999**, *121*, 4072-4073.
- 112 Cheng, M.; Attygalle, A. B.; Lobkovsky, E. B.; Coates, G. W. *J. Am. Chem. Soc.* **1999**, *121*, 11583-11584.
- 113 Chamberlain, B. M.; Cheng, M.; Moore, D. R.; Ovitt, T. M.; Lobkovsky, E. B.; Coates, G. W. *J. Am. Chem. Soc.* **2001**, *123*, 3229-3238.

- 114 Thomas, C.; Bibal, B. *Green Chem.* **2014**, *16*, 1687-1699.
- 115 Fevre, M.; Pinaud, J.; Gnanou, Y.; Vignolle, J.; Taton, D. *Chem. Soc. Rev.* **2013**, *42*, 2142-2172.
- 116 Kricheldorf, H. R.; Dunsing, R.; Serra, A. *Macromolecules* **1987**, *20*, 2050-2057.
- 117 Kricheldorf, H. R.; Dunsing, R. *Makromol. Chem.* **1986**, *187*, 1611-1625.
- 118 Sanda, F.; Fueki, T.; Endo, T. *Macromolecules* **1999**, *32*, 4220-4224.
- 119 Kricheldorf, H. R.; Jenssen, J. *J. Macromol. Sci., Pure Appl. Chem.* **1989**, *A26*, 631-644.
- 120 Kricheldorf, H. R.; Dunsing, R.; Serra, A. *Makromol. Chem.* **1987**, *188*, 2453-2466.
- 121 Bourissou, D.; Martin-Vaca, B.; Dumitrescu, A.; Graullier, M.; Lacombe, F. *Macromolecules* **2005**, *38*, 9993-9998.
- 122 Basko, M.; Kubisa, P. *J. Polym. Sci., Part A: Polym. Chem.* **2006**, *44*, 7071-7081.
- 123 Matsuo, J.; Nakano, S.; Sanda, F.; Endo, T. *J. Polym. Sci., Part A: Polym. Chem.* **1998**, *36*, 2463-2471.
- 124 Lou, X. D.; Detrembleur, C.; Jerome, R. *Macromolecules* **2002**, *35*, 1190-1195.
- 125 Shibasaki, Y.; Sanada, H.; Yokoi, M.; Sanda, F.; Endo, T. *Macromolecules* **2000**, *33*, 4316-4320.
- 126 Kim, M. S.; Seo, K. S.; Khang, G.; Lee, H. B. *Macromol. Rapid Commun.* **2005**, *26*, 643-648.
- 127 Hyun, H.; Kim, M. S.; Khang, G.; Lee, H. B. *J. Polym. Sci., Part A: Polym. Chem.* **2006**, *44*, 4235-4241.
- 128 Albertsson, A. C.; Palmgren, R. *J. Macromol. Sci., Pure Appl. Chem.* **1996**, *A33*, 747-758.
- 129 Takata, T.; Igarashi, M.; Endo, T. *J. Polym. Sci., Part A: Polym. Chem.* **1991**, *29*, 781-784.
- 130 Kricheldorf, H. R.; Boettcher, C. *Makromol. Chem.* **1993**, *194*, 1665-1669.
- 131 Jedlinski, Z.; Walach, W.; Kurcok, P.; Adamus, G. *Makromol. Chem.* **1991**, *192*, 2051-2057.
- 132 Kricheldorf, H. R.; Kreiser-Saunders, I. *Makromol. Chem.* **1990**, *191*, 1057-1066.
- 133 Keul, H.; Bacher, R.; Hocker, H. *Makromol. Chem.* **1986**, *187*, 2579-2589.
- 134 Kuhling, S.; Keul, H.; Hocker, H. *Makromol. Chem. Suppl.* **1989**, *15*, 9-13.
- 135 Hofle, G.; Steglich, W.; Vorbruggen, H. *Angew. Chem. Int. Ed. Engl.* **1978**, *17*, 569-583.

- 136 Spivey, A. C.; Arseniyadis, S. *Angew. Chem. Int. Ed.* **2004**, *43*, 5436-5441.
- 137 Lalanne-Tisné, M.; Mees, M. A.; Eyley, S.; Zinck, P.; Thielemans, W. *Carbohydr. Polym.* **2020**, *250*, 116974-116981.
- 138 Nederberg, F.; Connor, E. F.; Moller, M.; Glauser, T.; Hedrick, J. L. *Angew. Chem. Int. Ed.* **2001**, *40*, 2712-2715.
- 139 Helou, M.; Miserque, O.; Brusson, J. M.; Carpentier, J. F.; Guillaume, S. M. *Chem. Eur. J.* **2010**, *16*, 13805-13813.
- 140 Thillaye du Boullay, O.; Marchal, E.; Martin-Vaca, B.; Cossio, F. P.; Bourissou, D. *J. Am. Chem. Soc.* **2006**, *128*, 16442-16443.
- 141 Martin-Vaca, B.; Bourissou, D. *ACS Macro Lett.* **2015**, *4*, 792-798.
- 142 Hadjichristidis, N.; Iatrou, H.; Pitsikalis, M.; Sakellariou, G. *Chem. Rev.* **2009**, *109*, 5528-5578.
- 143 Trimaille, T.; Moller, M.; Gurny, R. *J. Polym. Sci. Part A: Polym. Chem.* **2004**, *42*, 4379-4391.
- 144 Trimaille, T.; Gurny, R.; Moeller, M. *Chimia* **2005**, *59*, 348-352.
- 145 Feng, H.; Dong, C. M. *J. Polym. Sci. Part A: Polym. Chem.* **2006**, *44*, 5353-5361.
- 146 Jaipuri, F. A.; Bower, B. D.; Pohl, N. L. *Tetrahedron: Asymmetry* **2003**, *14*, 3249-3252.
- 147 Vedejs, E.; Bennett, N. S.; Conn, L. M.; Diver, S. T.; Gingras, M.; Lin, S.; Oliver, P. A.; Peterson, M. J. *J. Org. Chem.* **1993**, *58*, 7286-7288.
- 148 Myers, M.; Connor, E. F.; Glauser, T.; Mock, A.; Nyce, G.; Hedrick, J. L. *J. Polym. Sci. Part A: Polym. Chem.* **2002**, *40*, 844-851.
- 149 Nyce, G. W.; Lamboy, J. A.; Connor, E. F.; Waymouth, R. M.; Hedrick, J. L. *Org. Lett.* **2002**, *4*, 3587-3590.
- 150 Movassaghi, M.; Schmidt, M. A. *Org. Lett.* **2005**, *7*, 2453-2456.
- 151 Jain, I.; Malik, P. *Eur. Polym. J.* **2021**, *150*, 110412-110425.
- 152 Connor, E. F.; Nyce, G. W.; Myers, M.; Mock, A.; Hedrick, J. L. *J. Am. Chem. Soc.* **2002**, *124*, 914-915.
- 153 Nyce, G. W.; Glauser, T.; Connor, E. F.; Mock, A.; Waymouth, R. M.; Hedrick, J. L. *J. Am. Chem. Soc.* **2003**, *125*, 3046-3056.
- 154 Dove, A. P.; Pratt, R. C.; Lohmeijer, B. G. G.; Culkin, D. A.; Hagberg, E. C.; Nyce, G. W.; Waymouth, R. M.; Hedrick, J. L. *Polymer* **2006**, *47*, 4018-4025.

- 155 Csihony, S.; Culkin, D. A.; Sentman, A. C.; Dove, A. P.; Waymouth, R. M.; Hedrick, J. L. *J. Am. Chem. Soc.* **2005**, *127*, 9079-9084.
- 156 Nederberg, F.; Lohmeijer, B. G. G.; Leibfarth, F.; Pratt, R. C.; Choi, J.; Dove, A. P.; Waymouth, R. M.; Hedrick, J. L. *Biomacromolecules* **2007**, *8*, 153-160.
- 157 Culkin, D. A.; Jeong, W.; Csihony, S.; Gomez, E. D.; Balsara, N. P.; Hedrick, J. L.; Waymouth, R. M. *Angew. Chem. Int. Ed.* **2007**, *119*, 2681-2684.
- 158 Dove, A. P. *ACS Macro Lett.* **2012**, *1*, 1409-1412.
- 159 Pratt, R. C.; Lohmeijer, B. G.; Long, D. A.; Waymouth, R. M.; Hedrick, J. L. *J. Am. Chem. Soc.* **2006**, *128*, 4556-4557.
- 160 Lohmeijer, B. G. G.; Pratt, R. C.; Leibfarth, F.; Logan, J. W.; Long, D. A.; Dove, A. P.; Nederberg, F.; Choi, J.; Wade, C.; Waymouth, R. M.; Hedrick, J. L. *Macromolecules* **2006**, *39*, 8574-8583.
- 161 Foresti, M. L.; Ferreira, M. L. *Macromol. Rapid Commun.* **2004**, *25*, 2025-2028.
- 162 Lalanne-Tisné, M.; Eyley, S.; Winter, J. D.; Favrelle-Huret, A.; Thielemans, W.; Zinck, P. *Carbohydr. Polym.* **2022**, *295*, 119840-119848.
- 163 Chuma, A.; Horn, H. W.; Swope, W. C.; Pratt, R. C.; Zhang, L.; Lohmeijer, B. G. G.; Wade, C. G.; Waymouth, R. M.; Hedrick, J. L.; Rice, J. E. *J. Am. Chem. Soc.* **2008**, *130*, 6749-6754.
- 164 Kiesewetter, M. K.; Shin, E. J.; Hedrick, J. L.; Waymouth, R. M. *Macromolecules* **2010**, *43*, 2093-2107.
- 165 Zhang, L.; Nederberg, F.; Pratt, R. C.; Waymouth, R. M.; Hedrick, J. L.; Wade, C. W. *Macromolecules* **2007**, *40*, 4154-4158.
- 166 Zhang, L.; Nederberg, F.; Messman, J. M.; Pratt, R. C.; Hedrick, J. L.; Wade, C. W. *J. Am. Chem. Soc.* **2007**, *129*, 12610-12611.
- 167 Dove, A. P.; Pratt, R. C.; Lohmeijer, B. G. G.; Waymouth, R. M.; Hedrick, J. L. *J. Am. Chem. Soc.* **2005**, *127*, 13798-13799.
- 168 Pratt, R. C.; Lohmeijer, B. G. G.; Long, D. A.; Lundberg, P. N. P.; Dove, A. P.; Li, H.; Wade, C. G.; Waymouth, R. M.; Hedrick, J. L. *Macromolecules* **2006**, *39*, 7863-7871.
- 169 Jain, I.; Malik, P. *Eur. Polym. J.* **2020**, *133*, 109791-109807.
- 170 Goldys, A. M.; Dixon, D. J. *Macromolecules* **2014**, *47*, 1277-1284.

171. Saito, T.; Aizawa, Y.; Tajima, K.; Isono, T.; Satoh, T. *Polym. Chem.* **2015**, *6*, 4374-4384.
- 172 Makiguchi, K.; Satoh, T.; Kakuchi, T. *Macromolecules* **2011**, *44*, 1999-2005.
- 173 Delcroix, D.; Couffin, A.; Susperregui, N.; Navarro, C.; Maron, L.; Martin-Vaca, B.; Bourissou, D. *Polym. Chem.* **2011**, *2*, 2249-2256.
- 174 Makiguchi, K.; Ogasawara, Y.; Kikuchi, S.; Satoh, T.; Kakuchi, T. *Macromolecules* **2013**, *46*, 1772-1782.
- 175 Chen, J.; Kan, S.; Xia, H.; Zhou, F.; Chen, X.; Jiang, X.; Guo, K.; Li, Z. *Polymer* **2013**, *54*, 4177-4182.
- 176 Lin, B.; Waymouth, R. M. *Macromolecules* **2018**, *51*, 2932-2938.
- 177 Burton, T. F.; Pinaud, J.; Giani, O. *Macromolecules* **2020**, *53*, 6598-6607.
- 178 Zaky, M. S.; Wirotius, A. L.; Coulembier, O.; Guichard, G.; Taton, D. *ACS Macro Lett.* **2022**, *11*, 1148-1155.
- 179 Zhang, X.; Jones, G. O.; Hedrick, J. L.; Waymouth, R. M. *Nat. Chem.* **2016**, *8*, 1047-1053.
- 180 Lin, B.; Waymouth, R. M. *J. Am. Chem. Soc.* **2017**, *139*, 1645-1652.
- 181 Coulembier, O.; Sanders, D. P.; Nelson, A.; Hollenbeck, A. N.; Horn, H. W.; Rice, J. E.; Fujiwara, M.; Dubois, P.; Hedrick, J. L. *Angew. Chem. Int. Ed.* **2009**, *48*, 5170-5173.
- 182 Thomas, C.; Peruch, F.; Deffieux, A.; Milet, A.; Desvergne, J. P.; Bibal, B. *Adv. Synth. Catal.* **2011**, *353*, 1049-1054.
- 183 Alba, A.; Schopp, A.; De Sousa Delgado, A. P.; Cheikh, R. C.; Martin-Vaca, B.; Bourissou, D. *J. Polym. Sci., Part A: Polym. Chem.* **2010**, *48*, 959-965.
- 184 Kadota, J.; Pavlovic, D.; Desvergne, J. P.; Bibal, B.; Peruch, F.; Deffieux, A. *Macromolecules* **2010**, *43*, 8874-8879.
- 185 Coady, D. J.; Fukushima, K.; Horn, H. W.; Rice, J. E.; Hedrick, J. L. *Chem. Commun.* **2011**, *47*, 3105-3107.
- 186 Xu, J.; Liu, J.; Li, Z.; Wang, H.; Wei, F.; Zhu, Y.; Guo, K. *Polymer* **2018**, *154*, 17-26.
- 187 Coulembier, O.; Josse, T.; Guillerm, B.; Gerbaux, P.; Dubois, P. *Chem. Commun.* **2012**, *48*, 11695-11697.
- 188 Basterretxea, A.; Gabirondo, E.; Jehanno, C.; Zhu, H.; Coulembier, O.; Mecerreyes, D.; Sardon, H. *Macromolecules* **2021**, *54*, 6214-6225.

Chapter 2

Organocatalyzed Regio-regular Polymerization of α -Aryl Trimethylene Carbonates

2.1 Introduction

Aliphatic polycarbonates are bio-degradable polymers and upon biodegradation it results in the formation of non-hazardous aliphatic diols. Since the commercially available aromatic polycarbonates biodegrade to hazardous bisphenol-A, a necessity to make an environmental friendly polycarbonate arises. To fulfill the need, polymer chemists have sought aliphatic polycarbonates as potential replacement for aromatic polycarbonates. In the first chapter of this thesis the advantages of using ROP for preparing aliphatic polycarbonates was discussed. Additionally, the catalysts available for the ROP of cyclic carbonates were also discussed. While a number of methods exist for ROP of cyclic carbonates, aliphatic polycarbonates need to match the physical properties exhibited by the aromatic polycarbonates to find commercial applications.

2.2 Background

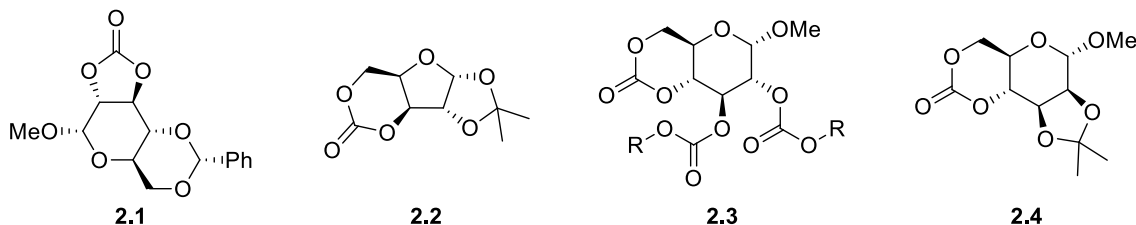
Poly(trimethylene carbonate) or polyTMC is the simplest aliphatic polycarbonate and is made by the ROP of trimethylene carbonate.¹⁻³ PolyTMC exists as a liquid polymer with glass transition temperature (T_g) of -20 °C. To improve the physical properties of aliphatic

polycarbonates, a variety of cyclic carbonates were designed, synthesized and subjected to ROP. These include sugar-based cyclic carbonates, β -substituted trimethylene carbonates and α -substituted cyclic carbonates.

2.2.1 Sugar Based Cyclic Carbonates

Sugars are one of the most easily available renewable resources and possess the required functional groups for synthesizing cyclic carbonates. Some of the cyclic carbonates synthesized from sugars are shown in Figure 2.1. The strained five-membered cyclic carbonate derived from glucose (**2.1**) undergoes anionic ROP to yield a regio-irregular amorphous polycarbonate.⁴⁻⁶ Polycarbonates obtained from **2.1** exhibit glass transition temperatures (T_g) in the range of 87-223 °C depending on the molar mass of the polymer. The ROP of six-membered cyclic carbonate derived from xylose (**2.2**) results in the formation of a regio-irregular semicrystalline polycarbonate.⁷⁻⁹ This semicrystalline polycarbonate exhibits T_g and T_m (melting temperature) at 128 °C and 228 °C respectively. Another six-membered cyclic carbonate derived from glucose (**2.3**) undergoes organocatalyzed ROP to produce regio-regular amorphous polycarbonate. These regio-regular polycarbonates exhibit T_g s in the range of 38-125 °C depending on the kind of side chain substituents.^{10, 11} Similarly, the six-membered cyclic carbonate derived from mannose (**2.4**) undergoes organocatalyzed ROP to yield regio-regular amorphous polycarbonate.¹² This amorphous polycarbonate exhibits T_g at 152 °C. Side chain functionalities of polycarbonates obtained from the sugar-based cyclic carbonates can be changed to desired functionalities in post-polymerization modifications. Even though the ROP of sugar-based cyclic carbonates results in the formation of stereo-regular polycarbonates, not all of them exist as crystalline polymer. Thus, there is a need for other structures that would easily pack

Figure 2.1. Structures of Sugar Based Cyclic Carbonates

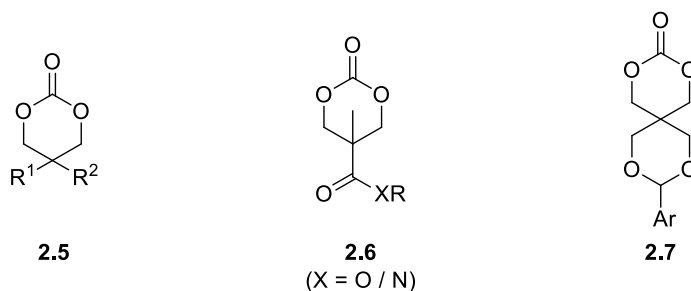


in an ordered manner and result in a crystalline polymer and possesses better physical property.

2.2.2 β -Substituted Trimethylene Carbonates

A large variety of β -substituted trimethylene carbonates (TMC) have been polymerized to produce aliphatic polycarbonates.¹³ Most of the synthesized β -substituted TMCs can be structurally divided into three kinds (Figure 2.2). The first kind of β -substituted TMCs (**2.5**, Figure 2.2) were synthesized from precursors such as dihydroxy acetone, glycerol, malonic acid diethyl ester and oxetane.¹⁴⁻²⁵ Using bis-MPA (2,2-bishydroxy(methyl)propionic acid), the second kind of β -substituted TMCs **2.6** were synthesized.²⁶⁻³⁶ Spiro cyclic β -substituted TMCs (**2.7**), which are third kind, were prepared from pentaerythritol.³⁷⁻⁴⁰ The general substituents mentioned in **2.5** and **2.6** include a wide range of groups such as alkyl, allyl, alkyl ether, allyl ether, aryl-alkyl ether, alkyl ester, aryl ester, alkyl-halogen, alkyl-azide, carbonate, carbamate, urea, guanidine, and sugars. ROP of β -substituted TMCs mostly results in the formation of amorphous polycarbonates. In some cases, crystalline polycarbonates were obtained for specific substituents.^{18, 24, 25} The overall T_g and T_m of polycarbonates synthesized from β -substituted TMCs are in the range of -40 to 128 °C and 24-153 °C respectively. ROP of β -substituted TMCs provides good scope for functionalization of aliphatic polycarbonates. However, the major drawback of ROP of β -

Figure 2.2. Structures of β -Substituted Trimethylene Carbonates



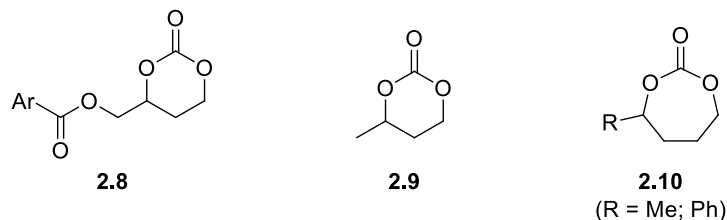
substituted TMCs is controlling the tacticity of polycarbonates. There are no reports related to the synthesis of stereo-regular polycarbonates using β -substituted TMCs.

2.2.3 α -Substituted Cyclic Carbonates

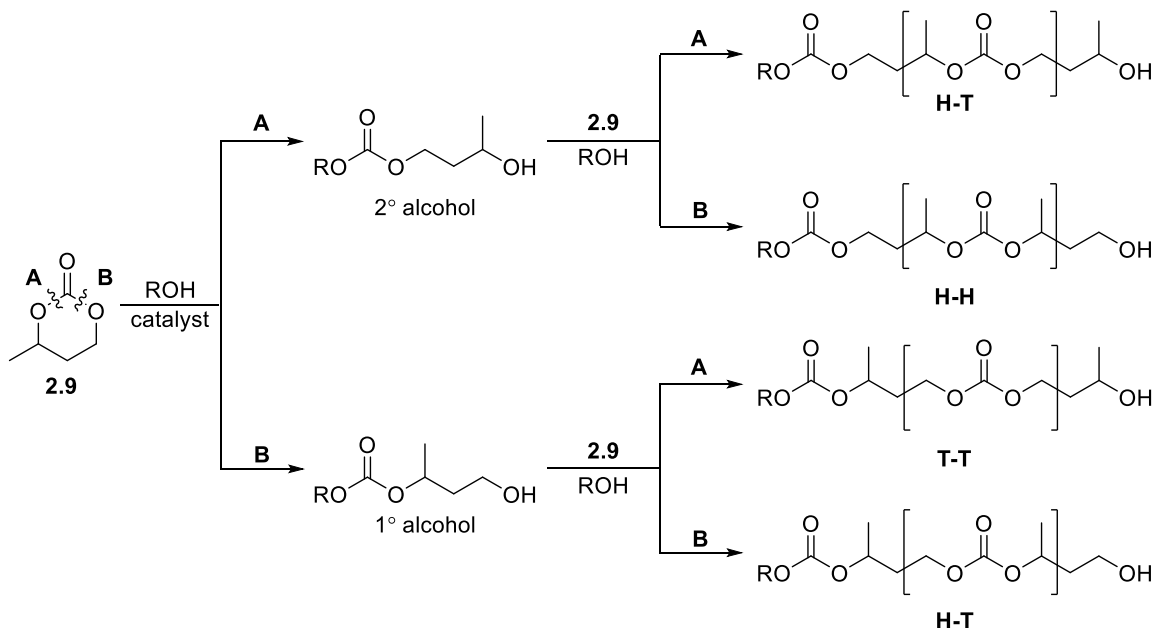
Compared to β -substituted TMCs, only a limited number of ROP of α -substituted cyclic carbonates have been reported. Some of the α -substituted cyclic carbonates used in the ROP are shown in the Figure 2.3.^{13, 21, 41-44} The challenging tasks in ROP of α -substituted cyclic carbonates are achieving high regio (head-to-tail linkages) and stereo-regularity. Both regio and stereo-regularity play significant roles in enhancing the physical properties of polymers.

The non-regioselective ROP of α -substituted cyclic carbonates lead to the formation of three types of carbonate linkages namely head-to-head (H-H), head-to-tail (H-T) and tail-to-tail (T-T) in the ratio of 1:2:1 (ROP of **2.9** represented in Scheme 2.1). ¹³C NMR is used in identifying and quantifying these linkages, which in turn gives the information about the regio-regularity of the polymer. In regio-random polymers, the carbonyl carbon appears as a pseudo triplet. Integration of each peak of the pseudo triplet of a regio-random polymer gives a ratio of 1:2:1. As shown in Scheme 2.1, H-T linkages can form in two different ways, and therefore, the central peak belongs to H-T carbonate linkages. The peaks on either

Figure 2.3. Structures of α -Substituted Cyclic Carbonates



Scheme 2.1. Formation of Three Kinds of Carbonate Linkages



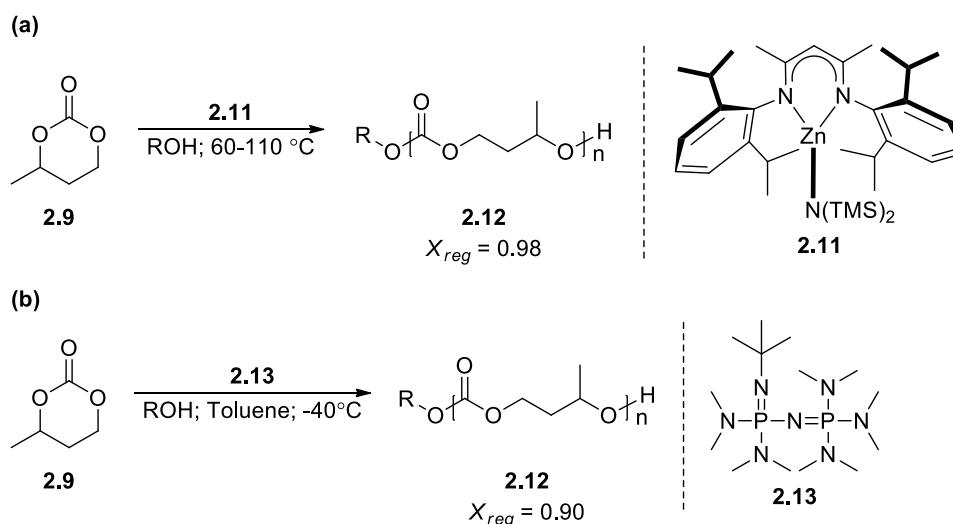
side of the central peak belong to H-H and T-T carbonate linkages. Expressing regio-regularity of a polymer in terms of percentage of H-T linkages is not convenient, as 50% of the linkages in regio-random polymers are H-T linkages. In order to express the regio-regularity in a more convenient manner, a term called X_{reg} with values between 0 and 1 is used.⁴¹ The formula used to calculate the regio-regularity in terms of X_{reg} is given as $[1 - (\text{relative intensity of H-H linkages} + \text{relative intensity of T-T linkages})]$ where the relative intensities are obtained by integrating the individual carbonyl peaks in the $^{13}\text{C}\{^1\text{H}\}$ NMR. The relative intensity of H-T linkages (the central peak) is normalized to 1. An X_{reg} value of

0 indicates complete regio-randomness, whereas an X_{reg} value of 1 indicates complete regio-regularity. Polymers with $X_{reg} \geq 0.9$ are usually termed as regio-regular polymers.

Guillaume and coworkers were the first to report a highly regio-regular bulk ROP of racemic α -methyl trimethylene carbonate **2.9** (α -MeTMC). The reaction was catalyzed by an organozinc complex **2.11** (Scheme 2.2a).⁴¹ The catalyst **2.11** was also employed for the ROP of α -methyl tetramethylene carbonate **2.10** with moderate regio-regularity.⁴⁴ Later, Odelius and coworkers have shown that a phosphazene can catalyze regio-regular ROP of α -MeTMC **2.13** (Scheme 2.2b).⁴² Both the Guillaume and Odelius groups reported that the α -MeTMC ring opens by the cleavage of acyl-oxygen bond nearer to the methyl substituent. This leads to secondary alcohol as the leaving group and therefore becomes the chain-end of the polymer. The regio-regular poly(α -MeTMC) reported by these groups exists as an amorphous polymer with $T_g = -16$ °C.

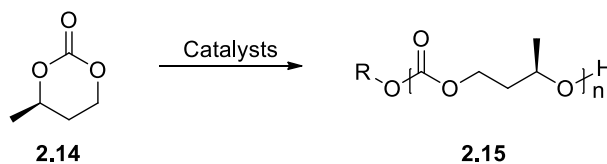
More recently Hillmyer and coworkers have reported the ROP of *R*- α -MeTMC to obtain regio and stereo-regular polycarbonate.^{43, 45} The ROP of *R*- α -MeTMC **2.14** using

Scheme 2.2. Regio-Regular ROP of α -MeTMC



phosphazene **2.13** as catalyst resulted in the formation of stereo-regular polycarbonate with X_{reg} ranging from 0.11 to 0.75 (Table 2.1, entries 1-3). The stereo-regular polycarbonate having X_{reg} lower than 0.75 exists as an amorphous polymer with T_g in the range of -12 to -18 °C (Table 2.1, entries 1 & 2). Above this value of X_{reg} a semicrystalline polymer with T_g and T_m of -4 °C and 54 °C respectively is obtained (Table 2.1, entry 3). The organozinc catalyzed ROP of *R*- α -MeTMC **2.14** resulted in the formation of polycarbonate with highest regio-regularity ($X_{reg} = 0.99$) (Table 2.1, entry 4). Stereo-regular poly(α -MeTMC) with higher X_{reg} exhibit crystallinity (Table 2.1, entries 2-4) compared to stereo-regular polycarbonates with lower X_{reg} . From the ROP of enantiopure *R*- α -MeTMC (**2.14**) and racemic α -MeTMC (**2.9**), it is evident that both regio and stereo-regularity are necessary for enhancing the physical properties of poly α -substituted TMCs (Table 2.1, entries 4 & 5).

Table 2.1. Regio-Regular ROP of *R*- α -MeTMC



entry ^{a,b}	catalyst	[M] ₀ /[I] ₀	[c] ^c (mol %)	solvent	temp (°C)	time (min)	conv ^d (%)	$M_{n,SEC}^e$ (g mol ⁻¹)	\bar{D}	X_{reg}	T_g	T_m
1	2.13	40	2.5	bulk	60	5	99	7800	1.60	0.11	-12 °C	-
2	2.13	40	2.5	toluene	-20	30	99	8000	1.40	0.44	-18 °C	-
3	2.13	40	2.5	toluene	-60	30	99	6600	1.20	0.75	-4 °C	54 °C
4	2.11	100	0.2	bulk	70	19	76	12500	1.10	0.99	-2 °C	73 °C
5 ^b	2.11	100	0.2	bulk	60	7	94	12600	1.28	0.98	-16 °C	-

^aROP of **2.14**; ^bROP of **2.9**; ^cwith respect to monomer; ^ddetermined by ¹H-NMR; ^eNumber average molar mass determined by Size Exclusion Chromatography.

2.3 Initial Hypothesis

One of the possible ways to improve the physical properties of poly α -substituted TMCs is to restrict the rotation of pendant groups in the polymer chain. DiStasio and coworkers have shown that restricting the rotation of pendant groups in a polymer chain can increase the T_g .⁴⁶ Since rigid substituents are more resistant to rotation than flexible substituents, we thought that replacing methyl with an aryl group in the α position of TMC would restrict the rotation of pendant groups and increase the T_g of polymer. Aryl groups in the backbone of poly(bisphenol-A) are responsible for inducing favorable physical properties. Also, the ability to vary its structure provides scope for tuning the properties of polymer. In order to replicate some of the favorable properties of aromatic polycarbonates under controlled polymerization conditions, we decided to pursue the ROP of α -ArTMCs. α -ArTMCs can be readily synthesized from the corresponding 1,3-diols which in turn can be readily synthesized from well-known synthetic reactions in a few steps. As mentioned earlier, both regio and stereo-regularity are necessary for achieving good physical properties of polymer. Once poly(α -ArTMC) with high regio-regularity is synthesized, stereo-regular polycarbonate can be readily synthesized using enantiopure α -ArTMC. Among the available catalysts for the ROP, we sought organocatalysts over organometallic catalysts to avoid remnant metal impurities in the polymer.

2.4 Results and Discussion

Synthesis of Monomer and Identification of Different Carbonate Linkages

We began our studies by synthesizing α -PhTMC using reported literature procedures (Scheme 2.3).^{47, 48} In the first step, the commercially available β -keto ester **2.16** was reduced

using sodium borohydride to yield 1,3-diol **2.17**.⁴⁷ The resultant diol **2.17** was converted to cyclic carbonate **2.18** using a mixture of CDI and pyridine.⁴⁸ ROP of the obtained monomer was then attempted using various catalysts and the regio-regularities were evaluated using ¹³C-NMR. In the case of poly(α -PhTMC) the chemical shift (δ) of H-T carbonate linkage is 153.80-153.51 ppm (Figure 2.4). The downfield (154.23-154.05 ppm) and upfield (153.03-152.86 ppm) carbonyl carbon peaks belong to either H-H or T-T carbonate linkages. The observed splitting of carbonyl carbon peak is due to the presence of different stereosequences (stereo-irregular).

Scheme 2.3. Synthesis of α -PhTMC

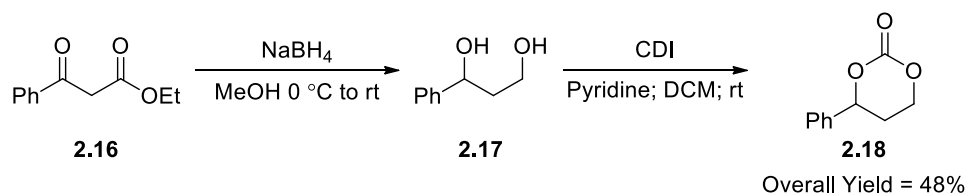
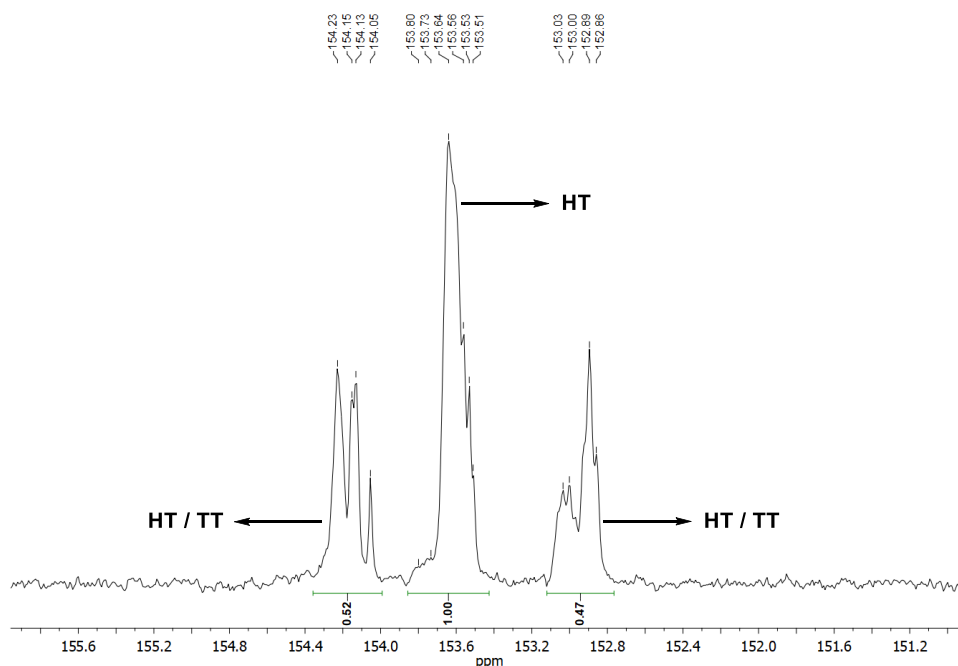
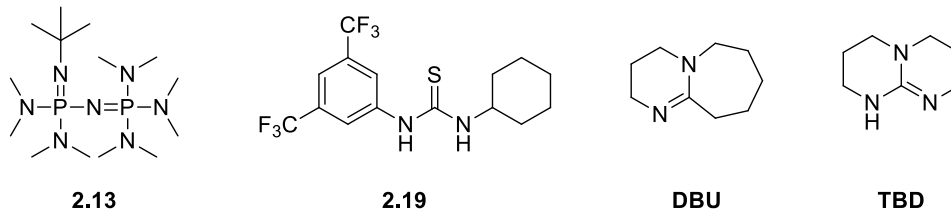
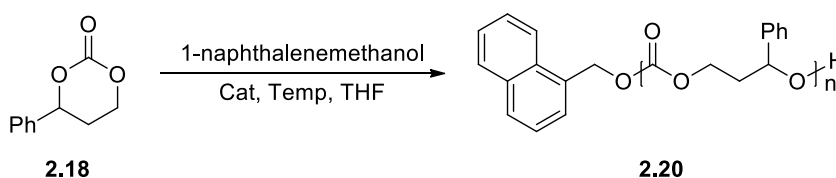


Figure 2.4. ¹³C{¹H} NMR Spectrum of Non-Regioselective ROP of α -PhTMC



Optimization of polymerization conditions

Phosphazene **2.13** (Figure 2.5) was chosen as the first catalyst to be tested, as it was successfully used for the regio-regular ROP of α -MeTMC.⁴² Using this catalyst, the ROP of α -PhTMC **2.18** was attempted with 1-naphthalene methanol as an initiator. Initially, the ROP was carried out in THF and toluene at room temperature using 0.5 mol% of phosphazene **2.13** with $[M]_0:[I]_0$ of 100:1 and $[M]_0 = 1$ M. The monomer conversion was observed to be 76% in 2.5 hours in THF (Table 2.2, entry 1) and 87% in 30 minutes in toluene (Table 2.2, entry 2). The polymerization reactions were quenched at these time points with 4 equivalents of benzoic acid (with respect to catalyst) and the polymer was obtained by precipitation in methanol to yield poly(α -PhTMC) as a white solid. The isolated polymers from both the reactions were observed to be regio-irregular. Since Odelius had reported that the phosphazene catalyzed ROP of α -MeTMC delivers high regio-regularity upon lowering the reaction temperature, we investigated the ROP of α -PhTMC at lower temperatures. When the ROP was carried out at -20 °C in THF, the reaction was observed to be very slow due to precipitation of monomer. In order to increase the rate of polymerization at lower temperatures, we increased the reaction concentration to 2 M and decreased the $[M]_0:[I]_0$ to 50:1. With these conditions, the ROP carried out in THF resulted in 75% conversion of monomer in 20 minutes. After isolation, the polymer was observed to be regio-random with a negligible change in the X_{reg} value (Table 2.2, entry 3). In case of toluene, the monomer was only partially soluble at -20 °C even with $[M]_0 = 1$ M. This retarded the polymerization rate and only 37% of monomer conversion was observed in 5 hours (Table 2.2, entry 4). Further lowering of reaction temperature to -45°C resulted in even poorer solubility of monomer in toluene. At the same temperature, the reaction in THF

Figure 2.5. Structure of catalysts used in the regio-regular polymerization of α -PhTMC **2.18****Table 2.2.** Optimization of Ring opening polymerization of α -PhTMC **2.18**

entry ^{a,b,c}	catalyst	$[M]_0/[I]_0$	[cat] ^d (mol%)	temp (°C)	time (min)	conv ^e (%)	$M_{n,theo}$ ^f (g mol ⁻¹)	$M_{n,NMR}$ ^g (g mol ⁻¹)	$M_{n,SEC}$ ^h (g mol ⁻¹)	\bar{D}	X_{reg}
1 ^a	2.13	100/1	0.5	27	150	76	13690	17800	11100	1.41	0.01
2 ^{a,c}	2.13	100/1	0.5	27	30	87	15650	19600	10400	1.48	0.00
3 ^b	2.13	50/1	0.5	-20	20	75	6920	8700	6500	1.40	0.03
4 ^{a,c}	2.13	50/1	0.5	-20	300	37	3540	nd ⁱ	nd	nd	nd
5 ^b	2.19 + DBU	50/1	2	27	750	98	8730	7500	4500	1.37	0.06
6 ^b	TBD	100/1	2	27	5	95	17070	17800	9200	1.43	0.40
7 ^b	TBD	50/1	2	-20	60	99	9060	10500	6600	1.36	0.61
8 ^a	TBD	50/1	2	-45	90	98	8880	8500	6100	1.32	0.70

Reactions were run either at ^a $[M]_0 = 1$ M or ^b $[M]_0 = 2$ M; ^cToluene was used as solvent; ^dwith respect to monomer; ^eReaction aliquots were quenched and conversions were determined by ¹H NMR recorded using CDCl₃ as solvent for room temperature reactions. For reactions run at lower temperatures, multiple reactions were set up side by side and were quenched at different time points to measure conversion; ^fCalculated using the formula $([M]_0/[I]_0) \times (\text{conversion}/100) \times (\text{molar mass of repeating unit} = 178 \text{ g mol}^{-1}) + (\text{molar mass of initiator} = 158 \text{ g mol}^{-1})$; ^gEstimated by ¹H NMR analysis in CDCl₃ (*Vide Infra*); ^hEstimated by SEC using THF as eluent against polystyrene standards (uncorrected data); ⁱNot determined.

was very slow and only 12% conversion of monomer was observed over 15 hours. In summary, phosphazene **2.13** was found to be ineffective in inducing regioselectivity in the case of ROP of α -PhTMC. This is in contrast to the results obtained in the ROP of α -MeTMC. Therefore, we decided to look for other catalysts that might promote a more regio-regular polymerization.

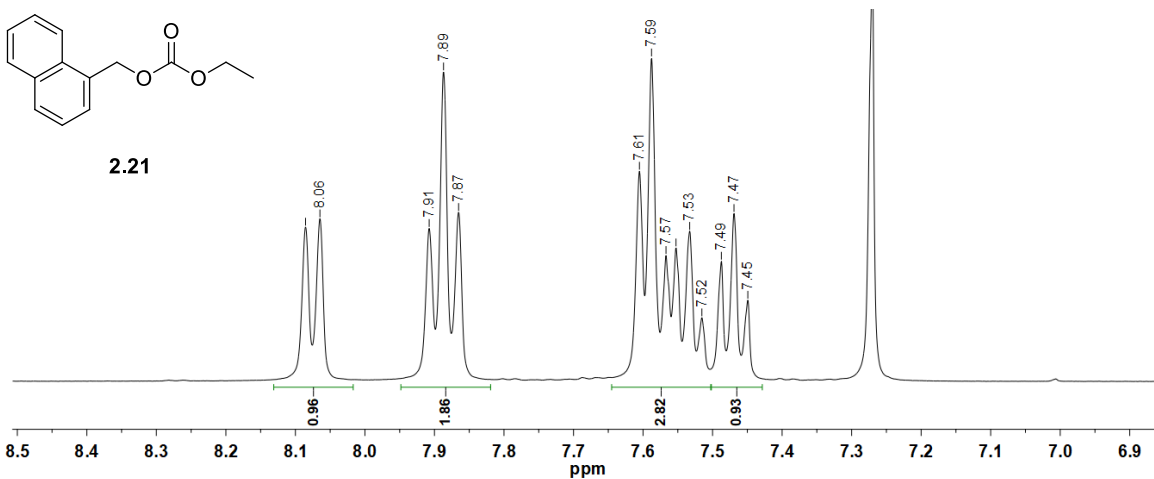
Combinations of thiourea and strong bases have been reported to be excellent organocatalysts for ROP of TMC and other cyclic monomers.^{1, 3, 49-52} When the ROP of α -PhTMC was carried out using the combination of thiourea **2.19** (Figure 2.5) and DBU, 98% monomer conversion was observed after 12.5 hours at room temperature for a $[M]_0:[I]_0$ of 50:1 (Table 2.2, entry 5). The precipitated polymer was found to be regio-random with X_{reg} of 0.06. In our next part of studies on the ROP of α -PhTMC, we decided to use commercially available strong base TBD as an organocatalyst. TBD was shown to induce high regio-regularity for the ROP of sugar-based cyclic carbonates.^{11, 12, 53} Wooley and coworkers have shown that the regio-regularity is dependent on the nature of substituents attached to the monomer ring.⁵³ Initially, the ROP of α -PhTMC catalyzed by TBD was attempted at room temperature in THF. In this reaction, 95% monomer conversion was observed within 5 minutes (Table 2.2, entry 6). The obtained polymer showed promising regio-regularity ($X_{reg} = 0.40$). Since TBD showed the best result among the screened catalysts, we decided to optimize the ROP with TBD to achieve better regio-regularity. When the reaction temperature was lowered to -20 °C the regio-regularity of the polymer increased to 0.61 (Table 2.2, entry 7). The regio-regularity of polymer improved to 0.7 when the reaction was carried out at -45 °C (Table 2.2, entry 8). Further improvement of regio-regularity was not possible because of the poor solubility of the monomer beyond -45 °C.

Estimation of Number Average Molar Mass of Poly(α -PhTMC)s

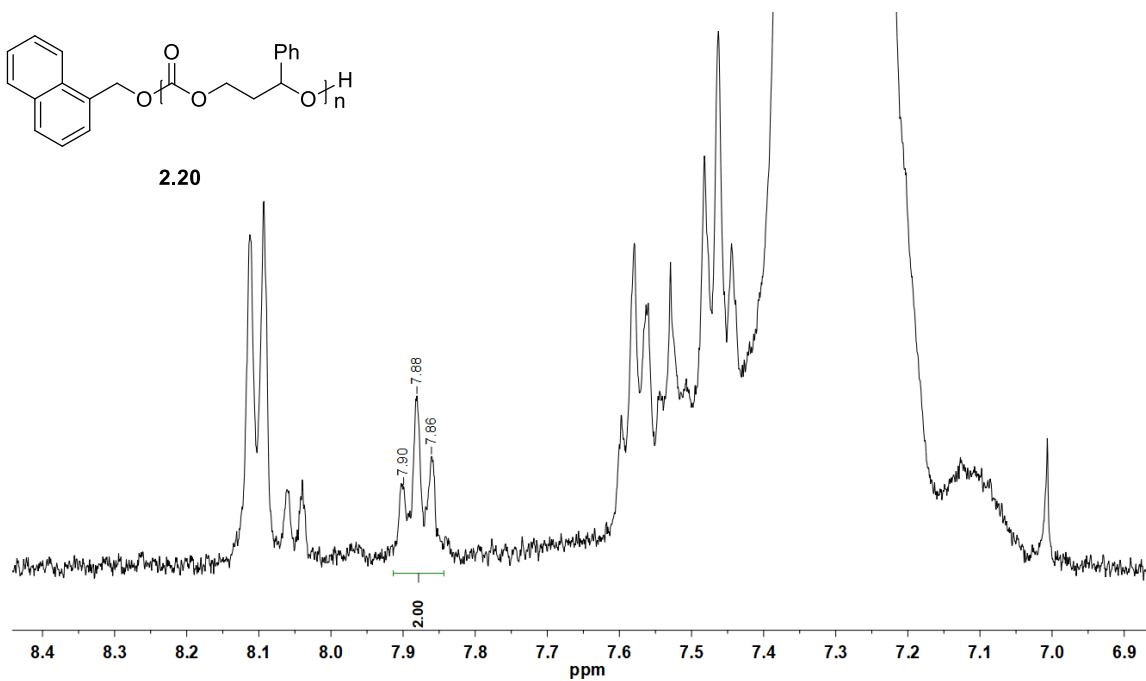
The number average molar mass (M_n) of synthesized polymers were determined by Size Exclusion Chromatography (SEC) and ^1H NMR (Table 2.2). In SEC, M_n was estimated against narrow disperse polystyrene standards by eluting polymer solution using THF in a polystyrene-*co*-divinylbenzene gel column. Here, the estimated $M_{n,\text{SEC}}$ are reported as raw uncorrected data. On the other hand, using ^1H NMR, M_n was estimated by analysis of end groups. In the synthesized poly(α -PhTMC)s, the naphthalene- CH_2 - moiety of initiator is one of the end groups. On examining the ^1H NMR of polycarbonate, we were able to identify an apparent triplet at δ 7.88 which is part of the naphthalene ring and integrates to two protons. To support this assignment, we have synthesized ethyl (naphthalen-1-ylmethyl) carbonate **2.21** (Figure 2.6a). The ^1H NMR of this compound shows an apparent triplet at δ 7.89 which integrates to two protons. Previously, ^1H NMR of methyl (naphthalen-1-ylmethyl) carbonate⁵⁴ and naphthalen-1-ylmethyl phenyl carbonate⁵⁵ have been reported. Both compounds show an apparent triplet at δ 7.89 that integrates to two protons. Based on this, we assigned the triplet at δ 7.88 in the polycarbonate to the naphthalene end group (Figure 2.6b). By integrating the triplet at δ 7.88 (represented as ● in the ^1H NMRs' of polycarbonate spectra) to two protons and then integrating the peaks belonging to the repeating unit in the alkyl region, M_n of the polycarbonate can be estimated. The integration of the aromatic protons present in the polymer samples is not accurate due to the overlap of residual CHCl_3 peak from the NMR solvent. The M_n estimated using ^1H NMR matched closely with the expected value calculated from the monomer to initiator ratio. The M_n measured by SEC showed lower than expected values. This is most likely due to the differences in the hydrodynamic radii of polystyrene and our polycarbonate.

Figure 2.6. Identification of End-Group Using ^1H NMR: (A) Expansion of Aromatic Region of ^1H NMR (CDCl_3) of Synthesized Carbonate **2.21**. (B) Expansion of Aromatic Region of ^1H NMR (CDCl_3) of poly(α -PhTMC) **2.20**

A



B



Synthesis of Poly(α -PhTMC)s of Various Degrees of Polymerization

Under the optimized polymerization condition, poly(α -PhTMC)s of various degrees of polymerization (DP) were synthesized by varying $[M]_0/[I]_0$ from 25 to 100 (Table 2.3). All the reactions were quenched only after high monomer conversions ($\geq 98\%$). In every reaction, the molar mass estimated using ^1H NMR was in good agreement with the expected molar mass. Initially, the ROP with $[M]_0/[I]_0$ of 25 resulted in X_{reg} of 0.63 (Table 2.3, entry 1). Interestingly, the value of X_{reg} jumped to 0.70 upon increasing the $[M]_0/[I]_0$ to 50 (Table 2.3, entry 2). Further increase of $[M]_0/[I]_0$ to 75 and 100 resulted in X_{reg} of 0.71 and 0.72 respectively (Table 2.3, entries 3 & 4).

Table 2.3. ROP of α -PhTMC **2.18** using TBD by varying monomer to initiator ratios.

entry ^a	$[M]_0/[I]_0$	time (min)	conv ^b (%)	$M_{n,theo}^c$ (g mol ⁻¹)	$M_{n,NMR}^d$ (g mol ⁻¹)	$M_{n,SEC}^e$ (g mol ⁻¹)	\bar{D}	X_{reg}	Yield (%)
1 ^f	25/1	90	99	4610	5500	4100	1.29	0.63	84
2	50/1	90	98	8880	8500	6100	1.32	0.70	82
3	75/1	120	98	13330	14200	7900	1.37	0.71	86
4	100/1	180	98	17610	17600	9600	1.39	0.72	83

^aSolvent = THF; temperature = -45 °C; $[M]_0 = 1$ M; $[cat] = 2$ mol% was used with respect to monomer;

^bMultiple reactions were set up side by side and were quenched at different time points to measure conversion; ^cCalculated using the formula $([M]_0/[I]_0) \times (\text{conversion}/100) \times (\text{molar mass of repeating unit} = 178 \text{ g mol}^{-1}) + (\text{molar mass of initiator} = 158 \text{ g mol}^{-1})$; ^dEstimated by ^1H NMR analysis in CDCl_3 ; ^eEstimated by SEC using THF as eluent against polystyrene standards (uncorrected data); ^fPrecipitation of the monomer was observed across four trials for this particular ratio of monomer to initiator. This led to a slowing down of the reaction.

Living Behavior of ROP of α -PhTMC

In order to show that the ROP of α -PhTMC exhibits living behavior we studied the reaction kinetics. For this purpose, multiple reactions were set up at the same time and were quenched at different time periods. Monomer conversions were determined using ^1H NMR. The plot of $\ln([M]/[M]_0)$ versus time was linear and this showed that the ROP was first order in monomer (Figure 2.7). In another experiment, the plot of M_n (SEC) versus monomer conversion showed a linear dependence with intercept at the origin (Figure 2.8). These two experiments along with excellent correlation of the observed molar mass with the monomer to initiator ratio suggests that the polymerization proceeds under living conditions.

Figure 2.7. Kinetic plot of $\ln([M]/[M]_0)$ versus time for ROP of **2.18**

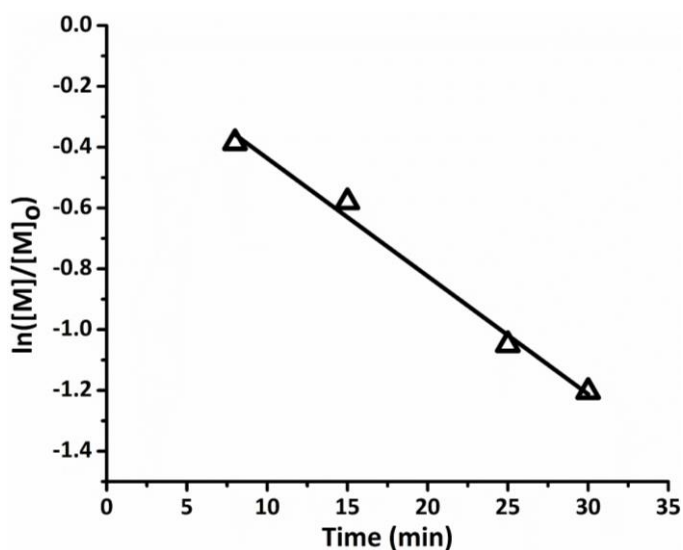
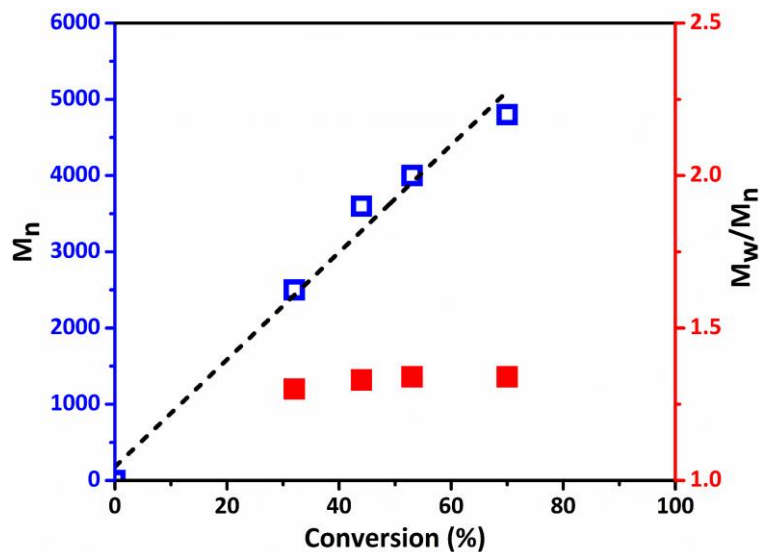


Figure 2.8. Plots of M_n and M_w/M_n versus monomer conversion for ROP of **2.18**



Effect of Substituents on the Regio-Regularity

To demonstrate the easy tunability of the polymer structure and to study the effect of substituents on the regio-regularity, we decided to evaluate monomers with various substitution patterns on the aromatic ring. In our studies, monomers with electron-donating and electron withdrawing groups on the para position of the phenyl ring were readily synthesized from corresponding diols, which were in turn obtained by reduction of β -keto esters. ROP of these substituted monomers were carried out under optimized condition with $[M]_0/[I]_0$ of 50. The monomer α -4-Me-PhTMC (**2.22**, Table 2.4) has poor solubility at -45 °C and precipitates out in some of the reactions. If the monomer precipitates during the polymerization, the rate of ROP reduces and about 97% of monomer conversion was observed in 6 hours (Table 2.4, entry 1). When the monomer remained soluble the polymerization reached above 90% in 2 hours and yielded polycarbonate with X_{reg} greater than the polycarbonate obtained from the slower reaction. Overall the ROP of α -4-Me-PhTMC **2.22** was observed to be slower than α -PhTMC. On the other hand, the electron

withdrawing substituents accelerate the ROP. The ROP of α -4-Br-PhTMC **2.23** reached 99% conversion within 30 minutes (Table 2.4, entry 2). The ROP was even faster in case of α -4-CF₃-PhTMC **2.24**, where 91% of conversion was observed within 5 minutes (Table 2.4, entry 3). Once again the molar mass estimated from ¹H NMR matched well with the expected value. Regarding the regio-regularity of the obtained polycarbonates, a clear trend was observed between X_{reg} and the nature of substituents. The electron-donating methyl group reduced the X_{reg} to 0.51 (Table 2.4, entry 1) while, the electron withdrawing groups Br and CF₃ significantly increased the X_{reg} value to 0.81 and 0.89 respectively (Table 2.4, entries 2 & 3). With the introduction of electron withdrawing CF₃ group on the α -PhTMC, a highly regio-regular polycarbonate was synthesized (Table 2.4, entry 3).

Table 2.4. ROP of α -ArTMC **2.22-2.24** using TBD as catalyst

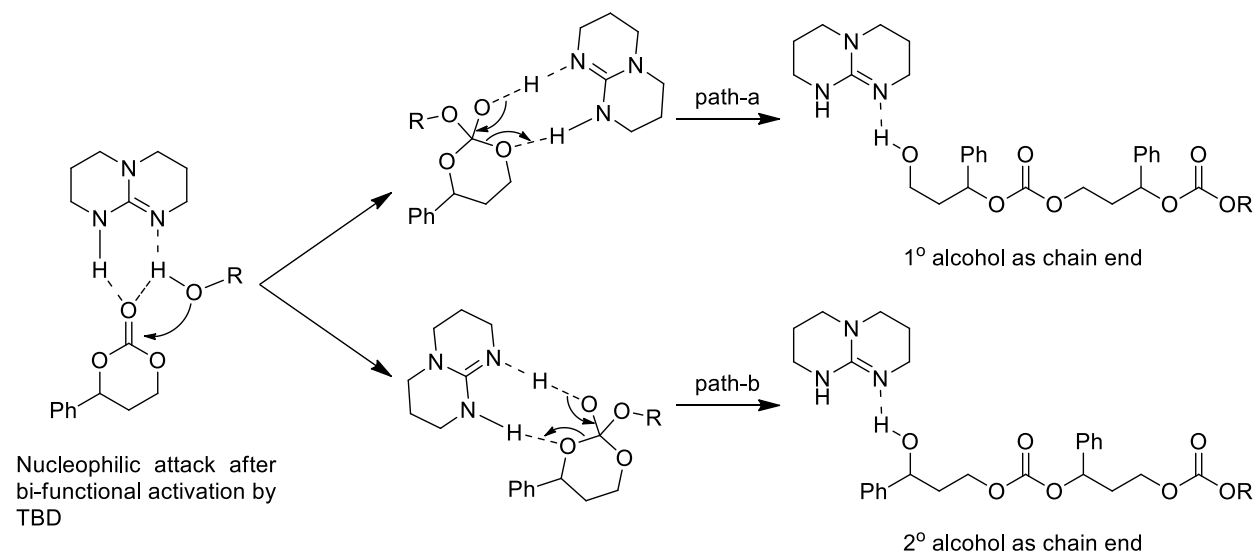
entry ^a	monomer	time (min)	conv ^b (%)	$M_{n,theo}^c$ (g mol ⁻¹)	$M_{n,NMR}^d$ (g mol ⁻¹)	$M_{n,SEC}^e$ (g mol ⁻¹)	\bar{D}	X_{reg}	Yield (%)
1	2.22 ^f	360	97	9570	10500	6500	1.40	0.51	83
2	2.23	30	99	13010	14000	7900	1.33	0.81	88
3	2.24	5	91	11470	12200	9700	1.35	0.89	70

^a[M]₀/[I]₀/[cat] = 50/1/1; [M]₀ = 1 M; ^bMultiple reactions were set up side by side and were quenched at different time points to measure conversion; ^cCalculated using the formula ([M]₀/[I]₀) X (conversion/100) X (molar mass of repeating unit = (**2.22** = 192 g mol⁻¹) (**2.23** = 257 g mol⁻¹) (**2.24** = 246 g mol⁻¹) + (molar mass of initiator = 158 g mol⁻¹); ^dEstimated by ¹H NMR analysis in CDCl₃; ^eEstimated by SEC using THF as eluent against polystyrene standards (uncorrected data); ^fThe monomer has solubility problem at -45 °C, if the monomer stays soluble from the start of polymerization, above 90% of conversion can be achieved in 120 mins with X_{reg} = 0.60.

Ring-opening Pathways and Regio-regularity

The ring opening pathways depicted in Scheme 2.1, clearly show that complete regio-regularity (H-T linkages) can be achieved when the monomer rings open to generate the same end group each time. ROP involving non-selective generation of both 1° and 2° alcohol end groups will lead to a regio-random polymer. Recently, Wooley and co-workers upon investigating the mechanism of TBD catalyzed ROP of glucose-based cyclic carbonates, reported that the protecting group of the monomer can influence regio-regularity of the polymer.⁵³ The monomer having carbonate protecting groups yields polymer with high regio-regularity while ether protecting groups lead to the formation of regio-random polymer. DFT calculations showed that in the transition state, a hydrogen bond exists between the carbonyl oxygen of the carbonate and the α -proton of TBD. This hydrogen bond is responsible for selective ring opening of the cyclic carbonate. In our case, the substituent on the aromatic ring is likely to be not present in a favorable position to have a direct interaction with the TBD. Therefore, it is likely that the substituent modulates the leaving-group ability. The two pathways for the ROP of carbonates catalyzed by TBD are shown in Figure 2.9. Here, the regioselective ring opening is likely to be determined by the preferential departure of one-alkoxide group over the other. The observed increase in regio-regularity with the electron withdrawing substituent on the aromatic ring suggests that the secondary alcohol is the leaving group (Figure 2.9, path b). Enhancement of the leaving group ability by the electron-withdrawing groups could be one reason for the increased regio-regularity.

Figure 2.9. Ring opening pathways for the formation of primary and secondary alcohol end groups.



Variation of T_g with Regio-regularity

As mentioned earlier, Hillmyer and co-workers had shown that stereo-regular poly(α -MeTMC) with low regio-regularity exists as an amorphous polymer. An increase in regio-regularity results in a semicrystalline polymer with greater T_g .⁴³ This implies that the regio-regularity significantly enhances the crystallinity of polymer by increasing the interactions between the polymer chains. Since our optimization of ROP of α -PhTMC resulted in polymers with different regio-regularities, we were interested in studying the effect of regio-regularity on T_g . In this study we selected three samples of poly(α -PhTMC) that were similar in degrees of polymerization (DP) and dispersity but had varying regio-regularities (Table 2.5, entries 1-3). All the three samples were found to be amorphous polymers, as only glass transition temperatures were observed in Differential Scanning Calorimetry (DSC). For regio-irregular poly(α -PhTMC), the T_g was found to be 39 °C (Table 2.5, entry 1) and this was observed to be significantly higher than the T_g of stereo and regio-regular poly(α -

Table 2.5. Comparison of Polycarbonate **2.20** of Varying X_{reg} with T_g

entry ^{a,b,c}	polymer	DP ^d	\bar{D}	X_{reg}	T_g
1 ^a	2.20	99	1.41	0.01	39 °C
2 ^b	2.20	99	1.43	0.40	50 °C
3 ^c	2.20	98	1.39	0.72	49 °C

^aTable-2.2 entry 1; ^bTable-2.2 entry 6; ^cTable-2.3 entry 4;

^dDegree of polymerization calculated from $M_{n,NMR}$

MeTMC) ($T_g = -2$ °C). The poly(α -PhTMC) with moderate regio-regularity ($X_{reg} = 0.40$) exhibits T_g of 50 °C (Table 2.5, entry 2), while the polymer with X_{reg} of 0.72 showed a T_g of 49 °C (Table 2.5, entry 3). This clearly shows that the T_g can be varied with the regio-regularity, as the T_g increase when going from a regio-random to a more regio-regular polymer. However, beyond a certain level of regio-regularity, the T_g remained unchanged with the increase in X_{reg} . This observation suggests that in the case of stereo-irregular poly(α -PhTMC) the effect of regio-regularity on the T_g is limited to a certain extent. This effect is likely to be greater in the case of stereo-regular poly(α -PhTMC).

Similarly, to study the effect of regio-regularity on T_g for the substituted poly(α -PhTMC)s, we synthesized three polymers that differ in X_{reg} for each substituent. Unlike poly(α -PhTMC), the variation of T_g with the regio-regularity is not significant in the case of substituted poly(α -PhTMC)s (Tables 2.6-2.8). For poly(α -4-Me-PhTMC)s **2.25**, there was a small increase of T_g (48 °C to 51 °C) when the X_{reg} was increased from 0.11 to 0.23 (Table 2.6, entries 1 & 2). Beyond X_{reg} of 0.23 there was no notable increase of T_g (Table 2.6, entry 3). Likewise, in poly(α -4-Br-PhTMC)s **2.26** a small increase of T_g (63 °C to 65 °C) was observed for an increase of X_{reg} from 0.16 to 0.57 (Table 2.7, entries 1 & 2). The T_g remained unchanged upon further increase of X_{reg} (Table 2.7, entry 3). In the case of poly(α -4-CF₃-PhTMC)s **2.27** once again, there was only a small increase in T_g (60 °C to 63 °C) for

the X_{reg} ranging from 0.36 to 0.89 (Table 2.8, entries 1-3). The above measurements suggest that there is a small effect of regio-regularity on the T_g for substituted poly(α -PhTMC)s. Overall, the DSC study shows that the replacement of methyl with a more rigid substituent such as aromatic ring in the α position of TMC improves the physical property of the aliphatic polycarbonate. This is due to the restricted rotation of the pendant groups. Additionally, the DSC study indicates that the variation of regio-regularity can lead to change in T_g to certain extent and also T_g can be varied with the substituents on the aromatic ring. In

Table 2.6. Comparison of Polycarbonate **2.25** of Varying X_{reg} with T_g

entry ^{a,b,c}	polymer	DP ^d	\bar{D}	X_{reg}	T_g
1 ^a	2.25	62	1.45	0.11	48 °C
2 ^b	2.25	55	1.38	0.23	51 °C
3 ^c	2.25	54	1.40	0.51	52 °C

All the reactions were carried out in THF with $[M]_0/[I]_0/[C]_0 = 50/1/1$; ^aReaction was carried out using **2.19 + DBU** as catalyst at 27 °C, time = 13 h (for 96% conversion) ; ^bReaction was carried out using **TBD** as catalyst at 27 °C, time = 7 mins (for 96% conversion); ^cTable-2.4 entry 1; ^dDegree of polymerization calculated from $M_{n,NMR}$

Table 2.7. Comparison of Polycarbonate **2.26** of Varying X_{reg} with T_g

entry ^{a,b,c}	polymer	DP ^d	\bar{D}	X_{reg}	T_g
1 ^a	2.26	41	1.35	0.16	63 °C
2 ^b	2.26	40	1.37	0.57	65 °C
3 ^c	2.26	47	1.32	0.81	65 °C

All the reactions were carried out in THF with $[M]_0/[I]_0/[C]_0 = 50/1/1$; ^aReaction was carried out using **2.19 + DBU** as catalyst at 27 °C, time = 5 h (for 96% conversion) ; ^bReaction was carried out using **TBD** as catalyst at 27 °C, time = 6 mins (for 93% conversion); ^cReaction condition similar to that of Table-2.4 entry 2; ^dDegree of polymerization calculated from $M_{n,NMR}$

Table 2.8. Comparison of Polycarbonate **2.27** of Varying X_{reg} with T_g

entry ^{a,b,c}	polymer	DP ^d	\bar{D}	X_{reg}	T_g
1 ^a	2.27	43	1.35	0.35	60 °C
2 ^b	2.27	42	1.39	0.70	61 °C
3 ^c	2.27	49	1.35	0.89	63 °C

All the reactions were carried out in THF with $[M]_0/[I]_0/[C]_0 = 50/1/1$; ^aReaction was carried out using **2.19 + DBU** as catalyst at 27 °C, time = 3.5 h (for 96% conversion) ; ^bReaction was carried out using **TBD** as catalyst at 27 °C, time = 4 mins (for 93% conversion); ^cTable-2.4 entry 3; ^dDegree of polymerization calculated from $M_{n,NMR}$

our study, the substituted poly(α -PhTMC)s shows higher T_g s than the unsubstituted, with the highest being poly(α -4-Br-PhTMC) **2.26** ($T_g = 65$ °C, Table 2.7, entry 3).

2.5 Conclusions

Among the different types of cyclic carbonates available for the synthesis of aliphatic polycarbonates *via* ROP, we had chosen α -substituted trimethylene carbonate as the monomer of our interest. These monomers can be readily accessible (including in enantiopure forms) and also it provides good scope for the introduction of various substituents. In this work, we had synthesized various α -ArTMCs as the monomer for ROP. The more rigid substituents such as aromatic ring would restrict the rotation of pendant groups and therefore can enhance the physical properties of polymer compared to the methyl substituent. Also, with the presence of aromatic ring, various kinds of substituents can be introduced to tune the properties of polymers. To solve the challenge of regioselective ROP of α -ArTMCs, we initially used organocatalysts such as phosphazene base and combination of thiourea and DBU. These catalysts yielded regio-random to low regio-regular polymers. The ROP of α -ArTMCs catalyzed by TBD in THF at -45 °C yielded moderate to high regio-

regular polymers depending on the kind of substituents. Electron-donating substituent methyl exhibited low regio-regularity ($X_{reg} = 0.51$), whereas electron withdrawing substituents Br ($X_{reg} = 0.81$) and CF_3 ($X_{reg} = 0.89$) exhibited moderate and high regio-regularity respectively. DSC studies showed that all poly(α -ArTMC)s exist as an amorphous polymers with T_g ranging from 39 °C to 65 °C depending on the molar mass, regio-regularity and substituents. This clearly shows that the poly(α -ArTMC)s has greater T_g than the regio and stereo-regular poly(α -MeTMC) ($T_g = -2$ °C and $T_m = 73$ °C). Also, it was found that the T_g increases with the regio-regularity to certain extent and the effect was observed to be more pronounced in poly(α -PhTMC). The T_g was also found to vary with the substituents on the aromatic ring. The physical properties of poly(α -ArTMC)s can be further improved by employing their respective enantiopure isomers for the regio-regular ROP. In the third chapter we will discuss about the synthesis and morphological studies of di-block copolymers having different electronic environments.

2.5 Experimental Section

Materials

All glasswares were dried overnight in an oven at 120 °C prior to use. Reactions were carried out under argon atmosphere using standard Schlenk techniques and were monitored by thin layer chromatography (TLC) using Merck TLC silica gel 60 F254. Polymerization reactions were carried out inside glove box (except for lower temperature reactions, where only measurements were carried out inside the glove box). Flash column chromatography was performed using silica gel of mesh size 230-400. Grease-free solvents for flash column chromatography were obtained by distillation. Methanol was distilled over Mg turnings. DCM was distilled over CaH_2 . Pyridine was distilled over CaH_2 . THF was

distilled over sodium-benzophenone after ketyl formation and stored in glove box. Distilled THF was dried over activated neutral alumina prior to use. TBD was dried azeotropically with dry benzene under argon atmosphere. 1-naphthalenemethanol was sublimed under high vacuum. Monomers were dried azeotropically using dry benzene under argon atmosphere prior to use. All other chemicals obtained from commercial sources were used without further purification.

Instrumentation and Characterization

Infrared spectra were recorded on Perkin Elmer FT-IR diamond crystal. ^1H and ^{13}C NMRs were recorded on a Bruker AVANCE-400 (400 MHz) Fourier transform NMR spectrometer. Chemical shifts are reported in parts per million (ppm) with respect to the residual solvent peak: CDCl_3 (^1H NMR: 7.27 ppm, ^{13}C { ^1H } NMR: 77.2 ppm); DMSO-d_6 (^1H NMR: 2.50 ppm, ^{13}C { ^1H } NMR: 39.5 ppm). HRMS were recorded using Agilent Q-TOF spectrometer. Melting points were measured using melting point apparatus from Techno Instruments and are uncorrected. Size exclusion chromatography (SEC) was performed on a Shimadzu, isocratic HPLC pump, refractive index detector (RID-10A), and a PLgel polystyrene-*co*-divinylbenzene gel column (Polymer Lab) 5 μm MiniMix-C (250x4.6 mm). The measurements were conducted at 40 $^\circ\text{C}$ with THF as eluent (flow rate set to 0.5 mL/min) against narrow disperse polystyrene standards. Data collection and analyses were carried out using Lab solutions software. Thermogravimetric analysis (TGA) was performed on a Mettler-Toledo model TGA/DSC 2, under nitrogen atmosphere with a heating rate of 10 $^\circ\text{C}/\text{min}$. The measurements were analyzed using Mettler-Toledo Star^e software. Glass transition temperatures (T_g) were measured by Differential scanning calorimetry (DSC) on a TA-DSC Q2000 under N_2 atmosphere with a heating and cooling rate of 5 $^\circ\text{C}/\text{min}$ from -20

°C to 150 °C. Measurements were analyzed using TA universal analysis software. The T_g was taken as the midpoint of the inflection tangent, upon the second heating scan.

Synthetic Procedures of Monomers

4-Phenyl-1,3-dioxan-2-one (2.18)

Procedure for the Synthesis of 1-Phenylpropane-1,3-diol (2.17):

A 500 mL two-neck round bottom flask was charged with 20 mL of ethyl benzoyl acetate (115.5 mmol). The flask was purged with argon following which 245 mL of dry MeOH was added. The flask was then cooled to 0 °C in an ice bath. To the clear solution, 13.16 g of sodium borohydride (346.5 mmol, 3 equivalents) was added portion-wise over two hours. After completion of addition, the contents were warmed to room temperature and stirred overnight. Upon completion (by TLC), the solvent was removed under reduced pressure to obtain a white viscous suspension. The suspension was diluted with 400 mL of water and extracted into ethyl acetate (3 × 200 mL). The combined organic layers were washed with 100 mL of brine, dried over Na₂SO₄ and concentrated to obtain 15.5 g of the crude product **2.17** (89% yield, average yield over two runs = 88%).⁴⁷ This was used in the subsequent step without further purification.

Characterization:

Pale yellow liquid; R_f : 0.43 in 70% EtOAc in Hexanes; ¹H NMR (400 MHz, CDCl₃): δ 7.38-7.28 (m, 5H), 4.98 (dt, 1H, J = 8.6, 3.0 Hz), 3.88 (dt, 2H, J = 9.2, 4.6 Hz), 2.86 (d, 1H, J = 2.5 Hz), 2.40 (br s, 1H), 2.08-1.91 (m, 2H).

Procedure for the Synthesis of 2.18:

The crude product **2.17** (15.5 g, 101.9 mmol) was dissolved in 100 mL of dry CH₂Cl₂ and transferred to a two-liter flask maintained under argon. An additional 820 mL of dry

CH₂Cl₂ was added followed by 22.2 mL of freshly distilled pyridine (275.2 mmol, 2.7 equivalents). To the clear solution, 18.2 g of 1,1'-carbonyldiimidazole (112.1 mmol, 1.1 equivalents) dissolved in 510 mL of dry CH₂Cl₂ was added dropwise over three hours. After stirring overnight, the reaction mixture was washed with 1M HCl (3 × 250 mL). The organic layer was further washed with 250 mL of water and 250 mL of brine. The organic layer was dried over Na₂SO₄ and concentrated to obtain a colorless liquid. The resulting liquid was recrystallized from 1:1 ethyl acetate and hexanes to obtain 9.8 g of pure product **2.18** (48% yield over two steps, average yield over two runs = 45%).⁴⁸

Characterization:

White solid; Mp: 58-60 °C; R_f: 0.33 in DCM; ¹H NMR (400 MHz, CDCl₃): δ 7.45-7.36 (m, 5H), 5.54 (dd, 1H, *J* = 9.8, 3.7 Hz), 4.56-4.46 (m, 2H), 2.37 (ddd, 1H, *J* = 14.6, 7.5, 3.7 Hz), 2.31-2.21 (m, 1H); ¹³C{¹H} NMR (100 MHz, CDCl₃): δ 148.9, 137.9, 129.12, 129.06, 125.7, 80.2, 67.0, 29.5; IR: 1720 cm⁻¹; HRMS (ESI/Q-TOF) *m/z*: [M+Na]⁺ calcd for C₁₀H₁₀NaO₃ 201.0522; Found 201.0511.

4-(p-Tolyl)-1,3-dioxan-2-one (2.22)

Procedure for the Synthesis of Ethyl 3-oxo-3-(p-tolyl)propanoate (2.28):

A 250 mL two-neck round bottom flask was charged with 50 mL of potassium hexamethyldisilazide (0.5 M in toluene, 25 mmol, 1.11 equivalents) under argon and diluted with 20 mL of dry THF. To the clear solution, 3.0 mL of 4-methyl acetophenone (22.5 mmol) in 20 mL of dry THF was added dropwise over a period of 15 minutes and stirred for 1 hour. To the brown suspension 13.6 mL of diethyl carbonate (112.4 mmol, 5.0 equivalents) was added dropwise for 10 minutes. After completion of addition, the reaction was refluxed for 2 hours. After two hours, the reaction mixture was quenched by slow

addition of 50 mL of water. The reaction mixture was then acidified with 50 mL of 1M HCl solution. Care should be taken to ensure the pH of the aqueous layer is maintained at 2. The reaction mixture was transferred to a separatory funnel and the aqueous layer was extracted with EtOAc (3 x 100 mL). The organic layers were combined and washed with 100 mL of brine solution. The organic layer was dried over Na₂SO₄ and concentrated to obtain 4.5 g of crude product as a brown liquid. The crude material was purified by column chromatography.

Column Chromatography:

Approximately 160 mL of silica was packed into a column using 5% EtOAc in hexanes as the solvent. The crude material was loaded as such on the column. Approximately 1400 mL of 5% EtOAc in hexanes was eluted. The eluted solvent was collected in 25 mL fractions. Fractions 30-37 contained product. The impure fractions were concentrated and subjected to another column under same condition. The pure fractions were concentrated to obtain 3.19 g of **2.28** (69% yield, average yield over two runs = 68%).⁵⁶

Characterization:

Pale yellow liquid; R_f: 0.20 in 6% EtOAc in hexanes; ¹H NMR (400 MHz, CDCl₃): δ 12.58 (s, 0.18x1H, enol), 7.84 (d, 0.82x2H, *J* = 8.2 Hz, keto), 7.67 (d, 0.18x2H, *J* = 8.3 Hz, enol), 7.27 (d, 0.82x2H, *J* = 8.8 Hz, keto), 7.22 (d, 0.18x2H, *J* = 8.1 Hz, enol), 5.63 (s, 0.18x1H, enol), 4.26 (q, 0.18x2H, *J* = 7.1 Hz, enol), 4.21 (q, 0.82x2H, *J* = 7.1 Hz, keto), 3.96 (s, 0.82x2H, keto), 2.42 (s, 0.82x3H, keto), 2.39 (s, 0.18x3H, enol), 1.33 (t, 0.18x3H, *J* = 7.1 Hz, enol), 1.26 (t, 0.82x3H, *J* = 7.1 Hz, keto).

Procedure for the Synthesis of 1-(p-Tolyl)propane-1,3-diol (2.29):

A 250 mL two-neck round bottom flask was charged with 7.64 g of **2.28** (37 mmol). The flask was purged with argon following which 80 mL of dry MeOH was added. The flask was then cooled to 0 °C in an ice bath. To the clear solution, 4.22 g of sodium borohydride (111 mmol, 3 equivalents) was added portion-wise over two hours. After completion of addition, the contents were warmed to room temperature and stirred for an additional two hours. Upon completion (by TLC), the solvent was removed under reduced pressure to obtain a white viscous suspension. The suspension was diluted with 200 mL of water and extracted into ethyl acetate (3 × 100 mL). The combined organic layers were washed with 100 mL of brine, dried over Na₂SO₄ and concentrated to obtain 5.85 g of the crude product **2.29** (95% yield, average yield over two runs = 94%).⁵⁷ This was used in the subsequent step without further purification.

Characterization:

Pale yellow liquid; R_f: 0.20 in 50% EtOAc in hexanes; ¹H NMR (400 MHz, CDCl₃): δ 7.24 (d, 2H, *J* = 7.9 Hz), 7.15 (d, 2H, *J* = 7.7 Hz), 4.90 (dd, 1H, *J* = 8.7, 3.5 Hz), 3.83-3.77 (m, 2H), 2.80 (br s, 2H), 2.34 (s, 3H), 2.03-1.86 (m, 2H).

Procedure for the Synthesis of 2.22:

The crude product **2.29** (5.85 g, 35.2 mmol) from the previous step was dissolved in 100 mL of dry CH₂Cl₂ and transferred to a one-liter flask maintained under argon. An additional 217 mL of dry CH₂Cl₂ was added followed by 7.7 mL of freshly distilled pyridine (95 mmol, 2.7 equivalents). To the clear solution, a solution of 6.3 g of 1,1'-carbonyldiimidazole (38.7 mmol, 1.1 equivalents) in 176 mL of dry CH₂Cl₂ was added dropwise over two hours. After stirring overnight, the reaction mixture was washed with 1M

HCl (3 × 125 mL). The organic layer was further washed with 125 mL of water and 125 mL of brine. The organic layer was dried over Na₂SO₄ and concentrated to obtain a pale yellow solid. The resulting solid was recrystallized from 1:1.25 ethyl acetate and hexanes to obtain 3.5 g of pure product **2.22** (52% yield over two steps, average yield over two runs = 51%).

Characterization:

White solid; Mp: 68-70 °C; R_f: 0.30 in DCM; ¹H NMR (400 MHz, CDCl₃): δ 7.25 (d, 2H, *J* = 8.6 Hz), 7.21 (d, 2H, *J* = 8.2 Hz), 5.49 (dd, 1H, *J* = 9.7, 3.7 Hz), 4.53-4.44 (m, 2H), 2.37 (s, 3H), 2.35-2.19 (m, 2H); ¹³C{¹H} NMR (100 MHz, CDCl₃): δ 149.0, 139.1, 135.0, 129.7, 125.7, 80.2, 67.0, 29.4, 21.3; IR: 1737 cm⁻¹; HRMS (ESI/Q-TOF) *m/z*: [M+Na]⁺ calcd for C₁₁H₁₂NaO₃ 215.0679; Found 215.0675.

4-(4-Bromophenyl)-1,3-dioxan-2-one (2.23)

Procedure for the Synthesis of 1-(4-Bromophenyl)propane-1,3-diol (2.30):

A 250 mL two-neck round bottom flask was charged with 10.0 g of ethyl 3-(4-bromophenyl)-3-oxopropanoate (37 mmol). The flask was purged with argon following which 80 mL of dry MeOH was added. The flask was then cooled to 0 °C in an ice bath. To the clear solution, 4.22 g of sodium borohydride (111 mmol, 3 equivalents) was added portion-wise over two hours. After completion of addition, the contents were warmed to room temperature and stirred for an additional two hours. Upon completion (by TLC), the solvent was removed under reduced pressure to obtain a white viscous suspension. The suspension was diluted with 200 mL of water and extracted into ethyl acetate (3 × 100 mL). The combined organic layers were washed with 100 mL of brine, dried over Na₂SO₄ and concentrated to obtain 8.12 g of the crude product **2.30** (95% yield, average yield over two runs = 94%).⁵⁸ This was used in the subsequent step without further purification.

Characterization:

Colorless liquid; R_f : 0.16 in 50% EtOAc in hexanes; ^1H NMR (400 MHz, CDCl_3): δ 7.47 (d, 2H, $J = 8.0$ Hz), 7.24 (d, 2H, $J = 8.0$ Hz), 4.92 (dd, 1H, $J = 8.1, 3.3$ Hz), 3.86-3.80 (m, 2H), 2.57 (br s, 2H), 2.00-1.86 (m, 2H).

Procedure for the Synthesis of 2.23:

The crude product **2.30** (8.12 g, 35.2 mmol) from the previous step was dissolved in 100 mL of dry CH_2Cl_2 and transferred to a one-liter flask maintained under argon. An additional 217 mL of dry CH_2Cl_2 was added followed by 7.7 mL of freshly distilled pyridine (95 mmol, 2.7 equivalents). To the clear solution, 6.3 g of 1,1'-carbonyldiimidazole (38.7 mmol, 1.1 equivalents) dissolved in 176 mL of dry CH_2Cl_2 was added dropwise over two hours. After stirring overnight, the reaction mixture was washed with 1M HCl (3×125 mL). The organic layer was further washed with 125 mL of water and 125 mL of brine. The organic layer was dried over Na_2SO_4 and concentrated to obtain a pale yellow liquid. The resulting liquid was recrystallized from 1:1.5 ethyl acetate and hexanes to obtain 4.8 g of pure product **2.23** (53% yield over two steps, average yield over two runs = 53%).

Characterization:

White solid; Mp: 66-68 °C; R_f : 0.30 in DCM; ^1H NMR (400 MHz, CDCl_3): δ 7.55 (d, 2H, $J = 8.4$ Hz), 7.25 (d, 2H, $J = 8.3$ Hz), 5.49 (dd, 1H, $J = 10.1, 3.5$ Hz), 4.56-4.45 (m, 2H), 2.34 (ddd, 1H, $J = 14.5, 7.1, 3.5$ Hz), 2.27-2.17 (m, 1H); $^{13}\text{C}\{^1\text{H}\}$ NMR (100 MHz, CDCl_3): δ 148.5, 137.0, 132.3, 127.4, 123.2, 79.5, 66.9, 29.4; IR: 1727 cm^{-1} ; HRMS (ESI/Q-TOF) m/z : $[\text{M}+\text{Na}]^+$ calcd for $\text{C}_{10}\text{H}_9\text{BrNaO}_3$ 278.9633 and 280.9612; Found 278.9617 and 280.9598.

4-(4-(Trifluoromethyl)phenyl)-1,3-dioxan-2-one (2.24)

Procedure for the Synthesis of Ethyl 3-oxo-3-(4-(trifluoromethyl)phenyl)propanoate (2.31):

A 100 mL two-neck round bottom flask was charged with 5.0 g of 4-(trifluoromethyl)benzoic acid (26.3 mmol). The flask was purged with argon following which 35 mL of dry THF was added. To the clear solution, 5.13 g of 1,1'-carbonyldiimidazole (31.55 mmol, 1.2 equivalents) was added portion-wise over 10 minutes at 0 °C and stirred for 45 minutes. The mixture was warmed to room temperature and stirred for 15 minutes. Separately, a 250 mL two-neck round bottom flask was charged with 3.5 mL of monoethyl malonate (31.55 mmol, 1.2 equivalents). The flask was purged with argon following which 85 mL of dry THF was added. To the clear solution, 8.0 mL of ⁱPrMgCl (2.0 M, 16.0 mmol, 0.6 equivalent) and 8.0 mL of ⁿBuLi (2.0 M, 16.0 mmol, 0.6 equivalent) was added at -78 °C. After stirring at room temperature for 45 minutes, the acylimidazole was added to this magnesium malonate solution over a period of 1 hour. The mixture was stirred at room temperature for 16 hours. Solvent was removed under reduced pressure and the residue was suspended in EtOAc (250 mL). The organic layer was washed with 1M HCl solution (100 mL). The organic layer was further washed with 100 mL of saturated NaHCO₃ solution and 100 mL of brine. The organic layer was dried over Na₂SO₄ and concentrated to obtain 5.5 g of crude product as a brown liquid. The crude material was purified by column chromatography.

Column Chromatography:

Approximately 200 mL of silica was packed into a column using 1% EtOAc in hexanes as the solvent. The crude material was loaded as such on the column. Approximately 400 mL of 1% EtOAc in hexanes, followed by 600 mL of 3% EtOAc in

hexanes was eluted. The eluted solvent was collected in 25 mL fractions. Fractions 14-40 contained product. The pure fractions were concentrated to obtain 3.88 g of **2.31** (57% yield, average yield over two runs = 50%).⁵⁹

Characterization:

Pale yellow liquid; R_f : 0.40 in 5% EtOAc in hexanes; $^1\text{H NMR}$ (400 MHz, CDCl_3): δ 12.57 (s, 0.47x1H, enol), 8.07 (d, 0.53x2H, $J = 8.1$ Hz, keto), 7.89 (d, 0.47x2H, $J = 8.2$ Hz, enol), 7.77 (d, 0.53x2H, $J = 8.3$ Hz, keto), 7.69 (d, 0.47x2H, $J = 8.3$ Hz, enol), 5.73 (s, 0.47x1H, enol), 4.30 (q, 0.47x2H, $J = 7.1$ Hz, enol), 4.23 (q, 0.53x2H, $J = 7.1$ Hz, keto), 4.02 (s, 0.53x2H, keto), 1.36 (t, 0.47x3H, $J = 7.1$ Hz, enol), 1.27 (t, 0.53x3H, $J = 7.1$ Hz, keto).

Procedure for the Synthesis of 1-(4-(trifluoromethyl)phenyl)propane-1,3-diol (2.32):

A 250 mL two-neck round bottom flask was charged with 9.0 g of **2.31** (34.8 mmol). The flask was purged with argon following which 73 mL of dry MeOH was added. The flask was then cooled to 0 °C in an ice bath. To the clear solution, 3.96 g of sodium borohydride (104.4 mmol, 3 equivalents) was added portion-wise over two hours. After completion of addition, the contents were warmed to room temperature and stirred for an additional two hours. Upon completion (by TLC), the solvent was removed under reduced pressure to obtain a white viscous suspension. The suspension was diluted with 250 mL of water and extracted into ethyl acetate (3 × 150 mL). The combined organic layers were washed with 100 mL of brine, dried over Na_2SO_4 and concentrated to obtain 6.94 g of the crude product **2.32** (91% yield, average yield over two runs = 90%).⁶⁰ This was used in the subsequent step without further purification.

Characterization:

Pale yellow liquid; R_f : 0.16 in 50% EtOAc in hexanes; ^1H NMR (400 MHz, CDCl_3): δ 7.62 (d, 2H, $J = 8.3$ Hz), 7.49 (d, 2H, $J = 8.1$ Hz), 5.05 (dd, 1H, $J = 7.8, 4.5$ Hz), 3.89 (t, 2H, $J = 5.4$ Hz), 2.54 (br s, 2H), 2.05-1.92 (m, 2H).

Procedure for the Synthesis of 2.24:

The crude product **2.32** (6.94 g, 31.56 mmol) from the previous step was dissolved in 100 mL of dry CH_2Cl_2 and transferred to a one-liter flask maintained under argon. An additional 185 mL of dry CH_2Cl_2 was added followed by 6.9 mL of freshly distilled pyridine (85.23 mmol, 2.7 equivalents). To the clear solution, 5.63 g of 1,1'-carbonyldiimidazole (34.7, 1.1 equivalents) in 158 mL of dry CH_2Cl_2 was added dropwise over two hours. After stirring overnight, the reaction mixture was washed with 1M HCl (3×150 mL). The organic layer was further washed with 150 mL of water and 150 mL of brine. The organic layer was dried over Na_2SO_4 and concentrated to obtain a pale yellow solid. The resulting solid was recrystallized from 1:4 ethyl acetate and hexanes to obtain 4.63 g of pure product **2.24** (59% yield over two steps, average yield over two runs = 56%).

Characterization:

White solid; Mp: 50-52 °C; R_f : 0.33 in DCM; ^1H NMR (400 MHz, CDCl_3): δ 7.69 (d, 2H, $J = 8.2$ Hz), 7.51 (d, 2H, $J = 8.2$ Hz), 5.60 (dd, 1H, $J = 10.1, 3.5$ Hz), 4.59-4.47 (m, 2H), 2.40 (ddd, 1H, $J = 14.5, 7.1, 3.5$ Hz), 2.29-2.19 (m, 1H); $^{13}\text{C}\{^1\text{H}\}$ NMR (100 MHz, CDCl_3): δ 148.3, 141.9, 131.4 (q, $J = 32.7$ Hz), 126.1 (q, $J = 3.8$ Hz), 126.05, 124.0 (q, $J = 272.3$ Hz), 79.3, 66.9, 29.5; IR: 1729 cm^{-1} ; HRMS (ESI/Q-TOF) m/z : $[\text{M}+\text{Na}]^+$ calcd for $\text{C}_{11}\text{H}_9\text{F}_3\text{NaO}_3$ 269.0401; Found 269.0392.

Synthetic Procedure of Ethyl (naphthalen-1-ylmethyl) carbonate (2.21)

A 10 mL two-neck round bottom flask was charged with 150 mg of 1-naphthalenemethanol (0.95 mmol). The flask was purged with argon following which 1 mL of dry DCM and 75 μ L of pyridine (0.94 mmol, 0.99 equivalent) were added. The flask was then cooled to 0 °C in an ice bath. To the clear solution, 90 μ L of ethyl chloroformate (0.94 mmol, 0.99 equivalent) was added dropwise. After completion of addition, the contents were warmed to room temperature and stirred overnight. Upon completion (by TLC), the reaction mixture was diluted with 15 mL of DCM and was washed with 10 mL of water. The DCM layer was further washed with 15 mL of 5% NaOH solution and 15 mL of brine. The DCM layer was dried over Na₂SO₄ and concentrated to obtain a colorless liquid. The crude material was purified by column chromatography.

Column Chromatography:

Approximately 30 mL of silica was packed into a column using 5% EtOAc in hexanes as the solvent. The crude material was loaded as such on the column. Approximately 300 mL of 5% EtOAc in hexanes was eluted. The eluted solvent was collected in 25 mL fractions. Fractions 4-7 contained product. The pure fractions were concentrated to obtain 128 mg of pure product **2.21** (63% yield).

Characterization:

Colorless liquid; R_f: 0.20 in 5% EtOAc in hexanes; ¹H NMR (400 MHz, CDCl₃): δ 8.08 (d, 1H, J = 8.3 Hz), 7.89 (app t, 2H, J = 8.5 Hz), 7.61-7.52 (m, 3H), 7.47 (t, 1H, J = 7.6 Hz), 5.65 (s, 2H), 4.24 (q, 2H, J = 7.1 Hz), 1.32 (t, 3H, J = 7.1 Hz); ¹³C{¹H} NMR (100 MHz, CDCl₃): δ ; 155.4, 133.9, 131.8, 131.1, 129.7, 128.9, 127.8, 126.9, 126.2, 125.4, 123.7,

67.9, 64.4, 14.4; IR: 2982, 1737 cm^{-1} ; HRMS (ESI/Q-TOF) m/z : $[\text{M}+\text{Na}]^+$ calcd for $\text{C}_{14}\text{H}_{14}\text{NaO}_3$ 253.0841; Found 253.0850.

Synthetic Procedures of Poly(α -ArTMC)s

Poly(α -PhTMC)s (2.20)

Procedure for the Polymerization of α -PhTMC (2.18):

For a typical experiment (Table 2.2, entry 8), a stock solution of TBD and initiator (0.084 M in each) was prepared by dissolving 11.7 mg of TBD and 13.3 mg of 1-naphthalenemethanol in dry THF. The monomer solution was prepared in a 10 mL flame dried schlenk tube by dissolving 150 mg of α -PhTMC **2.18** (0.84 mmol) in 0.64 mL of dry THF. The monomer solution was cooled to $-45\text{ }^\circ\text{C}$ for one minute. To this monomer solution, 0.2 mL of the stock solution containing TBD and initiator was added. The reaction mixture was stirred over appropriate time at $-45\text{ }^\circ\text{C}$. The reaction mixture was then quenched with 4 equivalents of benzoic acid in 1 mL of DCM. The solvents were removed under reduced pressure. The residue was dissolved in 1.0 mL of DCM and precipitated into 30 mL of stirring methanol. The precipitate initially appears as a semi-solid material. Methanol was decanted and the precipitate was washed with 30 mL of methanol. The polymer was then dried under high vacuum to obtain 126 mg of white solid **2.20** (82% yield, average yield over two runs = 80%).

Characterization:

^1H NMR (400 MHz, CDCl_3): δ 7.88 (app t, 2H, $J = 8.0\text{ Hz}$), 7.34-7.28 (m, 339H), 5.68-5.52 (m, 47H), 4.30-3.91 (m, 93H), 2.36-2.01 (m, 97H); $^{13}\text{C}\{^1\text{H}\}$ NMR (100 MHz, DMSO-d_6): δ 154.29-154.07 (Regio-irregular linkage), 153.79-153.52 (Head-to-Tail linkage), 153.02-152.88 (Regio-irregular linkage), 139.1, 128.5, 128.2, 126.1, 76.2, 63.9,

34.5; IR: 1739 cm^{-1} ; $M_{n,\text{NMR}} = 8500$ g/mol; $\bar{D} = 1.33$; $X_{\text{reg}} = 0.70$; $T_g = 48$ °C; TGA in N_2 : 200-272 °C, 94% weight loss.

Characterization of Poly(α -PhTMC) 2.20 (Table 2.3, Entry 1):

white solid (84% yield, average yield over two runs = 82%); ^1H NMR (400 MHz, CDCl_3): δ 7.88 (app t, 2H, $J = 8.2$ Hz), 7.35-7.29 (m, 160H), 5.65-5.55 (m, 30H), 4.35-4.00 (m, 59H), 2.39-2.02 (m, 63H); $^{13}\text{C}\{^1\text{H}\}$ NMR (100 MHz, DMSO-d_6): δ 154.39-154.05 (Regio-irregular linkage), 153.80-153.53 (Head-to-Tail linkage), 153.03-152.89 (Regio-irregular linkage), 139.1, 128.5, 128.2, 126.1, 76.2, 63.9, 34.5; $M_{n,\text{NMR}} = 5500$ g/mol; $\bar{D} = 1.29$; $X_{\text{reg}} = 0.63$; $T_g = 45$ °C; TGA in N_2 : 190-280 °C, 94% weight loss.

Characterization of Poly(α -PhTMC) 2.20 (Table 2.3, Entry 3):

white solid (86% yield, average yield over two runs = 83%); ^1H NMR (400 MHz, CDCl_3): δ 7.88 (app t, 2H, $J = 8.3$ Hz), 7.34-7.28 (m, 460H), 5.70-5.51 (m, 79H), 4.30-3.91 (m, 158H), 2.36-1.99 (m, 166H); $^{13}\text{C}\{^1\text{H}\}$ NMR (100 MHz, DMSO-d_6): δ 154.31-154.06 (Regio-irregular linkage), 153.80-153.54 (Head-to-Tail linkage), 153.00-152.90 (Regio-irregular linkage), 139.1, 128.5, 128.2, 126.1, 76.2, 63.9, 34.5; $M_{n,\text{NMR}} = 14200$ g/mol; $\bar{D} = 1.37$; $X_{\text{reg}} = 0.71$; $T_g = 47$ °C; TGA in N_2 : 200-280 °C, 94% weight loss.

Characterization of Poly(α -PhTMC) 2.20 (Table 2.3, Entry 4):

white solid (83% yield, average yield over two runs = 80%); ^1H NMR (400 MHz, CDCl_3): δ 7.88 (app t, 2H, $J = 8.1$ Hz), 7.34-7.29 (m, 544H), 5.64-5.52 (m, 98H), 4.23-3.90 (m, 196H), 2.31-2.00 (m, 210H); $^{13}\text{C}\{^1\text{H}\}$ NMR (100 MHz, DMSO-d_6): δ 154.27-153.96 (Regio-irregular linkage), 153.80-153.50 (Head-to-Tail linkage), 152.99-152.86 (Regio-irregular linkage), 139.1, 128.5, 128.2, 126.0, 76.2, 63.9, 34.5; $M_{n,\text{NMR}} = 17600$ g/mol; $\bar{D} = 1.39$; $X_{\text{reg}} = 0.72$; $T_g = 49$ °C; TGA in N_2 : 204-283 °C, 94% weight loss.

Poly(α -4-Me-PhTMC) (2.25)

Polymerized using a procedure similar to polymerization of **2.18** with a $M_0/I_0 = 50/1$.

Characterization of Poly(α -4-Me-PhTMC) 2.25 (Table 2.4, Entry 1):

white solid (83% yield, average yield over two runs = 82%); ^1H NMR (400 MHz, CDCl_3): δ 7.88 (app t, 2H, $J = 8.0$ Hz), 7.20-7.03 (m, 251H), 5.59-5.50 (m, 54H), 4.31-3.87 (br m, 107H), 2.48-2.07 (m, 280H); $^{13}\text{C}\{^1\text{H}\}$ NMR (100 MHz, DMSO-d_6): δ 154.30-153.99 (Regio-irregular linkage), 153.79-153.52 (Head-to-Tail linkage), 153.06-152.80 (Regio-irregular linkage), 137.6, 136.1, 129.0, 126.1, 76.2, 63.9, 34.4, 20.6; IR: 1740 cm^{-1} ; $M_{n,\text{NMR}} = 10500\text{ g/mol}$, $\bar{D} = 1.40$; $X_{\text{reg}} = 0.51$; $T_g = 52\text{ }^\circ\text{C}$; TGA in N_2 : $197\text{-}282\text{ }^\circ\text{C}$, 94% weight loss.

Poly(α -4-Br-PhTMC) (2.26)

Polymerized using a procedure similar to polymerization of **2.18** with a $M_0/I_0 = 50/1$.

Characterization of Poly(α -4-Br-PhTMC) 2.26 (Table 2.4, Entry 2):

white solid (88% yield, average yield over two runs = 88%). ^1H NMR (400 MHz, CDCl_3): δ 7.88 (app t, 2H, $J = 8.3$ Hz), 7.53-7.39 (m, 110H), 7.20-7.15 (m, 106H), 5.63-5.48 (m, 54H), 4.31-3.92 (m, 107H), 2.34-1.95 (m, 116H); $^{13}\text{C}\{^1\text{H}\}$ NMR (100 MHz, DMSO-d_6): δ 154.24-154.06 (Regio-irregular linkage), 153.61-153.46 (Head-to-Tail linkage), 152.83-152.70 (Regio-irregular linkage), 138.4, 131.4, 128.3, 121.5, 75.6, 63.9, 34.2; IR: 1739 cm^{-1} ; $M_{n,\text{NMR}} = 14000\text{ g/mol}$; $\bar{D} = 1.33$; $X_{\text{reg}} = 0.81$; $T_g = 65\text{ }^\circ\text{C}$; TGA in N_2 : $207\text{-}370\text{ }^\circ\text{C}$, 94% weight loss.

Poly(α -4-CF₃-PhTMC) (2.27)

Polymerized using a procedure similar to polymerization of **2.18** with a $M_0/I_0 = 50/1$.

Characterization of Poly(α -4-CF₃-PhTMC) 2.27 (Table 2.4, Entry 3):

white solid (70% yield, average yield over two runs = 67%). ^1H NMR (400 MHz,

CDCl₃): δ 7.88 (app t, 2H, $J = 7.9$ Hz), 7.63-7.53 (m, 101H), 7.44-7.39 (m, 100H), 5.74-5.56 (m, 49H), 4.35-3.92 (m, 98H), 2.37-1.97 (m, 100H); ¹³C{¹H} NMR (100 MHz, DMSO-d₆): δ 154.29-154.12 (Regio-irregular linkage), 153.66-153.50 (Head-to-Tail linkage), 152.83-152.70 (Regio-irregular linkage), 143.7, 128.8 (q, $J = 31.3$ Hz), 126.8, 125.4, 124.0 (q, $J = 272.1$ Hz), 75.6, 63.9, 34.3; IR: 1743 cm⁻¹; $M_{n,NMR} = 12200$ g/mol; $\bar{D} = 1.35$; $X_{reg} = 0.89$; $T_g = 63$ °C; TGA in N₂: 200-303 °C, 94% weight loss.

*General Procedure for the Polymerization of α -ArTMCs Using **2.19** + DBU as Catalysts:*

A stock solution of **2.19**, DBU and initiator (0.15 M in each) was prepared by dissolving 58.0 mg of **2.19**, 23 μ L of DBU and 24.7 mg of 1-naphthalenemethanol in dry THF. The monomer solution was prepared in a 4 mL oven dried vial by dissolving 0.78 mmol of α -ArTMC in 0.3 mL of dry THF at room temperature (27 °C). To this monomer solution, 0.1 mL of the stock solution containing **2.19**, DBU and initiator was added. The reaction mixture was stirred over appropriate time at 27 °C. The reaction mixture was then quenched with 4 equivalents of benzoic acid. The solvent was removed under reduced pressure. The residue was dissolved in 0.5 mL of DCM and precipitated into 30 mL of stirring methanol. Methanol was decanted and the precipitate was washed with 30 mL of methanol. The polymer was then dried under high vacuum to obtain poly(α -ArTMC) as a white solid.

Kinetics and Molar Mass versus Conversion Experiment (Using α -PhTMC **2.18**)

Identical reactions were set up at the same time and quenched at different time points. A stock solution of TBD and initiator (0.084 M in each) was prepared by dissolving 11.7 mg of TBD and 13.3 mg of 1-naphthalenemethanol in dry THF. The monomer solution was prepared in a 10 mL flame dried schlenk tube by dissolving 150 mg of α -PhTMC **2.18** (0.84

mmol) in 0.64 mL of dry THF. The monomer solution was cooled to -45 °C for one minute. To this monomer solution, 0.2 mL of the stock solution containing TBD and initiator was added. Each reaction was quenched at a different time point, by adding 4 equivalents of benzoic acid in 1 mL of DCM. The solvents were removed under reduced pressure. The conversion of monomer was determined by proton NMR of crude sample by integrating the methylene region (δ 4.56-4.46) of monomer and polymer (δ 4.30-3.91). The polymer sample was then analyzed by SEC to determine the M_n .

2.7 References

- 1 Nederberg, F.; Lohmeijer, B. G. G.; Leibfarth, F.; Pratt, R. C.; Choi, J.; Dove, A. P.; Waymouth, R. M.; Hedrick, J. L. *Biomacromolecules* **2007**, *8*, 153-160.
- 2 Helou, M.; Miserque, O.; Brusson, J. M.; Carpentier, J. F.; Guillaume, S. M. *Chem. Eur. J.* **2010**, *16*, 13805-13813.
- 3 Chan, J. M. W.; Zhang, X.; Brennan, M. K.; Sardon, H.; Engler, A. C.; Fox, C. H.; Frank, C. W.; Waymouth, R. M.; Hedrick, J. L. *J. Chem. Educ.* **2015**, *92*, 708-713.
- 4 Haba, O.; Tomizuka, H.; Endo, T. *Macromolecules* **2005**, *38*, 3562-3563.
- 5 Azechi, M.; Matsumoto, K.; Endo, T. *J. Polym. Sci. Part A: Polym. Chem.* **2013**, *51*, 1651-1655.
- 6 Felder, S. E.; Redding, M. J.; Noel, A.; Grayson, S. M.; Wooley, K. L. *Macromolecules* **2018**, *51*, 1787-1797.
- 7 Shen, Y.; Chen, X.; Gross, R. A. *Macromolecules* **1999**, *32*, 308-314.
- 8 Shen, Y.; Chen, X.; Gross, R. A. *Macromolecules* **1999**, *32*, 2799-2802.
- 9 Shen, Y.; Chen, X.; Gross, R. A. *Macromolecules* **1999**, *32*, 3891-3897.
- 10 Mikami, K.; Lonnecker, A. T.; Gustafson, T. P.; Zinnel, N. F.; Pai, P. J.; Russell, D. H.; Wooley, K. L. *J. Am. Chem. Soc.* **2013**, *135*, 6826-6829.
- 11 Song, Y.; Ji, X.; Dong, M.; Li, R.; Lin, Y. N.; Wang, H.; Wooley, K. L. *J. Am. Chem. Soc.* **2018**, *140*, 16053-16057.
- 12 Gregory, G. L.; Jenisch, L. M.; Charles, B.; Kociok-Kohn, G.; Buchard, A. *Macromolecules* **2016**, *49*, 7165-7169.

- 13 Tempelaar, S.; Mespouille, L.; Coulembier, O.; Dubois, P.; Dove, A. P. *Chem. Soc. Rev.* **2013**, *42*, 1312-1336.
- 14 He, F.; Wang, Y.; Feng, J.; Zhuo, R.; Wang, X. *Polymer* **2003**, *44*, 3215-3219.
- 15 Endo, T.; Kakimoto, K.; Ochiai, B.; Nagai, D. *Macromolecules* **2005**, *38*, 8177-8182.
- 16 Darensbourg, D. J.; Moncada, A. I.; Wei, S. H. *Macromolecules* **2011**, *44*, 2568-2576.
- 17 Helou, M.; Brusson, J. M.; Carpentier, J. F.; Guillaume, S. M. *Polym. Chem.* **2011**, *2*, 2789-2795.
- 18 Parzuchowski, P. G.; Jaroch, M.; Tryznowski, M.; Rokicki, G. *Macromolecules* **2008**, *41*, 3859-3865.
- 19 Yang, J.; Hao, Q.; Liu, X.; Ba, C.; Cao, A. *Biomacromolecules* **2004**, *5*, 209-218.
- 20 Chen, W.; Yang, H.; Wang, R.; Cheng, R.; Meng, F.; Wei, W.; Zhong, Z. *Macromolecules* **2010**, *43*, 201-207.
- 21 Nemoto, N.; Sanda, F.; Endo, T. *J. Polym. Sci. Part A: Polym. Chem.* **2001**, *39*, 1305-1317.
- 22 Hu, X.; Chen, X.; Xie, Z.; Cheng, H.; Jing, X. *J. Polym. Sci. Part A: Polym. Chem.* **2008**, *46*, 7022-7032.
- 23 Pyo, S. H.; Persson, P.; Lundmark, S.; Hatti-Kaula, R. *Green Chem.* **2011**, *13*, 976-982.
- 24 Zhu, W.; Wang, Y.; Zhang, Q.; Shen, Z. *J. Polym. Sci. Part A: Polym. Chem.* **2011**, *49*, 4886-4893.
- 25 Zhang, X.; Zhong, Z.; Zhuo, R. *Macromolecules* **2011**, *44*, 1755-1759.
- 26 Sanders, D. P.; Fukushima, K.; Coady, D. J.; Nelson, A.; Fujiwara, M.; Yasumoto, M.; Hedrick, J. L. *J. Am. Chem. Soc.* **2010**, *132*, 14724-14726.
- 27 Fukushima, K.; Pratt, R. C.; Nederberg, F.; Tan, J. P. K.; Yang, Y. Y.; Waymouth, R. M.; Hedrick, J. L. *Biomacromolecules* **2008**, *9*, 3051-3056.
- 28 He, F.; Wang, C. F.; Jiang, T.; Han, B.; Zhuo, R. *Biomacromolecules* **2010**, *11*, 3028-3035.
- 29 Hu, X.; Chen, X.; Xie, Z.; Liu, S.; Jing, X. *J. Polym. Sci. Part A: Polym. Chem.* **2007**, *45*, 5518-5528.
- 30 Al-Azemi, T. F.; Bisht, K. S. *Macromolecules* **1999**, *32*, 6536-6540.
- 31 Qiao, Y.; Yang, C.; Coady, D. J.; Ong, Z. Y.; Hedrick, J. L.; Yang, Y. Y. *Biomaterials* **2012**, *33*, 1146-1153.

- 32 Pratt, R. C.; Nederberg, F.; Waymouth, R. M.; Hedrick, J. L. *Chem. Commun.* **2008**, 114-116.
- 33 Tan, J. P. K.; Kim, S. H.; Nederberg, F.; Fukushima, K.; Coady, D. J.; Nelson, A.; Yang, Y. Y.; Hedrick, J. L. *Macromol. Rapid Commun.* **2010**, *31*, 1187-1192.
- 34 Cooley, C. B.; Trantow, B. M.; Nederberg, F.; Kiesewetter, M. K.; Hedrick, J. L.; Waymouth, R. M.; Wender, P. A. *J. Am. Chem. Soc.* **2009**, *131*, 16401-16403.
- 35 Bartolini, C.; Mespouille, L.; Verbruggen, I.; Willemb, R.; Dubois, P. *Soft Matter* **2011**, *7*, 9628-9637.
- 36 Suriano, F.; Pratt, R. C.; Tan, J. P. K.; Wiradharma, N.; Nelson, A.; Yang, Y. Y.; Dubois, P.; Hedrick, J. L. *Biomaterials* **2010**, *31*, 2637-2645.
- 37 Mei, L. L.; Yan, G. P.; Yu, X. H.; Cheng, S. X.; Wu, J. Y. *J. Appl. Polym. Sci.* **2008**, *108*, 93-98.
- 38 Xie, Z.; Lu, C.; Chen, X.; Chen, L.; Wang, Y.; Hu, X.; Shi, Q.; Jing, X. *J. Polym. Sci. Part A: Polym. Chem* **2007**, *45*, 1737-1745.
- 39 Chen, H.; Yan, G. P.; Li, L.; Ai, C. W.; Yu, X. H. *J. Appl. Polym. Sci.* **2009**, *114*, 3087-3096.
- 40 Chen, W.; Meng, F.; Li, F.; Ji, S. J.; Zhong, Z. *Biomacromolecules* **2009**, *10*, 1727-1735.
- 41 Brignou, P.; Carpentier, J. F.; Guillaume, S. M. *Macromolecules* **2011**, *44*, 5127-5135.
- 42 Hua, G.; Franzen, J.; Odelius, K. *Macromolecules* **2019**, *52*, 2681-2690.
- 43 DeRosa, C. A.; Luke, A. M.; Anderson, K.; Reineke, T. M.; Tolman, W. B.; Bates, F. S.; Hillmyer, M. A. *Macromolecules* **2021**, *54*, 5974-5984.
- 44 Brignou, P.; Gil, M. P.; Casagrande, O.; Carpentier, J. F.; Guillaume, S. M. *Macromolecules* **2010**, *43*, 8007-8017.
- 45 Hillmyer and Coworkers had used the following formula to calculate the regio-regularity of the polymer, $X_{reg} = H-T / (H-T + H-H + T-T)$.
- 46 Yu, X.; Jia, J.; Xu, S.; La, K. U.; Sanford, M. J.; Ramakrishnan, R. K.; Nazarenko, S. I.; Hoye, T. R.; Coates, G. W.; DiStasio Jr. R. A. *Nat. Commun.* **2018**, *9*, 2880.
- 47 Ozawa, J.; Kanai, M. *Org. Lett.* **2017**, *19*, 1430-1433.
- 48 Merkley, N.; Warkentin, J. *Can. J. Chem.* **2002**, *80*, 1187-1195.
- 49 Pratt, R. C.; Lohmeijer, B. G. G.; Long, D. A.; Lundberg, P. N. P.; Dove, A. P.; Li, H.; Wade, C. G.; Waymouth, R. M.; Hedrick, J. L. *Macromolecules* **2006**, *39*, 7863-7871.

- 50 Lohmeijer, B. G. G.; Pratt, R. C.; Leibfrath, F.; Logan, J. W.; Long, D. A.; Dove, A. P.; Nederberg, F.; Choi, J.; Wade, C.; Waymouth, R. M.; Hedrick, J. L. *Macromolecules* **2006**, *39*, 8574-8583.
- 51 Kazakov, O. I.; Datta, P. P.; Isajani, M.; Kiesewetter, E. T.; Kiesewetter, M. K. *Macromolecules* **2014**, *47*, 7463-7468.
- 52 Todd, R.; Rubio, G.; Hall, D. J.; Tempelaar, S.; Dove, A. P. *Chem. Sci.* **2013**, *4*, 1092-1097.
- 53 Song, Y.; Yang, X.; Shen, Y.; Dong, M.; Lin, Y. N.; Hall, M. B.; Wooley, K. L. *J. Am. Chem. Soc.* **2020**, *142*, 16974-16981.
- 54 Mukai, T.; Hirano, K.; Satoh, T.; Miura, M. *Org. Lett.* **2010**, *12*, 1360-1363.
- 55 Reddy, G. R.; Avadhani, A. S.; Rajaram, S. *J. Org. Chem.* **2016**, *81*, 4134-4141.
- 56 Neuvonen, A. J.; Pihko, P. M. *Org. Lett.* **2014**, *16*, 5152-5155.
- 57 Kim, J.; De Castro, K. A.; Lim, M.; Rhee, H. *Tetrahedron* **2010**, *66*, 3995-4001.
- 58 Borowiecki, P.; Wawro, A. M.; Winska, P.; Wielechowska, M.; Bretner, M. *Eur. J. Med. Chem.* **2014**, *84*, 364-374.
- 59 Baburajan, P.; Elango, K. P. *Tetrahedron Lett.* **2014**, *55*, 3525-3528.
- 60 Hayashi, Y.; Itoh, T.; Aratake, S.; Ishikawa, H. *Angew. Chem. Int. Ed.* **2008**, *47*, 2082-2084.

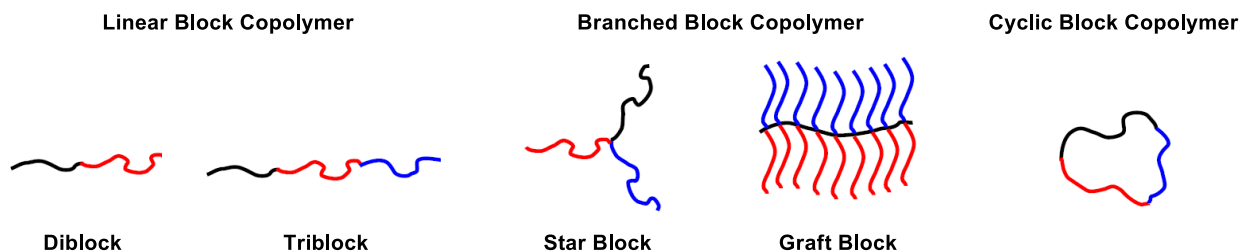
Chapter 3

Synthesis of Diblock Copolymers Containing Donor and Acceptor Blocks and Its AFM Studies

3.1 Introduction

Copolymers are polymers that are made up of different kinds of monomer units. The presence of different kinds of monomer units in a polymer can lead to the development of new properties that might be useful for specific applications. There are of three kinds of copolymers namely random, alternate and block copolymers. Block copolymers are made of two or more blocks of chemically different homopolymers that are covalently connected to each other. Broadly, block copolymers can be classified into three kinds (Figure 3.1) (i) linear block copolymers (di-, tri-, tetra-), (ii) branched block copolymers (star and graft block copolymers), and (iii) cyclic block copolymers.¹⁻³ Block copolymers can be synthesized by coupling different homopolymers using coupling reactions. This approach is

Figure 3.1. Representation of Three kinds of Block Copolymers



typified by the use of click reactions to couple homopolymers.⁴⁻⁶ Alternatively, living polymerizations can be used for the synthesis of block copolymers. In living polymerization, the chain end is active after complete consumption of the monomer. Upon addition of a second monomer, the polymerization is reinitiated to yield a diblock copolymer. There are several techniques that are useful for this approach including radical (ATRP, RAFT or NMP), anionic, and cationic polymerizations.^{1, 2, 7-12} The living nature of these techniques also allows the precise incorporation of an end group which can act as an initiator for a different kind of polymerization. Thus, diblock copolymers can be built by a combination of different polymerization techniques.¹³⁻¹⁵ These living polymerization techniques provide precise control over molecular weight, composition, architecture, and dispersity.

Among block copolymers, some linear triblock copolymers are commercially available and others are being explored or investigated in various applications. Poly(styrene-*b*-butadiene-*b*-styrene) (trade name Kraton) and poly(styrene-*b*-isoprene-*b*-styrene) are commercially available triblock copolymers that are being used as thermoplastic elastomers in products such as sealants, footwear soles, toys, adhesives, and road bitumens.^{1, 16, 17} Another commercially available triblock copolymer, poly(ethylene oxide-*b*-propylene oxide-*b*-ethylene oxide) (trade name Pluronic) has been used as antifoaming agent in cell cultures.¹⁶ Pluronic block copolymers and other amphiphilic block copolymers based on poly(ethylene oxide), poly(propylene glycol), and poly(N-isopropyl acrylamide) were investigated in drug delivery studies as nanocarriers for drug molecules.^{1, 16, 18-23} Diblock copolymers such as poly(styrene-*b*-methyl methacrylate), poly(styrene-*b*-ethylene oxide), poly(styrene-*b*-dimethylsiloxane) and poly(styrene-*b*-vinylpyridine) were identified as potential candidates for nanolithographic techniques, templates for patterning inorganic materials, and for studies

related to phase separations.^{1, 16, 24-29} Block copolymers incorporated with donor and acceptor moieties were explored in organic photovoltaics and organic light emitting devices in an attempt to enhance their performance.³⁰⁻³³

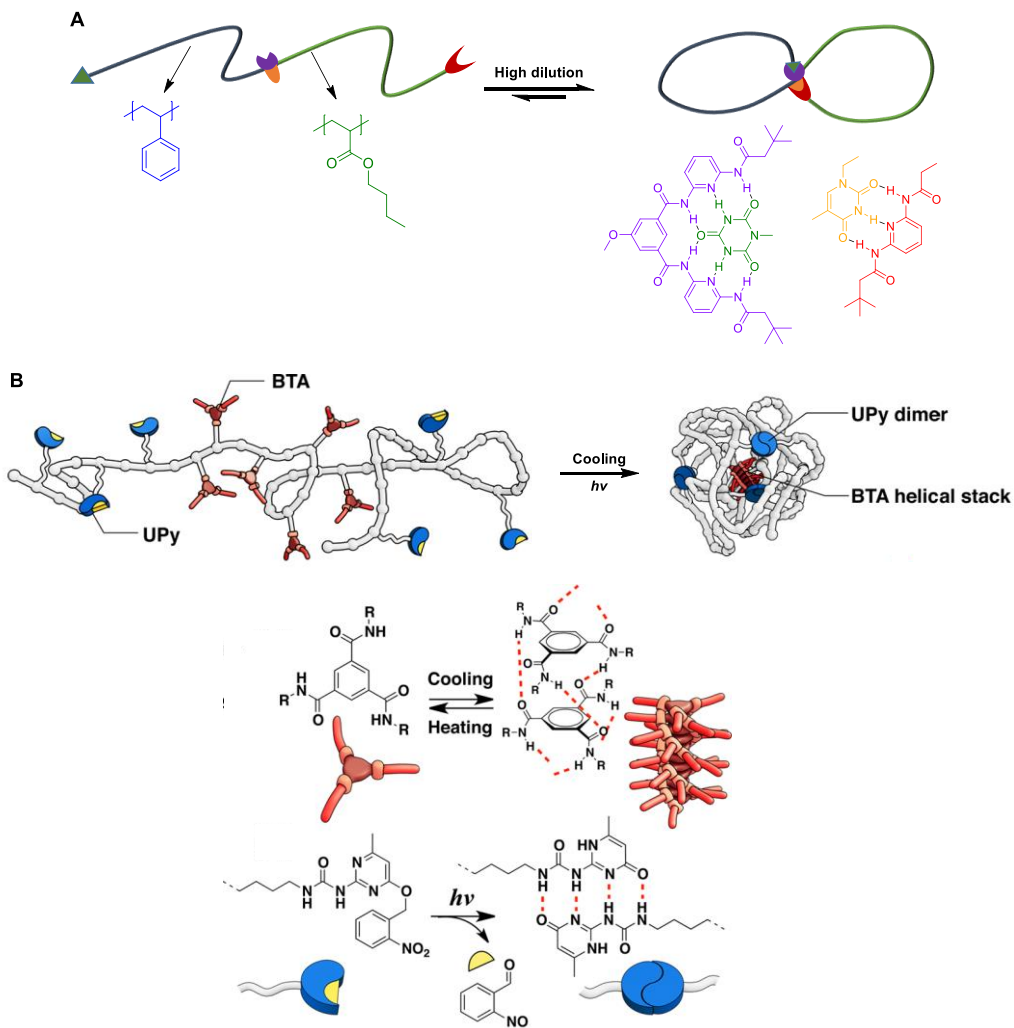
Apart from the above-mentioned applications, block copolymers incorporated with specific functional groups were used to mimic the folding behaviors of natural macromolecules and for the synthesis of single chain polymeric nanoparticles.³⁴⁻⁴¹ The process of a single block copolymer chain folding and single chain nanoparticle formation occurs due to favorable intramolecular interactions. The intramolecular interactions used in these studies can be broadly divided into non-covalent and covalent interactions. In this chapter, some of the non-covalent interactions responsible for the block copolymer chain folding and single chain nanoparticle formation will be explained briefly in section **3.2** (covalent interactions are not in the scope of this chapter).

3.2 Background

In the field of molecular biology, non-covalent interactions are very well known for stabilizing the complex structures of biomacromolecules.^{34, 42-44} Due to this reason, non-covalent interactions have been extensively employed in studies that try to mimic and understand the complex structures of biomacromolecules.^{34, 43-48} Similar studies have been carried out on the folding of block copolymers. Here, two kinds of non-covalent interactions were mainly used: hydrogen bonding and π - π interactions.

Barner-Kowollik and Meijer groups have independently synthesized various types of block copolymers that have multiple H-bonding sites to illustrate the folding of single polymer chain (Figure 3.2).^{35, 36, 49, 50} Some of the motifs with multiple H-bonding sites that

Figure 3.2. Folding of a Single Block Copolymer Chain *via* Intramolecular Hydrogen Bonding Interactions: (A) Barner-Kowollik and coworkers report.³⁵ (B) Meijer and coworkers report. Reprinted (adapted) with permission from Hosono, N.; Gillissen, M. A. J.; Li, Y.; Sheiko, S. S.; Palmans, A. R. A.; Meijer, E. W. *J. Am. Chem. Soc.* **2013**, *135*, 501-510. Copyright 2013 American Chemical Society.



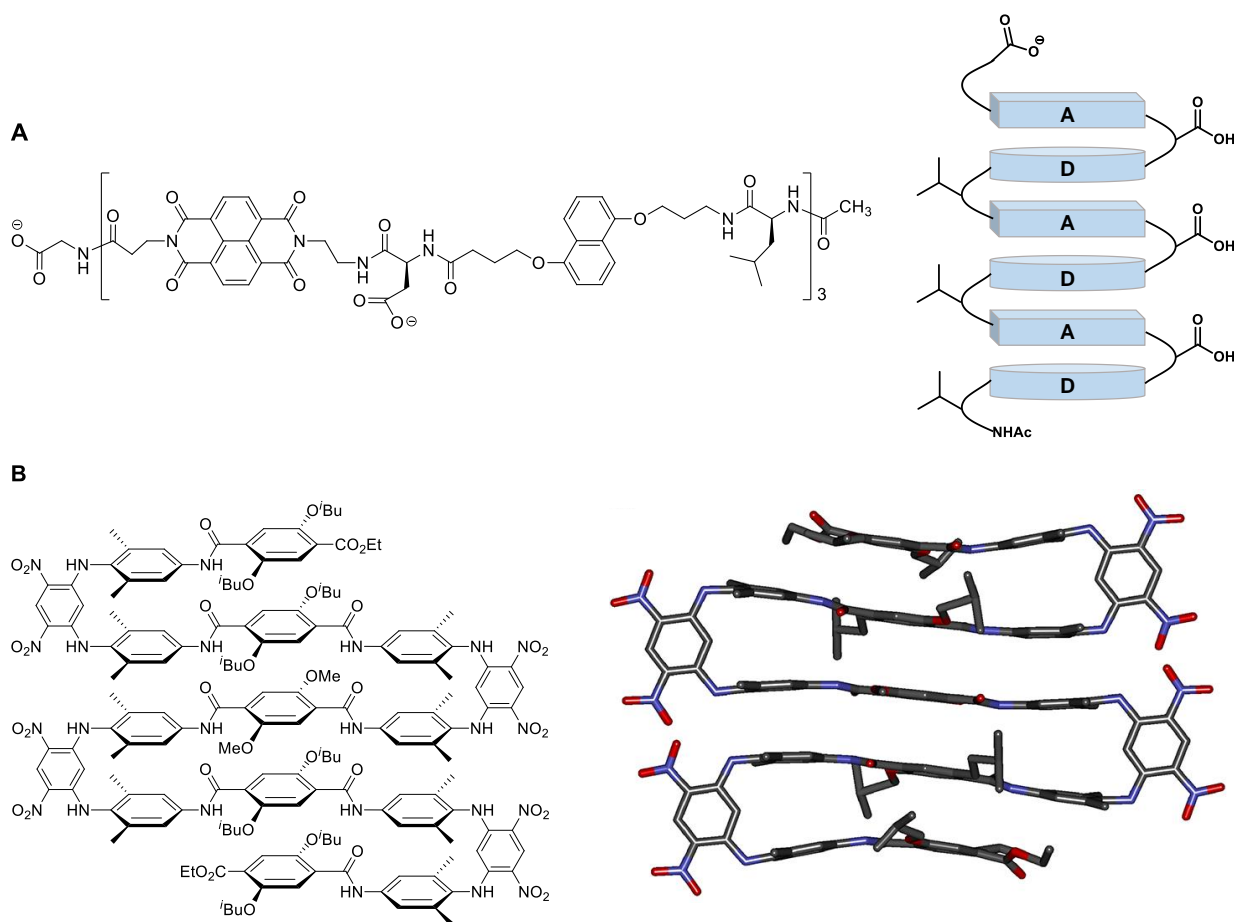
were incorporated in the block copolymers include Hamilton wedge, cyanuric acid, thymine, 2,6-diaminopyridine, benzene-1,3,5-tricarboxamide and 2-ureidopyrimidinone.

The other kind of non-covalent interaction responsible for the folding of block copolymers is π - π interaction. These interactions are most commonly observed between aromatic substituents in proteins. They are also observed in protein-small molecule complexes.^{42, 44, 51, 52} Synthetic foldamers that aim to mimic and study secondary structures

of proteins also use these interactions. A variety of aromatic systems that can involve in these interactions were used in synthetic foldamers (two examples were shown in Figure 3.3 for representation purpose).^{43, 53-58} In the case of block copolymers, the usage of π - π interactions for the folding has been studied to a limited extent.^{37, 59, 60}

Weck and coworkers synthesized a triblock copolymer and illustrated that the π - π stacking interactions can be used to fold a copolymer to mimic hairpin like structures. The triblock copolymer Poly(styrene-*b*-dimethylacrylamide-*b*-pentafluorostyrene), upon high dilution undergoes intramolecular chain folding due to π - π stacking. The stacking results

Figure 3.3. (A) Chemical Structure and Representation of Secondary Structure of Foldamer Based on Donor and Acceptor Interactions.⁴³ (B) Chemical and Crystal Structure of β -Sheet Foldamer Based on face-to-face π - π interactions.⁵⁵



from quadrupole interactions between the electron-rich phenyl rings of poly(styrene) block and electron-deficient pentafluorophenyl rings of poly(pentafluorostyrene) block (Figure 3.4).³⁷ Such interactions between phenyl and pentafluorophenyl ring have been well studied and is also used in various applications.^{44, 61-68} Weck and coworkers extended the usage of π - π stacking interactions between phenyl and pentafluorophenyl rings to the intramolecular folding of coil-helix diblock copolymer (Figure 3.5).⁵⁹ The same group had also used π - π stacking interactions between phenyl and pentafluorophenyl rings for stabilizing the β -turns of tetrablock copolymer to mimic β -sheet structures (Figure 3.6).⁶⁰

Figure 3.4. Schematic Representation of the Single-chain Folding of PS₃₀-PDMAA₂₀-PPFS₃₀ Block Copolymer in Solution. Reprinted (adapted) with permission from Lu, J.; Brummelhuis, N. T.; Weck, M. *Chem. Commun.* **2014**, 50, 6225-6227.

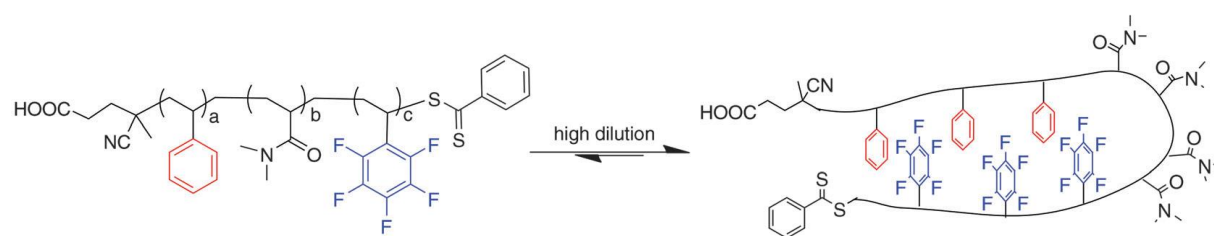


Figure 3.5. Chemical Structure of Coil-Helix Diblock Copolymer Comprised of Poly(styrene) and Poly(pentafluorophenyl isocyanide) Blocks and Representation of π - π Stacking Interactions Between Phenyl and Pentafluorophenyl Rings in Coil-Helix Diblock Copolymer. Reprinted (adapted) with permission from Wang, C.; Weck, M. *Macromol. Rapid Commun.* **2021**, 42, 2100368 (1-6).

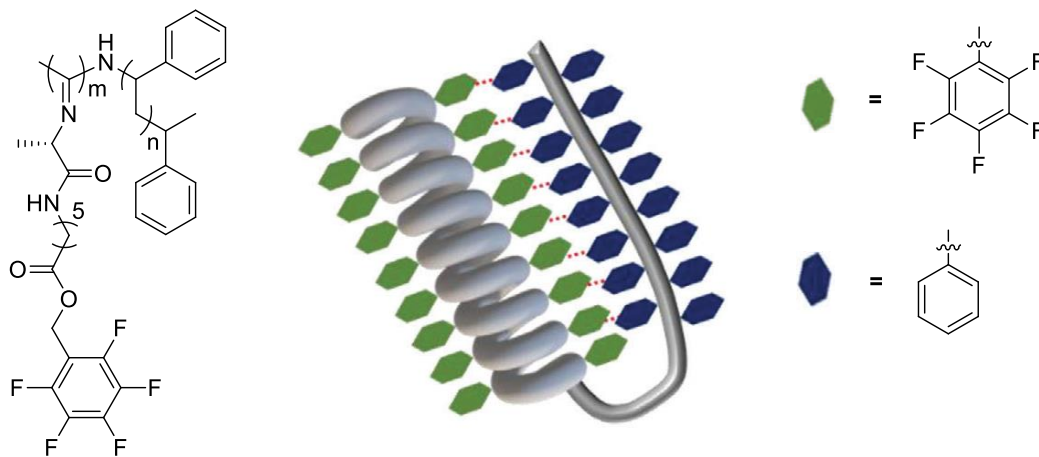
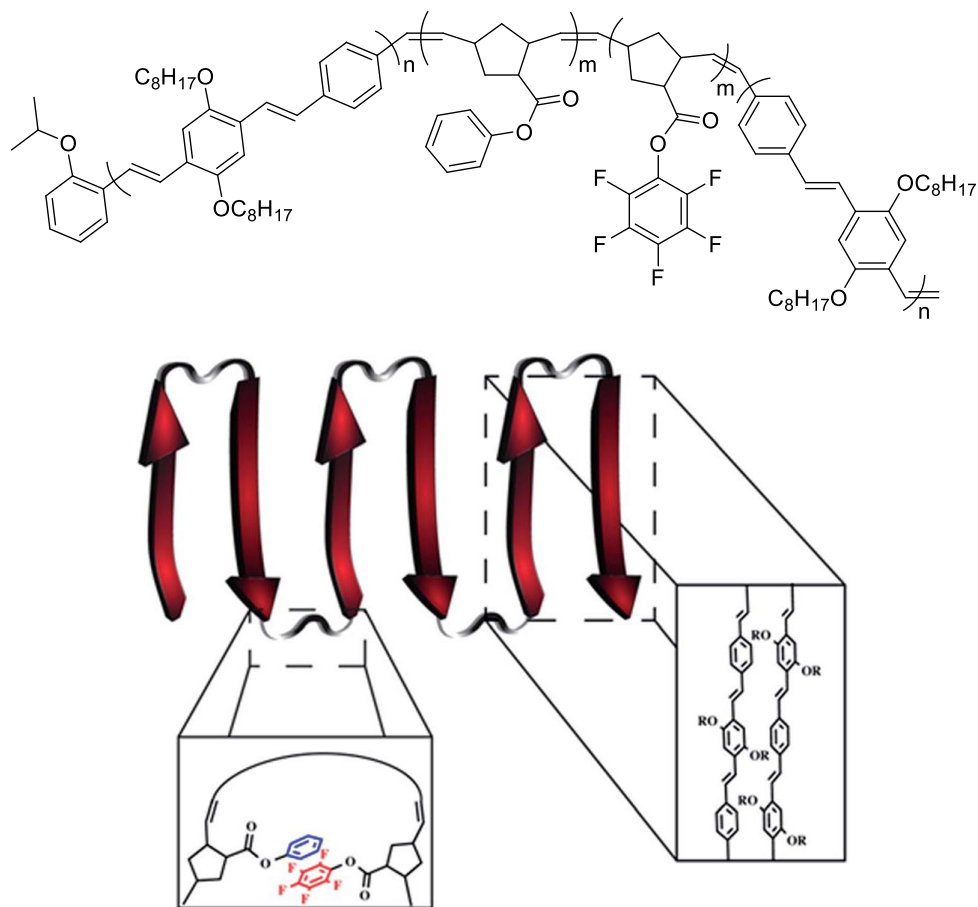


Figure 3.6. Chemical Structure of ABCA Tetrablock Copolymer Comprised of Poly(*p*-phenylene vinylene) (PPV) and Poly(norbornene) (PNB) Blocks and Schematic Representation of Synthetic β -Sheet Formation of PPV-(PNB-PNB-PPV)₅.⁶⁰



3.3 Our Approach

Our work in this chapter was inspired from the Weck and coworkers report on the intramolecular π - π stacking interactions between the electron-rich and electron-deficient blocks. In our work we sought to achieve intermolecular π - π stacking interactions between the electron-rich and electron-deficient blocks of a diblock copolymer in the bulk state. This in-turn can result in a high density of inter chain linkages in bulk state and eventually lead to strengthening of mechanical properties of a diblock copolymer. Although π - π interactions are weaker than hydrogen bonding, the overall contributions from large number of π - π

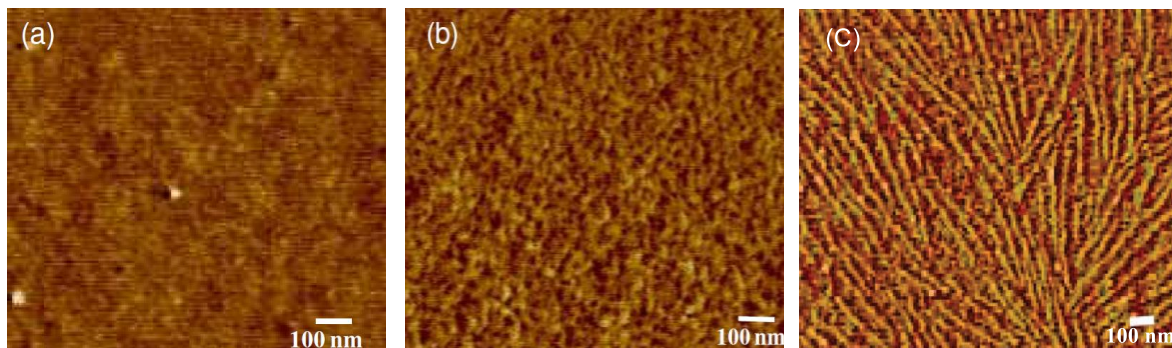
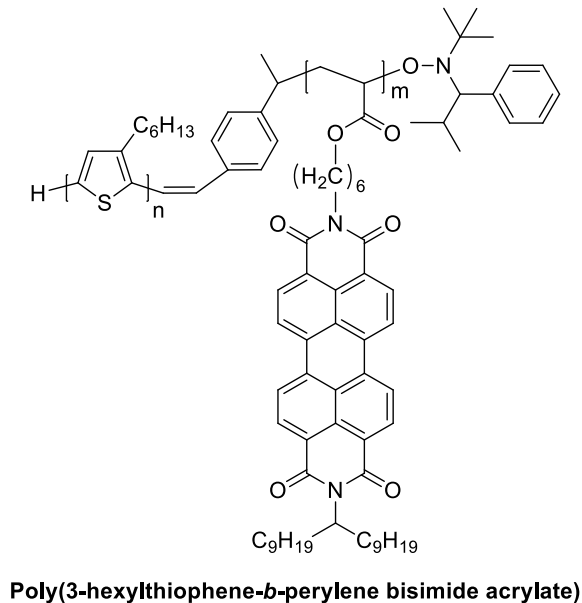
interactions will be high. This method of strengthening the mechanical properties of polymers will be more efficient than the simple blending of two different homopolymers (in this case electron-rich and electron-deficient homopolymers).

Diblock copolymers comprised of electron-rich and electron-deficient blocks have been extensively studied in the field of optoelectronics.³⁰⁻³³ In these studies, it has been shown that the donor and acceptor blocks micro-phase separate into molecularly pure domains.^{32, 69-71} For example the micro-phase separation of diblock copolymer comprised of electron-rich poly(3-hexylthiophene) and electron-deficient poly(perylene bisimide acrylate) blocks is shown in Figure 3.7.⁷¹ Generally, block copolymers tend to micro-phase separate (on a scale of 5-100 nm) in the bulk state. The driving force for the micro-phase separation of block copolymers is the Flory-Huggins interaction parameter (χ), which is the measure of incompatibility of blocks of copolymers.^{1, 3, 72} The Flory-Huggins interaction parameter χ_{AB} for the diblock copolymer is given by the equation 1.

$$\chi_{AB} = \left(\frac{Z}{k_B T} \right) \left[\varepsilon_{AB} - \frac{1}{2} (\varepsilon_{AA} + \varepsilon_{BB}) \right] \quad (1)$$

In the equation (1) Z corresponds to the number of nearest neighbor monomers per monomer in the diblock copolymer, ε_{AB} , ε_{AA} , and ε_{BB} represents the interaction energies per monomer between monomers A and B, A and A, and B and B respectively. The negative value for ε indicates favorable interaction, whereas a positive value indicates unfavorable interaction. Equation 1 shows that the sign of χ_{AB} is dependent on ε_{AB} . A positive value for χ_{AB} indicates net unfavorable interactions between monomers, while a negative value indicates favorable interactions. The product of χ_{AB} and N (degree of polymerization) which expresses the interaction per diblock copolymer chain, determines whether the micro-phase separation is

Figure 3.7. Structure of Poly(3-hexylthiophene-*b*-perylene bisimide acrylate) and SFM Phase Image of the Diblock Copolymer (a) As spun cast; (b) After thermal annealing at 150 °C for 20 min; (c) After annealing for 2h in toluene/chloroform vapor. Reprinted (adapted) with permission from Zhang, Q.; Cirpan, A.; Russell, T. P.; Emrick, T. *Macromolecules* **2009**, *42*, 1079-1082. Copyright 2009 American Chemical Society.



ordered or disordered. For the diblock copolymer with f_A (composition or volume fraction of block A) = 0.5, the critical value of χN for the order disorder transition is 10.5. If $\chi N \ll 10.5$ it results in a disordered micro-phase separation. The transition to ordered phase separation occurs when the $\chi N \approx 10.5$.

To achieve our goal of enhancing mechanical properties *via* intermolecular π - π stacking interactions, we need to prevent the micro-phase separation of diblock copolymers.

The studies on the diblock copolymers in the optoelectronics field clearly indicates that the mere placement of electron-rich and electron-deficient blocks does not prevent the micro-phase separation in the bulk state. Micro-phase separation of diblock copolymers can be prevented either by reducing the repulsions or by enhancing the favorable interactions between the blocks. With this thought, we wanted a diblock copolymer comprised of electron-rich and electron-deficient blocks that are almost identical in the backbones and in side chains. We believe that the near identical nature of two blocks can significantly reduce the repulsions between them. At the same time, favorable intermolecular π - π stacking interactions can be enhanced by tuning the electron-rich and electron-deficient blocks. Finally, this can lead to the phase mixing of two blocks in the bulk state. We sought to utilize this assumption to improve the mechanical properties of aliphatic polycarbonates. The aliphatic polycarbonates (poly(α -ArTMC)s) studied in the chapter II satisfies the above-mentioned conditions for the synthesis of diblock copolymers in order to prevent its micro-phase separation in the bulk state. To study the micro-phase behavior of synthesized diblock copolymers we planned to use atomic force microscopy.

3.4 Results and Discussion

The synthesis of diblock copolymers can be carried out either by sequential addition of monomers to the polymerization reaction mixture or by coupling of different homopolymers. As sequential addition of monomers can be done in a single pot, it is preferred over coupling of homopolymers. To enable sequential addition, the polymerization reaction has to have living characteristics. These characteristics include: (i) rate of initiation (k_i) being greater than rate of propagation (k_p); (ii) absence of chain termination; (iii) a molar mass dependence based on the monomer to initiator ratio; and (iv) polymer chain extension

by repeated monomer addition. Hence, the synthesis of block copolymers *via* sequential addition of monomers enables us to achieve (i) high block purity, (ii) control of block lengths, and (iii) required architectures.

In chapter II, we have shown that the ring opening polymerization of α -ArTMCs exhibits living polymerization behavior. We had shown that the polymerization is first order in monomer and that a plot of monomer conversion versus degree of polymerization was linear. As living polymerization techniques are known to support polymer chain extensions, in this chapter we decided to synthesis diblock copolymers *via* sequential addition of monomers.

Synthesis of Diblock Copolymers Containing Electron-Rich and Electron-Deficient Blocks

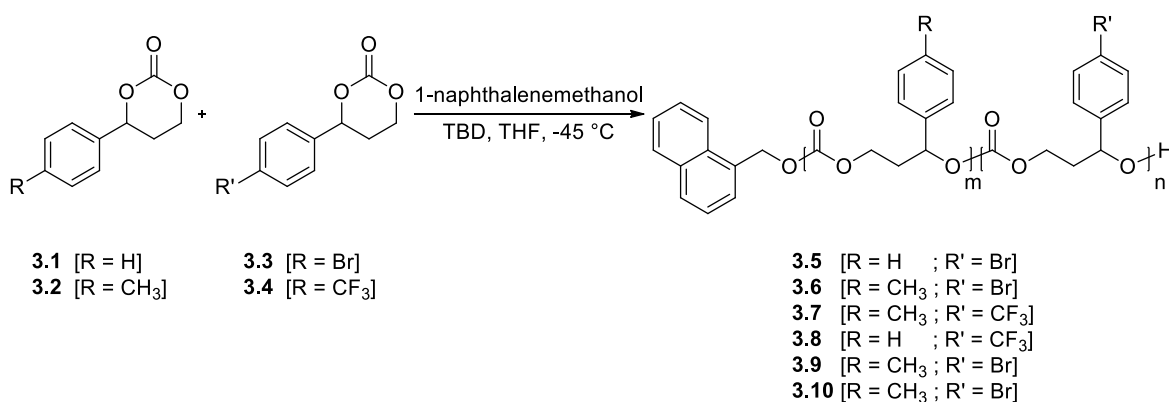
In the present work, we synthesized several diblock copolymers containing electron-rich and electron-deficient blocks from α -ArTMCs (monomers). All the diblock copolymers were prepared *via* sequential addition of monomers, wherein the electron-rich monomer was polymerized first followed by the electron-deficient monomer. The reason for polymerizing electron-rich monomer first is to minimize transesterification reactions (*vide infra*). As discussed in chapter II, the organocatalyzed ROP of α -ArTMCs results in polycarbonates with varying degrees of regio-regularity depending on reaction conditions. In order to prepare block copolymers with greater regio-regularity, conditions that gave higher X_{reg} value for the polymerization of α -ArTMCs were chosen.

Among the various conditions that were screened for ROP of α -ArTMCs, reactions that were carried out with TBD as catalyst in THF at -45 °C gave the highest regio-regularity. As before, 1-naphthalene methanol was used as an initiator in the polymerization. In the

synthesis of diblock copolymers, the monomers to initiator ratio used is given by $[M1]_0:[M2]_0:[I]_0 = 50:50:1$. With this ratio, the number of repeat units present in each block of the diblock copolymer will be approximately 50 and the overall repeat units in the diblock copolymer will be approximately 100. We started our first diblock copolymer synthesis by polymerizing α -PhTMC (**3.1**) using 2 mol% of TBD in THF at -45 °C (Table 3.1, entry 1). Based on our previous studies, the monomer reaches 98% conversion in 90 minutes. After 90 minutes, a cold solution of second monomer α -4-Br-PhTMC (**3.3**) in THF was added quickly to the reaction mixture (Table 3.1, entry 1). The progress of the diblock copolymer formation was monitored by ^1H NMR. After 40 minutes, 98% of the second monomer was consumed and immediately the reaction was quenched using 4 equivalents of benzoic acid with respect to TBD. The diblock copolymer poly(α -PhTMC-*b*- α -4-Br-PhTMC) (**3.5**) that contains a moderately electron-rich block was isolated as a white solid after precipitation of reaction mixture in methanol. In the second diblock copolymer **3.6**, a more electron-rich block was made by polymerizing α -4-Me-PhTMC (**3.2**) following the above reaction conditions (Table 3.1, entry 2). The monomer reached 97% conversion in 360 minutes and then a cold solution of α -4-Br-PhTMC (**3.3**) in THF was added to the reaction mixture. As in the previous synthesis, the reaction mixture was quenched after 40 minutes and the diblock copolymer was isolated as a white solid after precipitation in methanol. The third diblock copolymer **3.7** contains a more electron-deficient block compared to previous diblock copolymers. This was synthesized by polymerizing α -4-Me-PhTMC (**3.2**) following the optimized conditions (Table 3.1, entry 3). After the stipulated time, a cold solution of α -4-CF₃-PhTMC (**3.4**) in THF was added and the progress of the polymerization was monitored by ^1H NMR. After 15 minutes of adding the second monomer, 97% conversion was

observed. Immediately, the reaction mixture was quenched and precipitated into methanol to isolate **3.7** as a white solid. The last kind of diblock copolymer **3.8** contains a moderately electron-rich and a more electron-deficient block. This diblock copolymer was synthesized by polymerizing α -PhTMC (**3.1**), followed by the polymerization of α -4-CF₃-PhTMC (**3.4**) under the above-mentioned reaction conditions and reaction time (Table 3.1, entry 4). The diblock copolymer **3.8** was isolated as a white solid after precipitation of quenched reaction

Table 3.1. Synthesis of Different kinds of Diblock Copolymers Containing Electron-Rich and Electron-Deficient Blocks



entry ^{a,b,c}	copolymer	M1	time ^d (min)	conv ^e (%)	M2	time ^f (min)	conv ^g (%)	$M_{n,theo}^h$ (g mol ⁻¹)	$M_{n,NMR}^i$ (g mol ⁻¹)	m^j	n^k	$M_{n,SEC}^l$ (g mol ⁻¹)	\bar{D}	X_{reg}	Yield (%)
1	3.5	3.1	90	98	3.3	40	98	21470	21000	48	48	10200	1.37	0.73	85
2	3.6	3.2	360	97	3.3	40	98	21970	20900	45	47	11900	1.36	0.69	83
3	3.7	3.2	360	97	3.4	15	97	21180	18000	44	38	12600	1.39	0.69	66
4	3.8	3.1	90	98	3.4	15	97	20690	18500	48	40	12000	1.33	0.79	82
5 ^b	3.9	3.2	780	97	3.3	300	96	21710	21000	47	46	4900	1.41	0.12	56
6 ^c	3.10	3.2	7	96	3.3	6	90	20940	19200	43	42	8900	1.43	0.36	80

^aReactions were run with [M1]₀/[M2]₀/[I]₀/[TBD] = 50/50/1/1; [M1]₀ = 1 M; [M2]₀ = 0.7 M; ^bReaction was run using TU/DBU as catalyst instead of TBD at 27 °C; [M1]₀ = 2 M; [M2]₀ = 1.3 M; ^cReaction was run using TBD as catalyst at 27 °C; [M1]₀ = 1.95 M; [M2]₀ = 0.65 M; See experimental procedure for details; ^dTime taken by M1 to reach respective conversion; ^eConversion of M1, condition was optimized in chapter II; ^fTime taken by M2 to reach respective conversion; ^gReaction aliquots were quenched and conversions were determined by ¹H NMR recorded using CDCl₃ as solvent; ^hCalculated using the formula ([M1]₀/[I]₀) X (conversion/100) X (molar mass of repeating unit = (**3.1** = 178 g mol⁻¹) (**3.2** = 192 g mol⁻¹) (**3.3** = 257 g mol⁻¹) (**3.4** = 246 g mol⁻¹) + ([M2]₀/[I]₀) X (conversion/100) X (molar mass of repeating unit) + (molar mass of initiator = 158 g mol⁻¹); ⁱEstimated by ¹H NMR analysis in CDCl₃; ^jDegree of polymerization of 1st block; ^kDegree of polymerization of 2nd block; ^lEstimated by SEC using THF as eluent against polystyrene standards (uncorrected data).

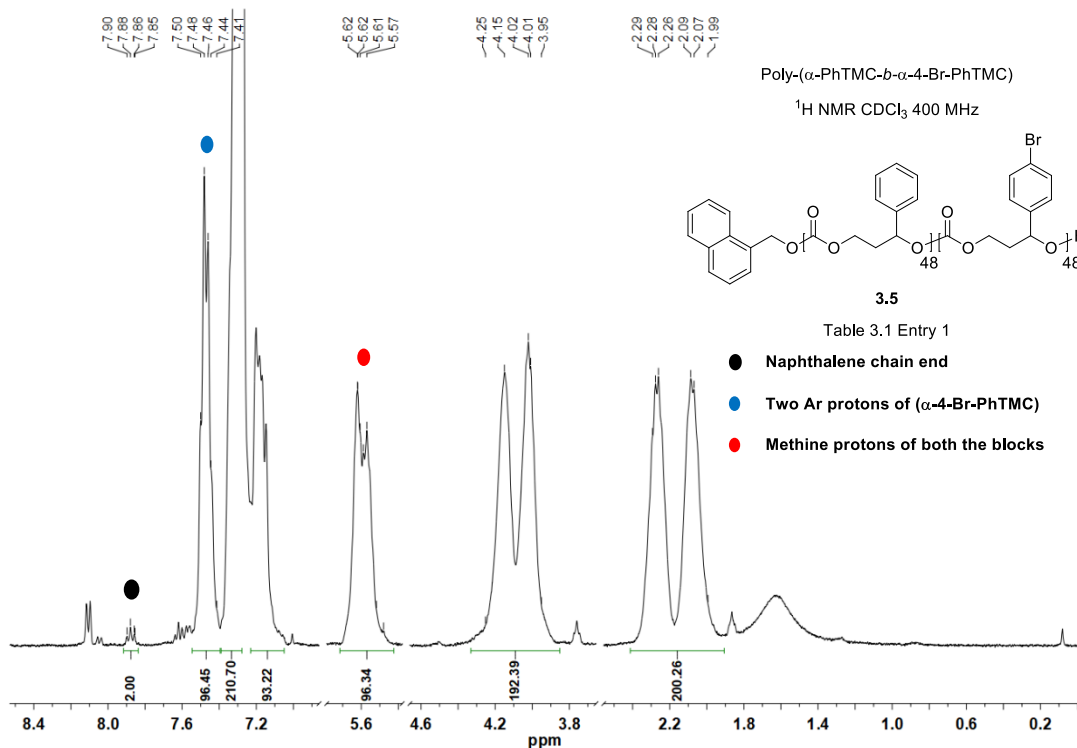
mixture in methanol. Apart from synthesizing four different kinds of diblock copolymers, we also synthesized two more diblock copolymers that are block-wise equivalent to **3.6**, but differing in regio-regularity. Using thiourea-DBU catalytic system, (reaction conditions were optimized in chapter II Table 2.6) the diblock copolymer **3.9** having a lower regio-regularity was synthesized and isolated as a white solid (Table 3.1, entry 5). The final diblock copolymer **3.10** having slightly higher regio-regularity compared to **3.9** was synthesized using TBD at 27 °C (Table 3.1, entry 6).

Estimation of Number Average Molar Mass, Block Lengths, and Regio-Regularity of Diblock Copolymers

We have estimated the M_n (number average molar mass) of synthesized diblock copolymers using ^1H NMR and Size Exclusion Chromatography (SEC) (Table 3.1). Using ^1H NMR, we were also able to determine the number of monomer units present in each block of the diblock copolymers. In chapter II, we have shown that the ^1H NMR of synthesized polycarbonate contains an apparent triplet at δ 7.88 and this corresponds to two naphthalene ring protons (part of 1-naphthalene methanol). Therefore, M_n of the polycarbonate can be estimated by first normalizing the integration of apparent triplet peak (δ 7.88) to two. The integration of methine protons of the polymer backbone indicates the number of monomer units present in the polymer. Similarly, the ^1H NMRs of all the diblock copolymers possess a distinct apparent triplet at δ 7.88. The methine protons corresponding to both the blocks of a diblock copolymer overlap and appear as a single multiplet at δ 5.73-5.46. Likewise, the two kinds of methylene protons belonging to both the blocks overlap and result in two kinds of multiplets at δ 4.29-3.91 and δ 2.36-1.96. The overall length of a diblock copolymer corresponds to the integral value of the peak belonging to the methine protons after

normalizing the peak at δ 7.88 to two. To estimate the length of each block in a diblock copolymer, we need to identify at least one peak that solely belongs to one of the blocks. In the case of poly(α -PhTMC-*b*- α -4-Br-PhTMC) (**3.5**), a distinct multiplet appears at δ 7.50-7.41. The chemical shift of this multiplet matches exactly with the doublet peak that corresponds to two aromatic protons in α -4-Br-PhTMC (**3.3**). Integration of the multiplet at δ 7.50-7.41 reveals that, 48 repeat units are present in the electron-deficient block (Table 3.1, entry 1) (Figure 3.8). With this data, the number of repeat units present in the other block can be calculated by subtracting 48 from the overall length of the copolymer. The integration of methine protons of **3.5** corresponds to 96 monomer units in the entire copolymer and therefore the number of repeat units present in the electron-rich block will be 48 (Table 3.1, entry 1) (Figure 3.8). Similarly, the multiplet at δ 7.50-7.41 was also seen in the diblock copolymer poly(α -4-Me-PhTMC-*b*- α -4-Br-PhTMC) (**3.6**). After integrating the necessary peaks, the number of repeat units present in the electron-rich and electron-deficient blocks are 45 and 47 respectively (Table 3.1, entry 2). The diblock copolymers **3.7** and **3.8** have an electron-deficient block in common. Inspection of the ^1H NMRs of **3.7** and **3.8** shows a distinct multiplet at δ 7.64-7.56. This was assigned to the electron-deficient block as its chemical shift matches with the doublet peak of two aromatic protons in α -4-CF₃-PhTMC **3.4**. ^1H NMR integrations in **3.7** reveal that there are 44 repeat units present in the electron-rich and 38 repeat units in the electron-deficient block (Table 3.1, entry 3). For the diblock copolymer **3.8**, the integrations show 48 and 40 repeat units in the electron-rich and electron-deficient blocks respectively (Table 3.1, entry 4). The block lengths of the remaining two diblock copolymers (**3.9** and **3.10**) were determined in a manner similar to **3.6**. Using this approach, the number of repeat units were determined to be 47 and 46 for diblock copolymer

Figure 3.8. An Example to Show the Block Lengths of a Diblock Copolymer Using ^1H NMR



3.9 (Table 3.1, entry 5). Similarly, there are 43 and 42 repeat units in **3.10** (Table 3.1, entry 6).

The M_{ns} (inclusive of block lengths) of synthesized diblock copolymers estimated by ^1H NMR were in close agreement with the expected M_{ns} . However, M_{ns} measured by SEC did not match well with the expected molar masses possibly due to differences in the hydrodynamic radii of our polymer and the polystyrene standards.

The process of determining the regio-regularity of polycarbonates was discussed in detail in the previous chapter. Calculating the regio-regularity of each block in the case of diblock copolymers using ^{13}C NMR was not possible due to the partial overlapping of carbonyl carbon peaks of both the blocks. In spite of partial overlap of carbonyl carbon peaks, various kinds of carbonate linkages were clearly distinguishable. As a result, a

number representing the overall regio-regularity of a diblock copolymer was measured. The regio-regularity (X_{reg}) of diblock copolymer **3.5** was found to be 0.73. Both **3.6** and **3.7** diblock copolymers had the same regio-regularity with $X_{reg} = 0.69$ (Table 3.1, entries 2 & 3). The highest regio-regularity was observed for the diblock copolymer **3.8** with $X_{reg} = 0.79$ (Table 3.1, entry 4). Diblock copolymers **3.9** and **3.10** that were structurally identical to **3.6** exhibit low regio-regularities with $X_{reg} = 0.36$ and 0.12, respectively (Table 3.1, entries 5 & 6).

Significance of Obtaining Diblock Copolymers with Low Dispersity (\mathcal{D})

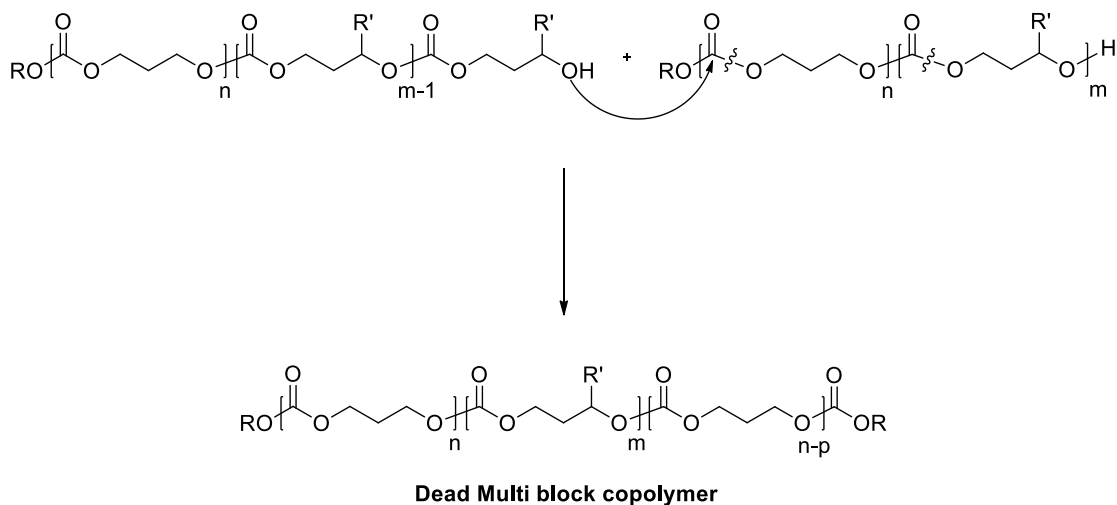
The living polymerization technique used for the synthesis of diblock copolymers should be completely free of chain transfer reactions (transesterification). In the case of polycarbonates synthesis, the chain transfer reactions can potentially lead to the formation of multi-block dead polymers (both ends of the polymer will be capped and cannot grow further) (Scheme 3.1a). Simultaneously, it can lead to the formation of multi-block copolymers with active chain ends (Scheme 3.1b). Therefore, transesterification has to be minimal to ensure block purity.

Some of the ways to assess the purity of synthesized block copolymers include: (i) observation of dispersity of copolymers, (ii) comparative experimental studies (such as ^1H NMR and DSC) between the diblock copolymers and random copolymers, and (iii) AFM studies on samples. In AFM studies, blocks that are incompatible with each other will micro-phase separate into well-ordered phase only when the diblock copolymer purity is high.

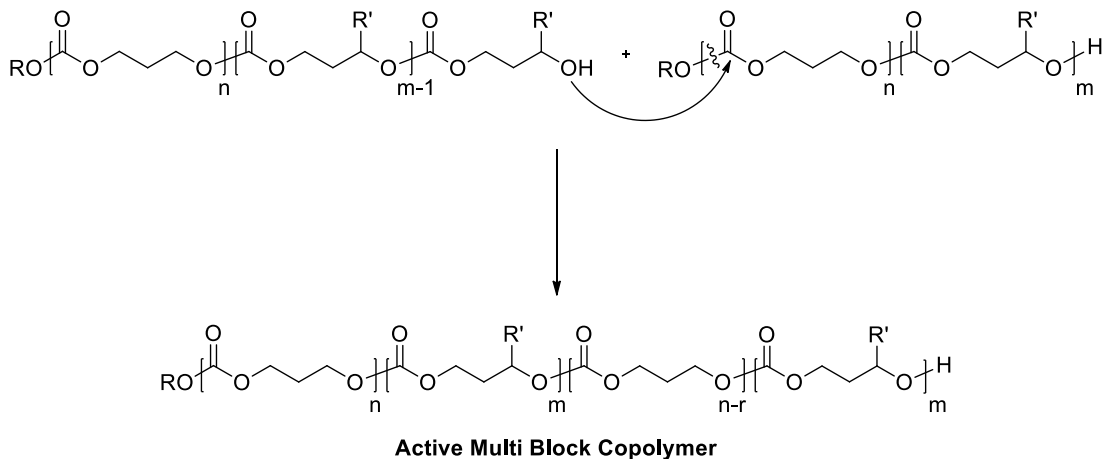
Dispersity (\mathcal{D}), which can be determined using SEC can predict the purity of diblock copolymers. Formation of impure blocks is a direct result of transesterification reactions. Transesterification also results in an increase in \mathcal{D} . Therefore, dispersity can be an indirect

Scheme 3.1. Transesterification of Polycarbonates Leading to the Formation of Dead Multi-Block Copolymer and Active Multi-Block Copolymer

A



B



measure of block purity. Diblock copolymers that are contaminated with multi-block copolymers due to extensive transesterification reactions will have high dispersity. On the other hand, the dispersity of pure diblock copolymers will be low. Moreover, the presence of multi-block dead polymers can be seen in the form of shoulders in the SEC traces.

Since TBD is known to catalyze transesterification reactions at high monomer conversions which can then lead to higher dispersity, we decided to monitor the increase of

dispersity with time. In the previous chapter, we reported that the TBD catalyzed ROP of α -PhTMC in THF reaches high monomer conversion in five minutes at room temperature (Table 3.2, entry 1). To assess the rate of transesterification, the polymerization was allowed to continue for 24 h. After quenching and precipitation, the obtained polymer was found to have a $\mathcal{D} = 2.34$ (Table 3.2, entry 2), due to transesterification reactions. Reactions quenched at five minutes showed significantly lower dispersity. In this work, the synthesis of diblock copolymers were carried out at $-45\text{ }^{\circ}\text{C}$ and quenched right after the monomer reached high conversions. Therefore, under this condition we expect that transesterification reactions will be minimal. This was reflected in SEC, where we obtained a unimodal peak without any low molar mass shoulders. In addition, the dispersity of synthesized diblock copolymers was in the range of 1.33-1.43. This indicates that the transesterification reactions were minimal during the course of diblock copolymer synthesis.

Apart from reaction conditions, the selection of monomer that needs to be polymerized first in a diblock copolymer synthesis also plays an important role in minimizing transesterification reactions. We can observe from Table 3.1 that electron-deficient monomers (**3.3** and **3.4**) are polymerized faster compared to electron-rich monomers (**3.1** and **3.2**). This clearly suggests that the rate of propagation of electron-deficient monomers is greater than that of electron-rich monomers. We can reasonably

Table 3.2. TBD Catalyzed Ring Opening Polymerization of α -PhTMC (**3.1**)

entry ^a	$[\text{M}]_0/[\text{I}]_0$	time	conv (%)	$M_{n,\text{theo}}$ (g mol ⁻¹)	$M_{n,\text{NMR}}$ (g mol ⁻¹)	$M_{n,\text{SEC}}$ (g mol ⁻¹)	\mathcal{D}	X_{reg}
1	100/1	5 min	95	17070	17800	9200	1.43	0.40
2	100/1	24 h	97	17420	nd ^b	8800	2.34	0.03

^aReactions were run using 2 mol% TBD in THF at 27 $^{\circ}\text{C}$; $[\text{M}]_0 = 2\text{ M}$; ^bnot determined

assume that the rate constant for transesterification (k_{te}) will be proportional to the propagation rate constant (k_p) as these steps are mechanistically similar. Based on this assumption, if the monomer with the higher k_p is polymerized first, then during the polymerization of the slower second block, extensive transesterification is possible in the first block. On the other hand, carrying out polymerization of the electron-rich monomer at the beginning and then polymerizing electron-deficient monomer can significantly reduce the level of transesterification reactions. The low dispersity observed in our diblock copolymer suggests that the isolated diblock copolymers were significantly pure. As dispersity and SEC traces give clarity on the purity of the synthesized diblock copolymers, we did not undertake the other studies to determine its purity.

Differential Scanning Calorimetry Studies of Diblock Copolymers

Differential scanning calorimetry (DSC) studies of all diblock copolymers showed a single glass transition temperature (T_g) (Table 3.3, entries 1-6). T_g s of diblock copolymers **3.5**, **3.6**, **3.8** and **3.9** were found to be an average of T_g s of individual blocks (Table 3.3, entries 1, 2, 4 and 5). While T_g s of **3.7** and **3.10** were found to be close to that of respective electron-deficient blocks (Table 3.3, entries 3 & 6).

Table 3.3. DSC Studies of Diblock Copolymers

copolymer	T_g
3.5	57 °C
3.6	59 °C
3.7	62 °C
3.8	56 °C
3.9	59 °C
3.10	64 °C

Atomic Force Microscope (AFM) Studies of Diblock Copolymers

Thin films of all four diblock copolymers were analyzed using AFM in tapping mode to study whether diblock copolymers micro-phase separate or phase mix. Figure 3.9A and 3.9B depict a $2\mu\text{m} \times 2\mu\text{m}$ cross section of the height and phase images of as spun-cast films of diblock copolymers **3.5** and **3.6**. Height images of the diblock copolymers suggests that the surface of the thin film is smooth with RMS roughness less than 0.3 nm. Typically, the RMS roughness will be significantly higher for thin films that exhibit ordered micro-phase separation. This observation suggests that there is no micro-phase separation in both the diblock copolymers. Further we wanted to verify whether there is disordered micro-phase separation in diblock copolymers. For this purpose, we extracted the phase profiles of both diblock copolymers and measured domain sizes. After collecting more than 200 data points we plotted the histogram of domain sizes and fitted the curve with Lorentzian function. If there is disordered micro-phase separation, then it should result in a narrow distribution of domain sizes with small standard deviation. In the case of our diblock copolymers the distribution is very broad with an average domain size of 25 nm and standard deviation of 14 nm (Figure 3.10A and 3.10B). As there is random distribution of domain sizes, we can conclude that that there is very little phase separation in as spun-cast films. Similarly, the as spun-cast thin films of the other two diblock copolymers (**3.7** and **3.9**) are smooth with RMS roughness less than 0.4 nm, which is an indication of phase mixing (Figure 3.11A and 3.11B).

Usually the thin films of diblock copolymers were thermally annealed above its glass transition temperature in order to obtain an equilibrated micro-phase separated system. In our studies we thermally annealed the thin films of diblock copolymers at 55 °C (which is

Figure 3.9. AFM Images of As Spun-Cast Thin Films of Diblock Copolymers: (A) 3.5; (B) 3.6

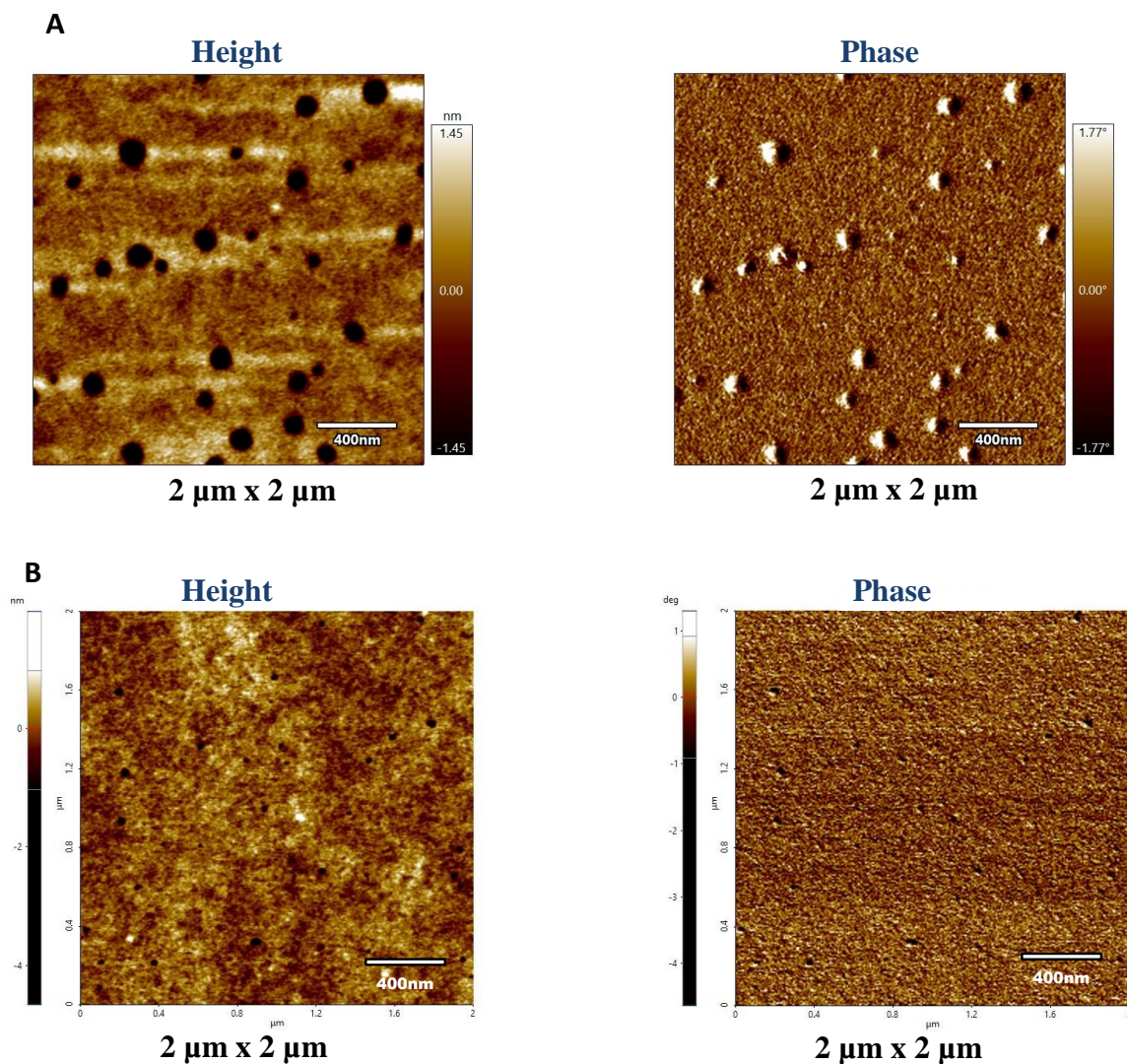


Figure 3.10. Curve Fitting of Histogram of Diblock Copolymers: (A) 3.5; (B) 3.6

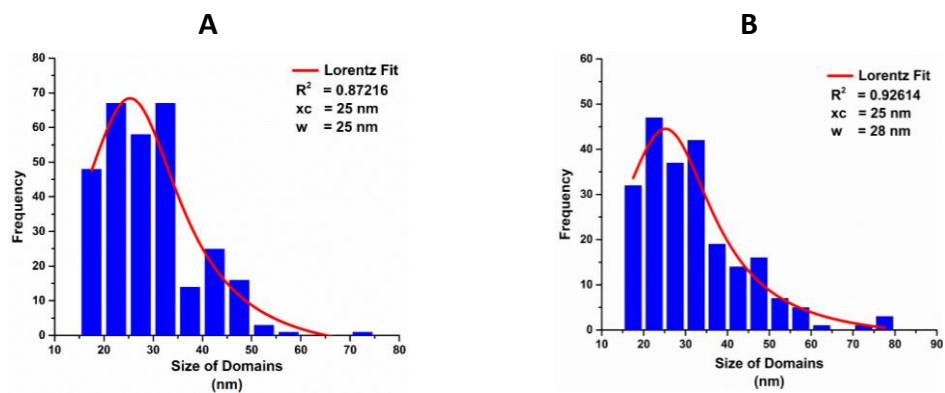
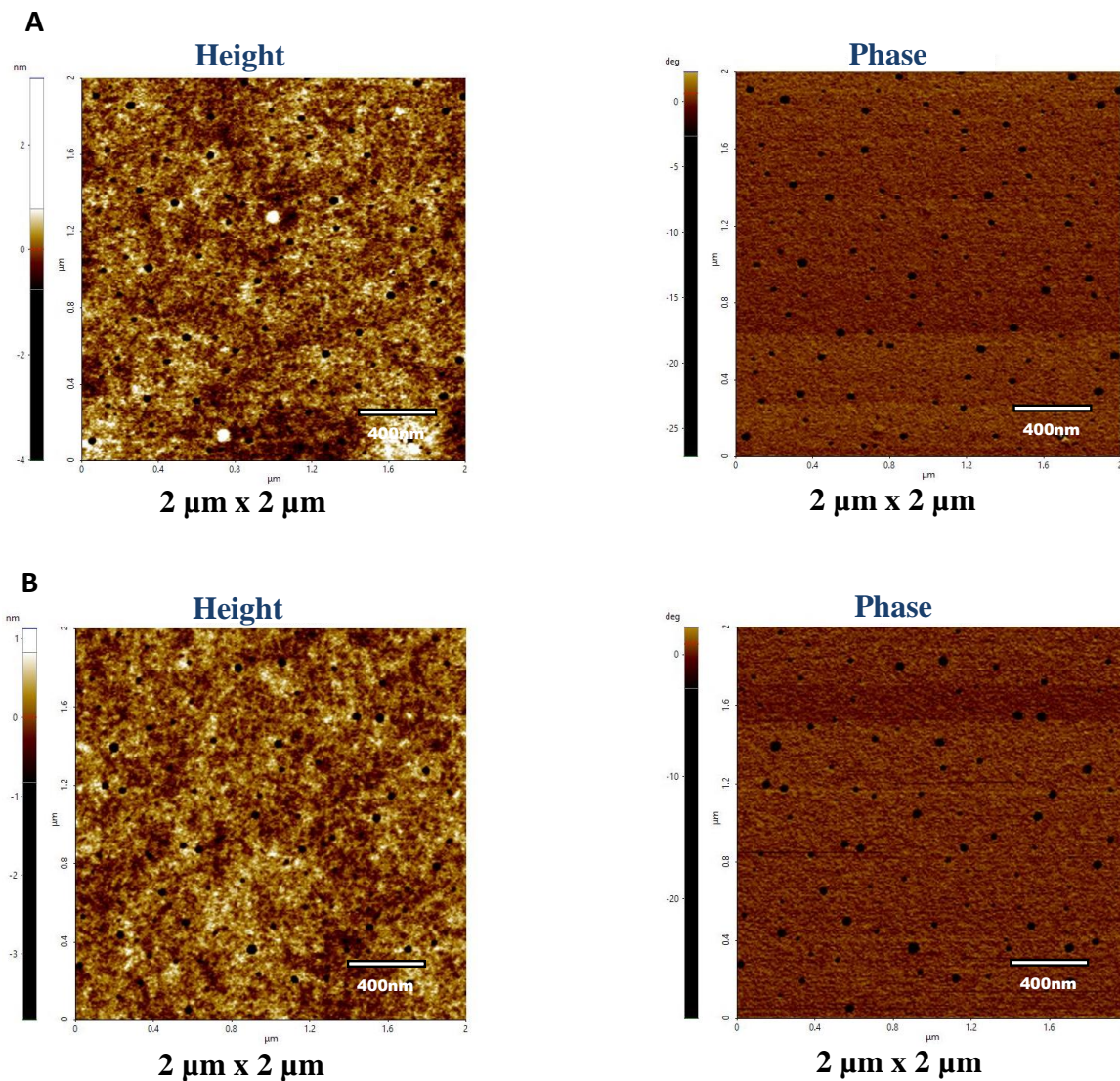


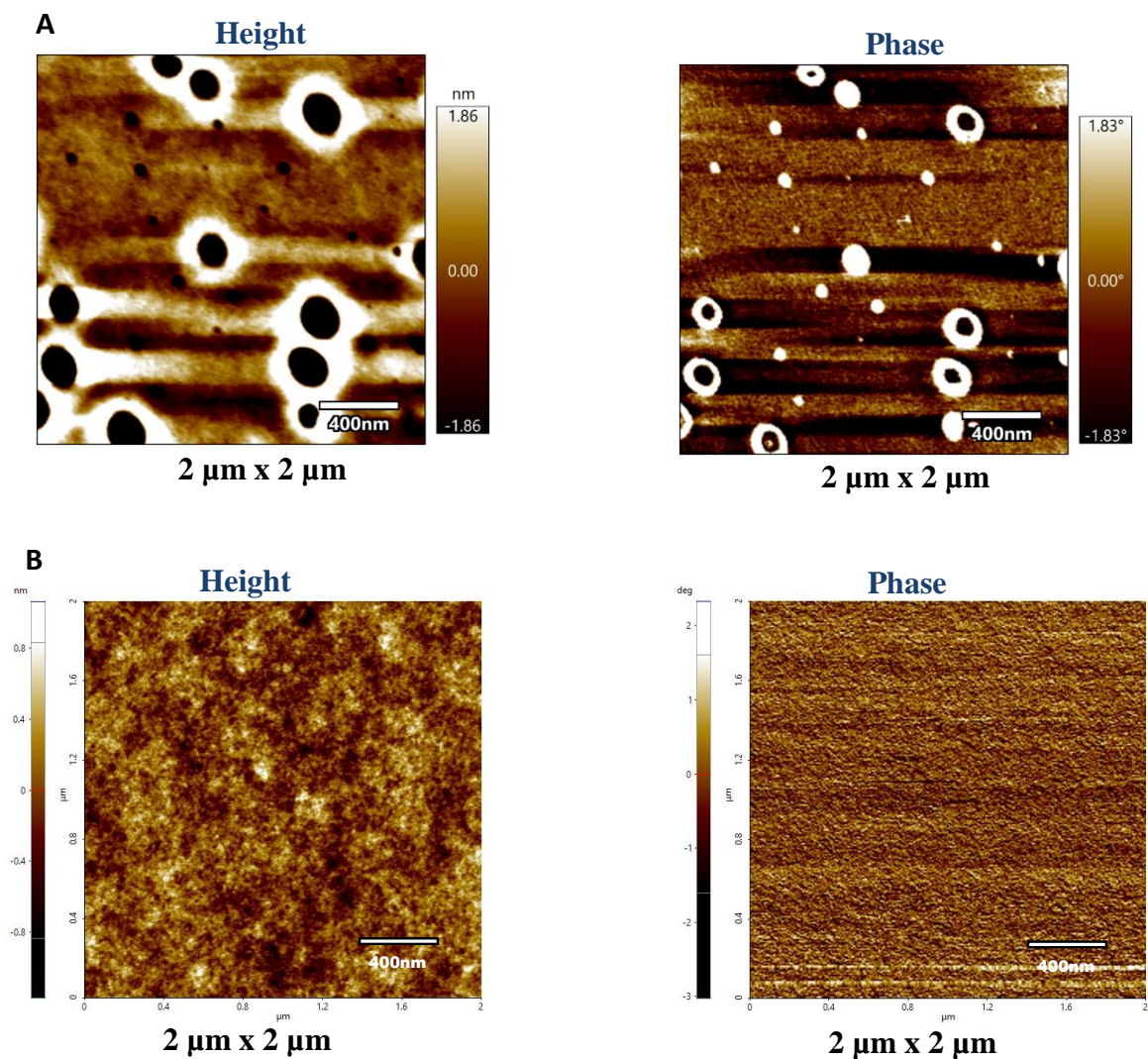
Figure 3.11. AFM Images of As Spun-Cast Thin Films of Diblock Copolymers: (A) **3.7**; (B) **3.8**

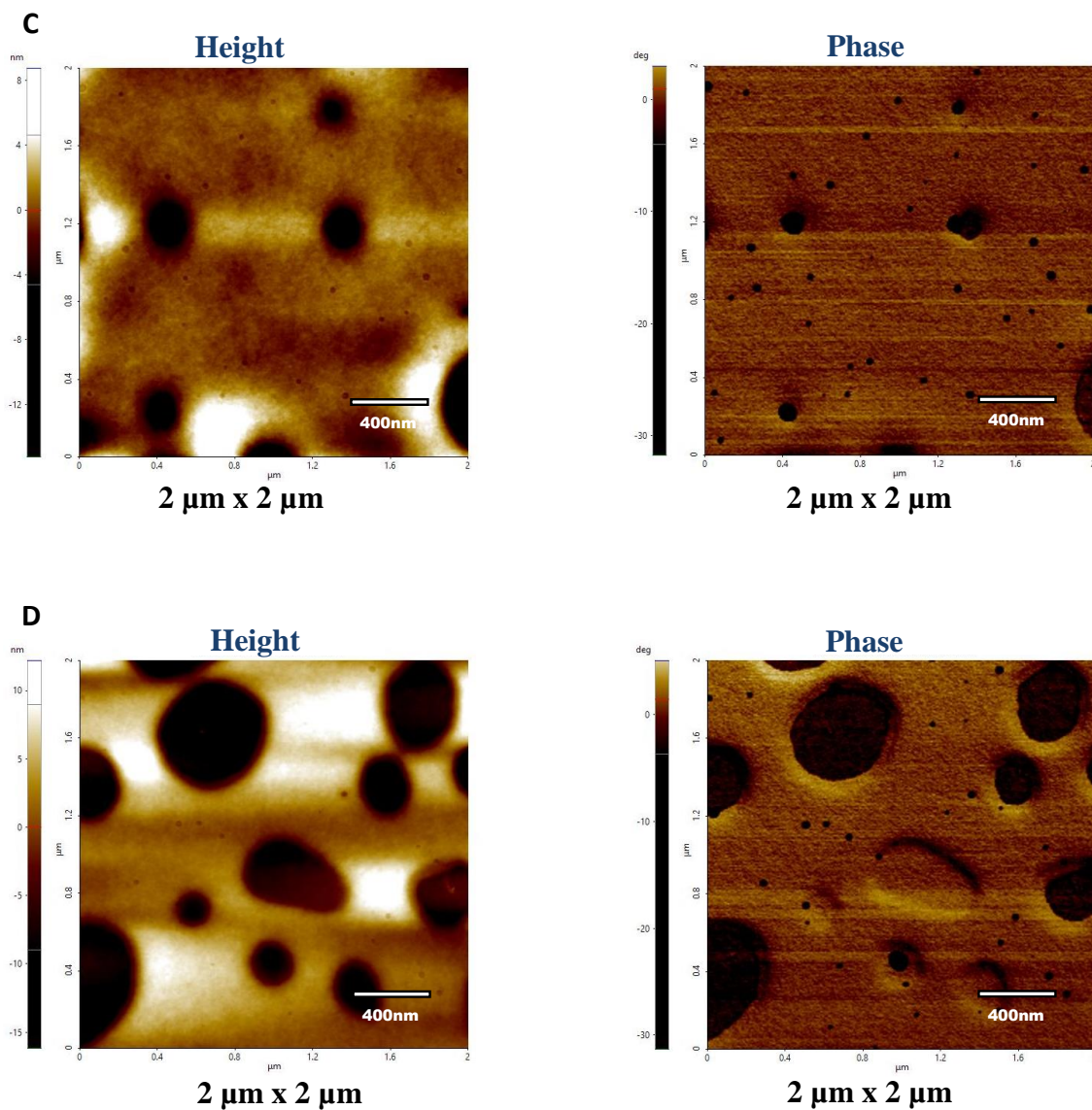


either the mid-point or the onset of transition) for 30 minutes and quenched to room temperature immediately to observe whether it phase separates. Figure 3.12(A-D) represents the height and phase images of thermally annealed thin films of diblock copolymers (**3.5-3.8**). All the thin films of diblock copolymers start dewetting upon thermal annealing at 55 °C which results in the formation of pin holes. In the case of diblock copolymer **3.6** we were able to image an area free of pin holes. The rate of dewetting in the case of diblock copolymers containing trifluoromethyl substituent was greater compared to bromo

substituted copolymers. Dewetting was observed to be severe at higher temperatures and longer time period. The average of RMS roughness measured in the area free of pin holes in all the height images of thin films were found to be low (0.3 to 0.5 nm). Also, the distribution of domain sizes calculated for diblock copolymers (3.5 and 3.6) were found to be completely random. This indicates that the diblock copolymers remain phase mixed upon thermal annealing up to 55 °C.

Figure 3.12. AFM Images of Thermally Annealed Thin Films of Diblock Copolymers: (A) 3.5; (B) 3.6; (C) 3.7; (D) 3.8





3.5 Conclusions

Diblock copolymers can be synthesized *via* sequential addition of monomers if the polymerization technique exhibits living behavior. In this chapter, we describe the synthesis of diblock copolymers using the chain extension approach. We sought a diblock copolymer wherein one block has an electron-rich aromatic pendant group while the other block has an electron-deficient aromatic pendant group. Using this approach, we expected to suppress phase separation and enhance interchain interactions *via* π - π interactions. The synthesis of

diblock copolymer was carried out by initially polymerizing the electron-rich monomer followed by addition of the electron-deficient monomer. This order of addition was chosen to minimize transesterification reactions and formation of dead chain ends. We have shown that transesterification is accompanied by a large increase in dispersity. In our synthesis, there is only a minimal change in dispersity upon addition of the second monomer. The molar mass of the polymers were measured by both SEC and ^1H NMR. As in the previous chapter, the molar mass measured by end group analysis correlated very well with the monomer to initiator ratio. On the other hand, the molar mass measured SEC did not match with the expected molar mass. Although the carbonyl signals for different linkages were distinct, the overlap of signals from the two different blocks prevented the estimation of regio-regularity for individual blocks. Therefore, we measured an overall regio-regularity. All diblock copolymers exhibited a single glass transition temperature. AFM studies indicated that there was minimal phase separation in all of the diblock copolymers. In future we will study the effect of phase mixing on mechanical properties. For this purpose, we need to prepare diblock copolymers on a larger scale. Also, we need to avoid dewetting of thin films in order to study the effect of thermal annealing at higher temperatures. This can be controlled by using other substrates or by synthesizing diblock copolymers having greater degree of polymerization.

3.6 Experimental Section

Materials

All glasswares were dried overnight in an oven at 120 °C prior to use. Polymerization reactions were carried out inside glove box (except for lower temperature reactions, where only weighings were carried out inside the glove box). THF was distilled

over sodium-benzophenone after ketyl formation and stored in glove box. Distilled THF was dried over activated neutral alumina prior to use. TBD was dried azeotropically with dry benzene under argon atmosphere. 1-naphthalenemethanol was sublimed under high vacuum. Monomers were dried azeotropically using dry benzene under argon atmosphere prior to use.

Instrumentation and Characterization

Infrared spectra were recorded on Perkin Elmer FT-IR diamond crystal. ^1H and ^{13}C NMRs were recorded on a Bruker AVANCE-400 (400 MHz) Fourier transform NMR spectrometer. Chemical shifts are reported in parts per million (ppm) with respect to the residual solvent peak: CDCl_3 (^1H NMR: 7.27 ppm, ^{13}C { ^1H } NMR: 77.2 ppm); DMSO-d_6 (^1H NMR: 2.50 ppm, ^{13}C { ^1H } NMR: 39.5 ppm). Size exclusion chromatography (SEC) was performed on a Shimadzu, isocratic HPLC pump, refractive index detector (RID-10A), and a PLgel polystyrene-*co*-divinylbenzene gel column (Polymer Lab) 5 μm MiniMix-C (250x4.6 mm). The measurements were conducted at 40 $^\circ\text{C}$ with THF as eluent (flow rate set to 0.5 mL/min) against narrow disperse polystyrene standards. Data collection and analyses were carried out using Lab solutions software. Thermogravimetric analysis (TGA) was performed on a Mettler-Toledo model TGA/DSC 2, under nitrogen atmosphere with a heating rate of 10 $^\circ\text{C}/\text{min}$. The measurements were analyzed using Mettler-Toledo Star^e software. Glass transition temperatures (T_g) were measured by Differential scanning calorimetry (DSC) on a TA-DSC Q2000 under N_2 atmosphere with a heating and cooling rate of 5 $^\circ\text{C}/\text{min}$ from -20 $^\circ\text{C}$ to 150 $^\circ\text{C}$. Measurements were analyzed using TA universal analysis software. The T_g was taken as the midpoint of the inflection tangent, upon the second heating scan. Phase mixing in thin films were analyzed using atomic force microscopy (AFM). AFM images of thin film of **3.5** were recorded using Oxford instruments Asylum Research Cypher

instrument in tapping mode with a 10 nm radius of Si tip scanning with 26 N/m force. AFM images of thin films of rest of diblock copolymers were recorded using Park Systems NX20 in tapping mode with a 10 nm radius of Si tip scanning with 26 N/m force.

Synthetic Procedures of Diblock Copolymers

Poly(α -PhTMC-*b*- α -4-Br-PhTMC) (3.5)

A stock solution of TBD and initiator (0.087 M in each) was prepared by dissolving 12.1 mg of TBD and 13.8 mg of 1-naphthalenemethanol in dry THF. The monomer solution was prepared in a 10 mL flame dried schlenk tube by dissolving 139 mg of α -PhTMC **3.1** (0.78 mmol) in 0.60 mL of dry THF. The monomer solution was cooled to -45 °C for one minute. To this monomer solution, 0.18 mL of the stock solution containing TBD and initiator was added. The reaction mixture was stirred for 90 minutes at -45 °C. Separately, 201 mg of α -4-Br-PhTMC **3.3** (0.78 mmol) was dissolved in 0.32 mL of dry THF and was cooled to -45 °C for one minute. This monomer solution was added to the polymer reaction mixture at -45 °C. The reaction mixture was stirred for 40 minutes at -45 °C. The reaction mixture was then quenched with 4 equivalents of benzoic acid in 1 mL of DCM. The solvents were removed under reduced pressure. The residue was dissolved in 2.0 mL of DCM and precipitated into 50 mL of stirring methanol. The precipitate initially appears as a semi-solid material. Methanol was decanted and the precipitate was washed with 50 mL of methanol. The polymer was then dried under high vacuum to obtain 292 mg of white solid **3.5** (85% yield, average yield over two runs = 83%).

Characterization:

$^1\text{H NMR}$ (400 MHz, CDCl_3): δ 7.88 (app t, 2H, $J = 7.8$ Hz), 7.50-7.41 (m, 96H), 7.39-7.28 (m, 209H), 7.20-7.12 (m, 93H), 5.67-5.57 (m, 96H), 4.25-3.91 (m, 191H), 2.36-

1.99 (m, 199H); $^{13}\text{C}\{^1\text{H}\}$ NMR (100 MHz, DMSO- d_6): δ 154.29-154.02 (Regio-irregular linkage), 153.77-153.34 (Head to Tail linkage), 153.08-152.67 (Regio-irregular linkage), 139.1, 138.5, 131.5, 128.5, 128.3, 128.2, 126.1, 121.5, 76.2, 75.6, 63.9, 34.5; IR: 1739 cm^{-1} ; $M_{n,\text{NMR}} = 21000$ g/mol; $\text{Đ} = 1.37$; $X_{\text{reg}} = 0.73$; $T_g = 57$ °C; TGA in N_2 : 198-295 °C, 94% weight loss.

Poly(α -4-Me-PhTMC-*b*- α -4-Br-PhTMC) (3.6)

A stock solution of TBD and initiator (0.087 M in each) was prepared by dissolving 12.1 mg of TBD and 13.8 mg of 1-naphthalenemethanol in dry THF. The monomer solution was prepared in a 10 mL flame dried schlenk tube by dissolving 150 mg of α -4-Me-PhTMC **3.2** (0.78 mmol) in 0.60 mL of dry THF. The monomer solution was cooled to -45 °C for one minute. To this monomer solution, 0.18 mL of the stock solution containing TBD and initiator was added. The reaction mixture was stirred for 360 minutes at -45 °C. Separately, 201 mg of α -4-Br-PhTMC **3.3** (0.78 mmol) was dissolved in 0.32 mL of dry THF and was cooled to -45 °C for one minute. This monomer solution was added to the polymer reaction mixture at -45 °C. The reaction mixture was stirred for 40 minutes at -45 °C. The reaction mixture was then quenched with 4 equivalents of benzoic acid in 1 mL of DCM. The solvents were removed under reduced pressure. The residue was dissolved in 2.0 mL of DCM and precipitated into 50 mL of stirring methanol. The precipitate initially appears as a semi-solid material. Methanol was decanted and the precipitate was washed with 50 mL of methanol. The polymer was then dried under high vacuum to obtain 295 mg of white solid **3.6** (83% yield, average yield over two runs = 80%).

Characterization:

^1H NMR (400 MHz, CDCl_3): δ 7.88 (app t, 2H, $J = 8.0$ Hz), 7.50-7.41 (m, 94H), 7.19-7.03 (m, 278H), 5.67-5.46 (m, 92H), 4.29-3.92 (m, 184H), 2.36-1.97 (m, 335H); $^{13}\text{C}\{^1\text{H}\}$ NMR (100 MHz, DMSO-d_6): δ 154.29-154.01 (Regio-irregular linkage), 153.73-153.35 (Head to Tail linkage), 153.08-152.72 (Regio-irregular linkage), 138.5, 137.5, 136.1, 131.5, 129.0, 128.3, 126.1, 121.4, 76.2, 75.6, 63.9, 34.4, 20.6; IR: 1739 cm^{-1} ; $M_{n,\text{NMR}} = 20900\text{ g/mol}$; $\text{Đ} = 1.36$; $X_{\text{reg}} = 0.69$; $T_g = 59\text{ }^\circ\text{C}$; TGA in N_2 : 202-301 $^\circ\text{C}$, 94% weight loss.

Poly(α -4-Me-PhTMC-*b*- α -4-CF₃-PhTMC) (3.7)

A stock solution of TBD and initiator (0.087 M in each) was prepared by dissolving 12.1 mg of TBD and 13.8 mg of 1-naphthalenemethanol in dry THF. The monomer solution was prepared in a 10 mL flame dried schlenk tube by dissolving 150 mg of α -4-Me-PhTMC **3.2** (0.78 mmol) in 0.60 mL of dry THF. The monomer solution was cooled to $-45\text{ }^\circ\text{C}$ for one minute. To this monomer solution, 0.18 mL of the stock solution containing TBD and initiator was added. The reaction mixture was stirred for 360 minutes at $-45\text{ }^\circ\text{C}$. Separately, 192 mg of α -4-CF₃-PhTMC **3.4** (0.78 mmol) was dissolved in 0.32 mL of dry THF and was cooled to $-45\text{ }^\circ\text{C}$ for one minute. This monomer solution was added to the polymer reaction mixture at $-45\text{ }^\circ\text{C}$. The reaction mixture was stirred for 15 minutes at $-45\text{ }^\circ\text{C}$. The reaction mixture was then quenched with 4 equivalents of benzoic acid in 1 mL of DCM. The solvents were removed under reduced pressure. The residue was dissolved in 2.0 mL of DCM and precipitated into 50 mL of stirring methanol. The precipitate initially appears as a semi-solid material. Methanol was decanted and the precipitate was washed with 50 mL of methanol. The polymer was then dried under high vacuum to obtain 228 mg of white solid **3.7** (66% yield, average yield over two runs = 65%).

Characterization:

^1H NMR (400 MHz, CDCl_3): δ 7.88 (app t, 2H, $J = 8.3$ Hz), 7.64-7.56 (m, 76H), 7.46-7.39 (m, 76H), 7.23-7.05 (m, 180H), 5.77-5.49 (m, 82H), 4.19-4.02 (m, 164H), 2.32-1.96 (m, 302H); $^{13}\text{C}\{^1\text{H}\}$ NMR (100 MHz, DMSO-d_6): δ 154.32-154.01 (Regio-irregular linkage), 153.75-153.38 (Head to Tail linkage), 153.03-152.68 (Regio-irregular linkage), 143.8, 137.5, 136.1, 129.0, 128.7 (q, $J = 30.4$ Hz), 126.8, 126.1, 125.4, 124.0 (q, $J = 272.2$ Hz), 76.2, 75.6, 63.9, 34.4, 20.6; IR: 1740 cm^{-1} ; $M_{n,\text{NMR}} = 18000\text{ g/mol}$; $\text{Đ} = 1.39$; $X_{\text{reg}} = 0.69$; $T_g = 62\text{ }^\circ\text{C}$; TGA in N_2 : $195\text{-}246\text{ }^\circ\text{C}$, 94% weight loss.

Poly(α -PhTMC-*b*- α -4-CF₃-PhTMC) (3.8)

A stock solution of TBD and initiator (0.087 M in each) was prepared by dissolving 12.1 mg of TBD and 13.8 mg of 1-naphthalenemethanol in dry THF. The monomer solution was prepared in a 10 mL flame dried schlenk tube by dissolving 139 mg of α -PhTMC **3.1** (0.78 mmol) in 0.60 mL of dry THF. The monomer solution was cooled to $-45\text{ }^\circ\text{C}$ for one minute. To this monomer solution, 0.18 mL of the stock solution containing TBD and initiator was added. The reaction mixture was stirred for 90 minutes at $-45\text{ }^\circ\text{C}$. Separately, 192 mg of α -4-CF₃-PhTMC **3.4** (0.78 mmol) was dissolved in 0.32 mL of dry THF and was cooled to $-45\text{ }^\circ\text{C}$ for one minute. This monomer solution was added to the polymer reaction mixture at $-45\text{ }^\circ\text{C}$. The reaction mixture was stirred for 15 minutes at $-45\text{ }^\circ\text{C}$. The reaction mixture was then quenched with 4 equivalents of benzoic acid in 1 mL of DCM. The solvents were removed under reduced pressure. The residue was dissolved in 2.0 mL of DCM and precipitated into 50 mL of stirring methanol. The precipitate initially appears as a semi-solid material. Methanol was decanted and the precipitate was washed with 50 mL of

methanol. The polymer was then dried under high vacuum to obtain 273 mg of white solid **3.8** (82% yield, average yield over two runs = 80%).

Characterization:

^1H NMR (400 MHz, CDCl_3): δ 7.88 (app t, 2H, $J = 8.4$ Hz), 7.61-7.53 (m, 80H), 7.46-7.31 (m, 280H), 5.73-5.51 (m, 88H), 4.28-3.92 (m, 176H), 2.36f-1.98 (m, 178H); $^{13}\text{C}\{^1\text{H}\}$ NMR (100 MHz, DMSO-d_6): δ 154.31-154.06 (Regio-irregular linkage), 153.75-153.35 (Head to Tail linkage), 153.15-152.69 (Regio-irregular linkage), 143.8, 139.1, 128.9 (q, $J = 32.7$ Hz), 128.5, 128.2, 126.8, 126.1, 125.4, 124.0 (q, $J = 272.3$ Hz), 76.4, 75.6, 63.9, 34.5; IR: 1740 cm^{-1} ; $M_{n,\text{NMR}} = 18500\text{ g/mol}$; $\text{Đ} = 1.33$; $X_{\text{reg}} = 0.79$; $T_g = 56\text{ }^\circ\text{C}$; TGA in N_2 : 197-260 $^\circ\text{C}$, 94% weight loss.

Poly(α -4-Me-PhTMC-*b*- α -4-Br-PhTMC) (3.9)

A stock solution of thiourea, DBU and initiator (0.156 M in each) was prepared by dissolving 58 mg of thiourea, 23 μL of DBU and 24.7 mg of 1-naphthalenemethanol in dry THF. The monomer solution was prepared in a 4 mL oven dried vial by dissolving 150 mg of α -4-Me-PhTMC **3.2** (0.78 mmol) in 0.30 mL of dry THF. To this monomer solution, 0.10 mL of the stock solution containing thiourea-DBU and initiator was added at room temperature (27 $^\circ\text{C}$). The reaction mixture was stirred for 780 minutes. Separately, 201 mg of α -4-Br-PhTMC **3.3** (0.78 mmol) was dissolved in 0.20 mL of dry THF. This monomer solution was added to the polymer reaction mixture at room temperature. The reaction mixture was stirred for 300 minutes. The reaction mixture was then quenched with 4 equivalents of benzoic acid in 1 mL of DCM. The solvents were removed under reduced pressure. The residue was dissolved in 2.0 mL of DCM and precipitated into 50 mL of stirring methanol. The precipitate initially appears as a semi-solid material. Methanol was

decanted and the precipitate was washed with 50 mL of methanol. The polymer was then subjected to second precipitation into 50 mL of methanol by dissolving in 1.0 mL of DCM. The precipitated polymer was then dried under high vacuum to obtain 197 mg of white solid **3.9** (56% yield, average yield over two runs = 55%).

Characterization:

^1H NMR (400 MHz, CDCl_3): δ 7.87 (app q, 2H, $J = 7.7$ Hz), 7.58-7.39 (m, 92H), 7.23-7.03 (m, 298H), 5.67-5.45 (m, 93H), 4.33-3.90 (m, 192H), 2.32-1.95 (m, 358H); $^{13}\text{C}\{^1\text{H}\}$ NMR (100 MHz, DMSO-d_6): δ 154.30-153.99 (Regio-irregular linkage), 153.67-153.40 (Head to Tail linkage), 153.06-152.66 (Regio-irregular linkage), 138.5, 137.5, 136.1, 131.4, 129.0, 128.4, 126.1, 121.4, 76.2, 75.7, 63.8, 34.4, 20.6; IR: 1738 cm^{-1} ; $M_{n,\text{NMR}} = 21000\text{ g/mol}$; $\text{Đ} = 1.41$; $X_{\text{reg}} = 0.12$; $T_g = 59\text{ }^\circ\text{C}$; TGA in N_2 : $196\text{-}308\text{ }^\circ\text{C}$, 94% weight loss.

Poly(α -4-Me-PhTMC-*b*- α -4-Br-PhTMC) (3.10)

A stock solution of TBD and initiator (0.156 M in each) was prepared by dissolving 21.7 mg of TBD and 24.7 mg of 1-naphthalenemethanol in dry THF. The monomer solution was prepared in a 4 mL oven dried vial by dissolving 150 mg of α -4-Me-PhTMC **3.2** (0.78 mmol) in 0.30 mL of dry THF. To this monomer solution, 0.10 mL of the stock solution containing TBD and initiator was added at room temperature ($27\text{ }^\circ\text{C}$). The reaction mixture was stirred for 7 minutes. Separately, 201 mg of α -4-Br-PhTMC **3.3** (0.78 mmol) was dissolved in 0.40 mL of dry THF. This monomer solution was added to the polymer reaction mixture at room temperature. The reaction mixture was stirred for 6 minutes. The reaction mixture was then quenched with 4 equivalents of benzoic acid in 1 mL of DCM. The solvents were removed under reduced pressure. The residue was dissolved in 2.0 mL of DCM and precipitated into 50 mL of stirring methanol. The precipitate initially appears as a

semi-solid material. Methanol was decanted and the precipitate was washed with 50 mL of methanol. The polymer was then dried under high vacuum to obtain 282 mg of white solid **2h** (80% yield, average yield over two runs = 80%).

Characterization:

^1H NMR (400 MHz, CDCl_3): δ 7.87 (app q, 2H, $J = 7.8$ Hz), 7.59-7.39 (m, 85H), 7.23-7.03 (m, 259H), 5.66-5.45 (m, 85H), 4.27-3.89 (m, 171H), 2.40-1.96 (m, 310H); $^{13}\text{C}\{^1\text{H}\}$ NMR (100 MHz, DMSO-d_6): δ 154.28-153.99 (Regio-irregular linkage), 153.72-153.33 (Head to Tail linkage), 153.12-152.64 (Regio-irregular linkage), 138.4, 137.5, 136.1, 131.4, 129.0, 128.3, 126.1, 121.4, 76.2, 75.6, 63.9, 34.4, 20.6; IR: 1739 cm^{-1} ; $M_{n,\text{NMR}} = 19200\text{ g/mol}$; $\text{Đ} = 1.43$; $X_{\text{reg}} = 0.36$; $T_g = 64\text{ }^\circ\text{C}$; TGA in N_2 : $198\text{-}310\text{ }^\circ\text{C}$, 94% weight loss.

Procedure for Preparation of Diblock Copolymer Thin Films

Silicon wafers were cleaned with 1:3 v / v solution of 98% H_2SO_4 / 30% H_2O_2 at $27\text{ }^\circ\text{C}$ for 30 minutes. The wafers were then rinsed thoroughly with DI water and sonicated in DI water for 30 minutes, followed by sonication in isopropanol for 30 minutes. Cleaned silicon wafers were then subjected to UV/ozone treatment for 20 minutes. The polymer films were spun-cast on these wafers using a 0.4 wt% solution of diblock copolymer in a 1:4 mixture of THF and toluene. A spin speed of 3000 rpm was used for 65 seconds. The as spun-cast films were imaged using AFM after 72 hours. The same film was then thermally annealed at $55\text{ }^\circ\text{C}$ for 30 minutes and quenched immediately at $27\text{ }^\circ\text{C}$. After 5 minutes, the annealed films were imaged using AFM.

3.7 References

- 1 Feng, H.; Lu, X.; Wang, W.; Kang, N. G.; Mays, J. W. *Polymers* **2017**, *9*, 494-524.
- 2 Hadjichristidis, N.; Iatrou, H.; Pitsikalis, M.; Mays, J. *Prog. Polym. Sci.* **2006**, *31*, 1068-1132.
- 3 Bates, F. S.; Fredrickson, G. H. *Phys. Today* **1999**, *52*, 32-38.
- 4 Opsteen, J. A.; van Hest, J. C. M. *Chem. Commun.* **2005**, *1*, 57-59.
- 5 Poelma, J. E.; Ono, K.; Miyajima, D.; Aida, T.; Satoh, K.; Hawker, C. J. *ACS Nano* **2012**, *6*, 10845-10854.
- 6 Inglis, A. J.; Sinnwell, S.; Davis, T. P.; Barner-Kowollik, C.; Stenzel, M. H. *Macromolecules* **2008**, *41*, 4120-4126.
- 7 Braunecker, W. A.; Matyjaszewski, K. *Prog. Polym. Sci.* **2007**, *32*, 93-146.
- 8 Chong, Y. K.; Le, T. P.; Moad, G.; Rizzardo, E.; Thang, S. H. *Macromolecules* **1999**, *32*, 2071-2074.
- 9 Nicolas, J.; Guillemeuf, Y.; Lefay, C.; Bertin, D.; Gigmès, D.; Charleux, B. *Prog. Polym. Sci.* **2013**, *38*, 63-235.
- 10 Hirao, A.; Loykulant, S.; Ishizone, T. *Prog. Polym. Sci.* **2002**, *27*, 1399-1471.
- 11 Matsuo, Y.; Konno, R.; Ishizone, T.; Goseki, R.; Hirao, A. *Polymers* **2013**, *5*, 1012-1040.
- 12 Hadjichristidis, N.; Pitsikalis, M.; Pispas, S.; Iatrou, H. *Chem. Rev.* **2001**, *101*, 3747-3792.
- 13 You, Y.; Hong, C.; Wang, W.; Lu, W.; Pan, C. *Macromolecules* **2004**, *37*, 9761-9767.
- 14 Aydoğan, C.; Kutahya, C.; Allushi, A.; Yilmaz, G.; Yagci, Y. *Polym. Chem.* **2017**, *8*, 2899-2903.
- 15 Dey, A.; Haldar, U.; De, P. *Front. Chem.* **2021**, *9*, 1-10.
- 16 Lazzari, M.; Torneiro, M. *Polymers* **2020**, *12*, 869-884.
- 17 Airey, G. D. *Fuel* **2003**, *82*, 1709-1719.
- 18 Batrakova, E. V.; Kabanov, A. V. *J. Control. Release* **2008**, *130*, 98-106.
- 19 Ghoroghchian, P. P.; Li, G.; Levine, D. H.; Davis, K. P.; Bates, F. S.; Hammer, D. A.; Therien, M. J. *Macromolecules* **2006**, *39*, 1673-1675.
- 20 Rosler, A.; Vandermeulen, G. W. M.; Klok, H. A. *Adv. Drug Deliv. Rev.* **2012**, *64*, 270-279.
- 21 Meng, F.; Engbers, G. H. M.; Feijen, J. *J. Control. Release* **2005**, *101*, 187-198.

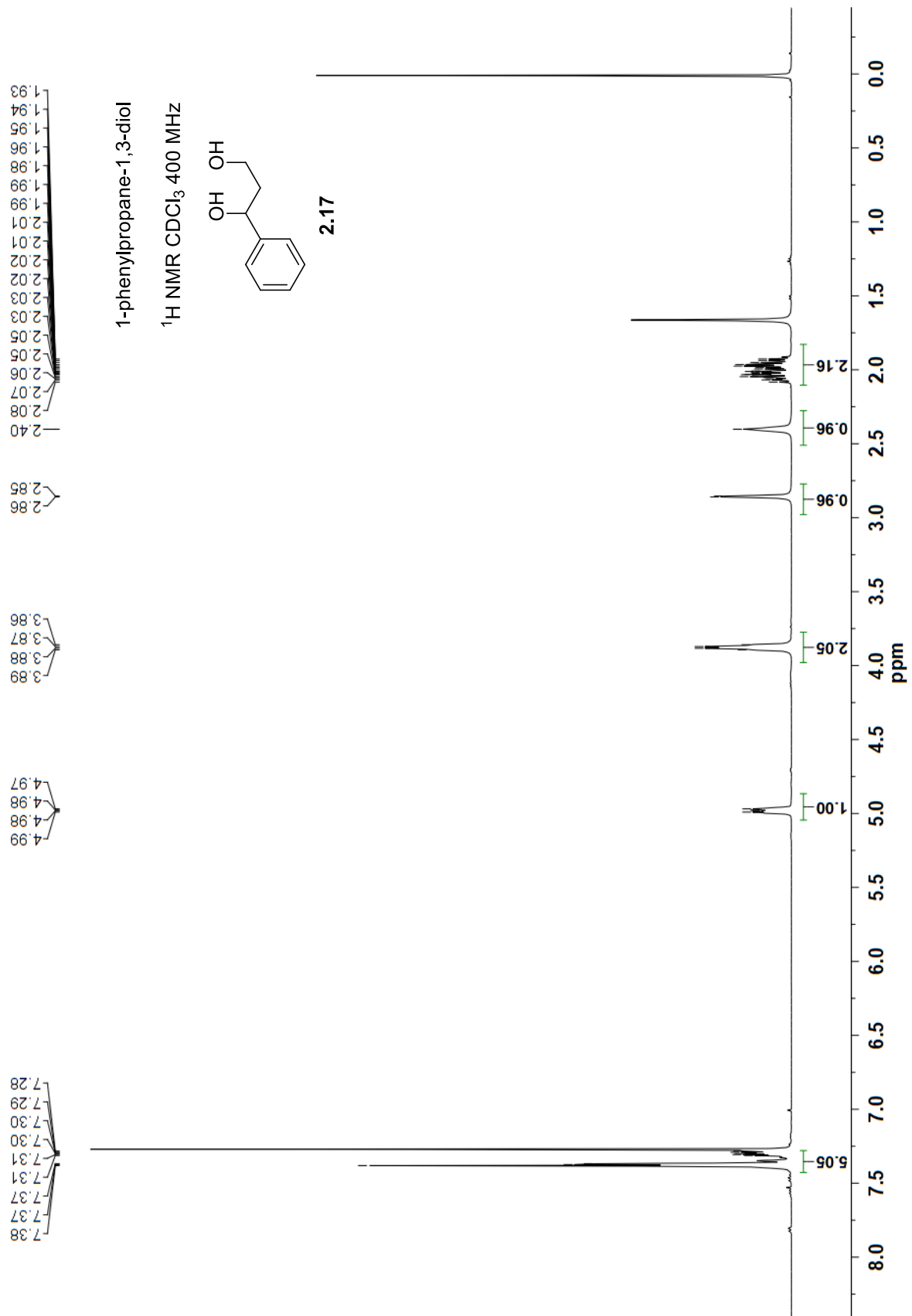
- 22 Farokhzad, O. C.; Jon, S.; Khademhosseini, A.; Tran, T. N. T.; LaVan, D. A.; Langer, R. *Cancer Res.* **2004**, *64*, 7668-7672.
- 23 Wei, H.; Cheng, S. X.; Zhang, X. Z.; Zhuo, R. X. *Prog. Polym. Sci.* **2009**, *34*, 893-910.
- 24 Krishnamoorthy, S.; Hinderling, C.; Heinzelmann, H. *Mater. Today* **2006**, *9*, 40-47.
- 25 Lazzari, M.; Lopez-Quintela, M. A. *Adv. Mater.* **2003**, *15*, 1583-1594.
- 26 Hamley, I. W. *Nanotechnology* **2003**, *14*, 39-54.
- 27 Nunns, A.; Gwyther, J.; Manners, I. *Polymer* **2013**, *54*, 1269-1284.
- 28 Hamley, I. W. *Prog. Polym. Sci.* **2009**, *34*, 1161-1210.
- 29 Kim, H. C.; Park, S. M.; Hinsberg, W. D. *Chem. Rev.* **2010**, *110*, 146-177.
- 30 Segalman, R. A.; McCulloch, B.; Kirmayer, S.; Urban, J. J. *Macromolecules* **2009**, *42*, 9205-9216.
- 31 de Boer, B.; Stalmach, U.; van Hutten, P. F.; Melzer, C.; Krasnikov, V. V.; Hadziioannou, G. *Polymer* **2001**, *42*, 9097-9109.
- 32 Yang, C.; Lee, J. K.; Heeger, A. J.; Wudl, F. *J. Mater. Chem.* **2009**, *19*, 5416-5423.
- 33 Becker, S.; Ego, C.; Grimsdale, A. C.; List, E. J. W.; Marsitzky, D.; Pogantsch, A.; Setayesh, S.; Leising, G.; Mullen, K. *Synthetic Metals* **2002**, *125*, 73-80.
- 34 Altintas, O.; Barner-Kowollik, C. *Macromol. Rapid Commun.* **2012**, *33*, 958-971.
- 35 Altintas, O.; Krolla-Sidenstein, P.; Gliemann, H.; Barner-Kowollik, C. *Macromolecules* **2014**, *47*, 5877-5888.
- 36 Hosono, N.; Palmans, A. R. A.; Meijer, E. W. *Chem. Commun.* **2014**, *50*, 7990-7993.
- 37 Lu, J.; Brummelhuis, N. T.; Weck, M. *Chem. Commun.* **2014**, *50*, 6225-6227.
- 38 Bertin, P. A.; Gibbs, J. M.; Shen, C. K. F.; Thaxton, C. S.; Russin, W. A.; Mirkin, C. A.; Nguyen, S. T. *J. Am. Chem. Soc.* **2006**, *128*, 4168-4169.
- 39 Kim, Y.; Pyun, J.; Frechet, J. M. J.; Hawker, C. J.; Frank, C. W. *Langmuir* **2005**, *21*, 10444-10458.
- 40 Harth, E.; Horn, B. V.; Lee, V. Y.; Germack, D. S.; Gonzales, C. P.; Miller, R. D.; Hawker, C. J. *J. Am. Chem. Soc.* **2002**, *124*, 8653-8660.
- 41 Adkins, C. T.; Muchalski, H.; Harth, E. *Macromolecules* **2009**, *42*, 5786-5792.
- 42 Anfinsen, C. B. *Science* **1973**, *181*, 223-230.
- 43 Hill, D. J.; Mio, M. J.; Prince, R. B.; Hughes, T. S.; Moore, J. S. *Chem. Rev.* **2001**, *101*, 3893-4011.

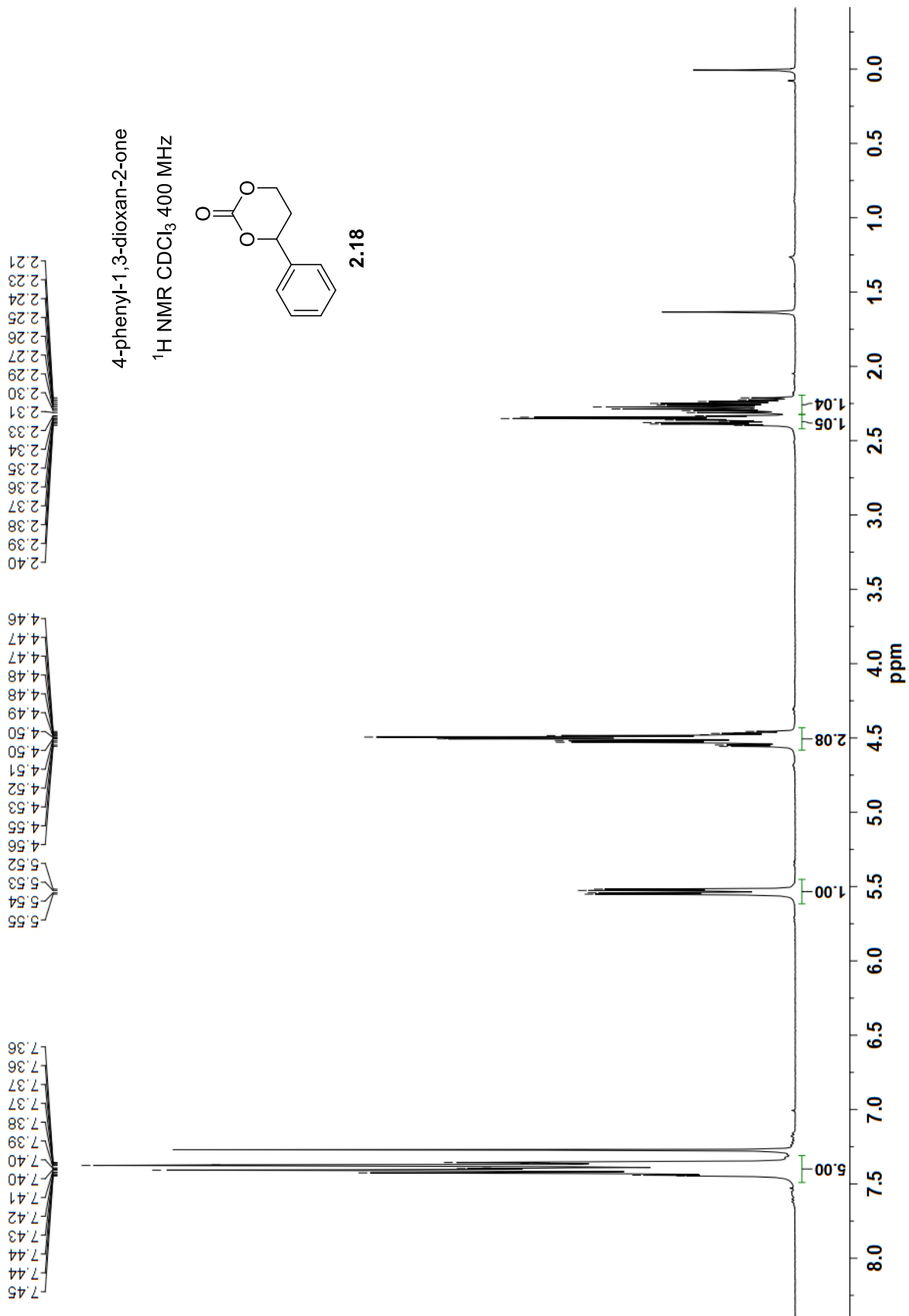
- 44 Meyer, E. A.; Castellano, R. K.; Diederich, F. *Angew. Chem. Int. Ed.* **2003**, *42*, 1210-1250.
- 45 Kudirka, R.; Tran, H.; Sanii, B.; Nam, K. T.; Choi, P. H.; Venkateswaran, N.; Chen, R.; Whitelam, S.; Zuckermann, R. N. *Biopolymers* **2011**, *96*, 586-595.
- 46 Altintas, O.; Lejeune, E.; Gerstel, P.; Barner-Kowollik, C. *Polym. Chem.* **2012**, *3*, 640-651.
- 47 Mes, T.; van der Weegen, R.; Palmans, A. R. A.; Meijer, E. W. *Angew. Chem. Int. Ed.* **2011**, *50*, 5085-5089.
- 48 Willenbacher, J.; Schmidt, B. V. K. J.; Schulze-Suenninghausen, D.; Altintas, O.; Luy, B.; Delaittre, G.; Barner-Kowollik, C. *Chem. Commun.* **2014**, *50*, 7056-7059.
- 49 Hosono, N.; Gillissen, M. A. J.; Li, Y.; Sheiko, S. S.; Palmans, A. R. A.; Meijer, E. W. *J. Am. Chem. Soc.* **2013**, *135*, 501-510.
- 50 Altintas, O.; Artar, M.; ter Huurne, G.; Voets, I. K.; Palmans, A. R. A.; Barner-Kowollik, C.; Meijer, E. W. *Macromolecules* **2015**, *48*, 8921-8932.
- 51 Burley, S. K.; Petsko, G. A. *Science* **1985**, *229*, 23-28.
- 52 Burley, S. K.; Petsko, G. A. *Adv. Protein Chem.* **1988**, *39*, 125-189.
- 53 Lokey, R. S.; Iverson, B. L. *Nature* **1995**, *375*, 303-305.
- 54 Berl, V.; Huc, I.; Khoury, R. G.; Krische, M. J.; Lehn, J. *Nature* **2000**, *407*, 720-723.
- 55 Sebaoun, L.; Maurizot, V.; Granier, T.; Kauffmann, B.; Huc, I. *J. Am. Chem. Soc.* **2014**, *136*, 2168-2174.
- 56 Bradford, V. J.; Iverson, B. L. *J. Am. Chem. Soc.* **2008**, *130*, 1517-1524.
- 57 Masu, H.; Sakai, M.; Kishikawa, K.; Yamamoto, M.; Yamaguchi, K.; Kohmoto, S. *J. Org. Chem.* **2005**, *70*, 1423-1431.
- 58 Nair, R. V.; Kheria, S.; Rayavarapu, S.; Kotmale, A. S.; Jagadeesh, B.; Gonnade, R. G.; Puranik, V. G.; Rajamohanan, P. R.; Sanjayan, G. J. *J. Am. Chem. Soc.* **2013**, *135*, 11477-11480.
- 59 Wang, C.; Weck, M. *Macromol. Rapid Commun.* **2021**, *42*, 2100368 (1-6).
- 60 Elacqua, E.; Geberth, G. T.; Bout, D. A. V.; Weck, M. *Chem. Sci.* **2019**, *10*, 2144-2152.
- 61 Patrick, C. R.; Prosser, G. S. *Nature* **1960**, *17*, 1021.
- 62 Hunter, C. A. *Angew. Chem. Int. Ed. Engl.* **1993**, *32*, 1584-1586.

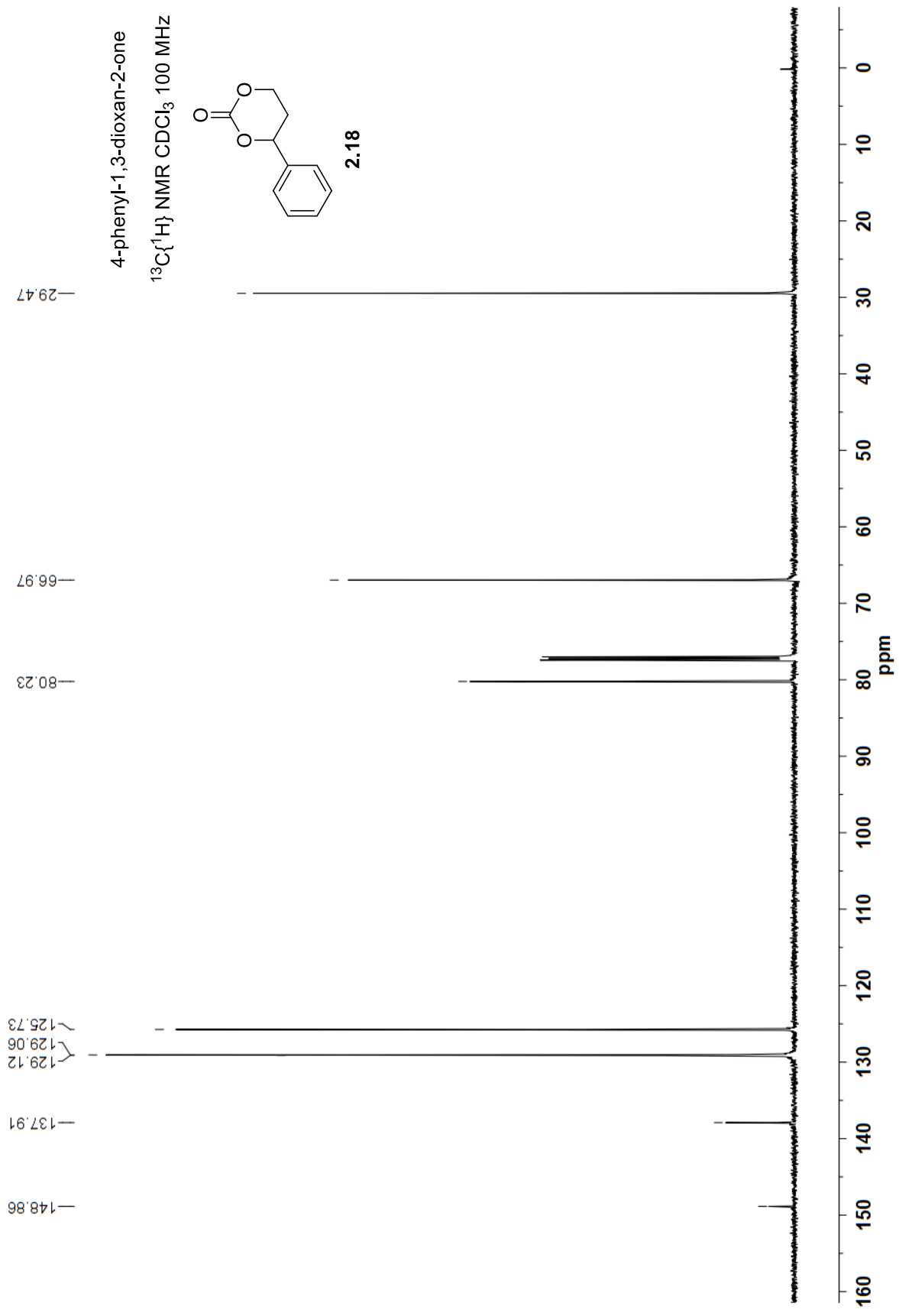
- 63 Cockroft, S. L.; Hunter, C. A.; Lawson, K. R.; Perkins, J.; Urch, C. J. *J. Am. Chem. Soc.* **2005**, *127*, 8594-8595.
- 64 Adams, H.; Blanco, J. J.; Chessari, G.; Hunter, C. A.; Low, C. M. R.; Sanderson, J. M.; Vinter, J. G. *Chem. Eur. J.* **2001**, *7*, 3494-3503.
- 65 Perez-Casas, S.; Hernandez-Trujillo, J.; Costas, M. *J. Phys. Chem. B* **2003**, *107*, 4167-4174.
- 66 Xu, R.; Schweizer, W. B.; Frauenrath, H. *Chem. Eur. J.* **2009**, *15*, 9105-9116.
- 67 Coates, G. W.; Dunn, A. R.; Henling, L. M.; Dougherty, D. A.; Grubbs, R. H. *Angew. Chem. Int. Ed. Engl.* **1997**, *36*, 248-251.
- 68 Weck, M.; Dunn, A. R.; Matsumoto, K.; Coates, G. W.; Lobkovsky, E. M.; Grubbs, R. H. *Angew. Chem. Int. Ed. Engl.* **1999**, *38*, 2741-2745.
- 69 Stalmach, U.; de Boer, B.; Videlot, C.; van Hutten, P. F.; Hadziioannou, G. *J. Am. Chem. Soc.* **2000**, *122*, 5464-5472.
- 70 Tao, Y.; McCulloch, B.; Kim, S.; Segalman, R. A. *Soft Matter* **2009**, *5*, 4219-4230.
- 71 Zhang, Q.; Cirpan, A.; Russell, T. P.; Emrick, T. *Macromolecules* **2009**, *42*, 1079-1082.
- 72 ten Brinke, G. *Phase Segregation / Polymer Blends / Microphase Separation*; Polymer Science: A Comprehensive Reference, Volume 1, 2012, p 287-313.

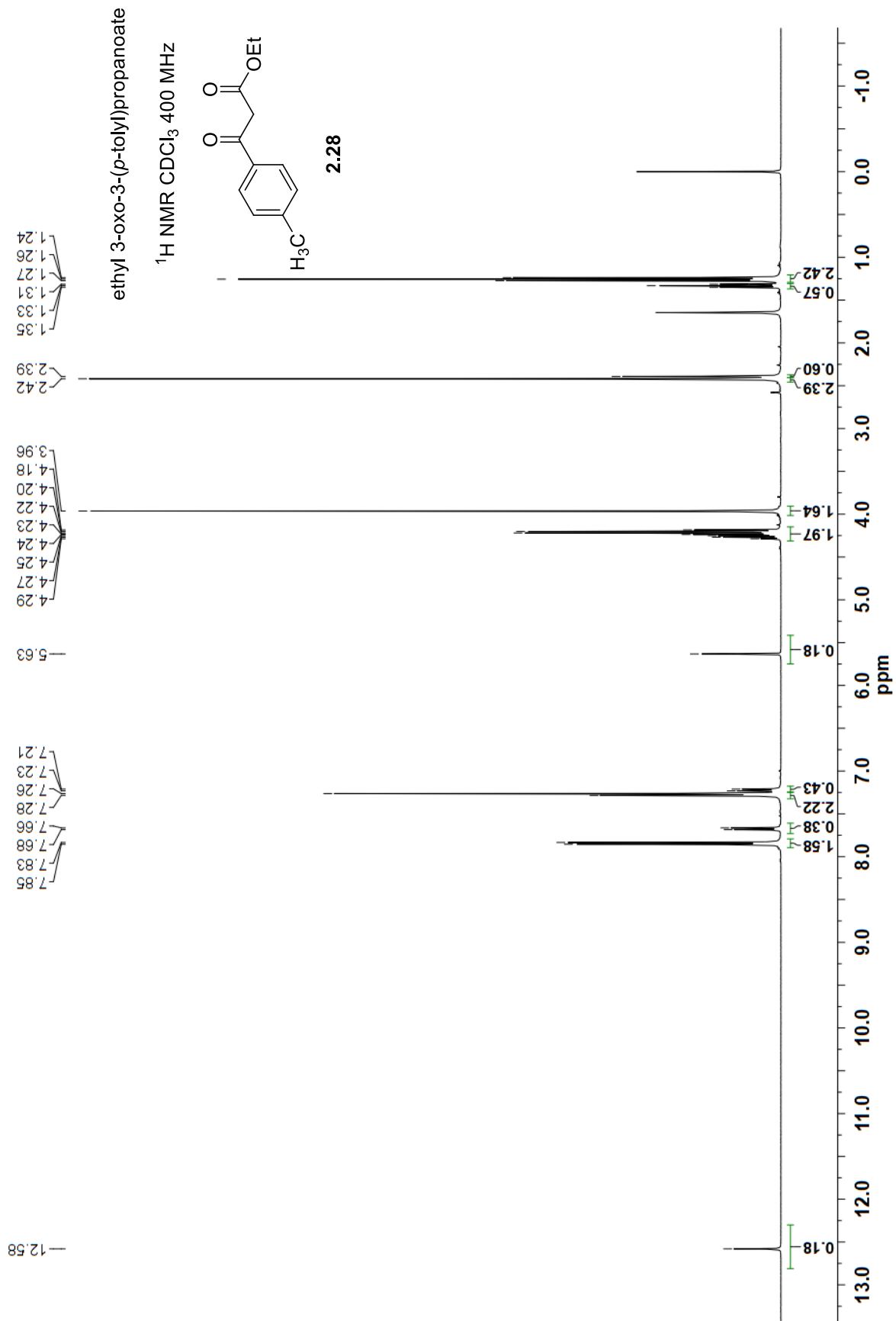
APPENDIX I

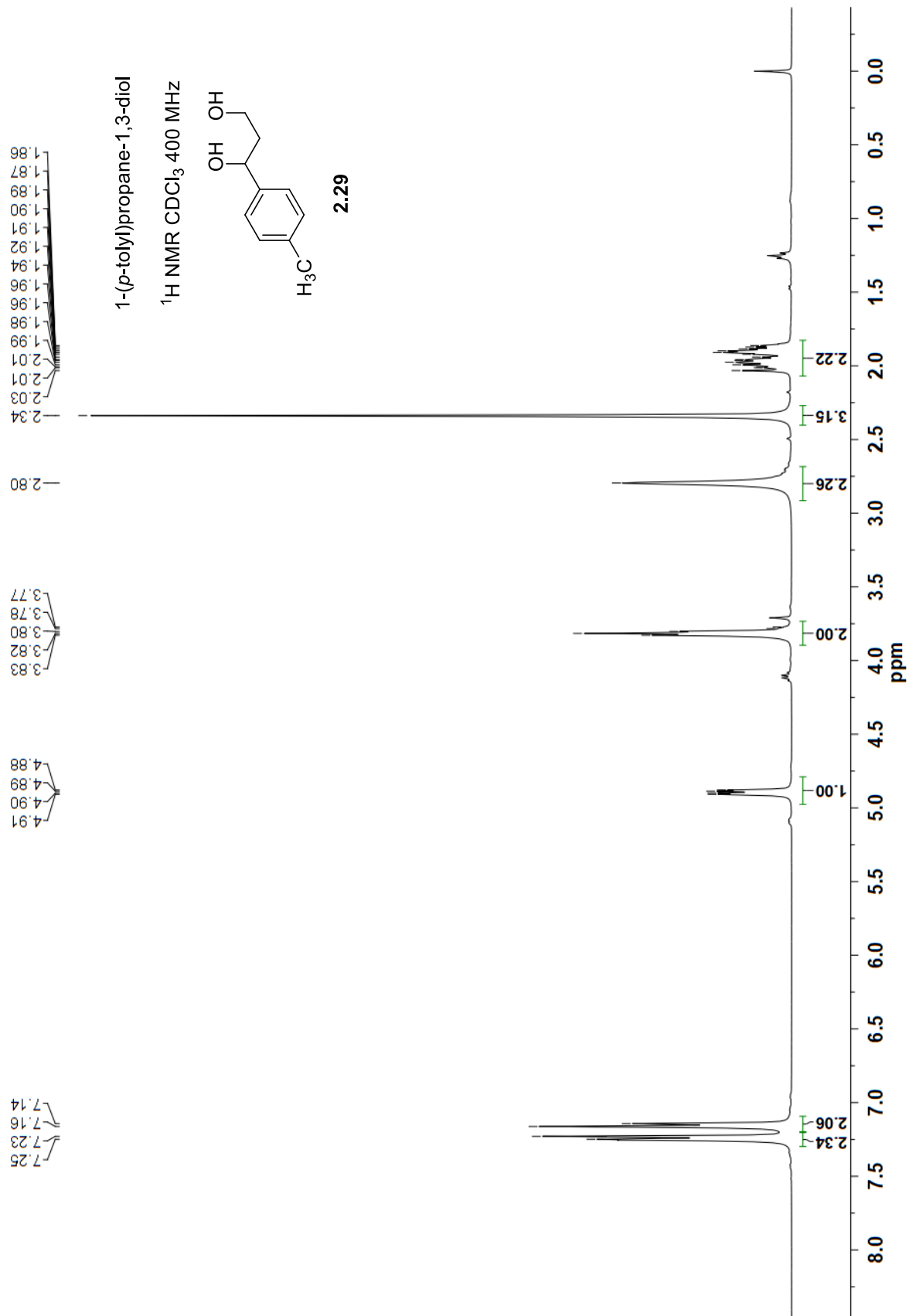
NMRs

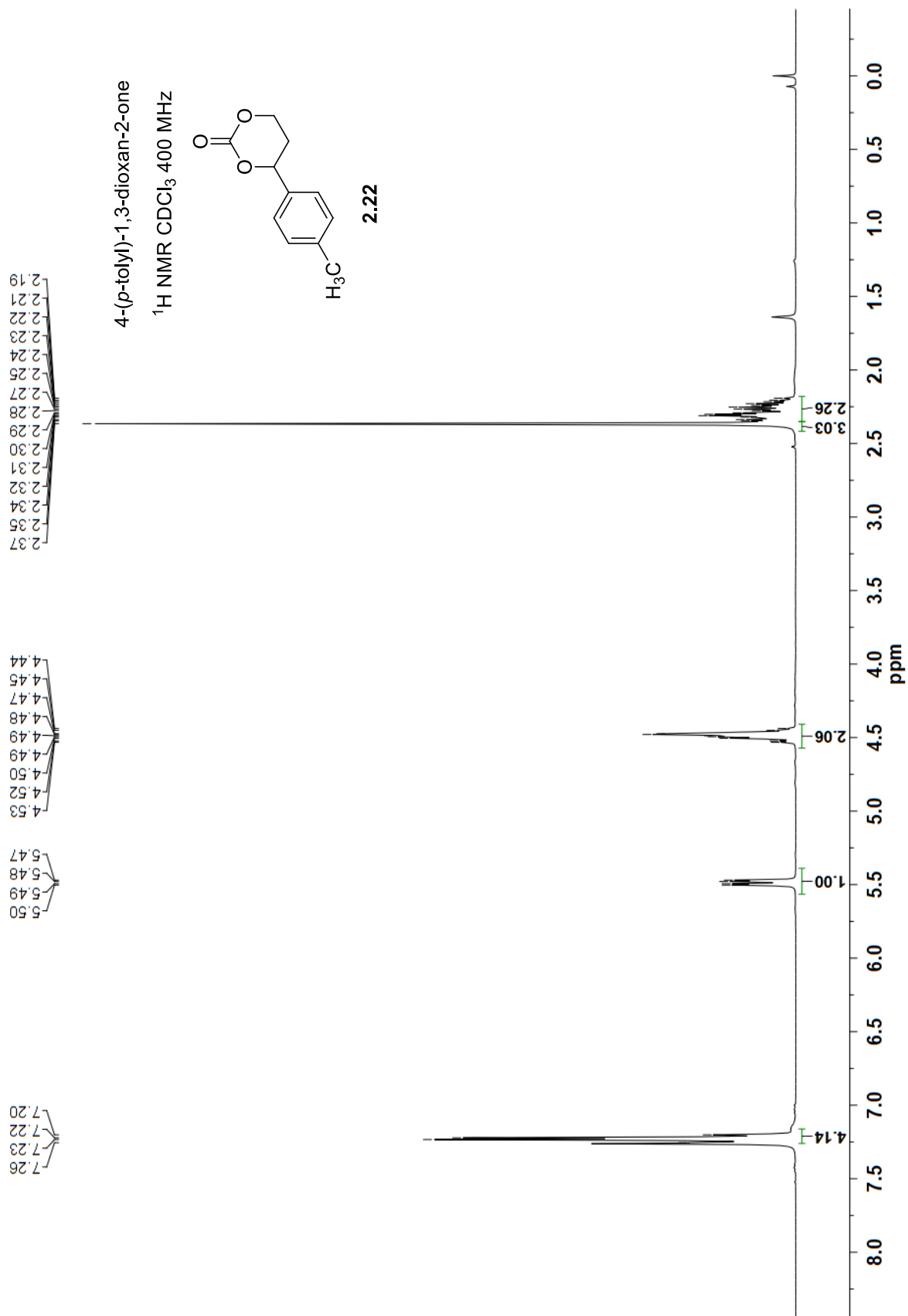


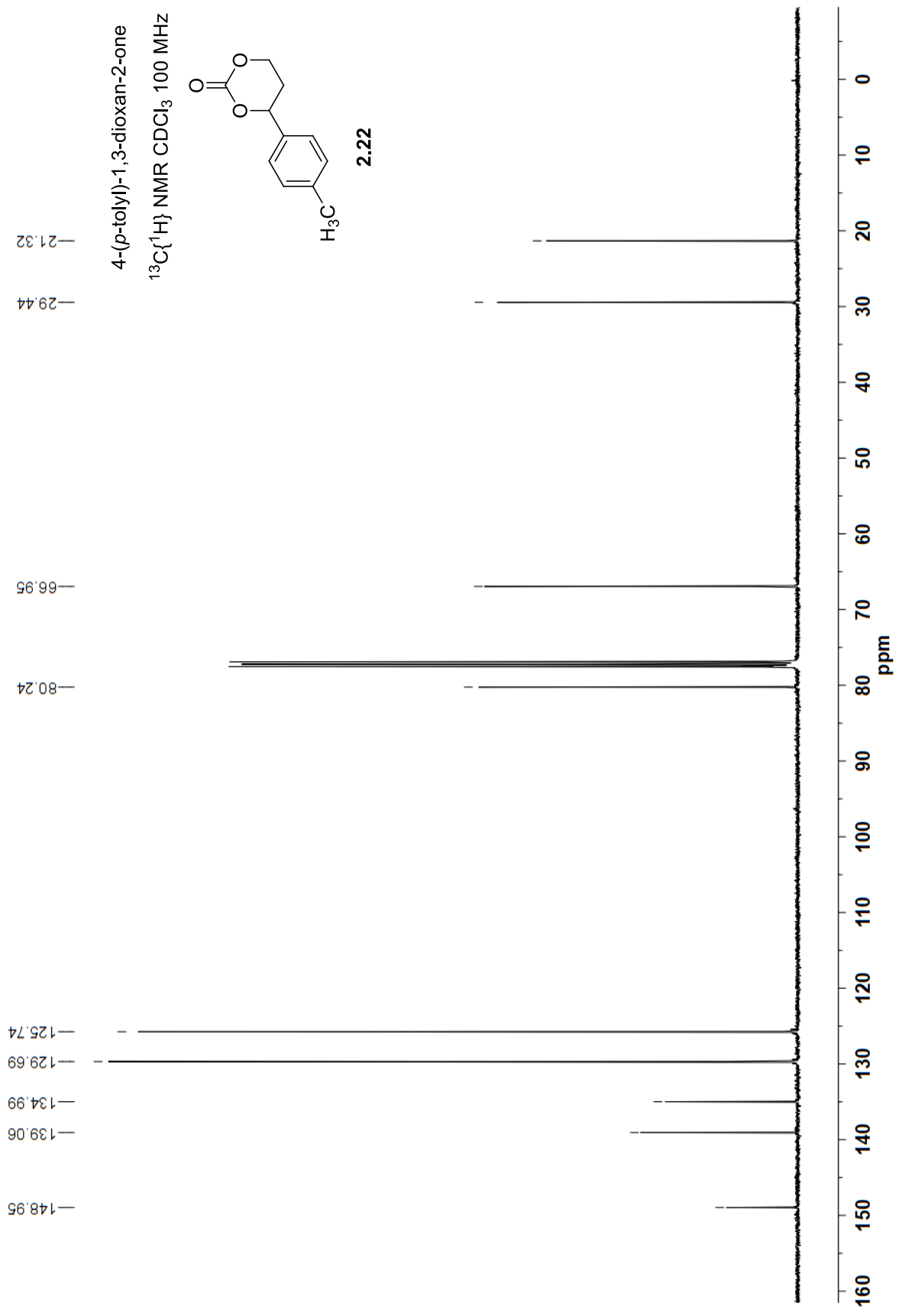


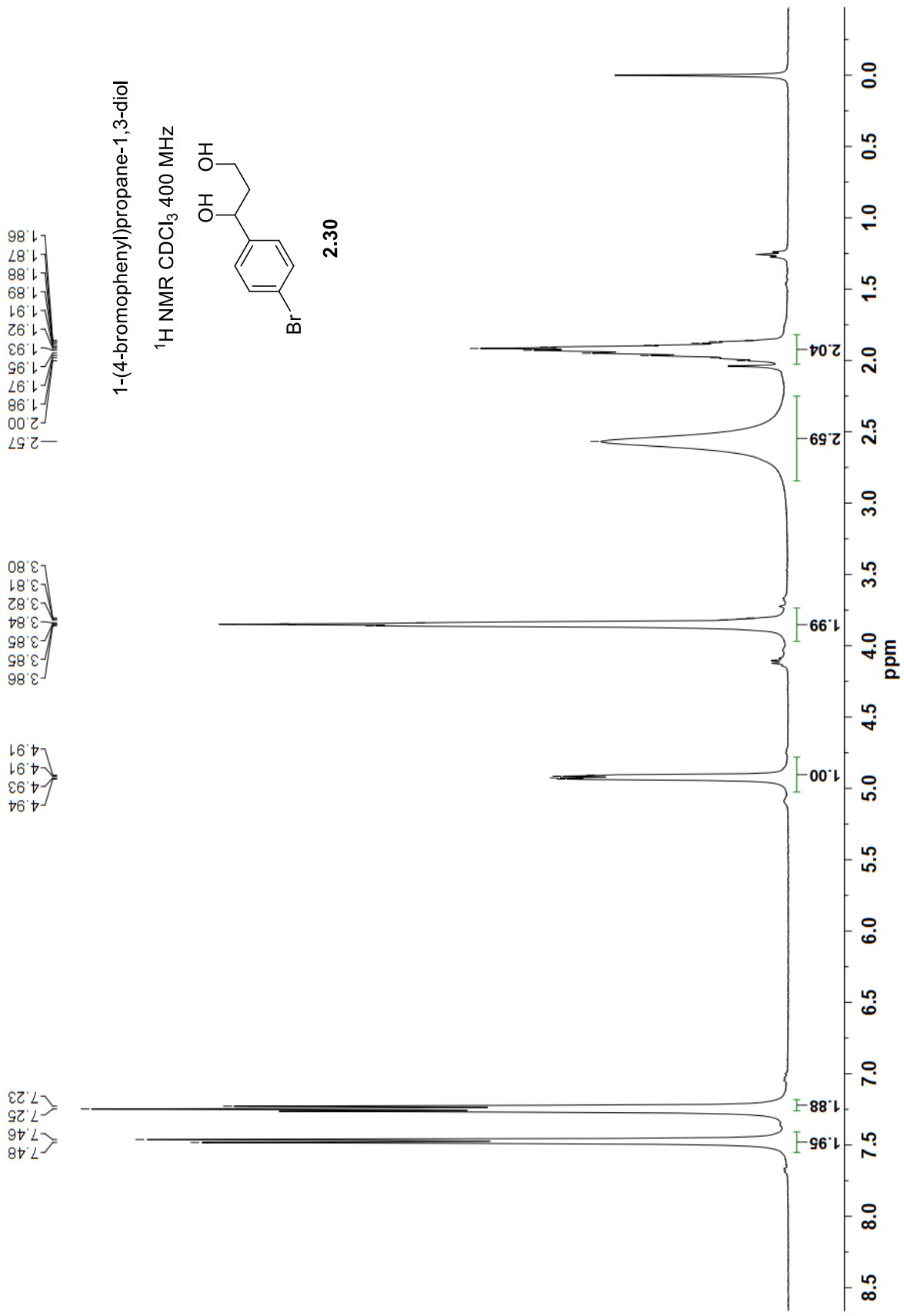


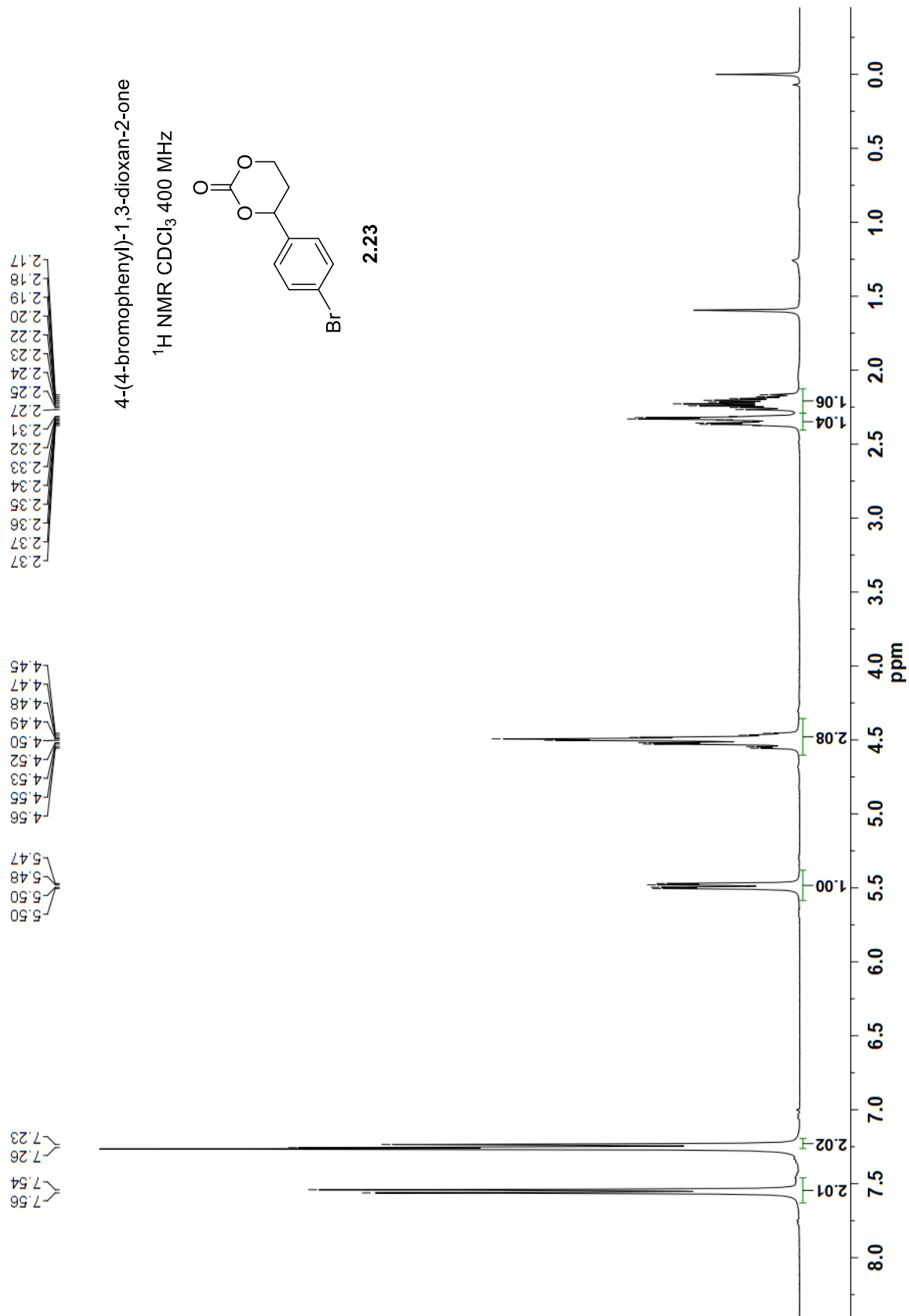


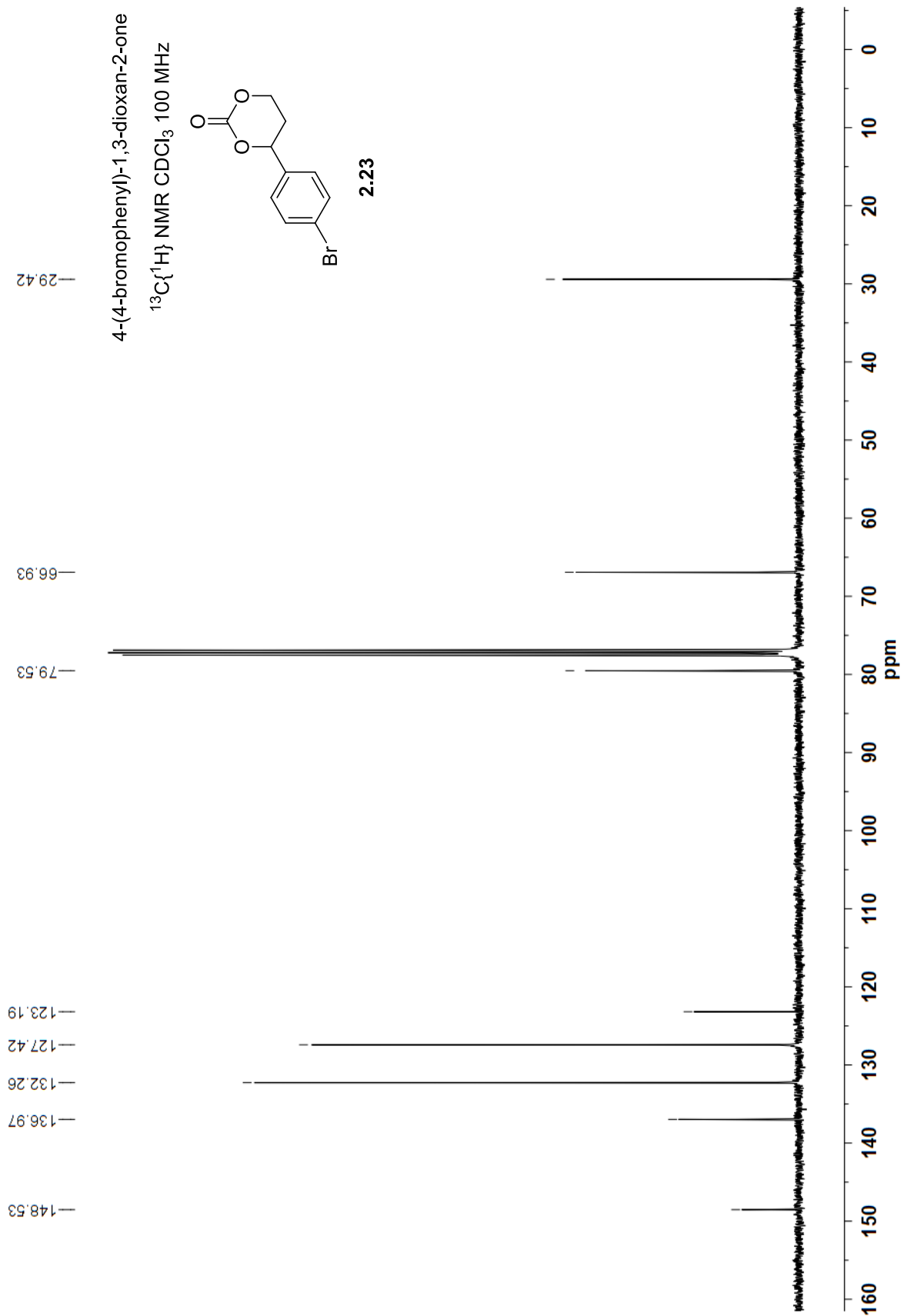


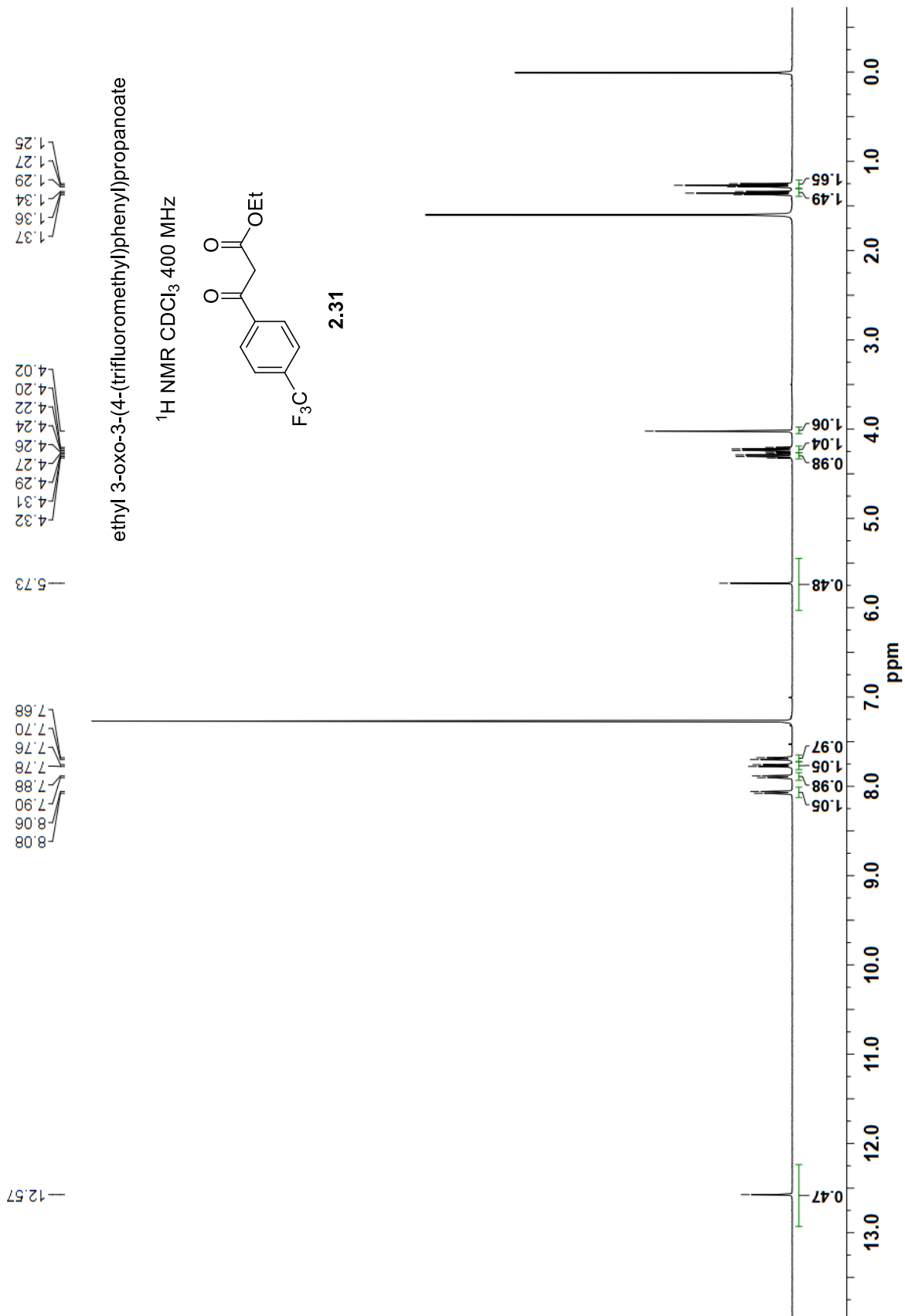


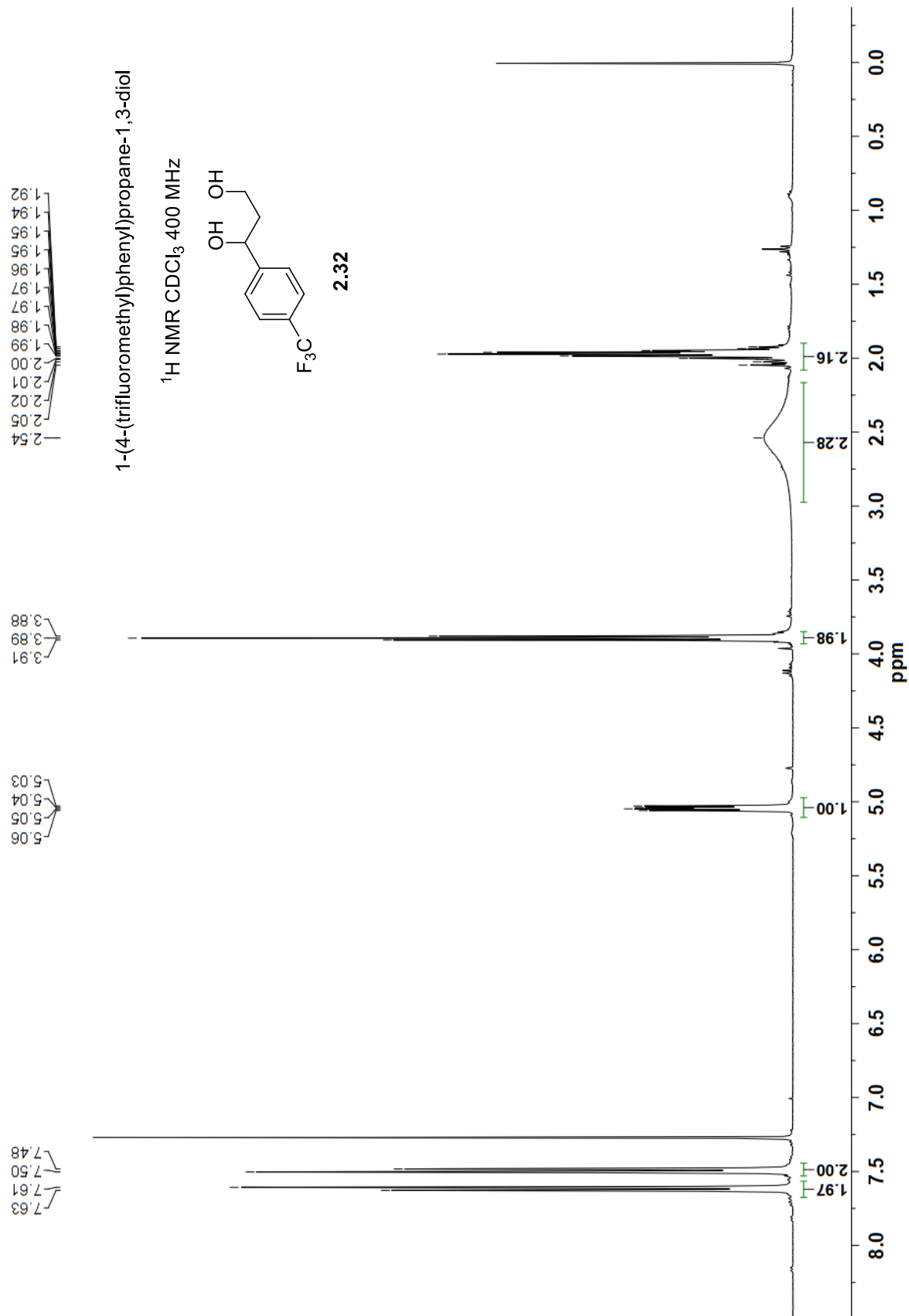


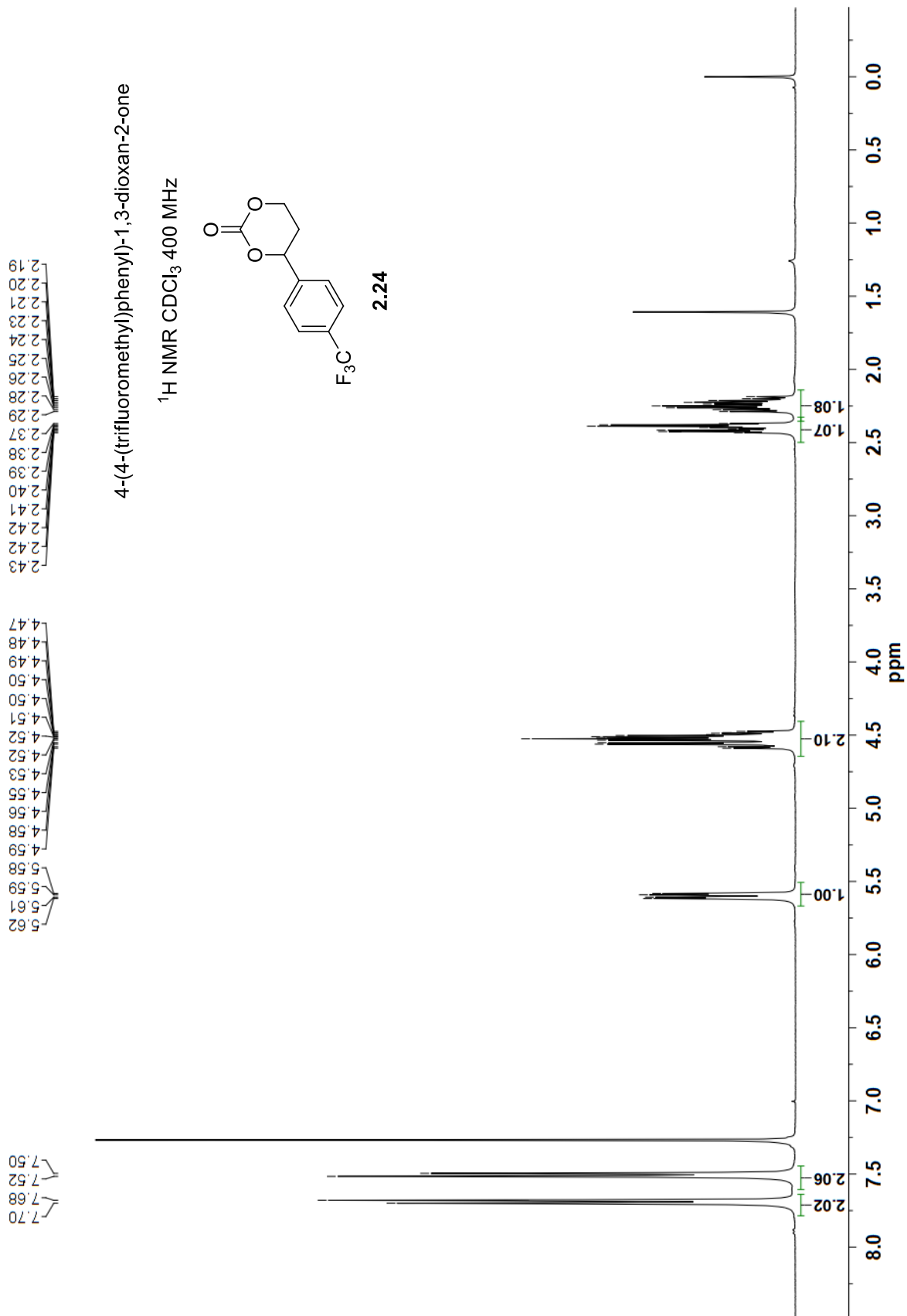


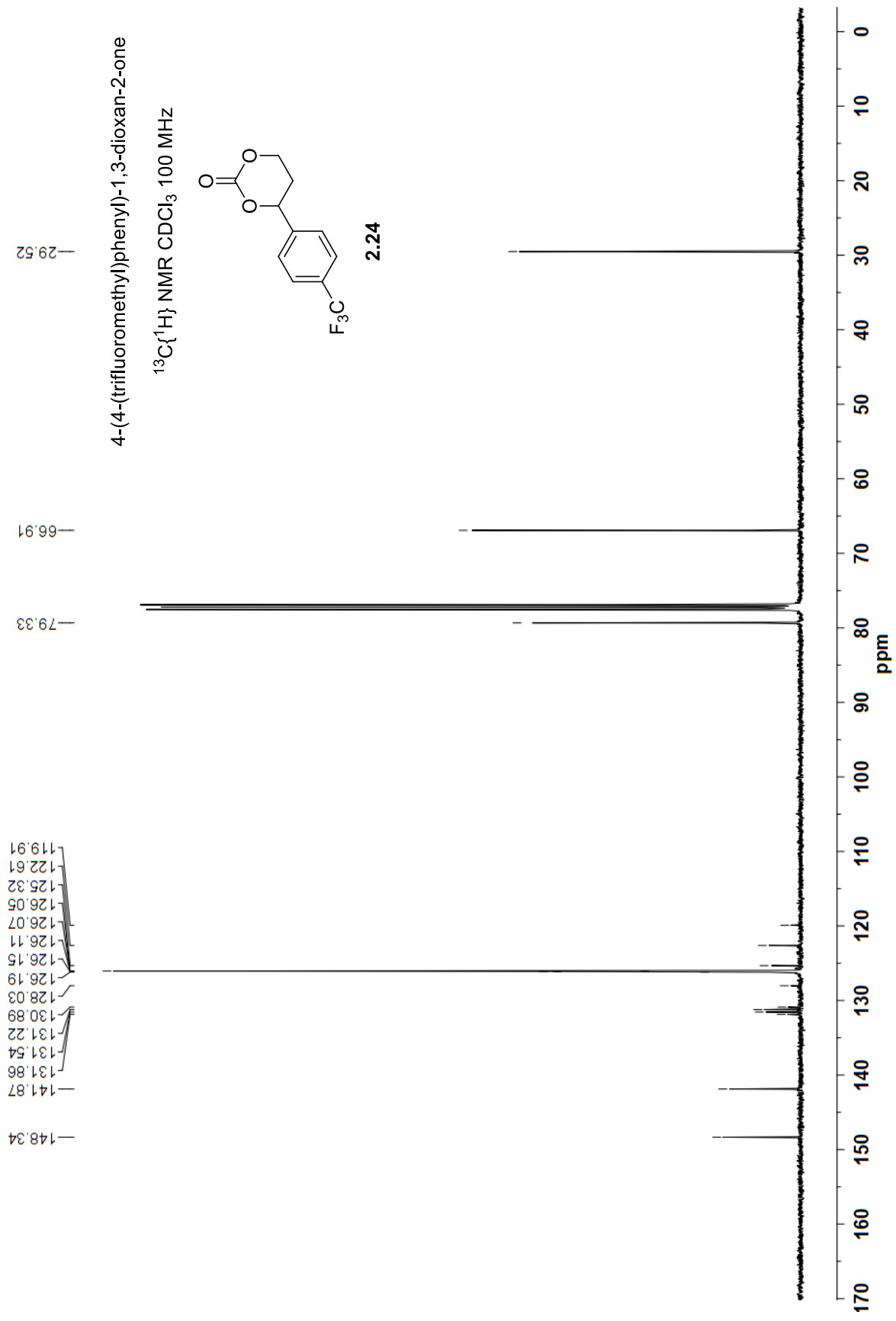


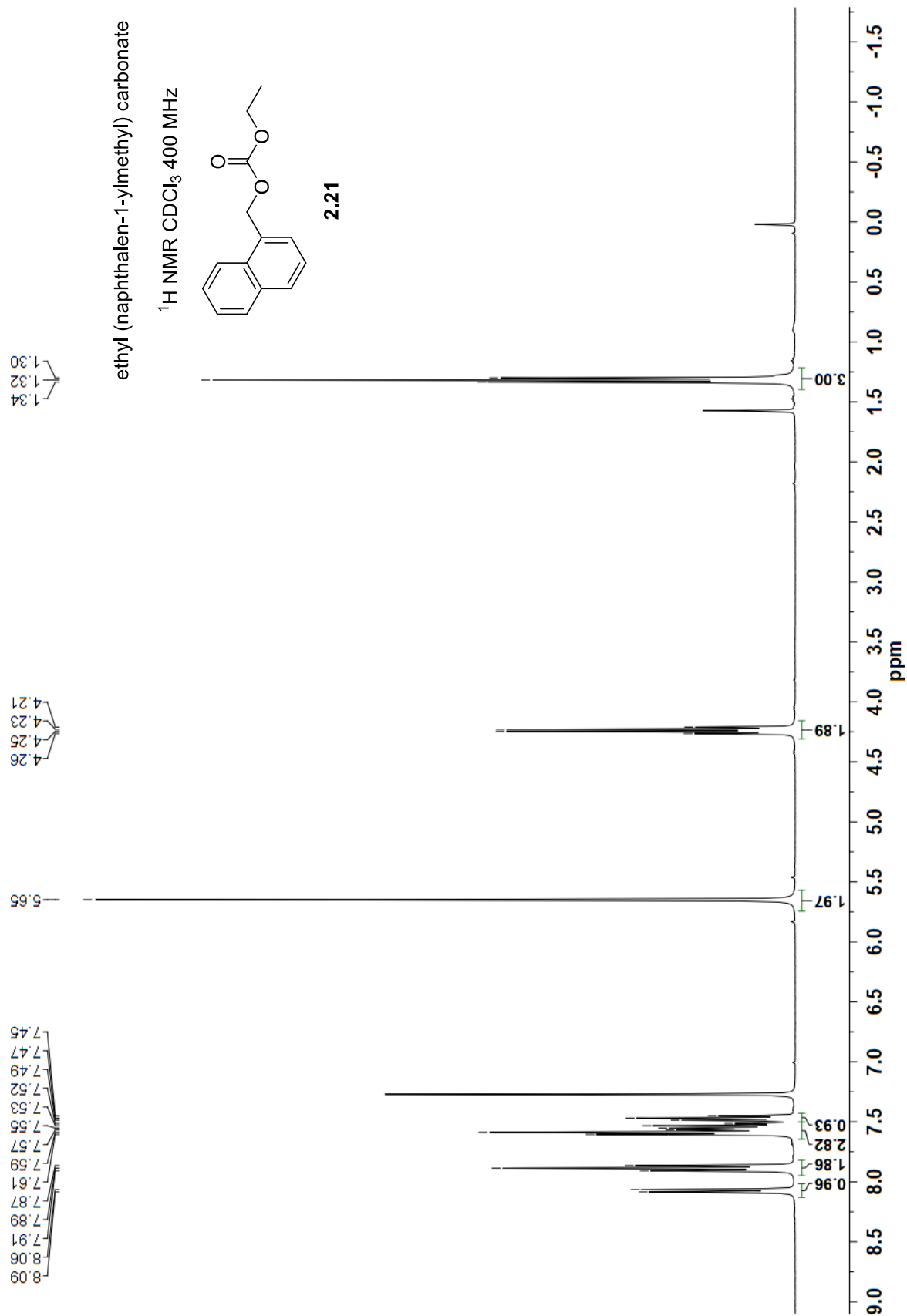


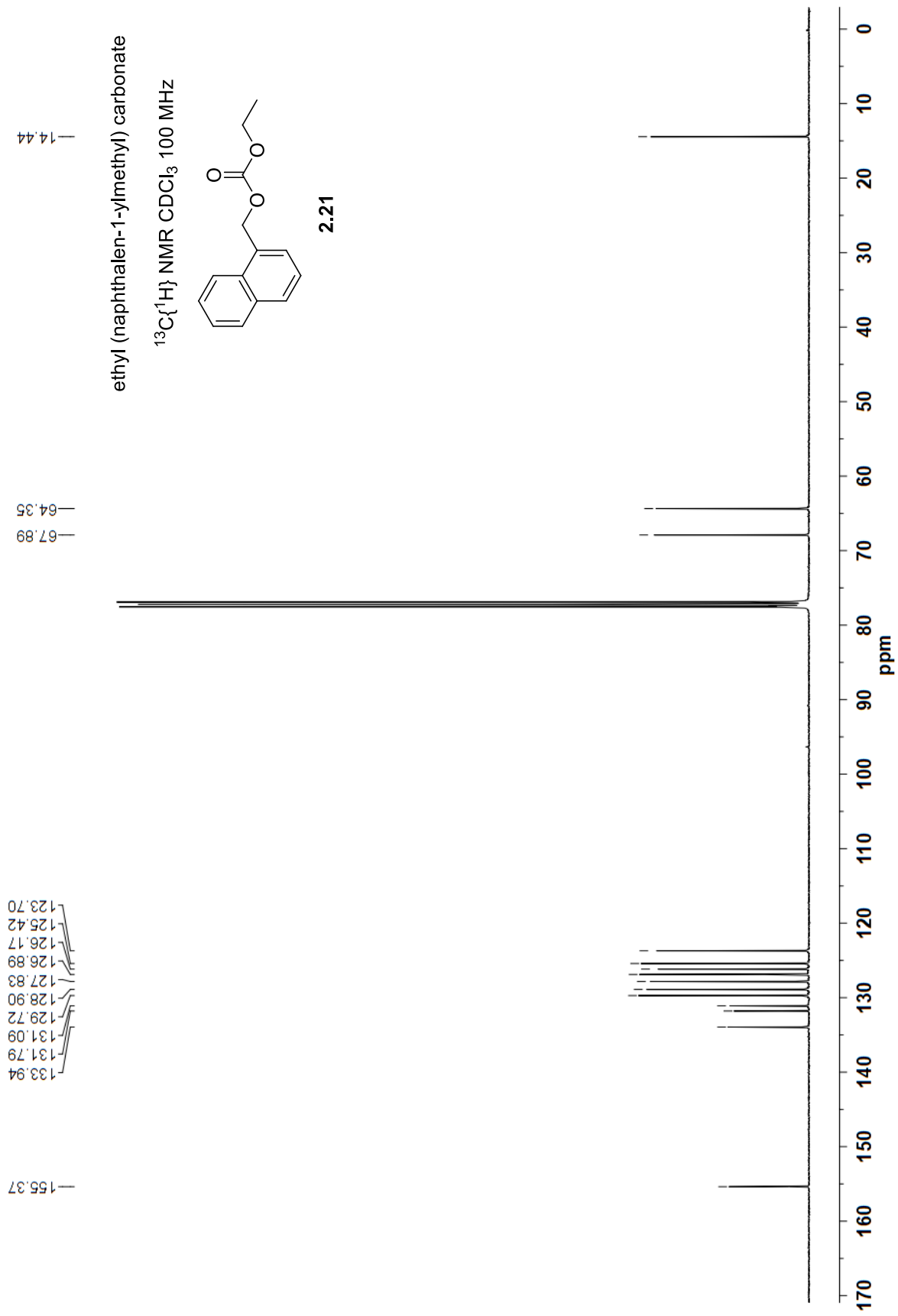


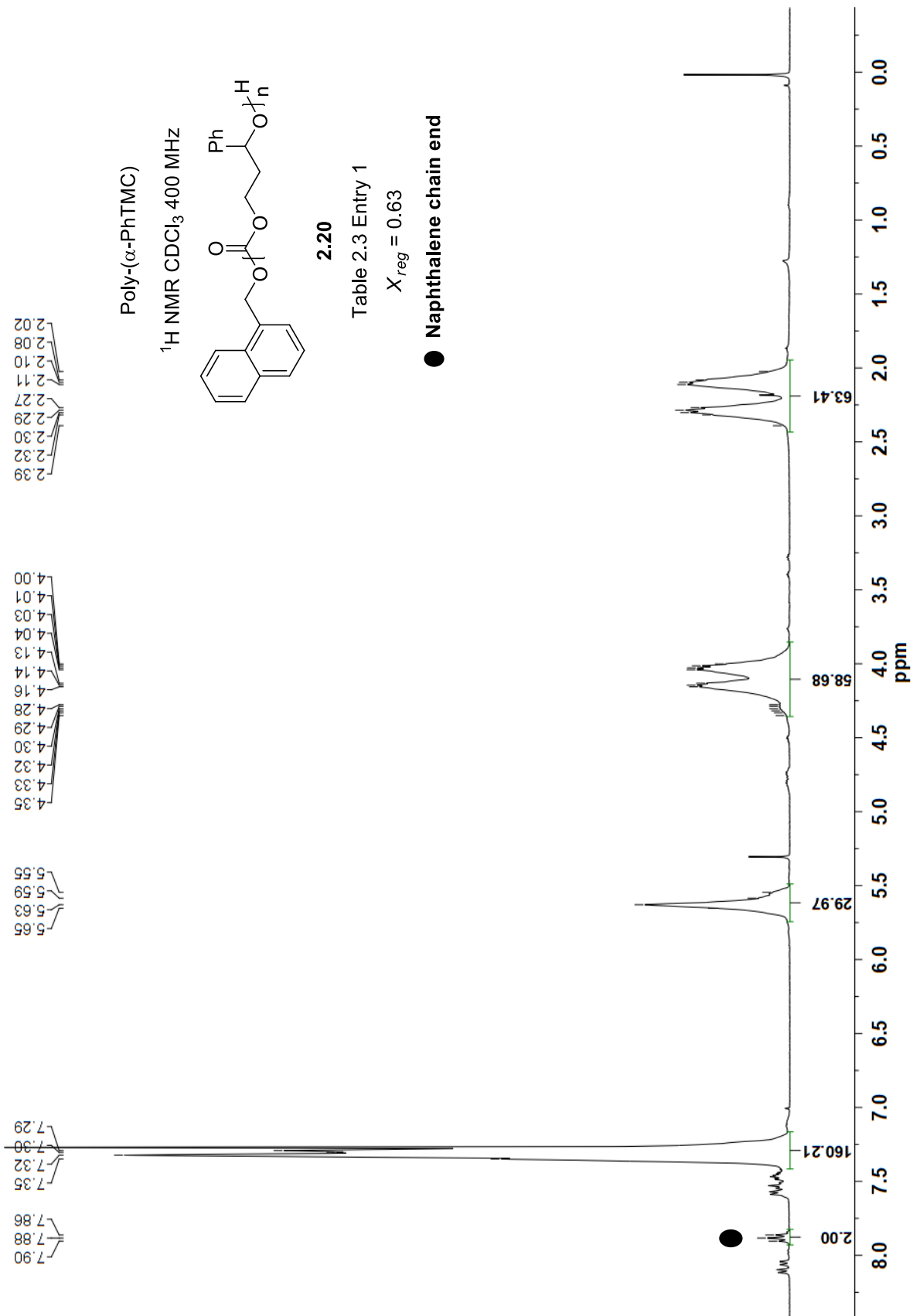


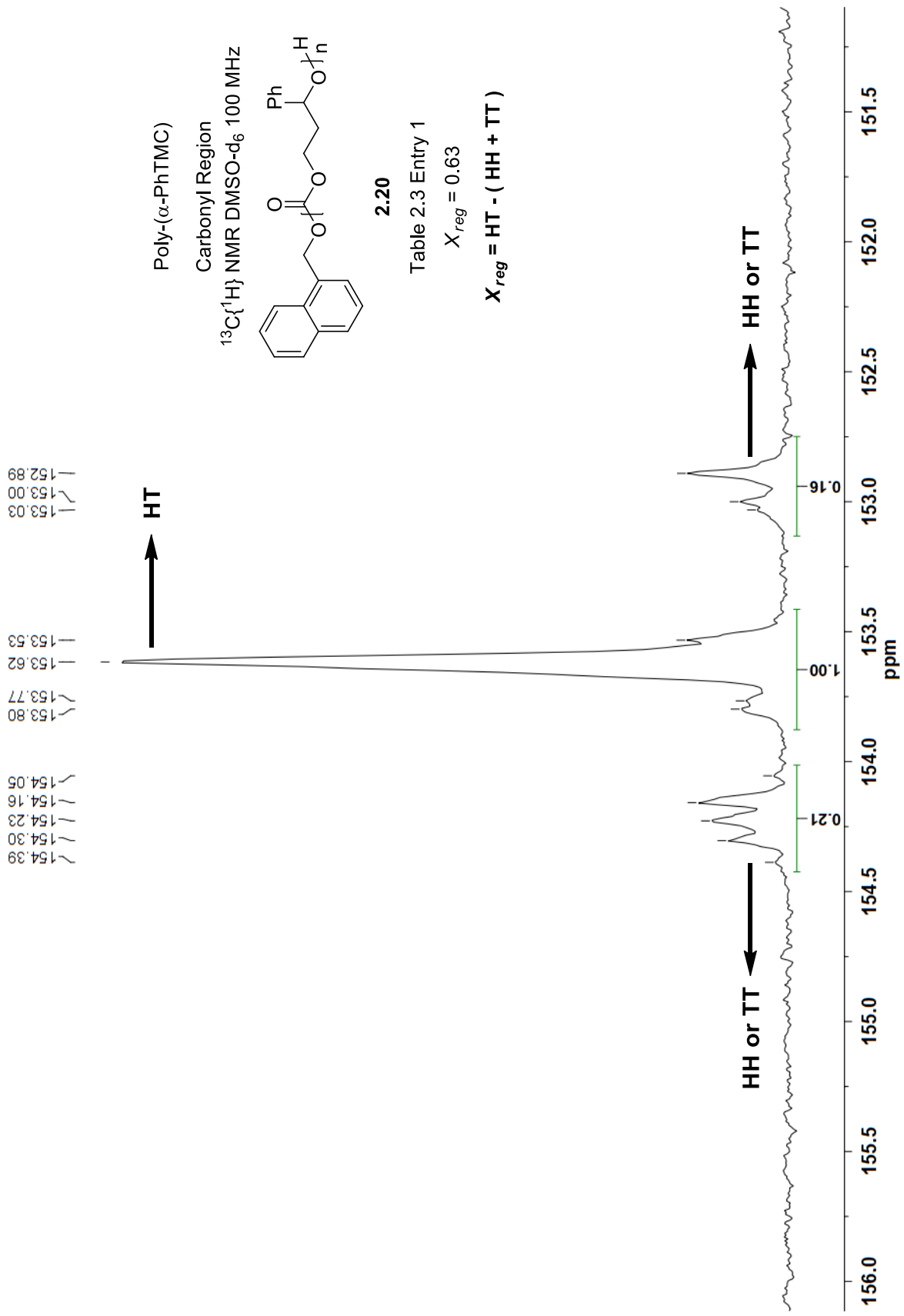


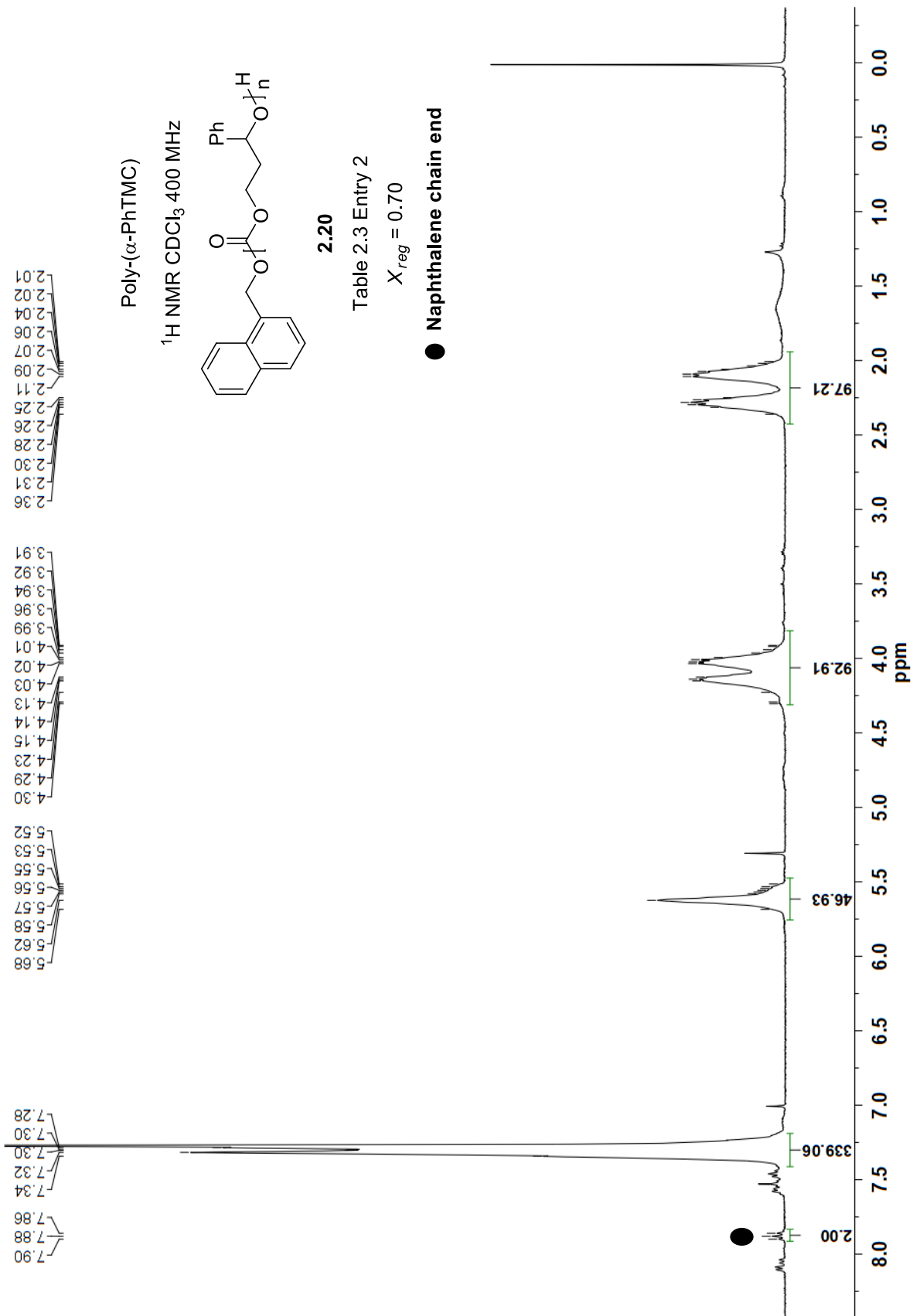


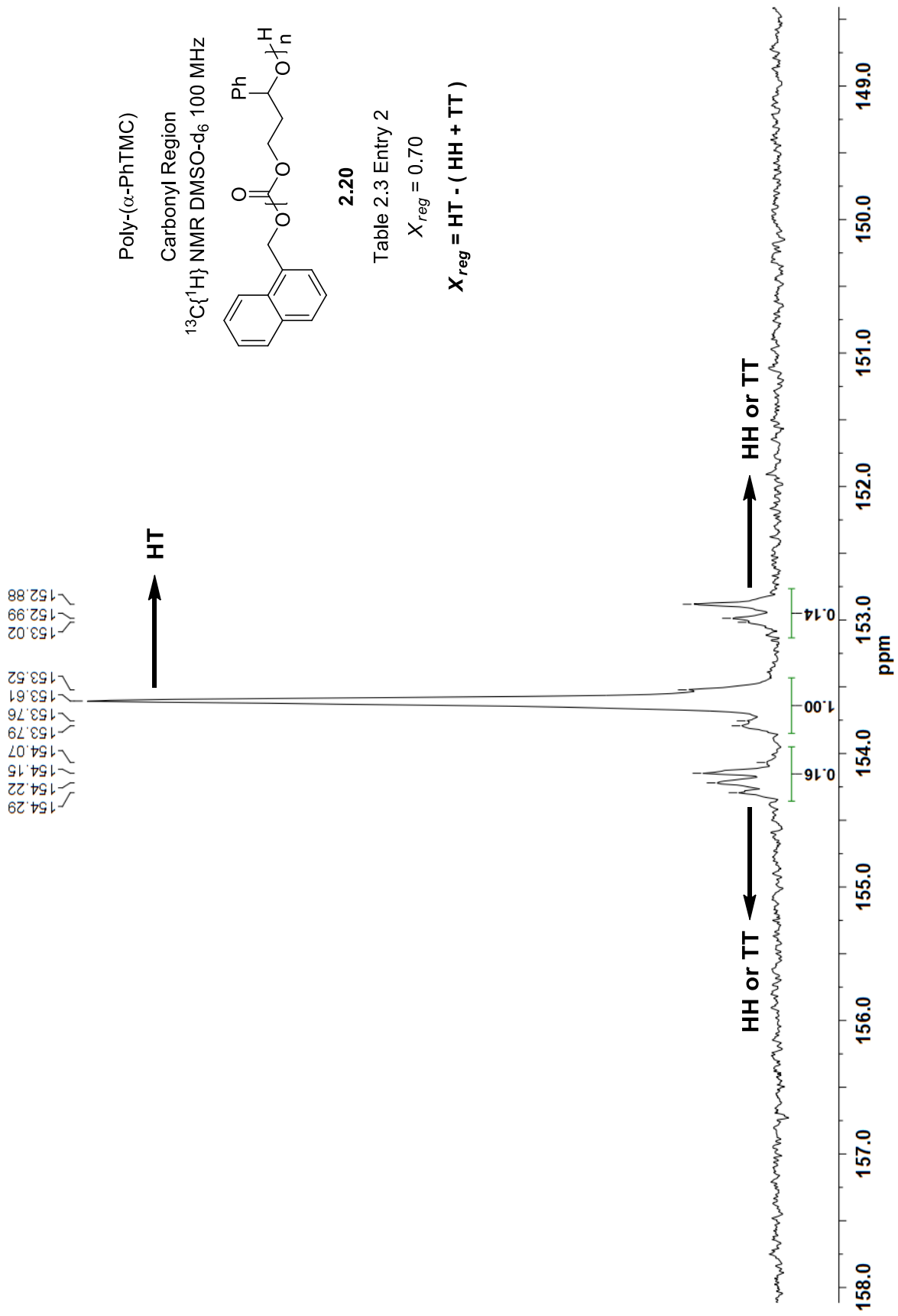


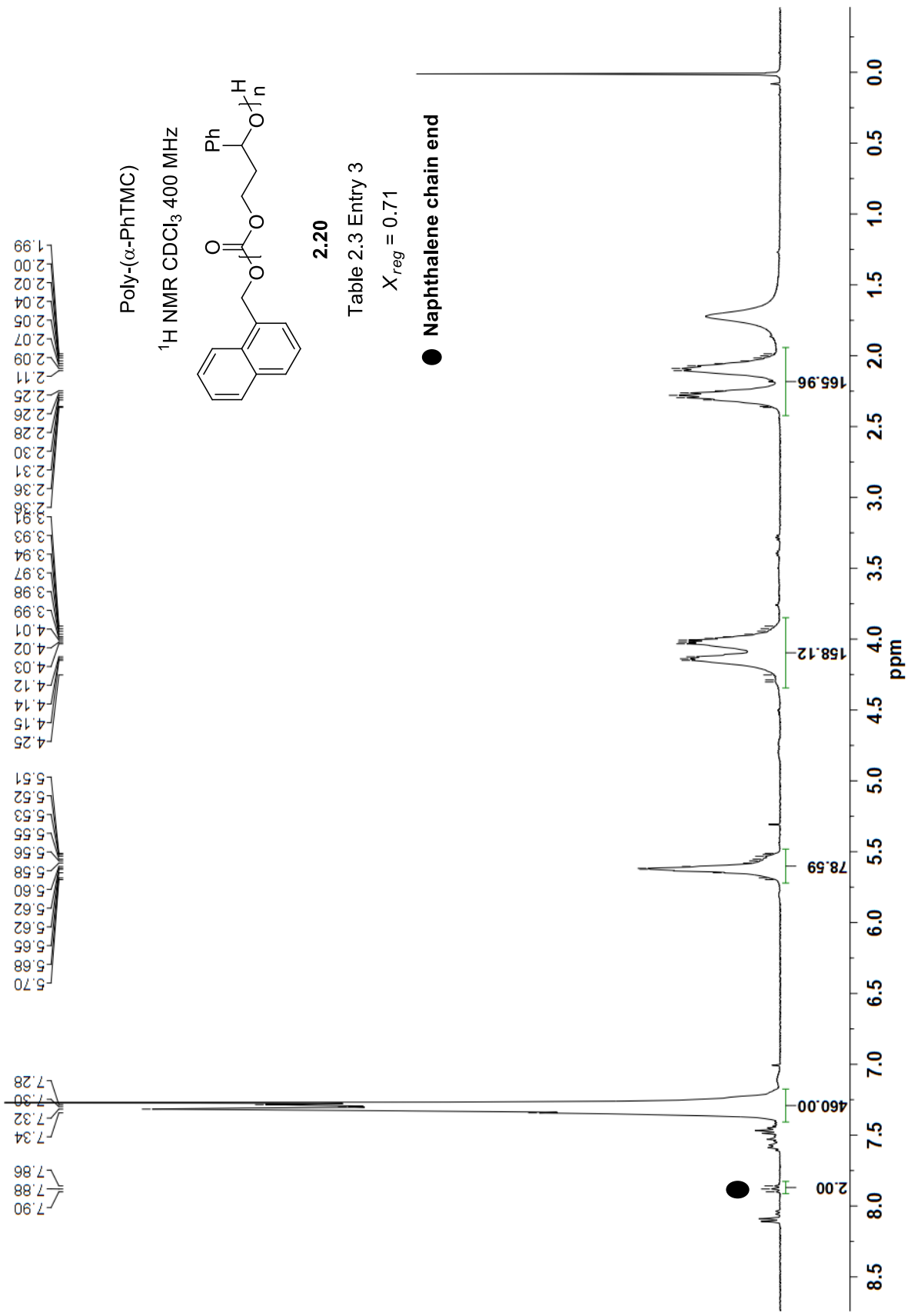


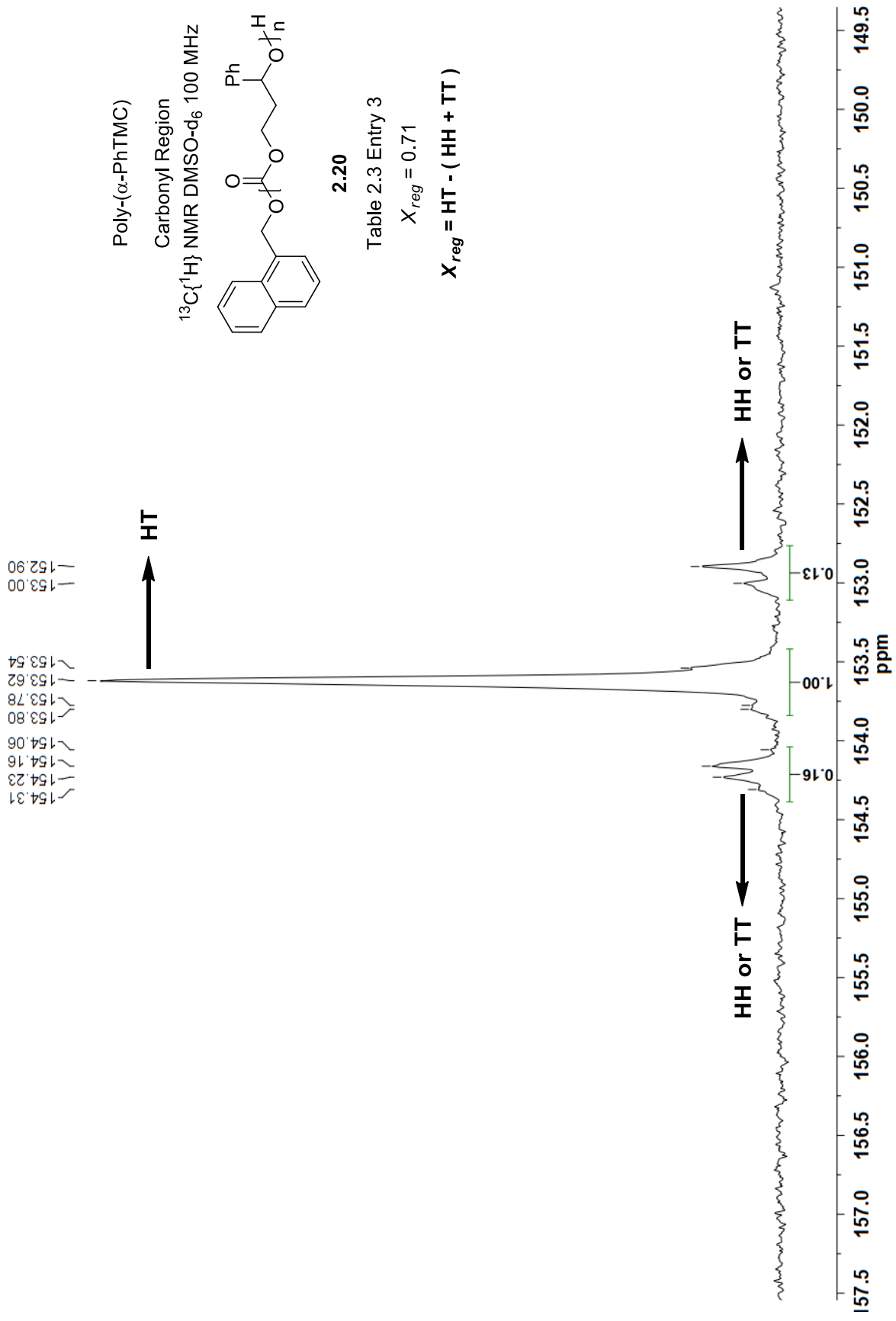


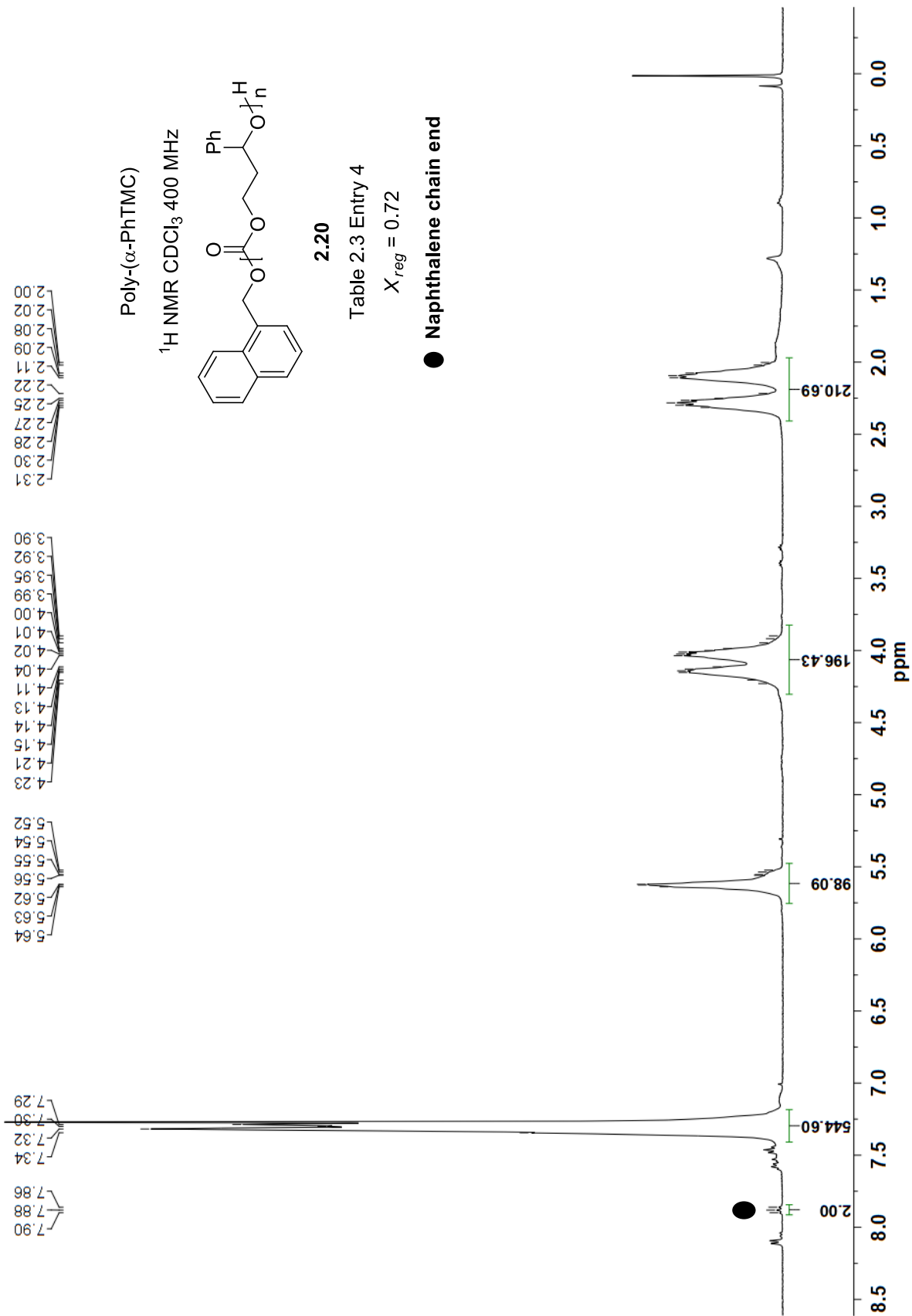


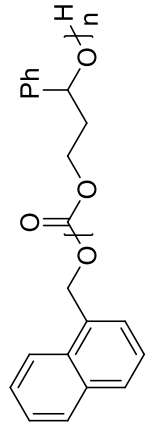
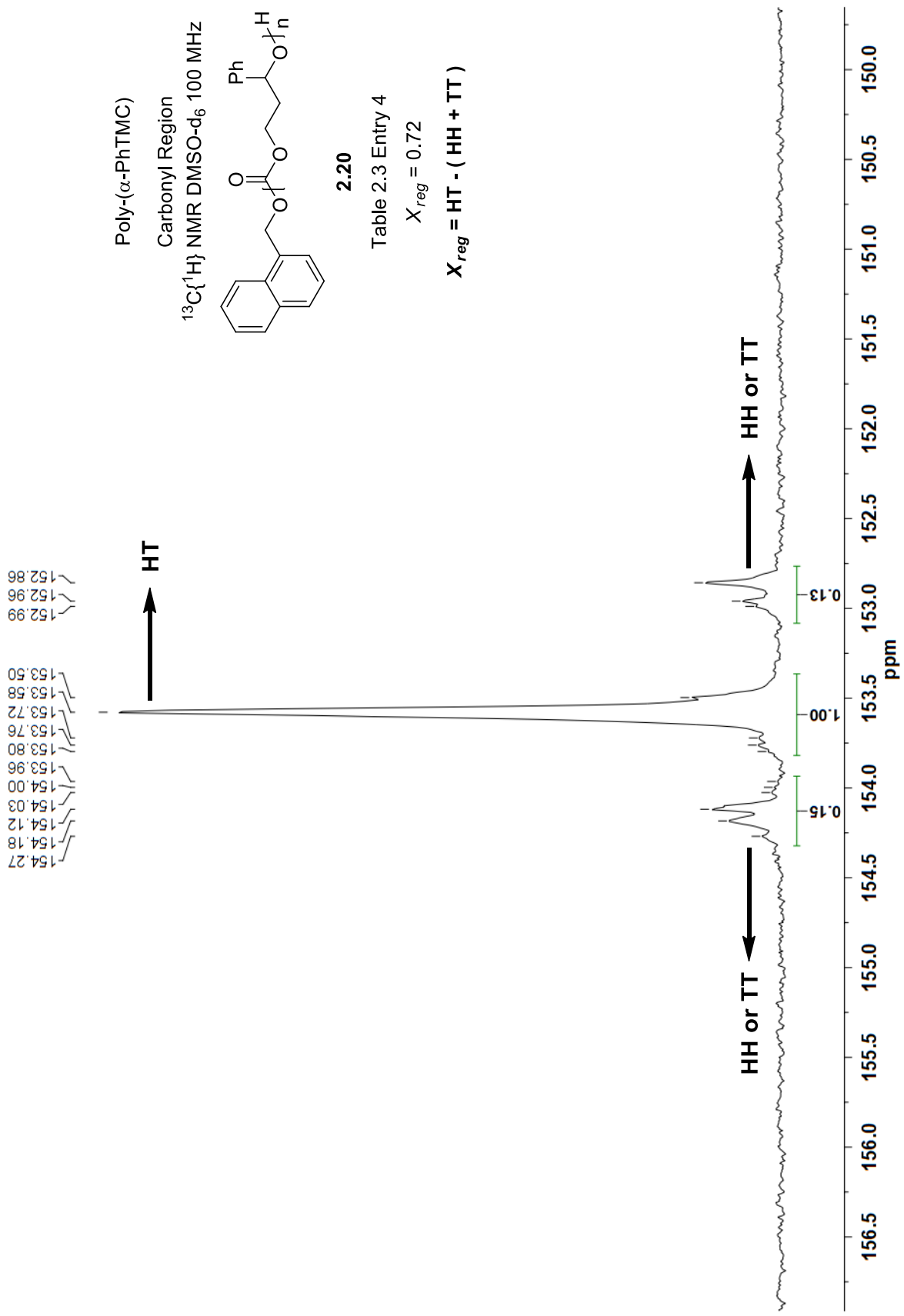










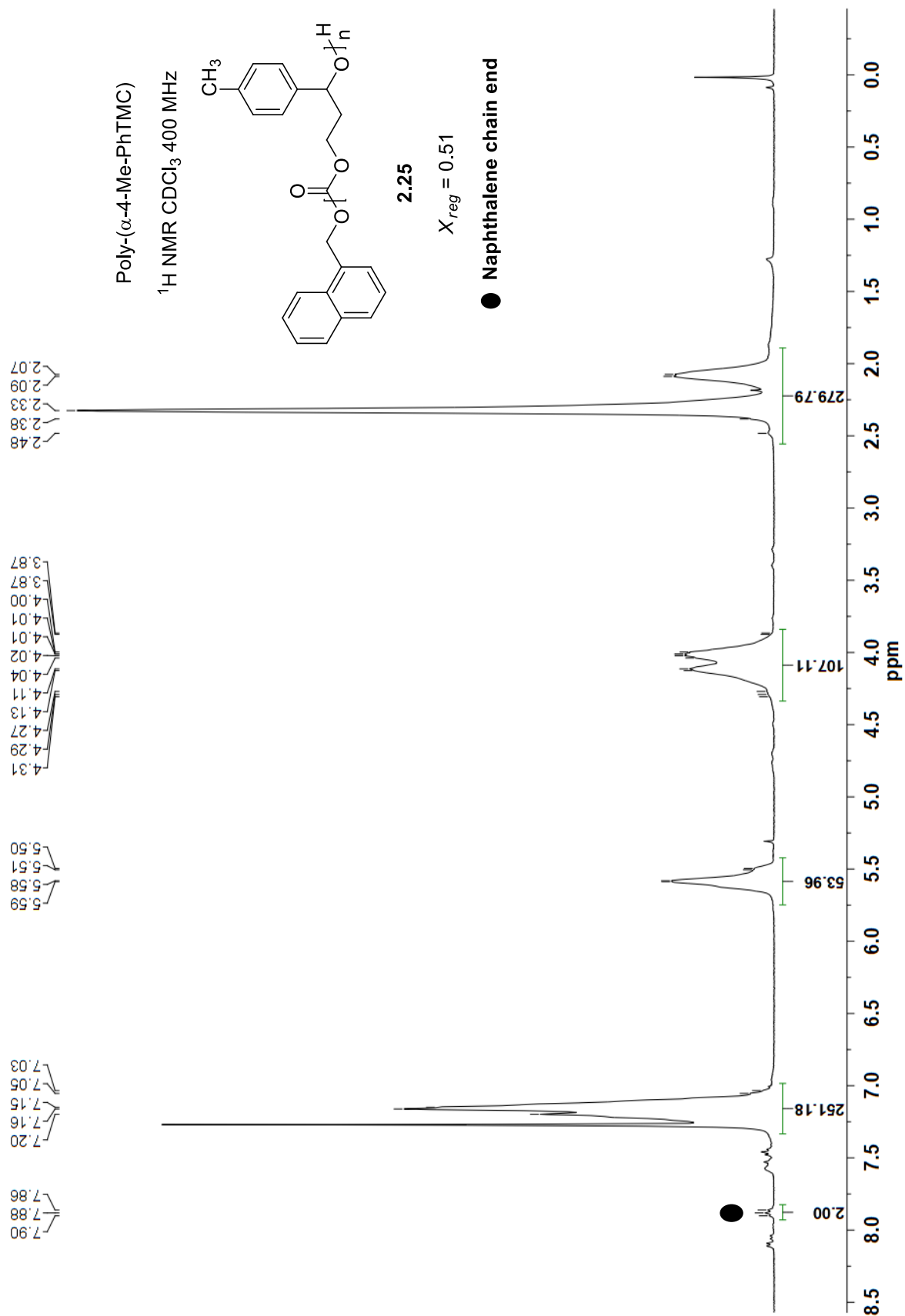


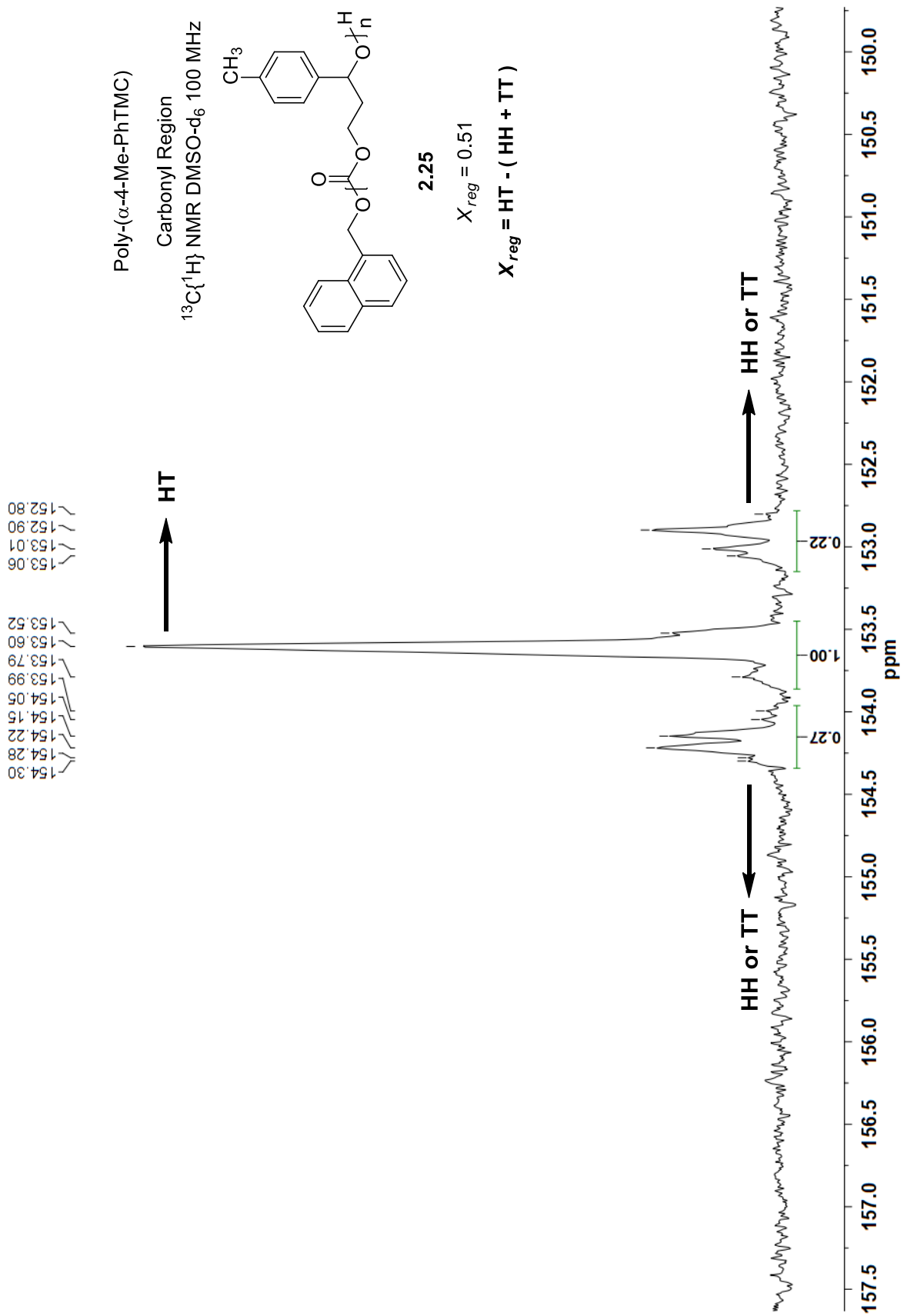
2.20

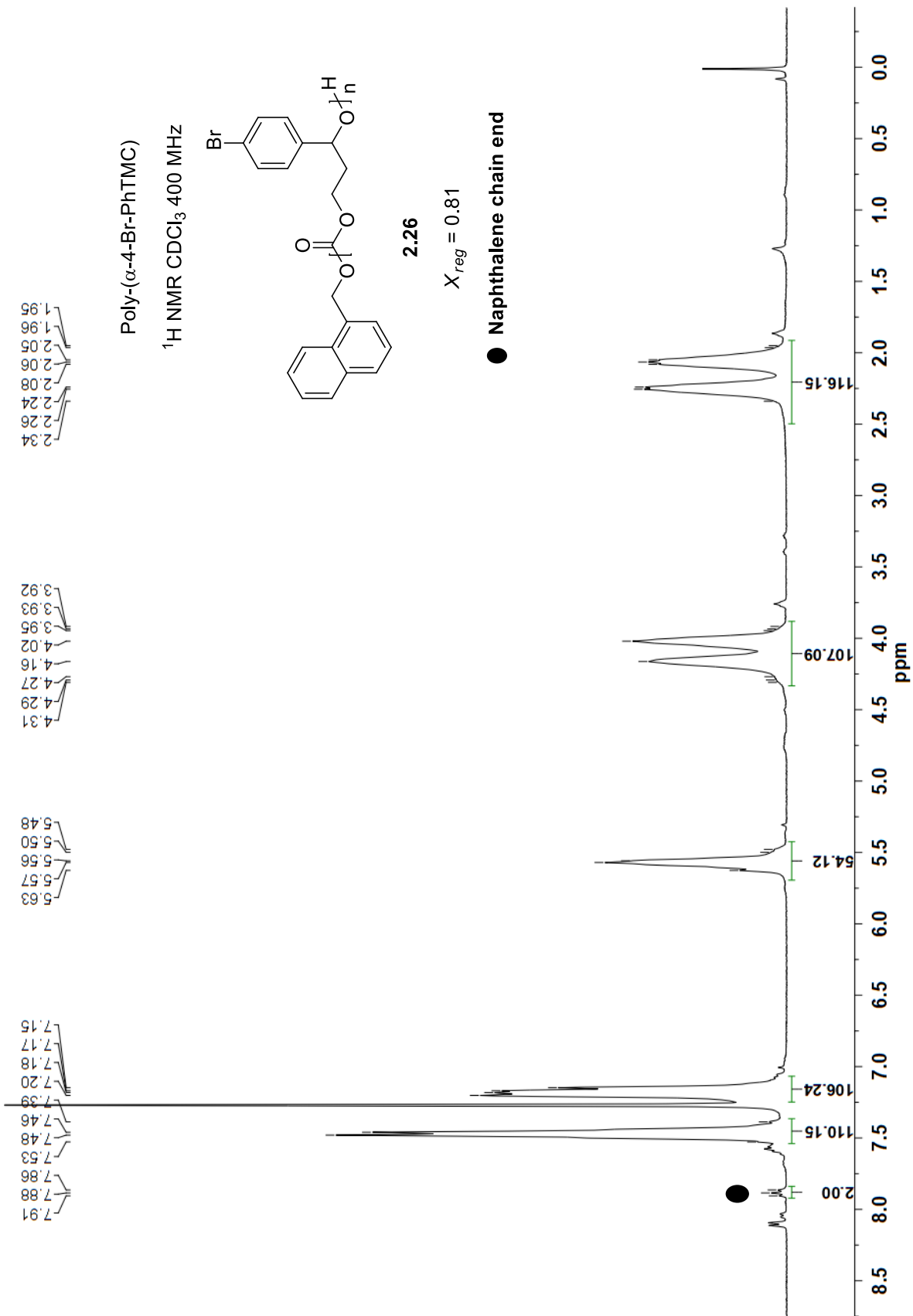
Table 2.3 Entry 4

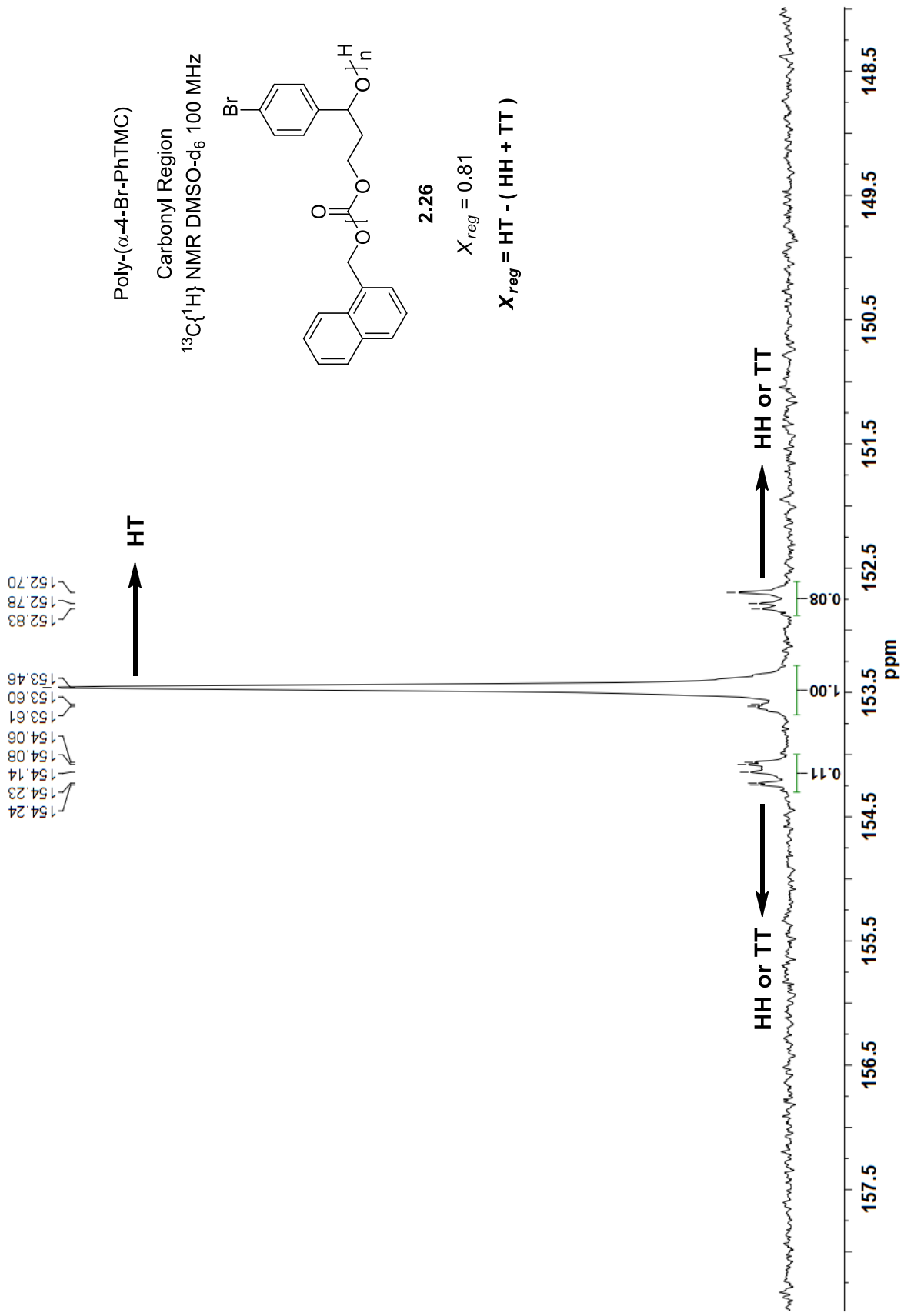
$$X_{reg} = 0.72$$

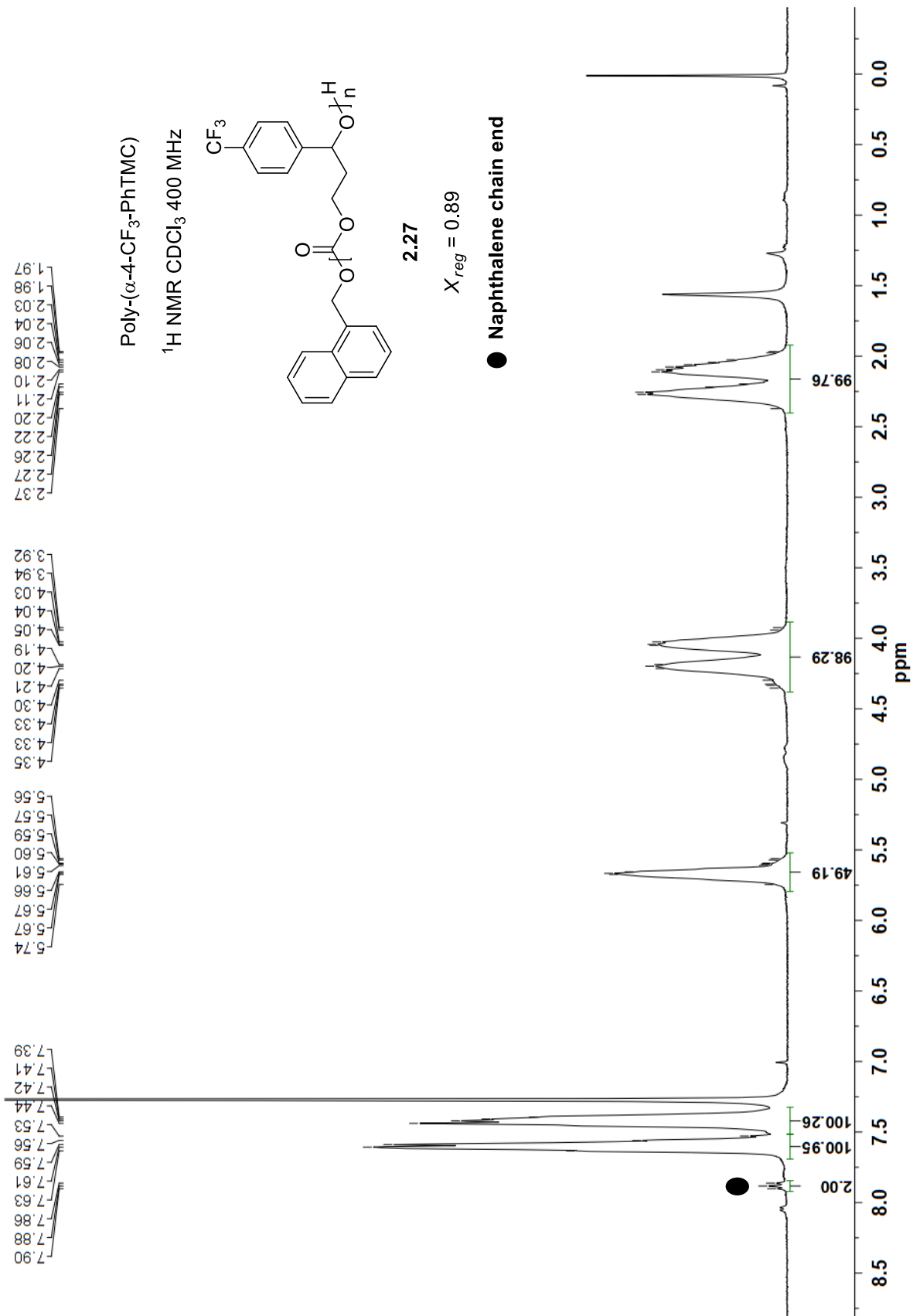
$$X_{reg} = HT - (HH + TT)$$

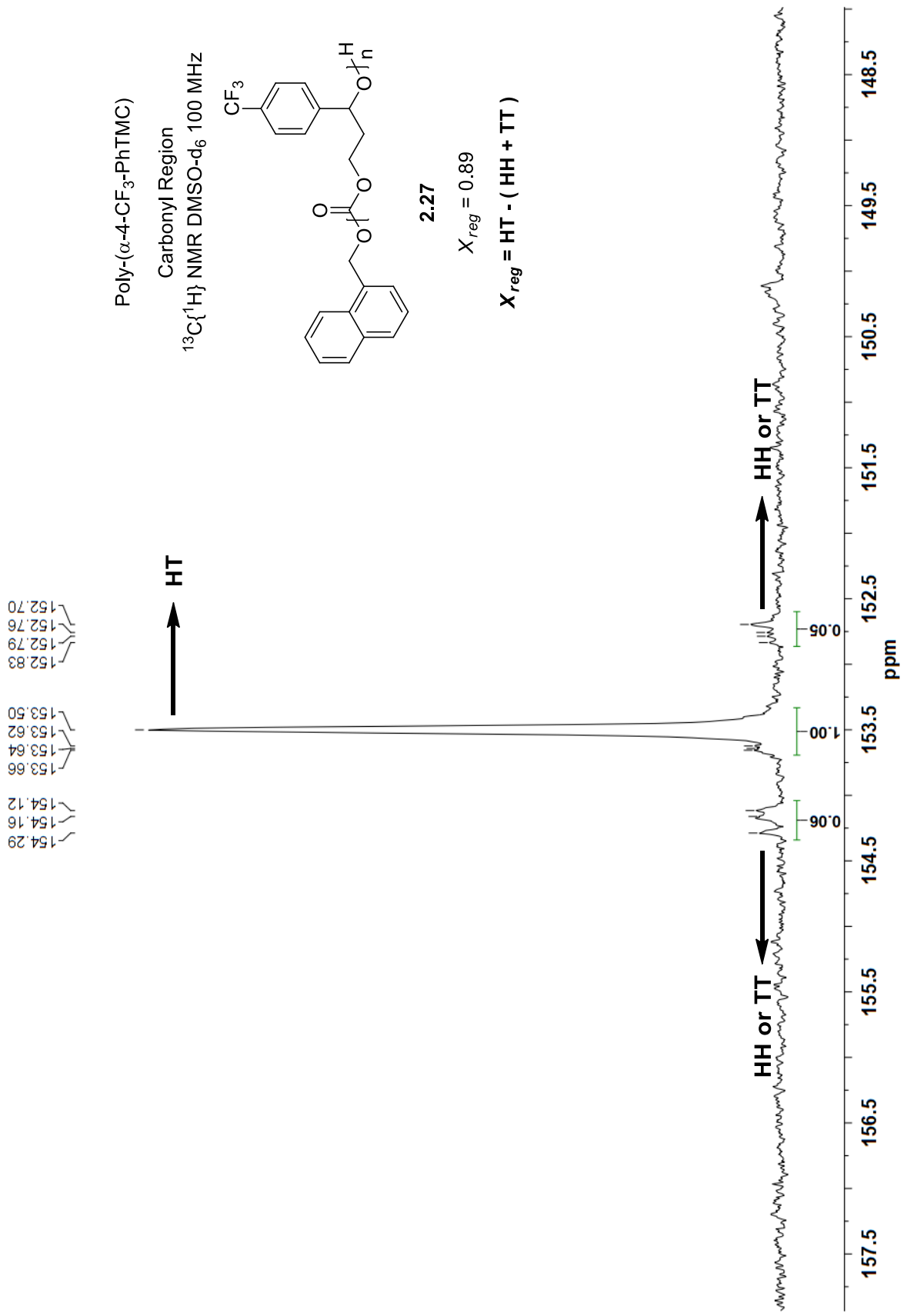


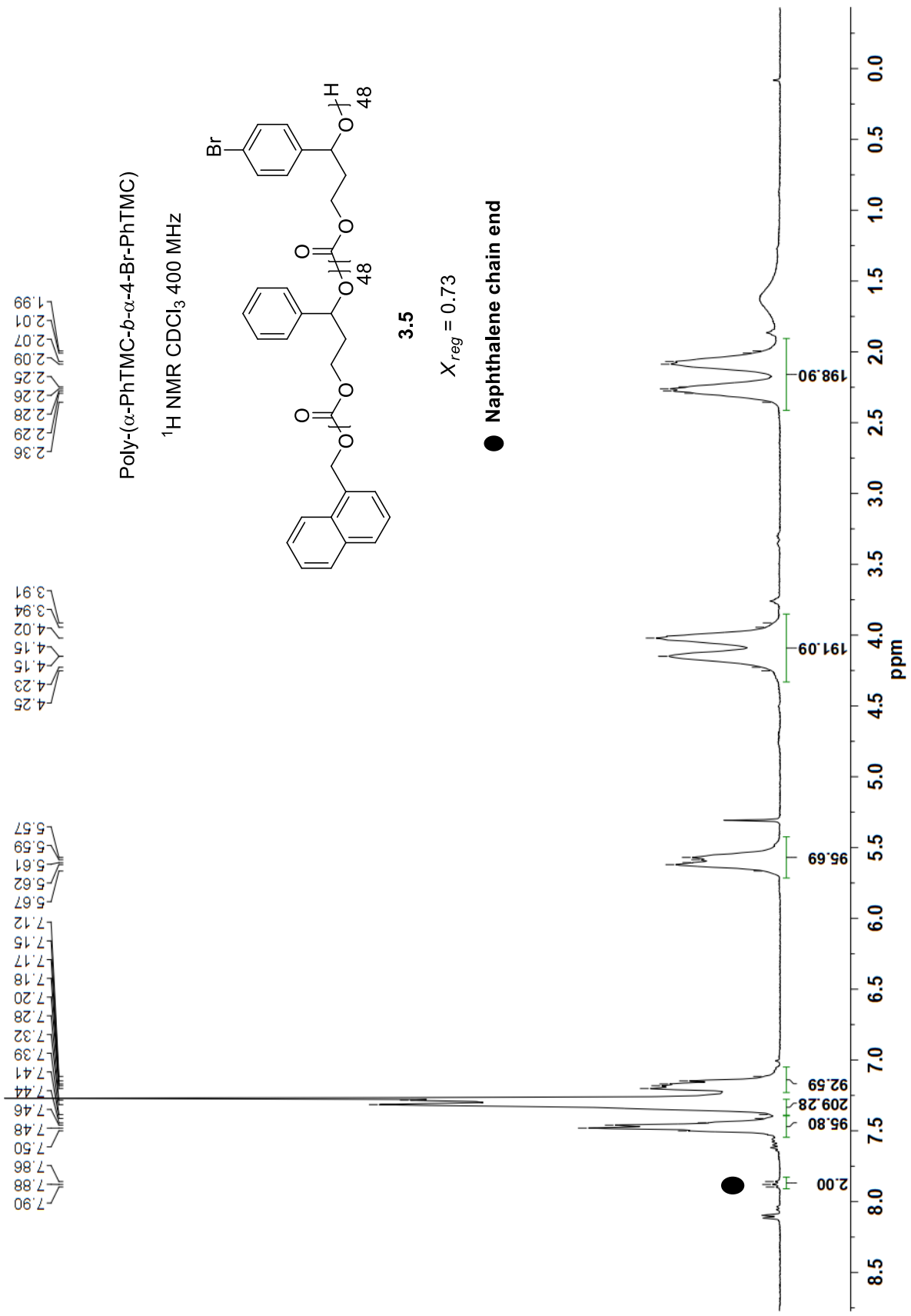


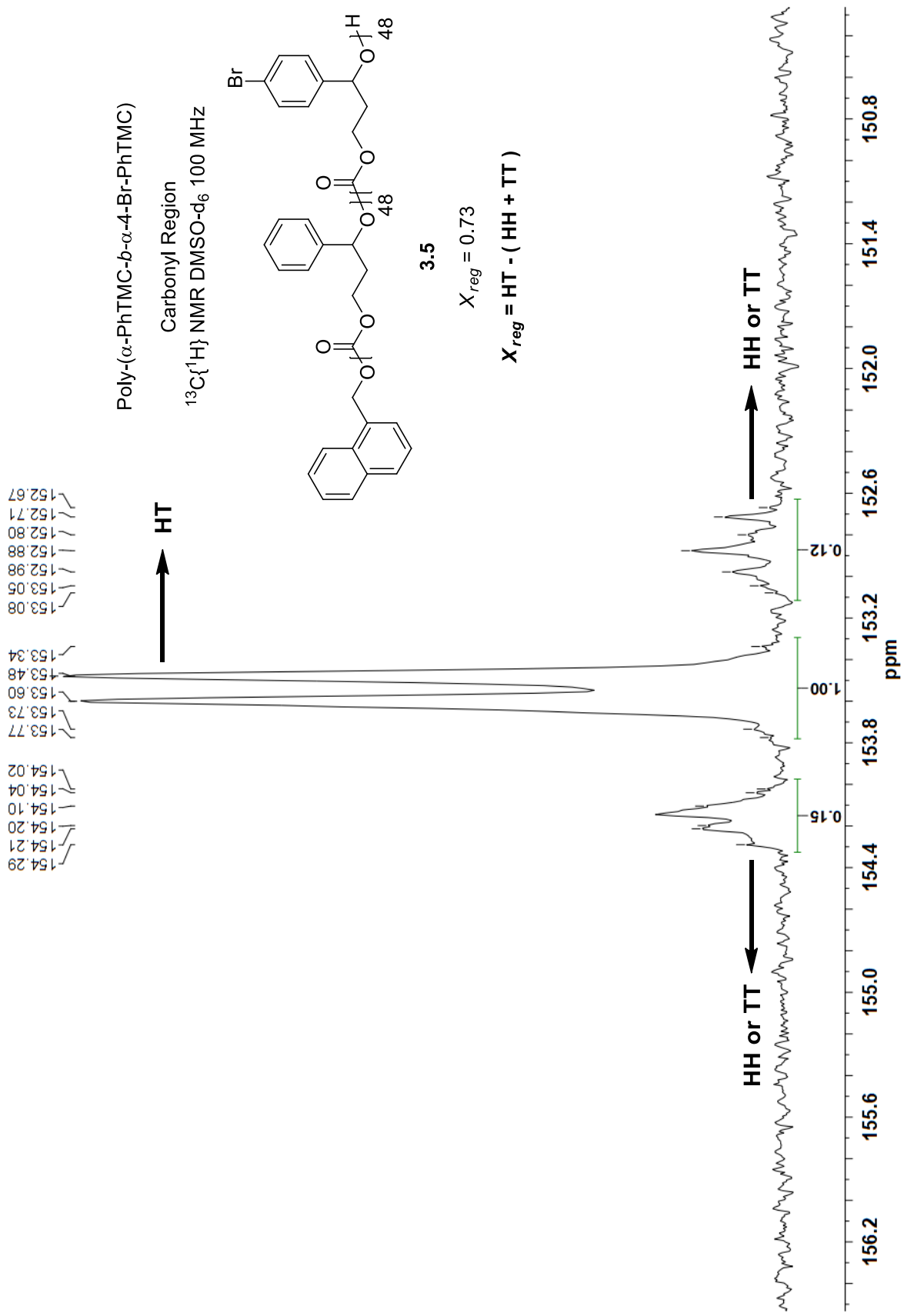


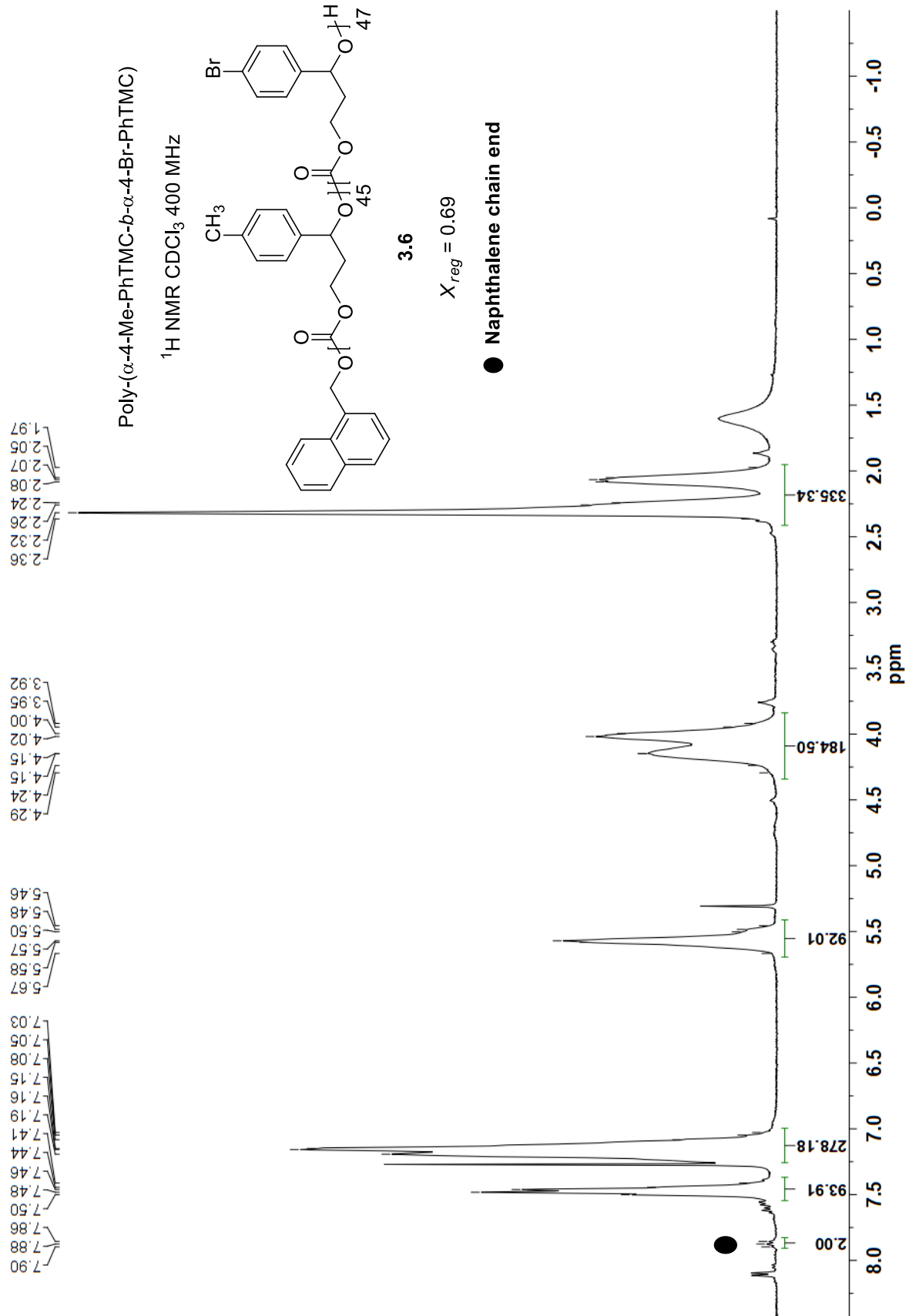


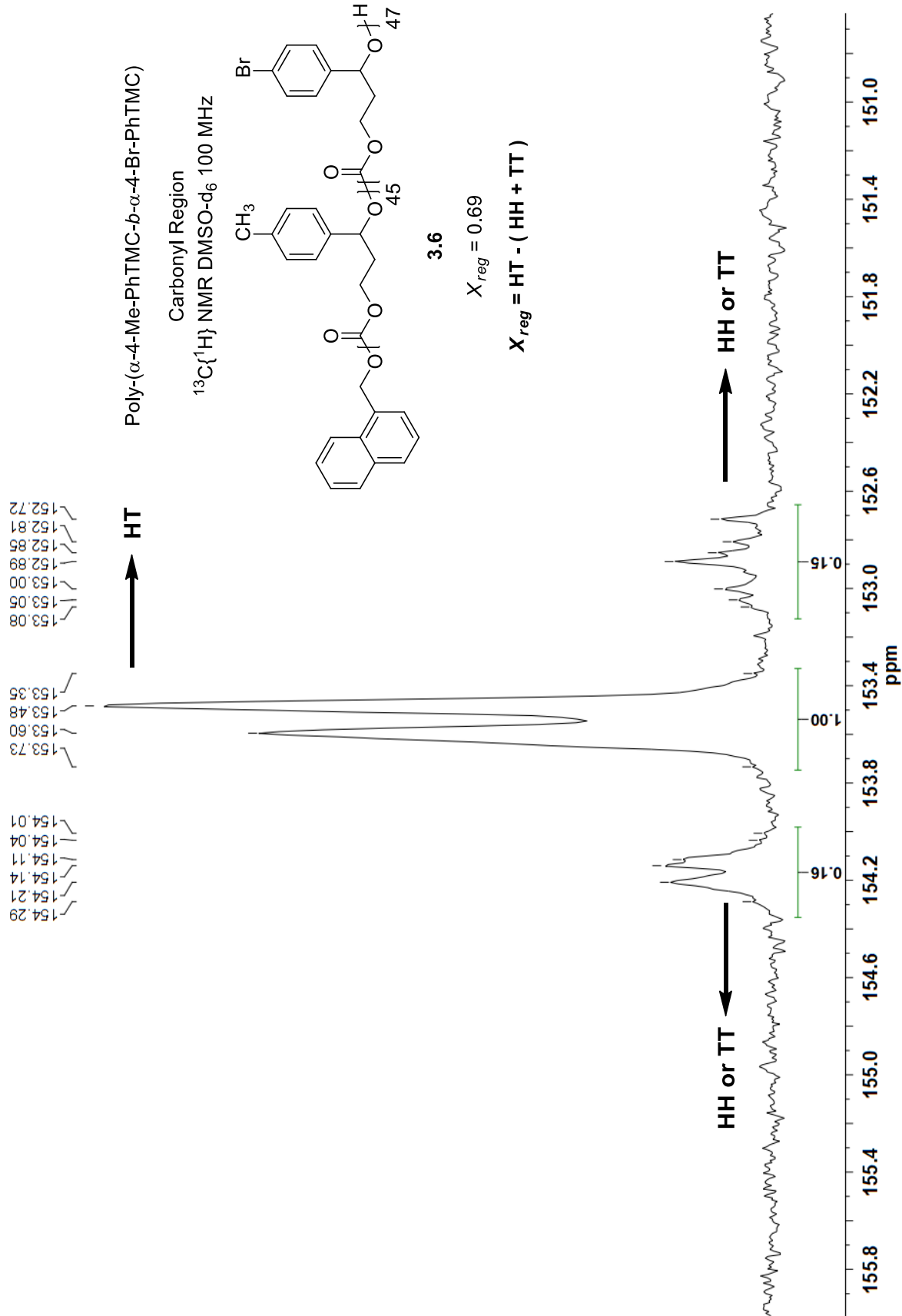


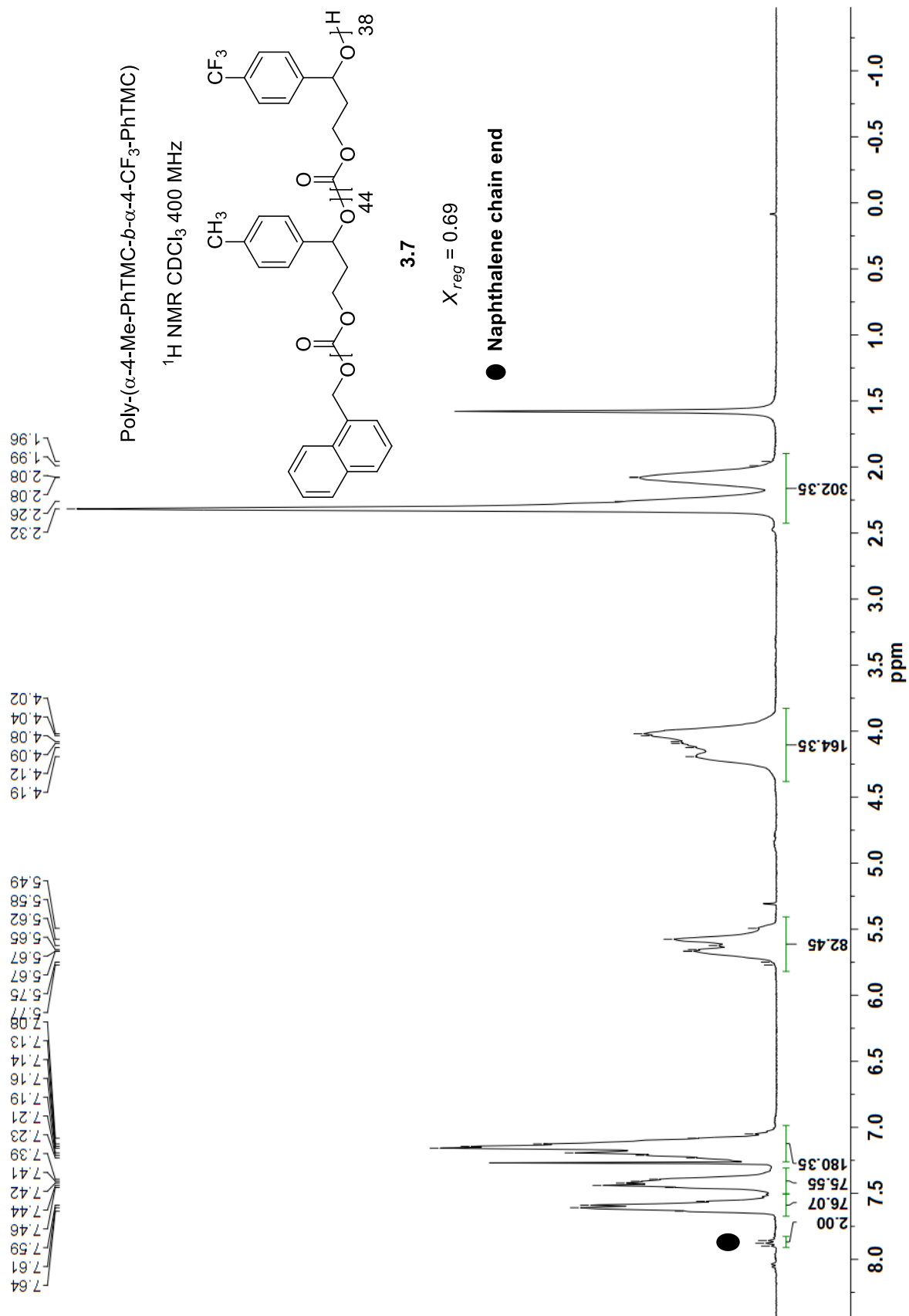


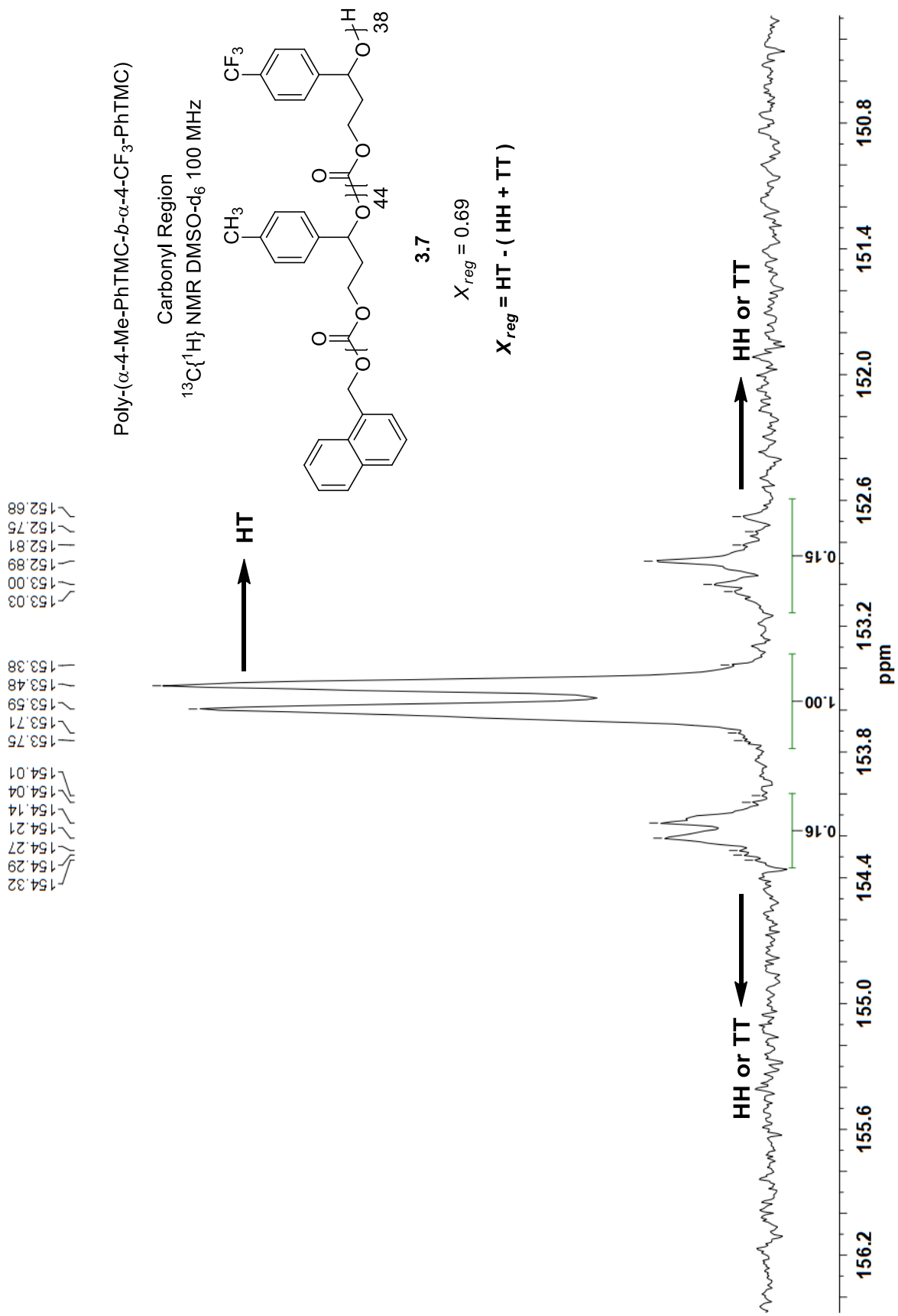


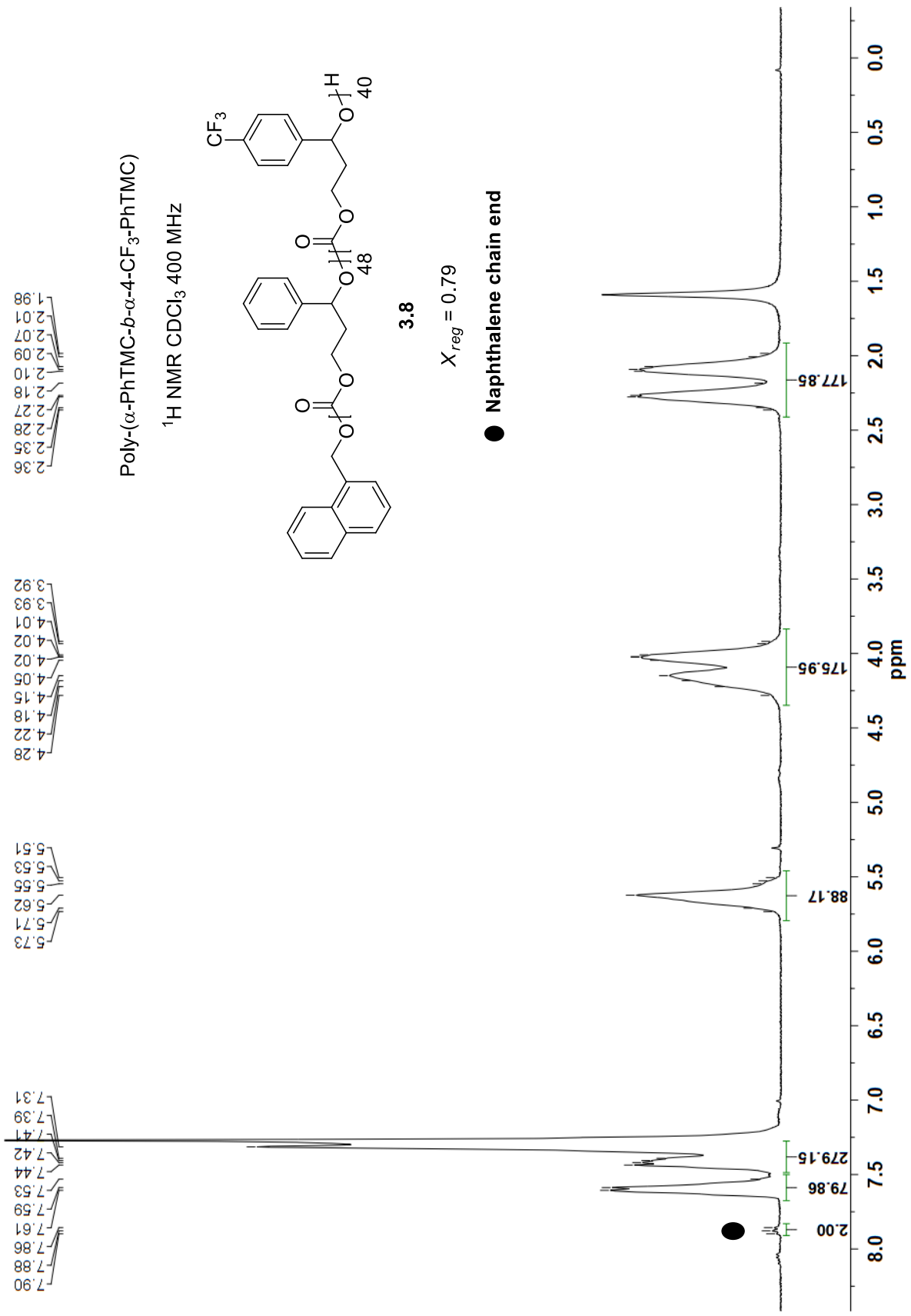


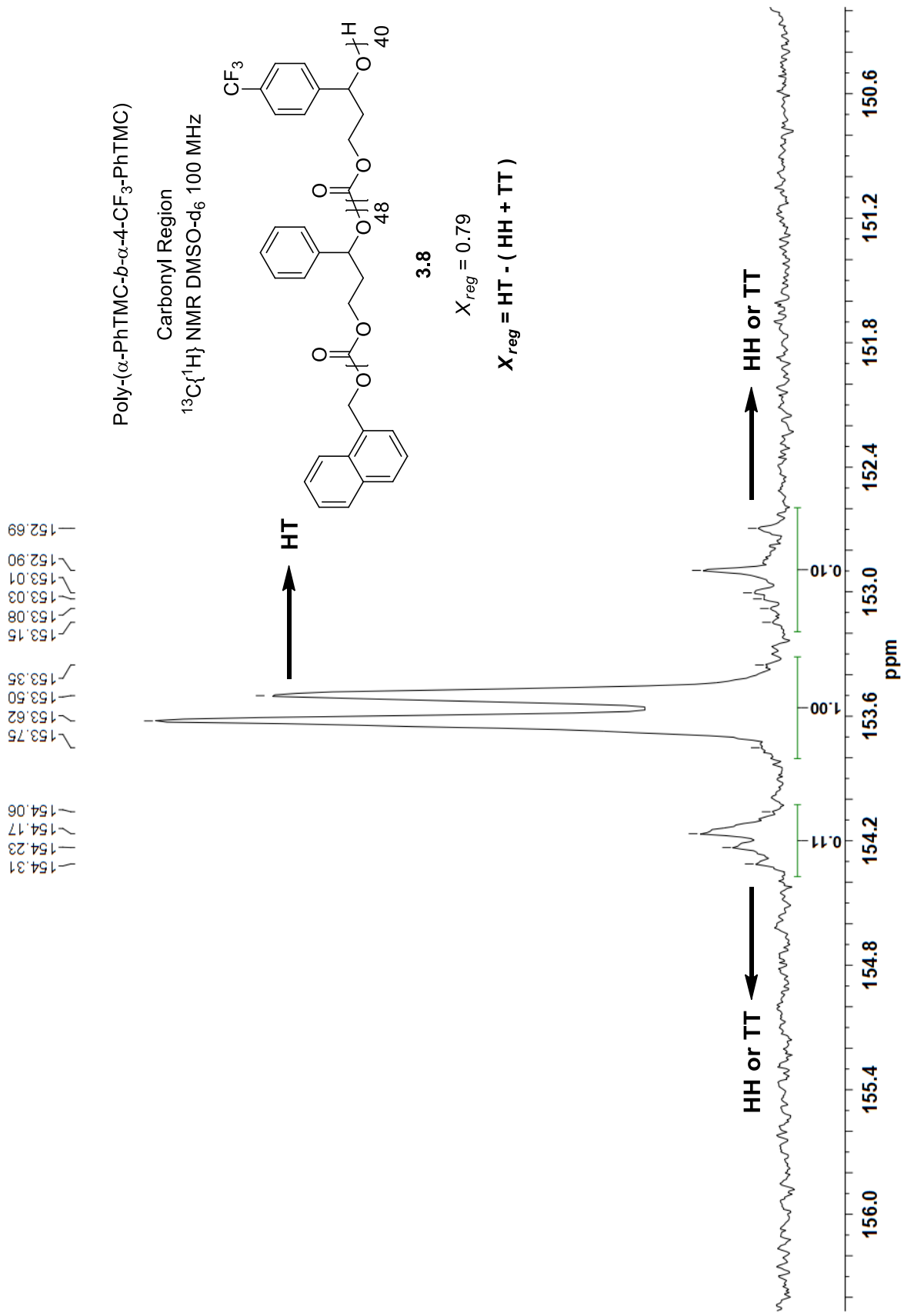


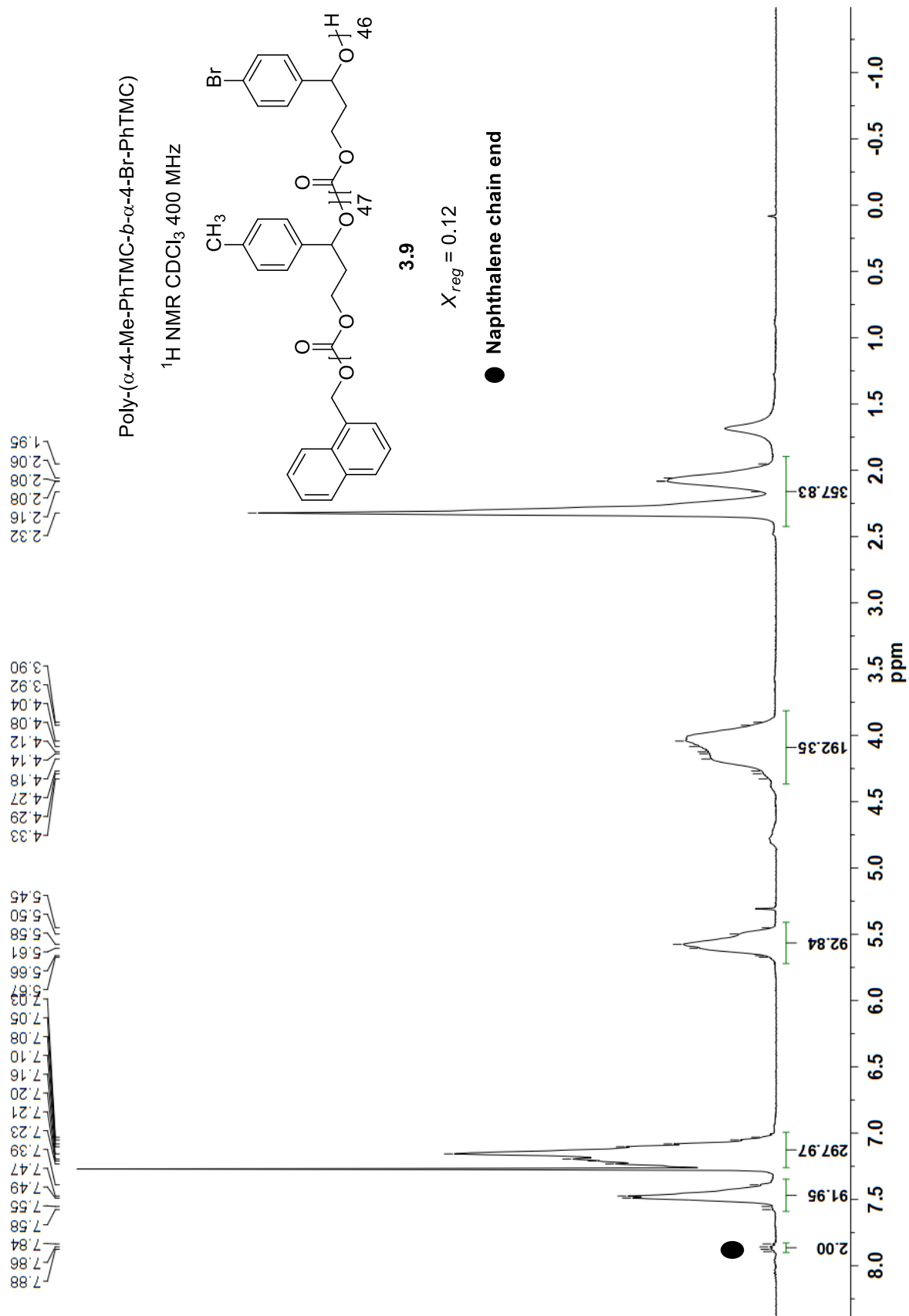


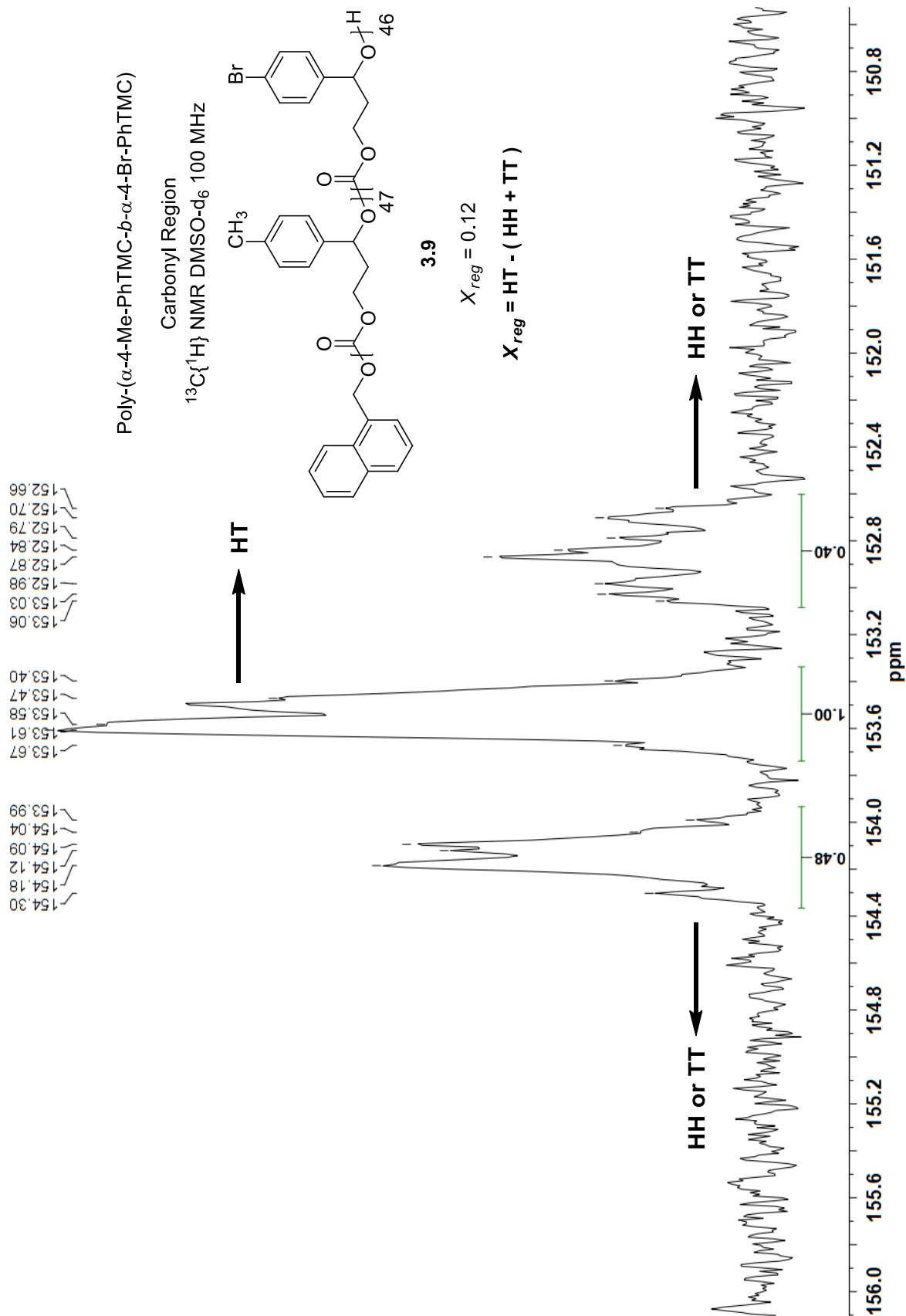


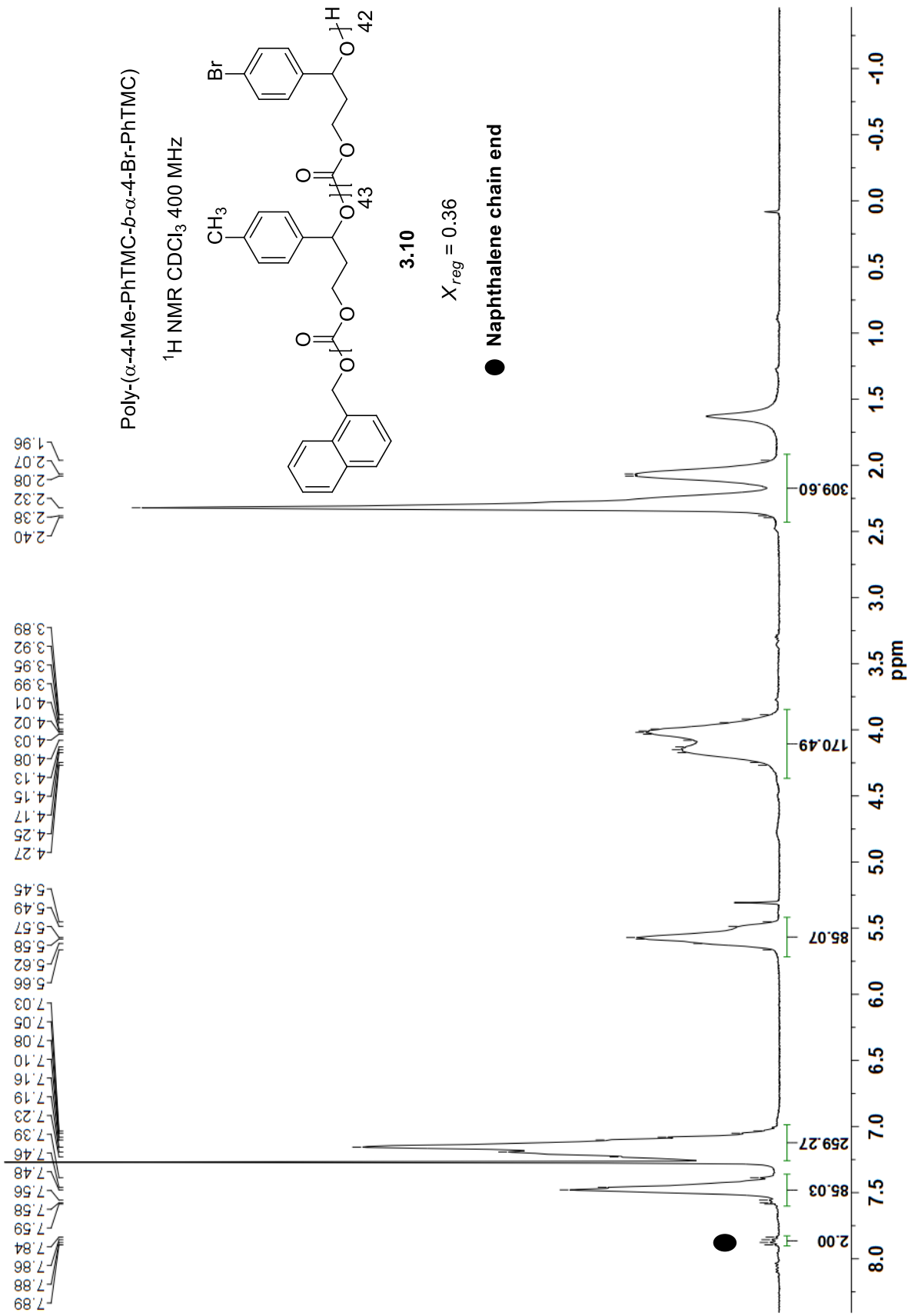


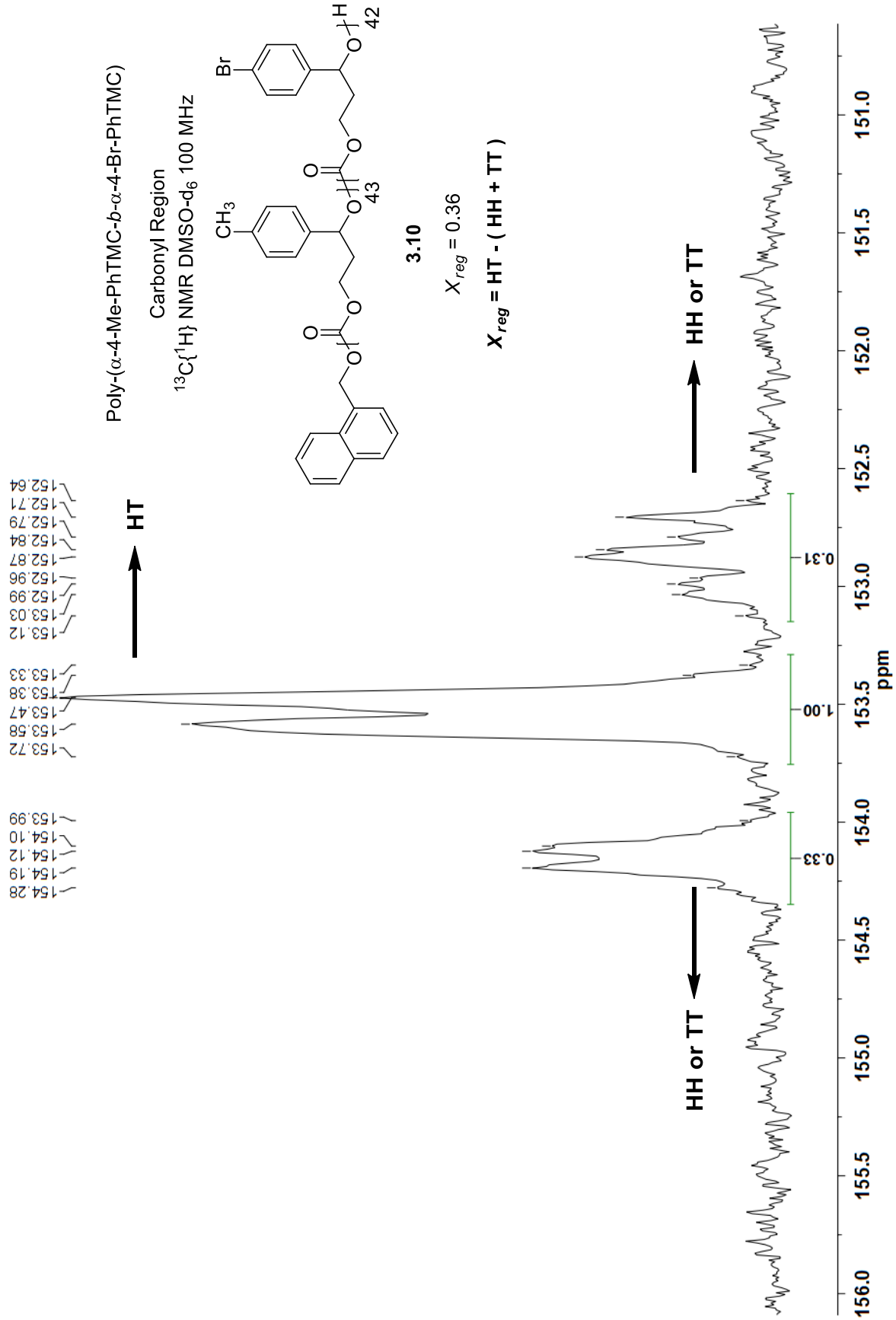




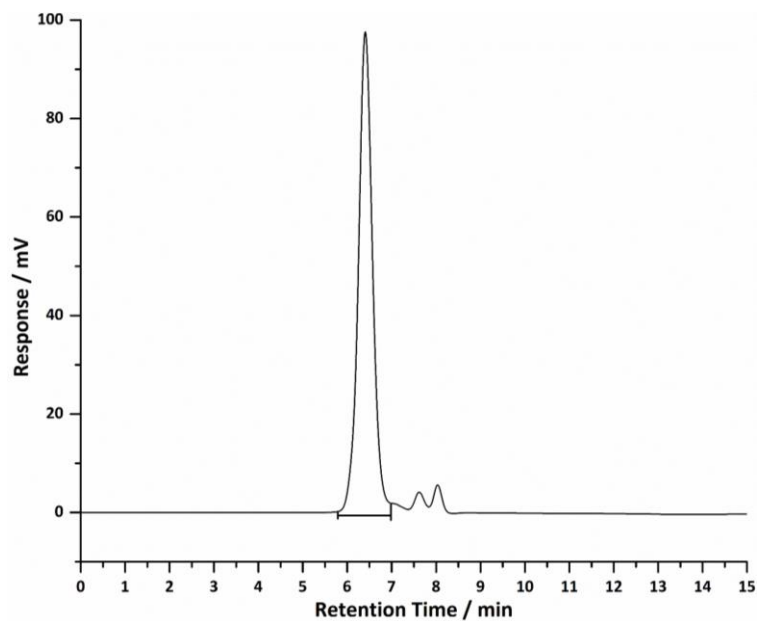






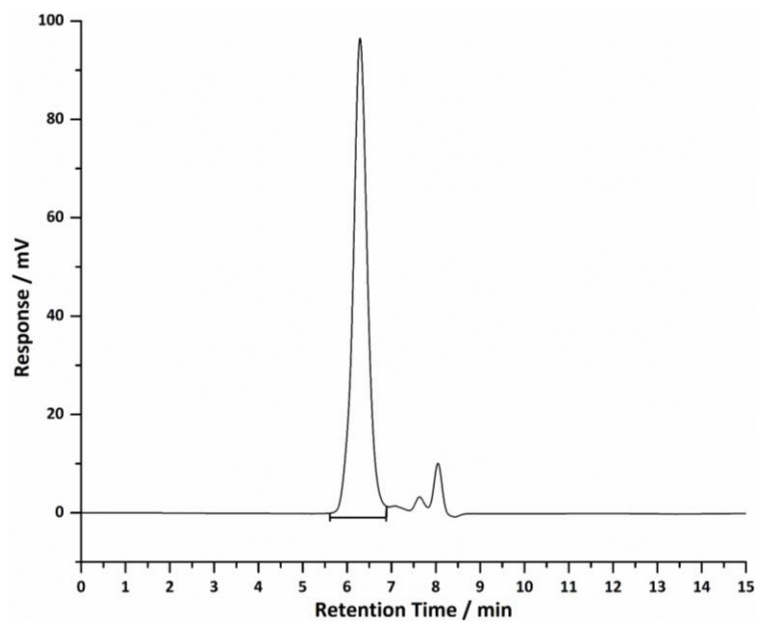


APPENDIX II
SEC TRACES



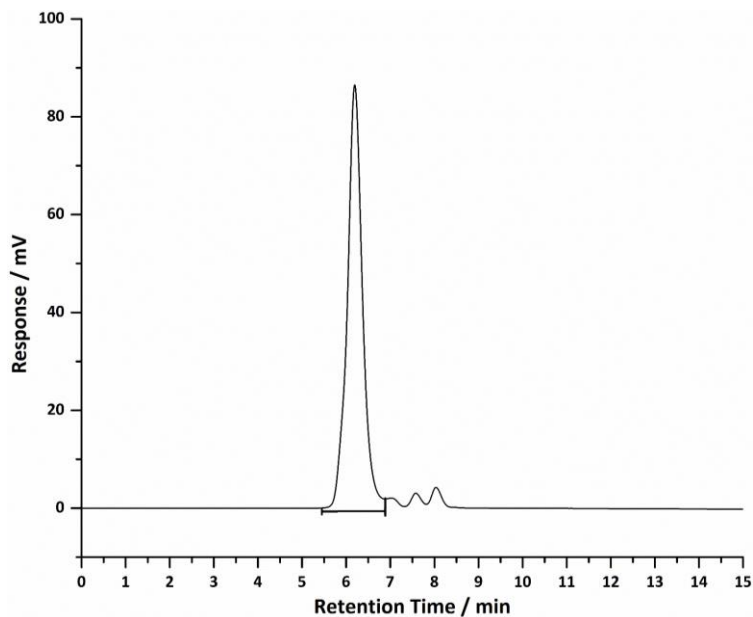
SEC trace of poly-(α -PhTMC) **2.20** (Table 2.3 Entry 1)

RT	M_n	M_w	\mathcal{D}
6.402	4100	5300	1.29



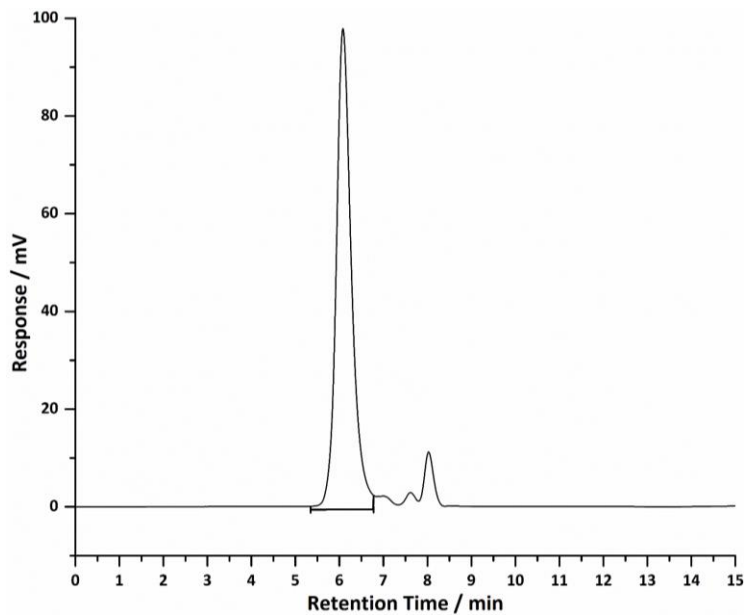
SEC trace of poly-(α -PhTMC) **2.20** (Table 2.3 Entry 2)

RT	M_n	M_w	\mathcal{D}
6.287	6100	8100	1.32



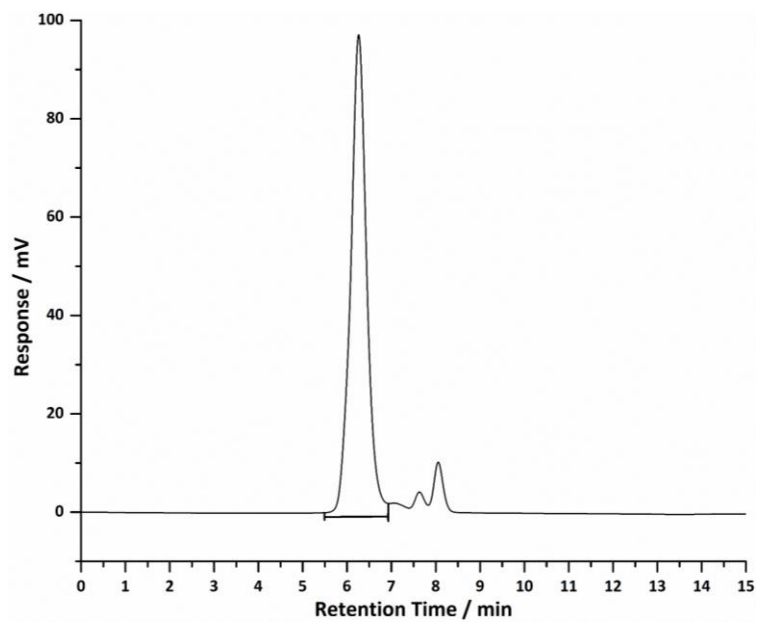
SEC trace of poly-(α -PhTMC) **2.20** (Table 2.3 Entry 3)

RT	M_n	M_w	\mathcal{D}
6.190	7900	10800	1.37



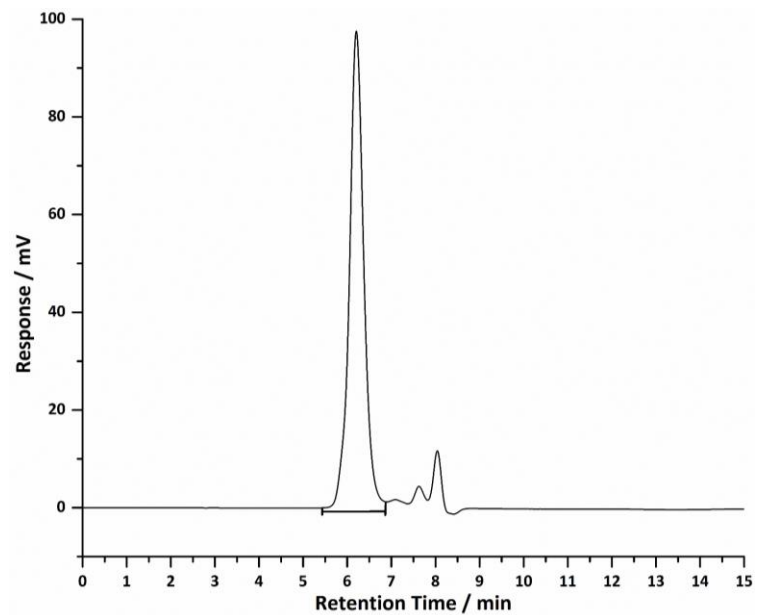
SEC trace of poly-(α -PhTMC) **2.20** (Table 2.3 Entry 4)

RT	M_n	M_w	\mathcal{D}
6.077	9600	13400	1.39



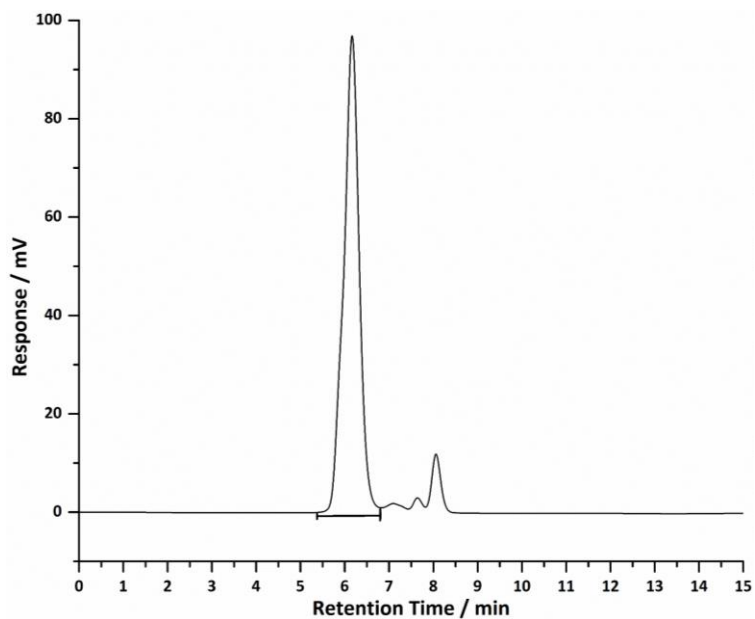
SEC trace of poly-(α -4-Me-PhTMC) **2.25** (Table 2.4 Entry 1)

RT	M_n	M_w	\bar{D}
6.258	6500	9100	1.40



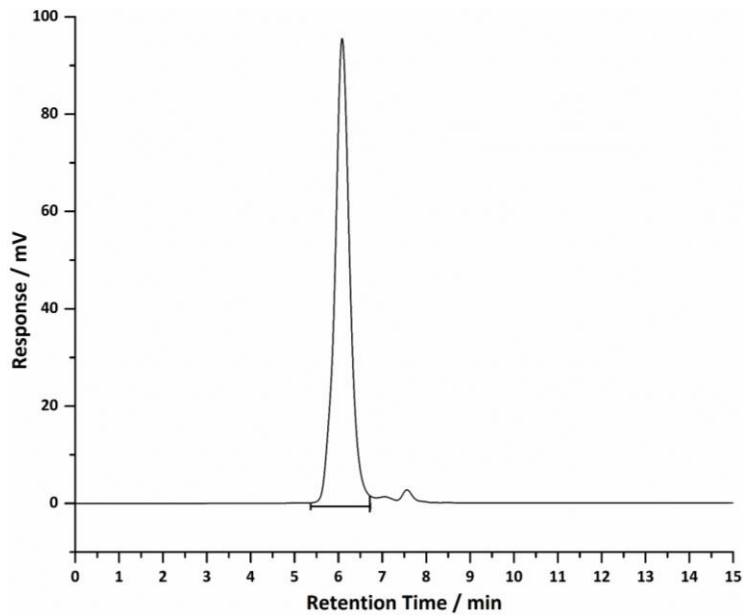
SEC trace of poly-(α -4-Br-PhTMC) **2.26** (Table 2.4 Entry 2)

RT	M_n	M_w	\bar{D}
6.202	7900	10500	1.33



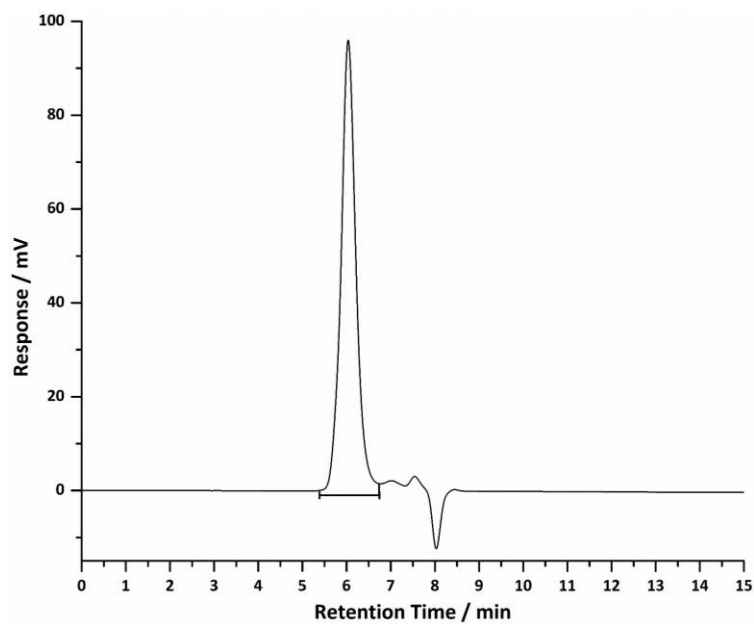
SEC trace of poly-(α -4-CF₃-PhTMC) **2.27** (Table 2.4 Entry 3)

RT	M_n	M_w	\mathcal{D}
6.162	9700	13100	1.35



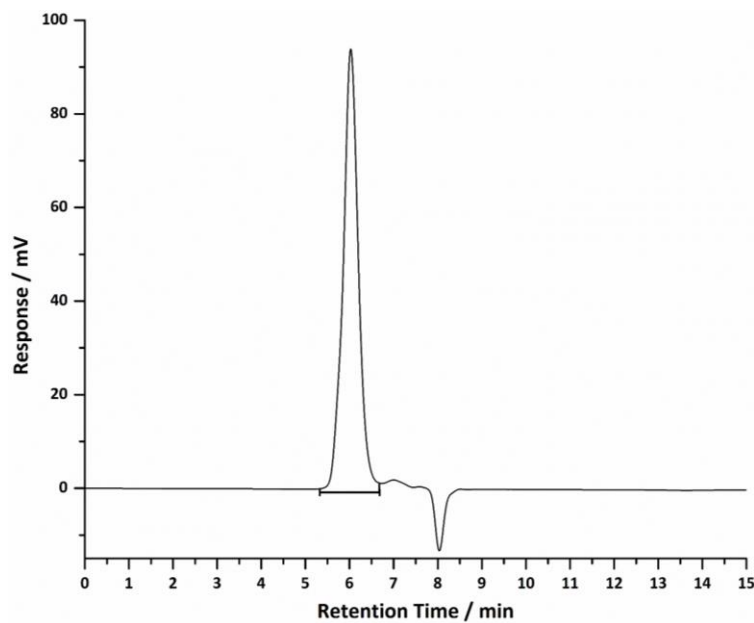
SEC trace of poly-(α -PhTMC-*b*- α -4-Br-PhTMC) **3.5** (Table 3.1 Entry 1)

RT	M_n	M_w	\mathcal{D}
6.080	10200	14000	1.37



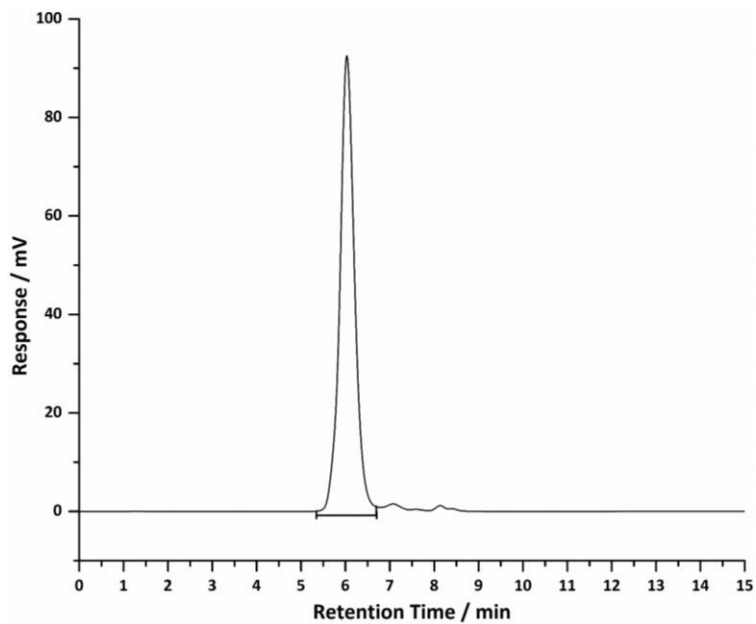
SEC trace of poly-(α -4-Me-PhTMC-*b*- α -4-Br-PhTMC) **3.6** (Table 3.1 Entry 2)

RT	M_n	M_w	\mathcal{D}
6.032	11900	16200	1.36



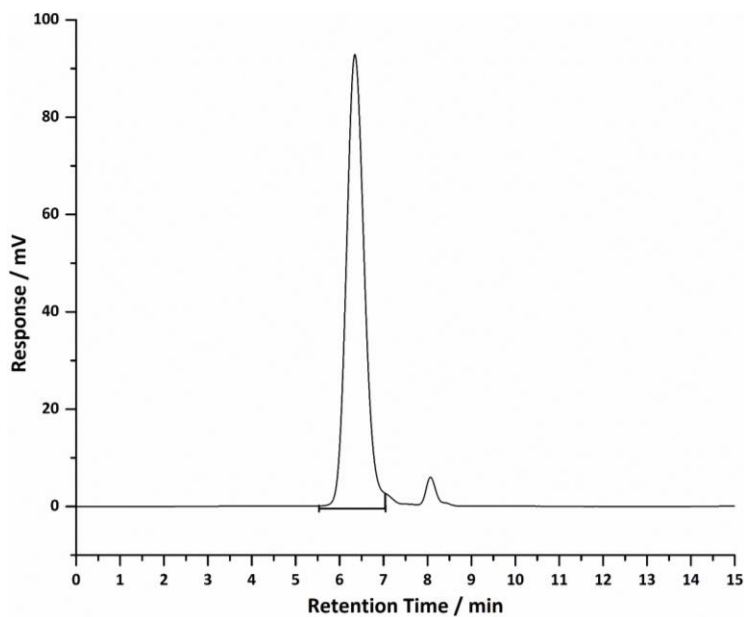
SEC trace of poly-(α -4-Me-PhTMC-*b*- α -4-CF₃-PhTMC) **3.7** (Table 3.1 Entry 3)

RT	M_n	M_w	\mathcal{D}
6.025	12600	17500	1.39



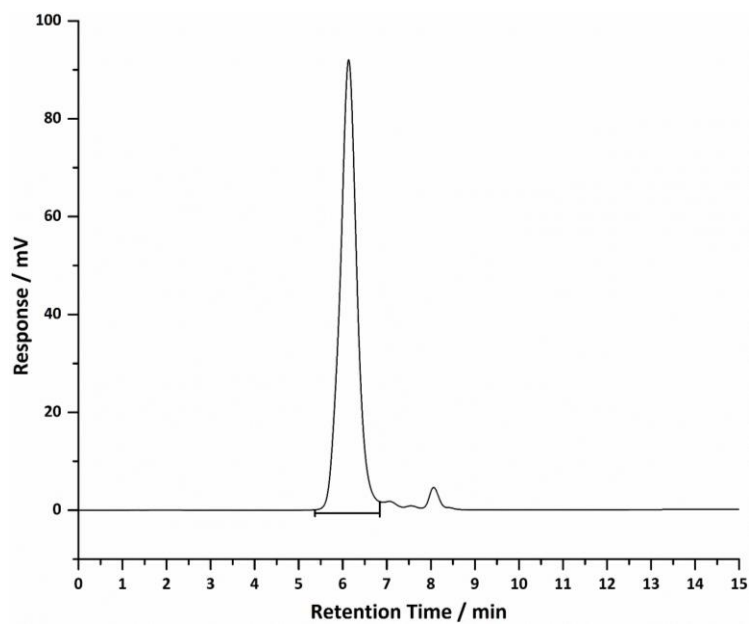
SEC trace of poly-(α -PhTMC-*b*- α -4-CF₃-PhTMC) **3.8** (Table 3.1 Entry 4)

RT	M_n	M_w	\mathcal{D}
6.028	12000	16000	1.33



SEC trace of poly-(α -4-Me-PhTMC-*b*- α -4-Br-PhTMC) **3.9** (Table 3.1 Entry 5)

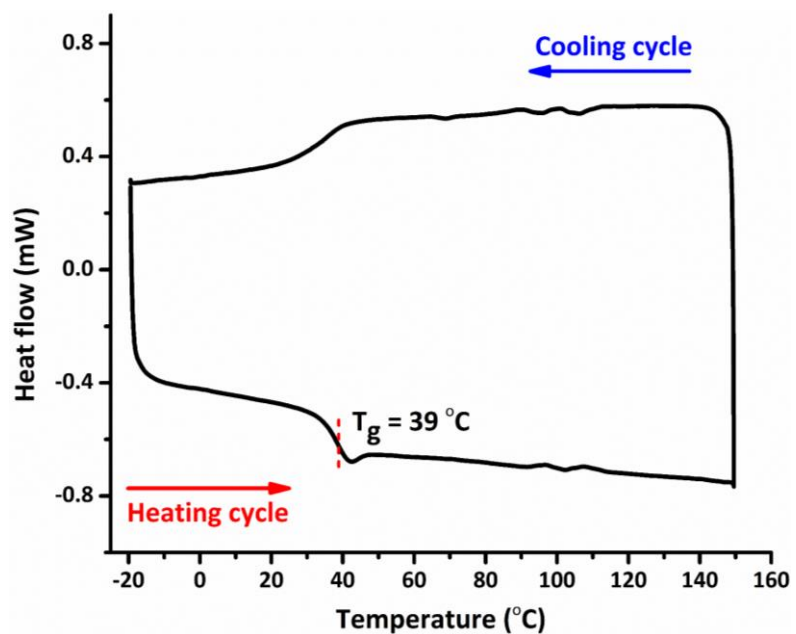
RT	M_n	M_w	\mathcal{D}
6.343	4900	6900	1.41



SEC trace of poly-(α -4-Me-PhTMC-*b*- α -4-Br-PhTMC) **3.10** (Table 3.1 Entry 6)

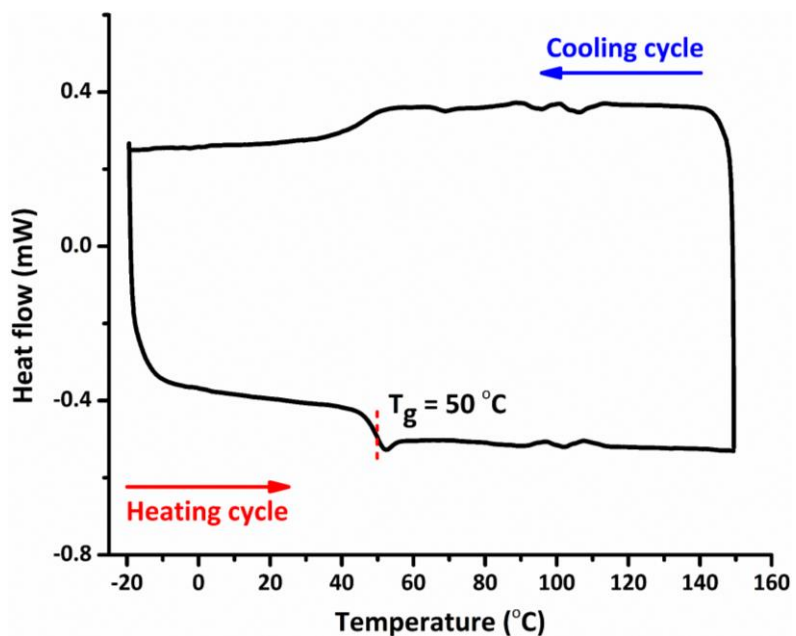
RT	M_n	M_w	\bar{D}
6.140	8900	12700	1.43

APPENDIX III
DSC TRACES



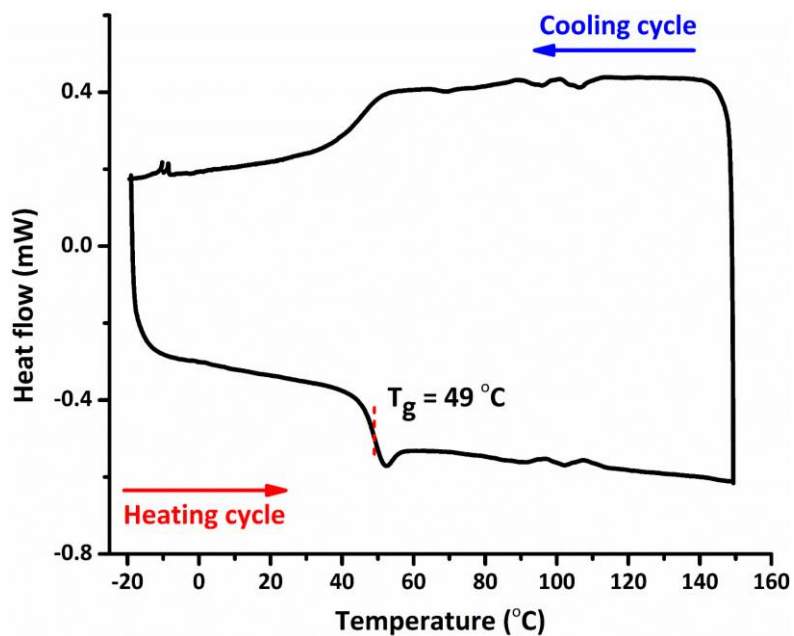
DSC curve of poly-(α -PhTMC) **2.20** (Table 2.5 Entry 1)

X_{reg}	DP_{NMR}	\bar{D}	T_g
0.01	99	1.41	39 °C



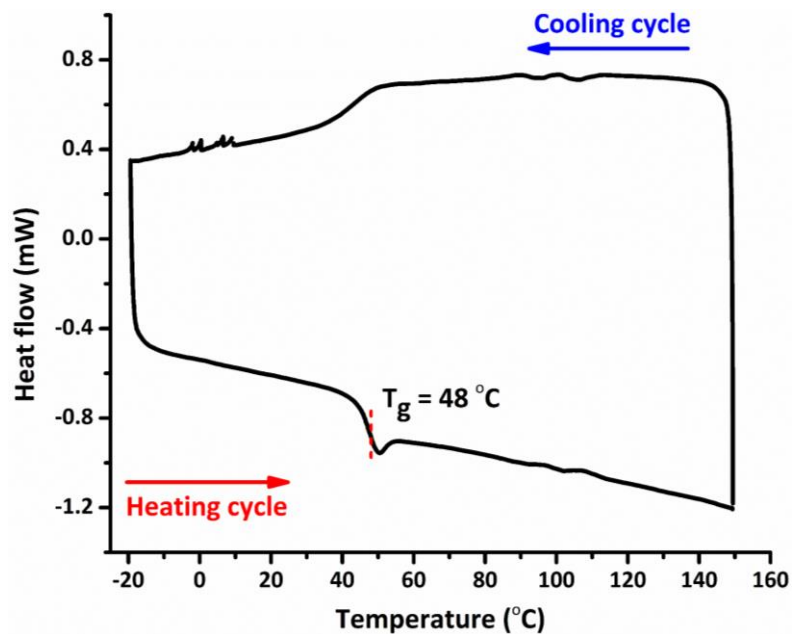
DSC curve of poly-(α -PhTMC) **2.20** (Table 2.5 Entry 2)

X_{reg}	DP_{NMR}	\bar{D}	T_g
0.40	99	1.43	50 °C



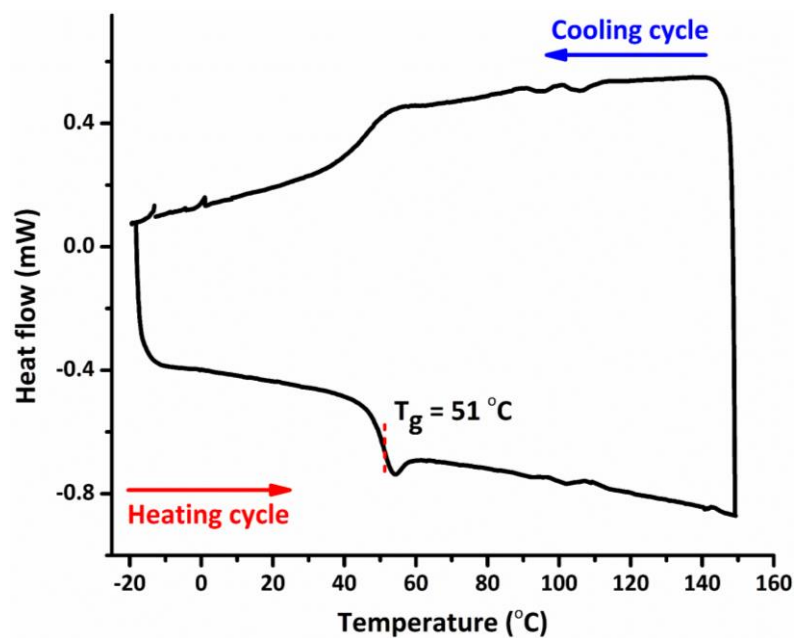
DSC curve of poly-(α -PhTMC) **2.20** (Table 2.5 Entry 3)

X_{reg}	DP_{NMR}	\bar{D}	T_g
0.72	98	1.39	49° C



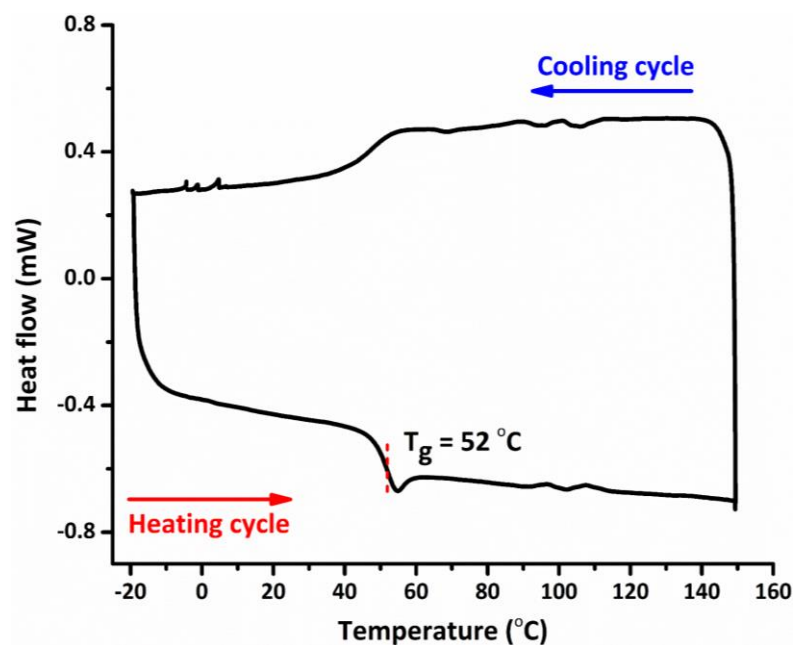
DSC curve of poly-(α -4-Me-PhTMC) **2.25** (Table 2.6 Entry 1)

X_{reg}	DP_{NMR}	\bar{D}	T_g
0.11	62	1.45	48° C



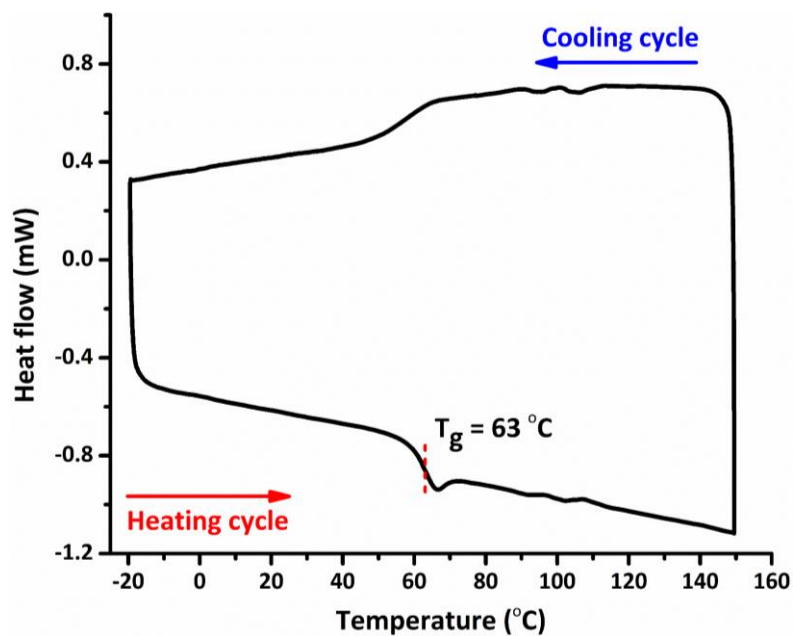
DSC curve of poly-(α -4-Me-PhTMC) **2.25** (Table 2.6 Entry 2)

X_{reg}	DP_{NMR}	\bar{D}	T_g
0.23	55	1.38	51 $^{\circ}$ C



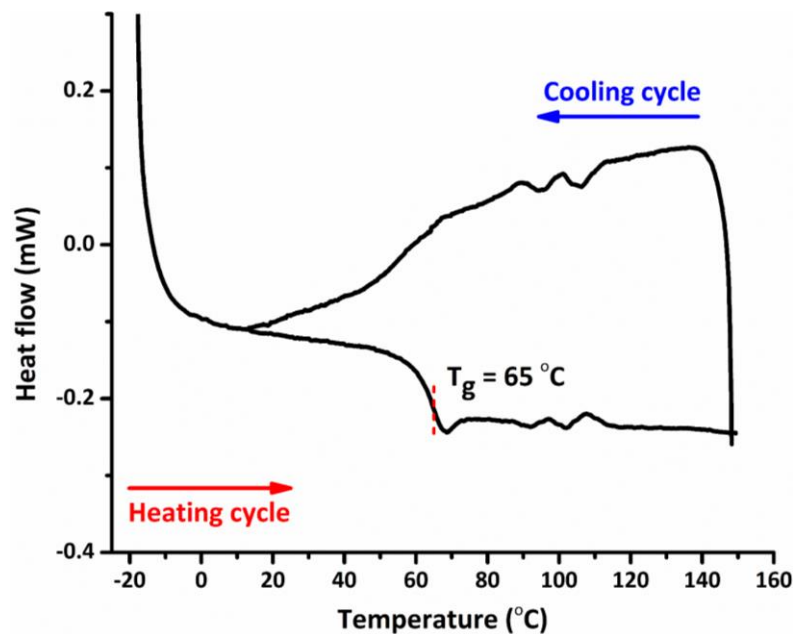
DSC curve of poly-(α -4-Me-PhTMC) **2.25** (Table 2.6 Entry 3)

X_{reg}	DP_{NMR}	\bar{D}	T_g
0.51	54	1.41	52 $^{\circ}$ C



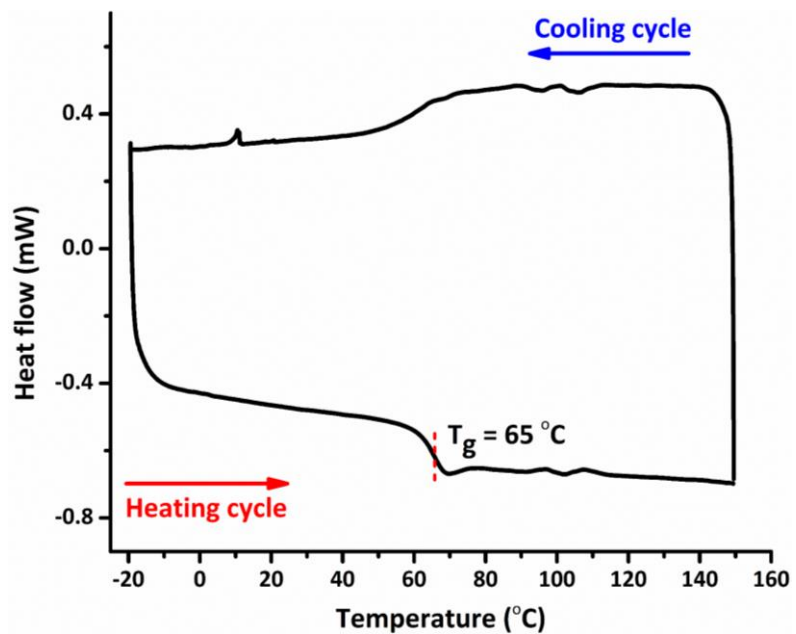
DSC curve of poly-(α -4-Br-PhTMC) **2.26** (Table 2.7 Entry 1)

X_{reg}	DP_{NMR}	\bar{D}	T_g
0.16	41	1.35	63 °C



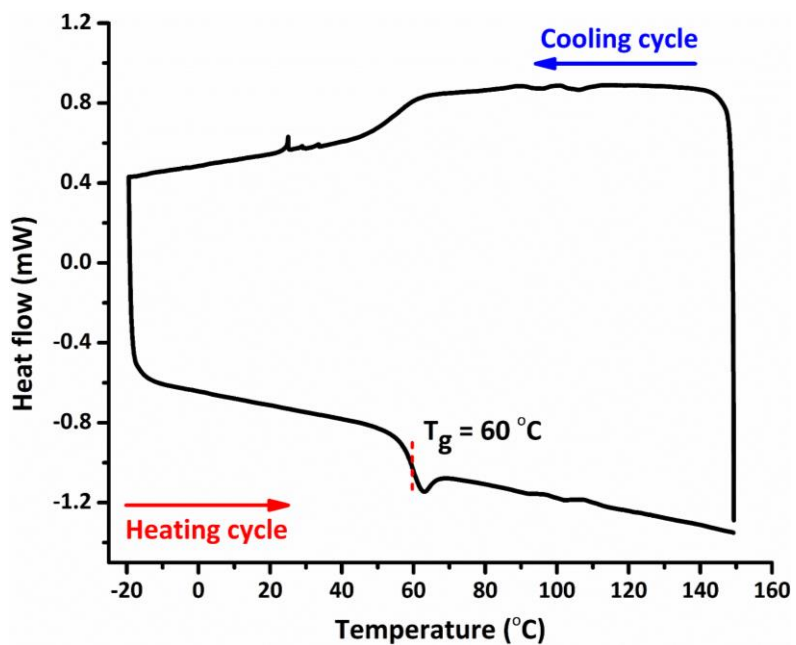
DSC curve of poly-(α -4-Br-PhTMC) **2.26** (Table 2.7 Entry 2)

X_{reg}	DP_{NMR}	\bar{D}	T_g
0.57	40	1.37	65 °C



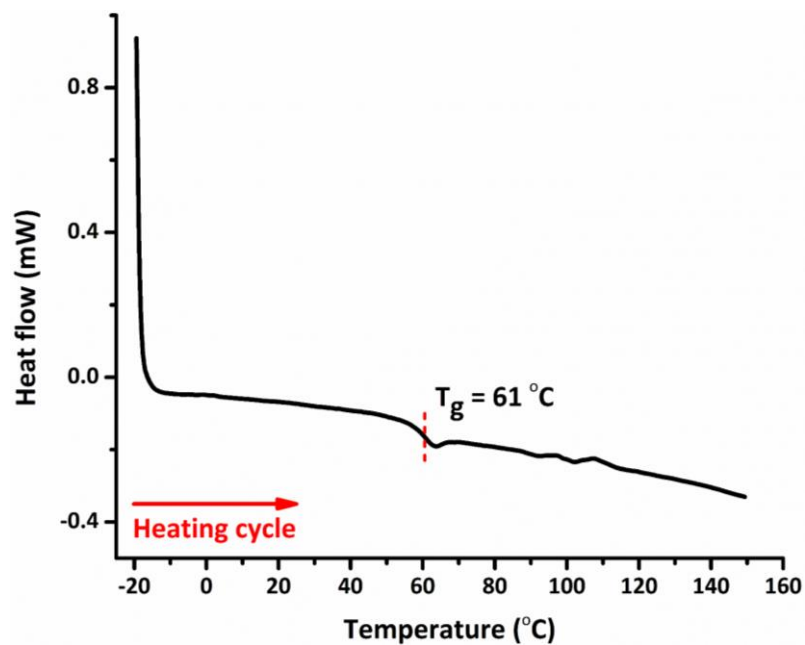
DSC curve of poly-(α -4-Br-PhTMC) **2.26** (Table 2.7 Entry 3)

X_{reg}	DP_{NMR}	\bar{D}	T_g
0.81	47	1.32	65 °C



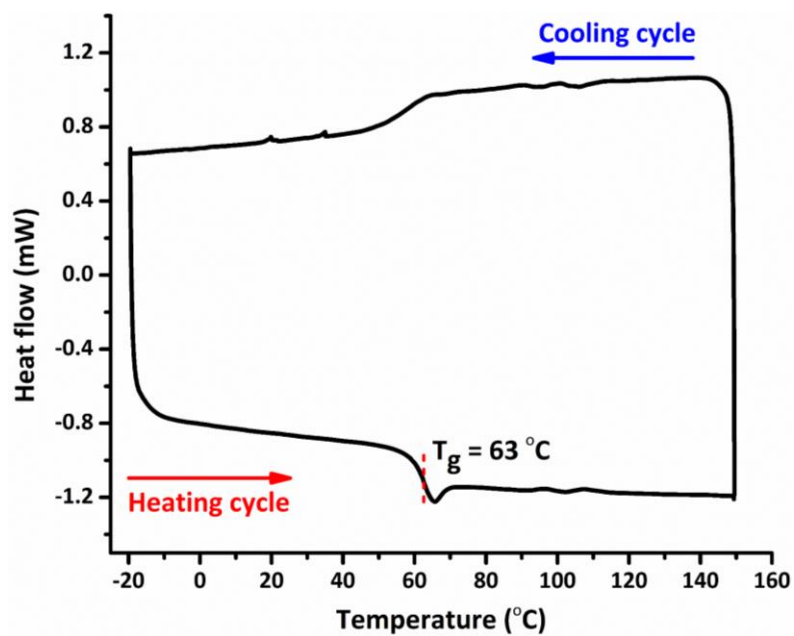
DSC curve of poly-(α -4-CF₃-PhTMC) **2.27** (Table 2.8 Entry 1)

X_{reg}	DP_{NMR}	\bar{D}	T_g
0.35	43	1.35	60 °C



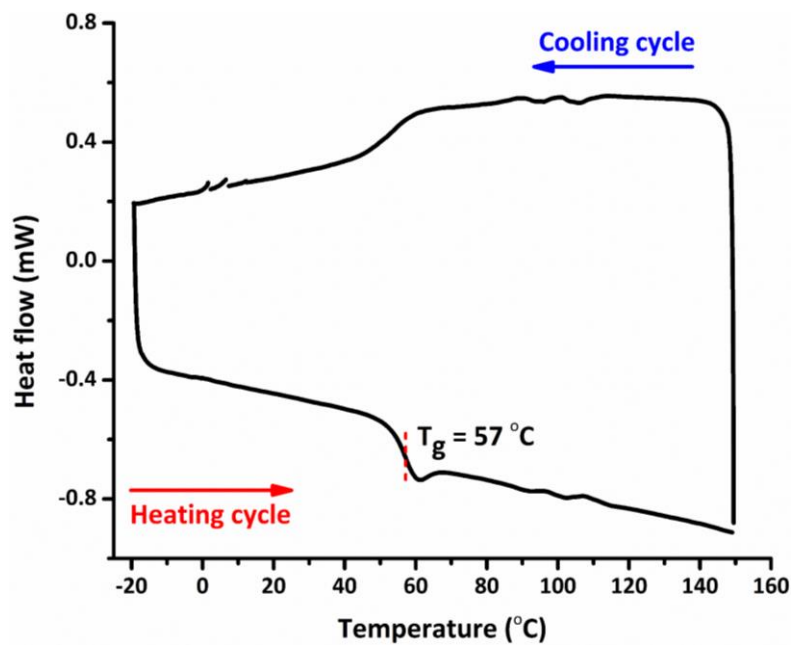
DSC curve of poly-(α -4-CF₃-PhTMC) **2.27** (Table 2.8 Entry 2)

X_{reg}	DP _{NMR}	\bar{D}	T_g
0.70	42	1.39	61 °C



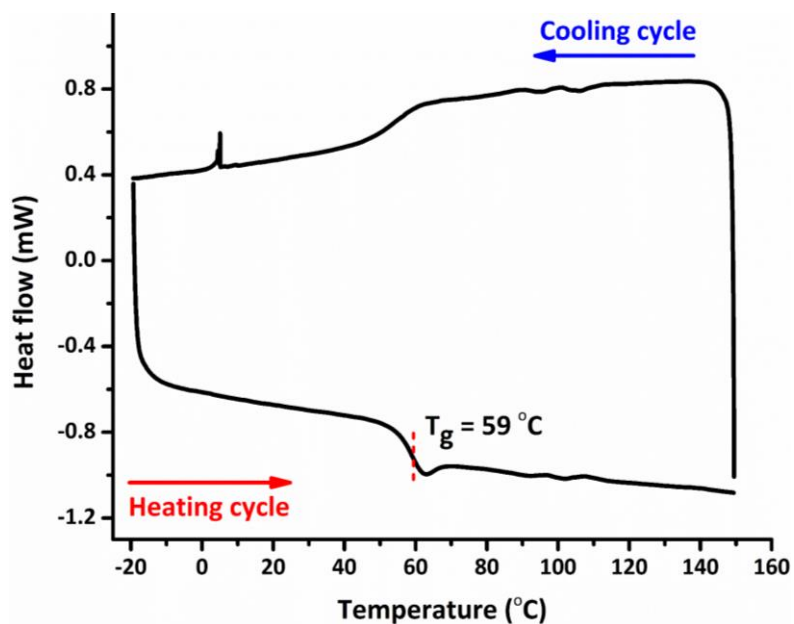
DSC curve of poly-(α -4-CF₃-PhTMC) **2.27** (Table 2.8 Entry 3)

X_{reg}	DP _{NMR}	\bar{D}	T_g
0.89	49	1.35	63 °C



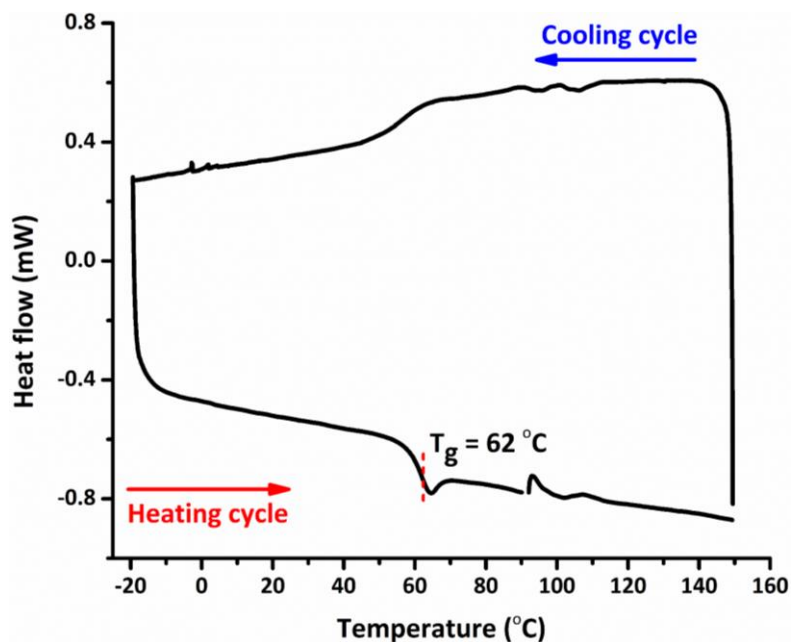
DSC curve of poly-(α -PhTMC-*b*-4-Br-PhTMC) **3.5** (Table 3.2 Entry 1)

X_{reg}	DP_{NMR}	\bar{D}	T_g
0.73	96	1.37	57 °C



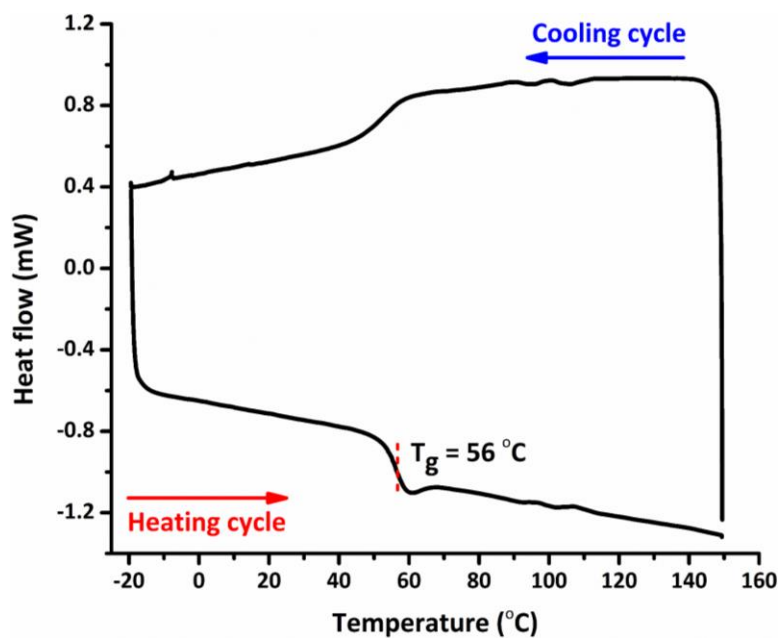
DSC curve of poly-(α -4-Me-PhTMC-*b*-4-Br-PhTMC) **3.6** (Table 3.2 Entry 2)

X_{reg}	DP_{NMR}	\bar{D}	T_g
0.69	92	1.36	59 °C



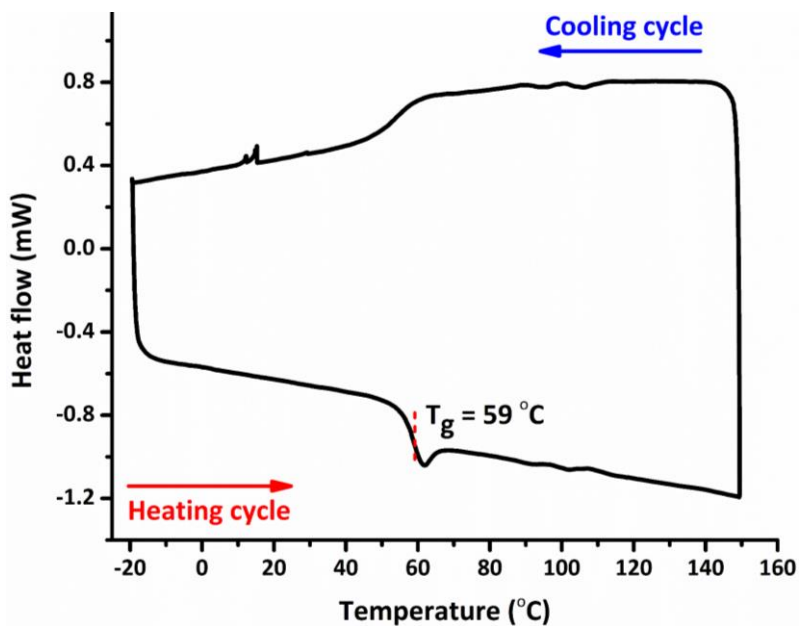
DSC curve of poly-(α -4-Me-PhTMC-*b*-4-CF₃-PhTMC) **3.7** (Table 3.2 Entry 3)

X_{reg}	DP _{NMR}	\bar{D}	T _g
0.69	82	1.39	62 °C



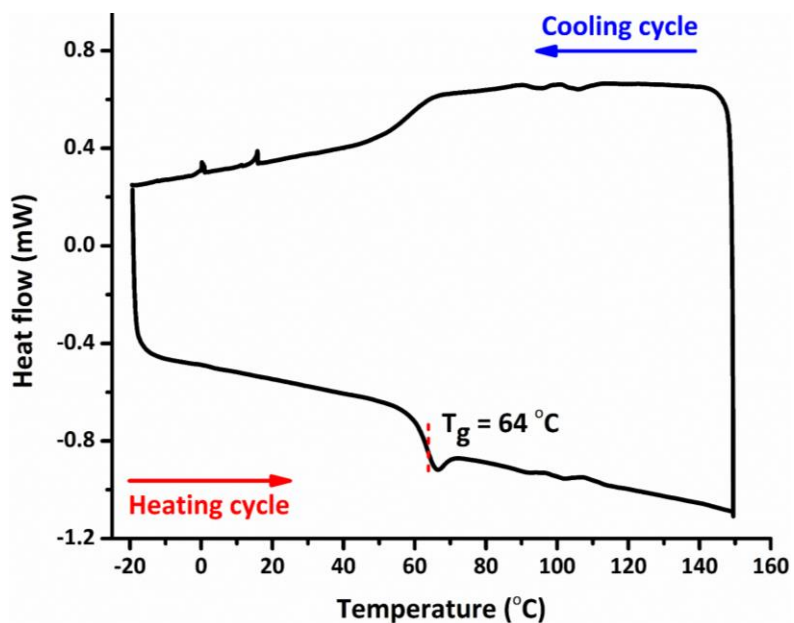
DSC curve of poly-(α -PhTMC-*b*-4-CF₃-PhTMC) **3.8** (Table 3.2 Entry 4)

X_{reg}	DP _{NMR}	\bar{D}	T _g
0.79	88	1.33	56 °C



DSC curve of poly-(α -4-Me-PhTMC-*b*-4-Br-PhTMC) **3.9** (Table 3.2 Entry 5)

X_{reg}	DP_{NMR}	\bar{D}	T_g
0.12	93	1.41	59 °C



DSC curve of poly-(α -4-Me-PhTMC-*b*-4-Br-PhTMC) **3.10** (Table 3.2 Entry 6)

X_{reg}	DP_{NMR}	\bar{D}	T_g
0.36	85	1.43	64 °C